



The University of
Nottingham

**Asphalt Mixture Moisture Sensitivity Evaluation
using Surface Energy Parameters**

by

Naveed Ahmad

GEORGE GREEN LIBRARY OF
SCIENCE AND ENGINEERING

Department of Civil Engineering

**Thesis submitted to the University of Nottingham for
the degree of Doctor of Philosophy**

March 2011

ABSTRACT

Asphalt mixture is mainly used for the construction of roads throughout the world. Large amounts of capital are spent for construction and maintenance of roads. Water is one of the major contributors towards the damage of the road structure. It is considered as the worst enemy of a pavement structure by directly causing a distress or indirectly magnifying a distress and hence damaging the road structure. Asphalt mixture loses its strength in the presence of water either through loss of cohesion within the bitumen or loss of adhesive bond between bitumen and aggregate. All the conventional techniques that are used for the determination of the moisture susceptibility of an asphalt mixture assess the material as a whole by using some mechanical testing technique without taking into account the individual physico-chemical characteristics of both the bitumen and the aggregates. The surface energy properties of the materials, which are used to quantify their interfacial adhesion, play an important role in the final adhesive bond strength between these materials. The aim of this research is to produce detailed experimental techniques to measure the surface energy properties of bitumen and aggregate, and then combine them with a mechanical moisture sensitivity test procedure. This can greatly contribute towards the development of a powerful material screening protocol/tool for selection of bitumen-aggregate combinations that are less susceptible to moisture damage.

This thesis describes the work that was carried out towards the development of a physico-chemical laboratory at the Nottingham Transportation Engineering Centre (NTEC). Four types of equipment were used, namely goniometer and dynamic contact angle analyser for determining the surface energy properties of the bitumen samples, and the dynamic vapour sorption and microcalorimeter systems for the surface energy properties of the aggregates. Large amount of material testing was carried out with these equipment and testing protocols were developed and improved over the course of experimental work. It was found that the dynamic contact angle technique and dynamic vapour sorption technique provides consistent results for bitumen and aggregates respectively as compared to the other two test equipment. The surface energy properties of the bitumen and the aggregates were then combined thermodynamically to determine the adhesive bond strength between the two materials, and the reduction in the adhesive properties if water is introduced into the

system. The results showed that these thermodynamic properties generally correlate well with the moisture damage performance of these combinations from the laboratory testing. SATS mechanical test technique was used to determine the moisture susceptibility of different bitumen-aggregate combinations. The virgin material and the recovered material from the SATS tested cores were tested for the surface energy properties. It was found that the surface energy properties combined with SATS results can be used, with some exceptions, to identify compatible bitumen-aggregate combinations and hence improved moisture damage performance of the resulting asphalt mixture.

Keywords: Surface Energy, Asphalt Mixture, Moisture Damage, Saturation Ageing Tensile Stiffness (SATS) Test.

DEDICATION

To my parents and teachers

ACKNOWLEDGEMENTS

First and foremost, I owe enormous gratitude to Professor Gordon Airey, my supervisor, for providing me with the opportunity to work on this project and extending his help and guidance throughout the research period despite his own heavy work load. I am grateful to him for his technical and moral support in each and every meeting. I always got out energised and refreshed after meeting him. He not only helped me with this research but also encouraged me by providing opportunities to interact with other national and international research groups. I feel honoured to have worked with him and have got groomed a lot both on academic and personal level. I will always cherish the time I have spent under his supervision.

Secondly, I would like to express my sincere gratitude to Professor Andrew Collop for allowing me to take admission at this esteemed institute and be a part of his research team. I would also like to thank him for his valuable suggestions and encouragement during the meetings.

I am grateful to Dr. James Grenfell, my second supervisor, for his academic support and especially for listening to all my problems as a friend. He has been an enormous help throughout the project.

I would also like to acknowledge all the technical staff of NTEC (Nottingham Transportation Engineering Centre) especially Jon Watson, Mick Winfield, Lawrence Pont, Richard Blakemore and Martyn Barrett for their help during the laboratory work.

I appreciate the support and company of my colleagues especially Rawid Khan, Lelio Brito, Fauzan Jakarni, Naeem Memon, Mohammed Mubarak, Oluwaseyi Oke, Xiaoyi Shi, Jiantao Wu, Junwei Wu, Izzi Yusoff and Said Zahran.

Finally, I would like to thank my parents for their continuous moral and financial support throughout my studies and my wife for her patience and encouragement during this research.

DECLARATION

The research described in this thesis was conducted at the University of Nottingham, Department of Civil Engineering between December 2006 and March 2010. I declare that the work is my own and has not been submitted for a degree of another university.

Naveed Ahmad
Nottingham
March 2011

TABLE OF CONTENTS

Abstract	i	
Dedication	iii	
Acknowledgements	iv	
Declaration	v	
List of Figures	xi	
List of Tables	xvi	
Glossary	xviii	
Chapter 1	Introduction	1
1.1	Background	1
1.2	Problem Statement	3
1.3	Research Objectives and Deliverables	4
1.4	Research Methodology	5
1.5	Thesis Outline	7
Chapter 2	Literature Review	9
2.1	Introduction	9
2.2	Moisture Damage	9
2.3	Sources of Moisture	10
2.3.1	Internal	10
2.3.2	External	10
2.4	Types of Moisture Damage	11
2.5	Effect of Moisture Damage	12
2.6	Factors Effecting Moisture Sensitivity	13
2.6.1	Aggregate Physical Properties	13
2.6.2	Aggregate Chemistry	14
2.6.3	Presence of Clay	14
2.6.4	Bitumen properties	14
2.6.5	Bitumen-Aggregate Interactions	15
2.6.6	Factors other than Material Properties	15

2.7	Moisture Damage Mechanisms	15
2.7.1	Advective Flow through an Asphalt Mixture	16
2.7.2	Diffusion Leading to Bitumen-Aggregate Interface Failure	16
2.7.3	Diffusion Causing Dispersion of the Bitumen Film	16
2.7.4	Emulsification	16
2.7.5	Pore Pressures	16
2.8	Moisture Sensitivity Assessment	17
2.8.1	Tests on Loose Coated Aggregates	17
2.8.2	Tests on Compacted Asphalt Mixtures	19
2.8.3	Latest Advancements	26
2.9	Surface Energy and Moisture Sensitivity	31
2.9.1	Background	31
2.9.2	Surface Energy Theory	32
2.9.3	General Principles	34
2.9.4	Bitumen-Aggregate Adhesion and Moisture Susceptibility	37
2.9.5	Bitumen-Aggregate Bond Energy Ratios	41
Chapter 3	Surface Energy Testing of Binders	43
3.1	Background	43
3.2	Contact Angle Technique	46
3.3	Theories for Surface Energy Calculation from Contact Angle Data	47
3.3.1	Critical Surface Tension Approach	47
3.3.2	Geometric Mean Approach	48
3.3.3	Harmonic Mean Approach	49
3.3.4	Acid-Base Approach	49
3.4	Sessile Drop/Static Contact Angle Technique	50
3.5	Dynamic Contact Angle-DCA Technique	53
3.6	Calculation of Surface Energy Parameters - Example Solution	55
3.7	Results and Discussion	60
3.7.1	Test/Probe Liquids	60
3.7.2	Sample Preparation Techniques and Test Parameters	62
3.7.3	Contact Angle Data Selection	64
3.7.4	SFE Using Different Number of Probe Liquids	66

3.7.5	Goniometer versus DCA	67
Chapter 4	Surface Energy Testing of Aggregates	72
4.1	Background	72
4.2	Dynamic Vapour Sorption-DVS Technique	72
4.3	Microcalorimeter Technique	75
4.4	Determination of Surface Energy Parameters - Example Solution	77
4.5	Results and Discussion	80
4.5.1	Probe Liquids	81
4.5.2	DVS Results	81
4.5.3	Microcalorimeter Results	89
Chapter 5	Bitumen-Aggregate Adhesion and Moisture Sensitivity	93
5.1	Introduction	93
5.2	Bond Energy Parameters	93
5.3	Moisture Sensitivity Parameters	94
5.4	Bitumen-Aggregate Combinations and Moisture Sensitivity	95
Chapter 6	Moisture Damage Performance of Asphalt using SATS Protocol	100
6.1	Introduction	100
6.2	SATS Protocol	101
6.2.1	Summary of Test Procedure	102
6.3	Testing and Material Variables	103
6.3.1	Effect of Changing Individual Parameters	105
6.3.2	Effect of Changing Multiple Parameters	117
6.4	Summary and Conclusions	131

Chapter 7	Moisture Sensitivity Interpretation for SATS Tested Asphalt Mixtures	133
7.1	Introduction	133
7.2	Material Combinations	133
7.3	Binder Recovery and Rheological Testing	135
7.3.1	Rheology Testing of Control and SATS Recovered Binders	135
7.3.2	Results	143
7.4	Data Analysis for Moisture Sensitivity Determination	143
7.4.1	SATS Retained Stiffness Modulus and Moisture Damage	143
7.4.2	Age Hardening (Ageing Factor)	144
7.4.3	Pressure Factor	150
7.4.4	Moisture Factor	151
7.5	Results and Conclusions	153
Chapter 8	Surface Energy and SATS Protocol	156
8.1	Introduction	156
8.2	Surface Energy Testing of SATS Material	156
8.2.1	Surface Energy Properties of Binders	157
8.2.2	Binder Rheology and Surface Energy	164
8.2.3	Surface Energy Properties of Aggregates	167
8.3	Bitumen-Aggregate Bond Energies and Moisture Sensitivity	169
8.4	SATS Moisture Factors versus SE Moisture Sensitivity Ratios	174
Chapter 9	Conclusions and Recommendations	176
9.1	Overview	176
9.2	Conclusions	177
9.3	Recommendations for Future Work	179
References		182
Appendix A		195

Appendix B	218
Appendix C	240
Appendix D	266
Appendix E	279
Appendix F	280
Curriculum Vitae	286

LIST OF FIGURES

Figure 2.1: Sources of Water in an Asphalt Pavement	11
Figure 2.2: Pavement Distresses	12
Figure 2.3: Moisture Effect on Fatigue Response	13
Figure 2.4: Adhesion Test Fixture	21
Figure 2.5: Hamburg Wheel Tracker	21
Figure 2.6: Vialit Plate Test	24
Figure 2.7: Sketch of the Tapered Double Cantilever Beam Specimen	24
Figure 2.8: Peel Test	25
Figure 2.9: Time-to-Failure (Creep-Rupture) Test	25
Figure 2.10: Pneumatic Adhesion Tensile Testing Instrument	27
Figure 2.11: A Schematic of Blister Apparatus	27
Figure 2.12: SATS	29
Figure 2.13: Work of Cohesion	36
Figure 2.14: Work of Adhesion	37
Figure 3.1: Surface Tension	43
Figure 3.2: Surface Tension Measurement using Wilhelmy Plate	44
Figure 3.3: Surface Tension Measurement using Du-Nouy Ring	45
Figure 3.4: Young's Contact Angle Formula	46
Figure 3.5: Contact Angle-Sessile Drop Technique	47
Figure 3.6: Critical Surface Energy of Solid	48
Figure 3.7: Contact Angles	51
Figure 3.8: Goniometer Schematic	52
Figure 3.9: Static Contact Angle; Process Steps	52
Figure 3.10: Schematic of Dynamic Contact Angle Analyser	53
Figure 3.11: Contact Angle Measurement; Wilhelmy Plate Technique	54
Figure 3.12: Variation of Wetting Force versus Depth of Immersion	54
Figure 3.13: Neumann Plot	65
Figure 3.14: Change of Contact Angle and Drop Width with Time (with Diiodomethane)	68
Figure 3.15: Contact Angle vs. Time (with Diiodomethane)	69
Figure 3.16: Change of Contact Angle and Drop Width with Time (with Glycerol)	69
Figure 3.17: Contact Angle vs. Time (with Glycerol)	70

Figure 4.1: DVS Partial Pressure Plot	82
Figure 4.2: DVS Isotherm	83
Figure 4.3: BET Line-Fit Plot	83
Figure 4.4: Partial Pressure and Aggregate Change in Mass	84
Figure 4.5: Typical Adsorption Isotherm Plots	85
Figure 4.6: A Typical Heat Flow Curve	90
Figure 5.1: Bitumen-Aggregate Compatibility Ratio 3	98
Figure 5.2: Bitumen-Aggregate Compatibility Ratio 4	99
Figure 6.1a: SATS Pressure Vessel	102
Figure 6.1b: SATS Specimen Tray	102
Figure 6.2: Gradation Curves for All Aggregate Types	105
Figure 6.3: SATS results for specimens from different aggregate type made using 15pen binder and tested under standard conditions (85°C, 65 hours and 2.1MPa)	106
Figure 6.4: SATS results for specimens from different aggregate type made using 50pen binder and tested under standard conditions (85°C, 65 hours and 2.1MPa)	107
Figure 6.5: SATS results for Aggregate A specimens made using 15 and 50pen binders and tested under standard conditions (85°C, 65 hours and 2.1MPa)	108
Figure 6.6: SATS results for 50pen Aggregate A specimens tested under different pressures for 65 hours at 85°C	109
Figure 6.7: SATS results for 50pen Aggregate B specimens tested under different pressures for 65 hours at 85°C	110
Figure 6.8: SATS results for 50pen Aggregate A specimens tested at different temperatures for 65 hours at 2.1MPa	111
Figure 6.9: SATS results for 50pen Aggregate A specimens tested at different temperatures for 65 hours at 0.5MPa	112
Figure 6.10: SATS results for 50pen Aggregate B specimens tested at different durations at 85°C and 2.1MPa	113
Figure 6.11: SATS results for 50pen Aggregate A specimens made with different binder contents tested at different temperatures and durations under 0.5MPa and 2.1MPa pressure	114

Figure 6.12: SATS results for 50pen Aggregate A and D specimens made with 4% and 5% binder, tested at 85°C, 0.5MPa and 24 hours	115
Figure 6.13: SATS results for 50pen Aggregate A specimens made with different air void contents tested at different temperatures and durations under 0.5MPa and 2.1MPa pressure	116
Figure 6.14: SATS results for 50pen Aggregate A and D specimens made with different air void contents tested at 85°C, 0.5MPa and 24 hours	117
Figure 6.15: SATS results for different 50pen mixture types tested at 60°C and 0.5MPa for a duration of 65 hours	118
Figure 6.16: SATS results for different 50pen mixture types tested at 30°C and 0.5MPa for a duration of 65 hours	119
Figure 6.17: SATS results for 50pen Aggregate A mixture types tested at 30, 60 and 85°C at either 0.5 or 2.1MPa for a duration of 65 hours	119
Figure 6.18: SATS results for different 50pen mixture types tested at 85°C and 0.5MPa for a duration of 24 hours	121
Figure 6.19: SATS results for 50pen Aggregate A mixture types tested at 85°C at either 0.5 or 2.1MPa for different durations	121
Figure 6.20: SATS results for different 50pen mixture types tested at 60°C and 0.5MPa for a duration of 24 hours	122
Figure 6.21: SATS results for different 50pen mixture types tested at 30°C and 0.5MPa for a duration of 24 hours	123
Figure 6.22: SATS results for 50pen Aggregate A specimens tested at different temperatures under 0.5MPa pressure for a duration of 65 hours	124
Figure 6.23: SATS results for 50pen Aggregate B specimens tested at different temperatures under 0.5MPa pressure for a duration of 65 hours	124
Figure 6.24: SATS results for 50pen Aggregate D specimens tested at different temperatures under 0.5MPa pressure for a duration of 65 hours	125
Figure 6.25: SATS results for 50pen Aggregate A specimens tested at different temperatures under 0.5MPa pressure for a duration of 24 hours	126
Figure 6.26: SATS results for 50pen Aggregate B specimens tested at different temperatures under 0.5MPa pressure for a duration of 24 hours	127
Figure 6.27: SATS results for 50pen Aggregate D specimens tested at different temperatures under 0.5MPa pressure for a duration of 24 hours	127

Figure 6.28: SATS results for 50pen Aggregate A specimens tested at different durations at a temperature of 60°C under 0.5MPa pressure	128
Figure 6.29: SATS results for 50pen Aggregate B specimens tested at different durations at a temperature of 60°C under 0.5MPa pressure	129
Figure 6.30: SATS results for 50pen Aggregate A specimens tested at different durations at a temperature of 30°C under 0.5MPa pressure	130
Figure 6.31: SATS results for 50pen Aggregate B specimens tested at different durations at a temperature of 30°C under 0.5MPa pressure	130
Figure 7.1: Dynamic Shear Rheometer	136
Figure 7.2: DSR Test; Sample Preparation	136
Figure 7.3: DSR-Control Software	137
Figure 7.4: DSR-Result Analysis	137
Figure 7.5: Typical Shift Factor Plot	138
Figure 7.6: Master Curves Comparison (15pen Binder & SATS Conditions-A)	139
Figure 7.7: Master Curves Comparison (50pen Binder & SATS Conditions-B)	139
Figure 7.8: Master Curves Comparison (50pen Binder & SATS Conditions-C)	140
Figure 7.9: Penetration and Softening Point vs. Normalised Shear Complex Modulus	145
Figure 7.10: Comparison of 2Hz Sinusoidal Load and ITSM Pulse Load	146
Figure 7.11: Predicted Asphalt Mixture Stiffness Moduli	147
Figure 7.12: Ageing Factor of Mixture against Normalised DSR G^* Data	148
Figure 7.13: Effect of Retained Saturation on Normalised Shear Complex Modulus	149
Figure 7.14: Predicted Ageing Factor Plotted as a Function of Retained Saturation	149
Figure 7.15: Chart showing $f_{ageing} \times f_{pressure}$ of Standard SATS	151
Figure 7.16: Moisture Factors for 15 and 50pen Binders with Basic Aggregate	153
Figure 7.17: Moisture Factors for Different SATS Test Conditions	154
Figure 7.18: Moisture Factors for Basic (A) and Acidic (D) Aggregates	154
Figure 7.19: Moisture Factor versus Retained Stiffness Modulus	155
Figure 8.1: Effect of Ageing and Moisture on Contact Angle	160
Figure 8.2: Effect of Binder Grade and SATS Conditions on Contact Angle	160
Figure 8.3: Effect of Ageing and Moisture on Cohesive Bond Strength	161

Figure 8.4: Cores above Water versus Cores Submerged in Water (SATS)	162
Figure 8.5: ^1H NMR (400 MHz, CDCl_3 , 25°C) of 50pen Binder with added DCM	163
Figure 8.6: ^1H NMR (400 MHz, CDCl_3 , 25°C) of SATS Recovered Binder	163
Figure 8.7: Effect of Presence of Air on Binder Rheology and SE	164
Figure 8.8: SATS Results and Binder Rheology	166
Figure 8.9: SATS Results and Binder SE	166
Figure 8.10: SATS Moisture Factors versus SE Bond Ratios	174

LIST OF TABLES

Table 3.1: Surface Energy Components of the Probes (Example Solution)	57
Table 3.2: Contact Angle Results (Example Solution)	57
Table 3.3: Probes for the Analysis of Bitumen	62
Table 3.4: Contact Angle Data (Neumann Plot)	65
Table 3.5: Surface Energy Data using Five Probes	66
Table 3.6: Surface Energy Data using Three Probes	67
Table 3.7: Comparison of Goniometer and DCA Contact Angle Data	67
Table 3.8: Variability; DCA Data	70
Table 3.9: Variability; Goniometer Data	70
Table 4.1: Surface Energy Parameters of the Test Liquids (Example Solution)	78
Table 4.2: Obtained Spreading Pressures (DVS Test Results)	78
Table 4.3: Probes for Aggregate Analysis	81
Table 4.4: SSA of Aggregates (DVS)	86
Table 4.5: Aggregates Spreading Pressure Values (DVS)	87
Table 4.6: Aggregates SE Parameters; DVS Analysis	87
Table 4.7: Aggregates SE Parameters (Pre-heated)	89
Table 4.8: Aggregates SE Parameters (DVS)	89
Table 4.9: Heat of Immersion (erg/cm^2)	91
Table 5.1: Binder SE; Compatibility Analysis	96
Table 5.2: Bitumen-Aggregate Compatibility Ratios	96
Table 5.3: Parameters to Predict the Bitumen-Aggregate Moisture Susceptibility	97
Table 6.1: Aggregate Properties	104
Table 7.1: Material Combinations for Binder Recovery and Analysis	134
Table 7.2: Recovered Binder Complex Modulus Data at 0.4 Hz and 25°C	140
Table 7.3: Pressure Factors for Aggregate Types A, B, C and D with 50pen	150
Table 7.4: Moisture Factors for Aggregate Type 'A'	152
Table 8.1: SATS Binder, SE Parameters	157
Table 8.2: Binder Cohesion	159
Table 8.3: Test Results; Executive Summary	165
Table 8.4: SSA of Aggregates (SATS)	168
Table 8.5: Aggregates Spreading Pressure Values (SATS)	168

Table 8.6: Aggregates SE Parameters (SATS)	169
Table 8.7: Binder Surface Energy (SATS Material)	170
Table 8.8: Binder Cohesion (SATS Material)	170
Table 8.9: Bitumen-Aggregate Compatibility Ratios (Aggregates 'A' & 'C')	171
Table 8.10: Bitumen-Aggregate Compatibility Ratios (Aggregates 'B' & 'D')	171
Table 8.11: Prediction of Moisture Susceptibility of a Bitumen-Aggregate System	173

GLOSSARY

- AASHTO*: American Association of State Highway and Transportation Officials
- ASTM*: American Society for Testing and Materials
- CA*: Contact Angle
- COSHH*: Care of Substances Hazardous To Health
- CMV*: Clean Mirror Value
- DCA*: Dynamic Contact Angle Analyser
- DCC*: Dynamic Contamination Control
- DCM*: Dichloromethane
- Diiodomethane*:
In some parts of this literature diiodomethane is also referred as methylene iodide.
- DPA*: Dew Point Analyser
- DSR*: Dynamic Shear Rheometer
- DVS*: Dynamic Vapour Sorption System
- GVOC*: Good-Van Oss-Chaudhury
- HPLC*: High Performance Liquid Chromatography
- Hydrophobic*: Hydrophobic is also referred as lyophobic (liquid hating) and vice versa.
- Hydrophilic*: Hydrophilic is also referred as lyophilic (liquid loving) and vice versa.
- ITSM*: Indirect Tensile Stiffness Modulus
- MFC*: Mass Flow Controller
- MPK*: Methyl Propyl Ketone
- MSDS*: Material Safety Data Sheet
- NTEC*: Nottingham Transportation Engineering Centre
- PMB*: Polymer Modified Bitumen

<i>PP:</i>	Partial Pressure
<i>PPE:</i>	Personal Protective Equipment
<i>PTFE:</i>	Poly Tetra Fluoro Ethylene
<i>SATS:</i>	Saturation Ageing Tensile Stiffness
<i>SBS:</i>	Styrene Butadiene Styrene
<i>SE:</i>	Surface Energy Surface Energy is also referred as Surface Free Energy (SFE)
<i>SMS:</i>	Surface Measurement Systems
<i>USD:</i>	Universal Sorption Device
<i>WEL:</i>	Work Exposure Limit
<i>ZDOI:</i>	Zero Depth of Immersion

CHAPTER 1

INTRODUCTION

1.1 Background

Majority of the roads throughout the world are constructed by using asphalt mixtures. Like any other man-made structures, asphalt pavements deteriorate with the passage of time. Moisture damage is considered as one of the major causes of distress in an asphalt pavement. Almost 2.5 billion pounds are spent annually by the local authorities in England and Wales (ALARM, 2006) for road maintenance and rehabilitation works. Though all the damage is not caused directly by the moisture, its presence increases the extent and severity of already existing distresses like cracking, potholes and patches, and rutting (Miller and Bellinger, 2003). The presence of moisture results in the degradation of the mechanical properties of the asphalt mixture i.e. loss of stiffness and mechanical strength which could ultimately lead to the failure of the road structure. Moisture damage can thus have a great economic impact as it could cause premature pavement failure and hence results in increased rehabilitation work and maintenance costs.

Bitumen and aggregates are the main constituents of an asphalt mixture. Moisture damage is normally related to the loss of adhesion between bitumen and aggregate and/or loss of cohesion within the bitumen in the presence of water (Terrel and Al-Swailmi, 1994). Replacement of bitumen film from the aggregate surface by water is termed as stripping (Kandhal et al., 1994). The phenomenon of stripping largely depends on the chemical composition of bitumen and aggregates, and their affinity towards each other (Emery and Seddik, 1997). Hence the individual properties of the material along with the properties of the resulting asphalt mixture largely affect the structural performance of the road pavement.

It is important to identify materials and mixtures that are prone to moisture damage. A number of laboratory tests have been developed to determine the moisture susceptibility of asphalt mixtures but they do not show good correlation between the results obtained in the laboratory and the field performance of the mixtures (Solaimanian et al., 2003). In most of these tests the moisture sensitivity/damage is

just related to the mechanical properties of the asphalt mixture. The physical and chemical properties of the individual material (bitumen and aggregate), also referred to as physico-chemical properties, are not addressed by these tests. These properties are related to the adhesion characteristics of the two materials and are responsible for adhesion or debonding of the materials (MS-24, 2007). Surface energy properties of the materials are used to assess these adhesion characteristics (Bhasin, 2006). Surface energy is believed to truly represent the physico-chemical surface characteristics of the bitumen and aggregate material and is considered as a tool for selection of moisture resistant material (Cheng, 2002).

This physico-chemical approach is being used at NTEC to assess the moisture susceptibility of the asphalt mixtures. Four different types of test equipment namely, Goniometer, Wilhelmy Plate Device, Microcalorimeter and Dynamic Vapour Sorption System have been commissioned. Goniometer and Wilhelmy Plate devices are used to measure the contact angle values of different probe liquids with the bitumen while the Microcalorimeter and the Dynamic Vapour Sorption System are used to measure the heat of adhesion and adsorption of different probe liquids respectively with the aggregates. Surface energy characteristics of the bitumen and aggregates are calculated by using the results obtained from these equipment which are then used to assess the adhesive and cohesive bond characteristics of the two materials, with and without the presence of water.

Different types of bitumen and aggregates have been tested by using the above mentioned equipment. Different sample preparation techniques and test variables have been considered and the experimental procedures have been updated accordingly. SATS, a combined ageing and moisture sensitivity protocol, has been selected to study the applicability and validation of the surface energy theory. Bitumen and aggregate material is recovered from the asphalt cores that have been tested under various conditions of the SATS protocol. The recovered material is then tested for its surface energy properties. The surface energy properties of the virgin material are compared with that of the aged and moisture damaged material. The rheological properties for both the virgin and recovered binder are also obtained and compared. It has been observed that the surface energy results generally correspond well with the results obtained from the SATS and rheology testing.

This dissertation describes the work that has been carried out to produce detailed experimental protocols for the measurement of surface energy properties of bitumen and aggregate, and to determine the moisture sensitivity of the bitumen-aggregate combinations that are generally used in the UK.

1.2 Problem Statement

Surface energy properties of the bitumen and aggregates are used to assess the cohesive and adhesive bond strengths of the two materials. The effect of moisture/water on the bond strength of a bitumen-aggregate system is also studied by using this thermodynamic technique (Bhasin et al. 2006a, Cheng et al. 2002b, and Cheng et al. 2002c). The laboratory test techniques that have been developed in the past to measure the moisture sensitivity of asphalt mixtures do not provide good correlation between the results obtained by these tests and the field performance of asphalt mixtures (Birgisson et al. 2005, Solaimanian et al. 2003) as, they do not focus on measuring the fundamental material properties related to adhesion and cohesion and hence cannot explain the cause of poor and good performance. Researchers believe that the surface energy technique can correctly predict the moisture susceptibility of an asphalt mixture (Bhasin et al. 2006). However, because of the complex nature of the asphalt material and the fact that the surface energy properties of the material can be considerably different than its bulk chemistry (Kim, 2009), it is not that straight forward.

A complete characterization of the surface energy technique can be done if the results obtained by this technique are compared with that of some mechanical tests. Tests like AASHTO T-283 and SATS are considered good for the comparative analysis of moisture susceptibility of various mixtures (Airey et al., 2007). Considering this, SATS technique along with the dynamic mechanical analysis has been chosen to compare the surface energy results with the mechanical parameters obtained by these tests.

1.3 Research Objectives and Deliverables

Lack of compatibility between the constituent bitumen and aggregate is one of the main causes of moisture damage in an asphalt mixture. Bitumen film is removed from the surface of aggregates in the presence of water because of weak adhesive bond between the two materials. According to the literature, the physico-chemical characteristics of bitumen and aggregates are mainly responsible for the adhesion between the two materials. Surface energy properties of the two materials are used to assess the adhesion between these materials which is then related to the moisture sensitivity of the resulting asphalt mixture.

The main objectives of this research are to:

- Set up experimental devices for the measurement of surface energy properties of bitumen and aggregate.
- Perform surface energy analysis with different bitumen and aggregate samples and develop detailed experimental testing protocols for the determination of surface energy properties of bitumen and aggregate.
- Combine surface energy testing techniques with a mechanical moisture sensitivity assessment technique for identification of compatible bitumen-aggregate combinations. This will be achieved by:
 - Using SFE to determine dry and wet adhesion parameters and dry/wet bond ratios
 - Determining moisture damage parameter for asphalt mixtures from SATS test, and
 - Establishing correlations between adhesion ratios and moisture damage parameters obtained from SATS test.

This research will contribute towards the better understanding of the moisture susceptibility of the asphalt mixtures. Developed testing protocols will help users to effectively and efficiently determine the surface energy properties of the bitumen and the aggregates. Adhesive bond strength of an asphalt mixture calculated from the surface energy properties of the constituent bitumen and aggregate can be used to compliment available mixture design methods by identifying compatible bitumen-aggregate combinations. Surface energy properties of the materials combined with the

parameters obtained by conventional moisture sensitivity assessment techniques can also contribute towards the development of a material screening protocol for determining the best combinations of bitumen and aggregates for the local road material providing better bitumen-aggregate adhesion and less susceptibility to moisture damage/stripping.

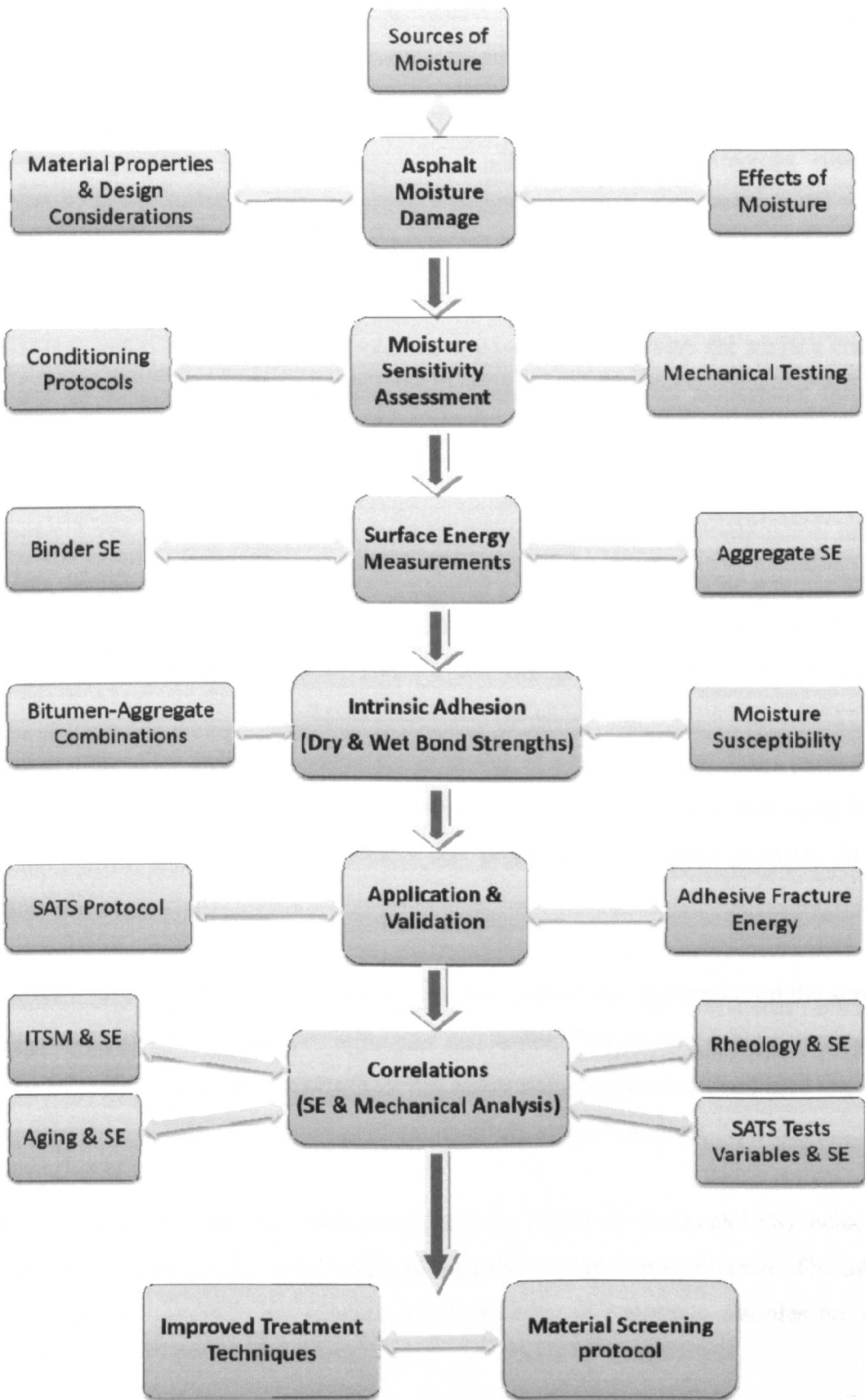
1.4 Research Methodology

In order to attain the research objectives, the following main tasks were undertaken:

- A detailed review of the published research literature on moisture sensitivity assessment of asphalt mixture was done with particular review of:
 - Moisture sensitivity evaluation techniques
 - Chemistry of bitumen-aggregate interaction
 - Bitumen-aggregate adhesion testing techniques
 - Surface energy characteristics of the bitumen and aggregate, and methods to measure surface energy values
- Commissioning of the surface energy equipment was carried out.
- Sample preparation techniques and testing procedures were developed with the newly installed equipment for obtaining the surface energy properties of the bitumen and the aggregates.
- Surface energy testing of different bitumen and aggregate samples was carried out. The surface energy properties of the two materials were then combined together to predict the moisture sensitivity of the resulting asphalt mixture.
- SATS protocol was selected to study the applicability of the surface energy technique. Material recovered from the SATS cores were tested for their surface energy properties. Recovered binders were also tested for the rheological properties. The results obtained for the recovered material were then compared with the ones obtained from the virgin material. Different types of materials and SATS test conditions were used to study and correlate the obtained results.

A brief outline of the thought process behind this research is provided in the following chart:

Flow Chart



1.5 Thesis Outline

The thesis has been divided into nine chapters.

Chapter 1 provides a background to the asphalt mixture moisture damage problem and relevant importance of bitumen-aggregate adhesion. It also presents research objectives and scope along with a brief outline of the research methodology.

Chapter 2 presents a literature review on moisture damage of asphalt mixture, and moisture sensitivity and adhesion testing techniques. It also covers the surface energy concept of bitumen-aggregate adhesion and moisture sensitivity assessment through this theory.

Chapter 3 covers the work that has been carried out for the determination of the surface energy properties of the bitumen samples by using Goniometer and Wilhelmy plate techniques, and the development of the experimental testing protocols for each equipment. The detailed test procedures are provided in the appendices of this thesis.

Chapter 4 provides with the surface energy testing of aggregates and fillers carried out by using dynamic vapour sorption and microcalorimeter techniques, with main focus on the former technique. The detailed test procedures are again provided in the appendices.

Chapter 5 discusses the moisture sensitivity of an asphalt mixture based on the surface energy components of bitumen, aggregate and water. The surface energy parameters of the bitumen and the aggregates from the above two chapters are combined together to assess the moisture susceptibility of the resulting asphalt mixture.

Chapter 6 discusses the use of Saturation Ageing Tensile Stiffness (SATS) technique for mechanical assessment of moisture susceptibility of an asphalt mixture. The SATS test results for two different binders and four different aggregate samples are also provided.

Chapter 7 combines the retained saturation values determined through the SATS test with the rheological properties of the virgin and the SATS recovered binder in order to determine the moisture sensitivity factors for the SATS tested materials.

Chapter 8 presents surface energy data of bitumen and aggregates for both the virgin and SATS recovered material. The bond energy ratios for the available bitumen-aggregate combinations are then correlated with the SATS data.

Conclusions from this research and recommendations for the future work are outlined in Chapter 9.

CHAPTER 2

LITERATURE REVIEW

2.1 Introduction

This chapter is divided into three main parts. The first two parts provide a summary of asphalt mixture moisture damage, moisture sensitivity assessment and bitumen-aggregate adhesion testing. The third part discusses the concept of bitumen-aggregate adhesion, surface energy and related theories.

2.2 Moisture Damage

Water is the worst enemy of asphalt pavements. The presence of water (or moisture) often results in premature failure of pavements in the form of isolated distress caused by debonding of the bitumen film from the aggregate surface or early rutting/fatigue cracking due to reduced mixture strength (Lu and Harvey, 2007). Moisture sensitivity has long been recognized as an important mixture design consideration. Francis Hveem, in 1940, realized the importance of water resistance and identified it as a critical engineering property that needs to be determined in the selection of quality material for pavement construction (Santucci, 2002).

Moisture sensitivity is primarily concerned with the potential for loss of adhesion between the binder and aggregate in the presence of moisture, commonly called stripping. Critical situations leading to stripping largely relate to the extent of moisture saturation in the asphalt mixture and level of traffic stress, which can be avoided by considering the pavement design, mixture design and construction factors that can lead to this moisture saturation. Sensitivity to moisture damage in a particular asphalt mixture is further influenced by the characteristics of component materials, particularly the type and proportion of aggregates, filler and binder. The detrimental effects of moisture damage are required to be minimized to achieve the goal of perpetual pavements.

The susceptibility of road material (aggregate & bitumen) to moisture damage is dependent on the interfacial characteristics of the material and is determined by using the surface energy characteristics of the material (Airey et al., 2007).

2.3 Sources of Moisture

An asphalt pavement is exposed to several cycles of precipitation during its service life. Sources of moisture in an asphalt pavement can be either internal or external.

2.3.1 Internal

Moisture is left inside the pavement before construction in the form of inadequately dried aggregate (Santucci, 2002). Also, if water comes in contact with hot bitumen it is converted into steam and its volume increases which can result in foaming and boil-over of hot bitumen (Read and Whiteoak, 2003). Warm mix technologies can be more prone to this type of phenomenon.

2.3.2 External

The following three can be considered as the external sources of moisture:

- Moisture entering the pavement from surface because of poor drainage, poor construction (compaction) or mixture design having high air voids and thus more permeability.
- Moisture entering from sides because of poorly constructed shoulders and poor side drainage.
- Moisture from beneath the subgrade because of high water table and poor drainage characteristics of base and subbase material.

Figure 2.1 below illustrates different sources of moisture in a pavement structure.

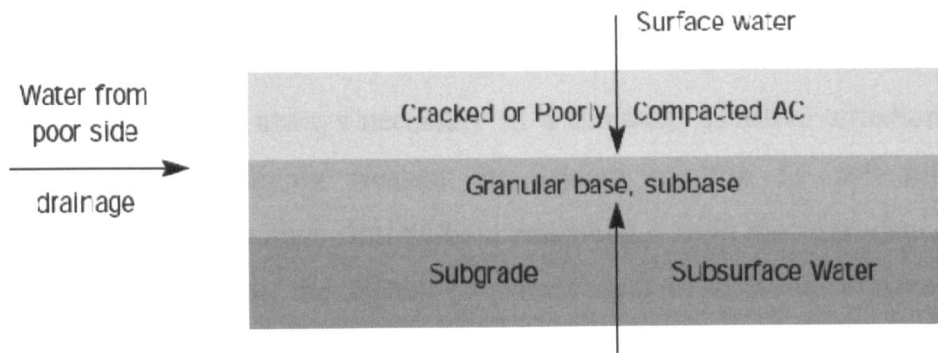


Figure 2.1: Sources of Water in an Asphalt Pavement (Santucci, 2002)

2.4 Types of Moisture Damage

Presence of moisture either causes certain types of pavement distresses and/or increases the severity of already existing distresses.

Pavement distresses that are directly caused by moisture damage include:

- *Stripping*
Adhesive failure between the bitumen film and aggregate surface results in debonding which, in an advanced state, is identified as “stripping”. Stripping converts a high strength asphalt treated pavement layer to a much weaker untreated aggregate section. When it occurs in isolated spots throughout the pavement, it can rapidly develop into potholes.
- *Corrugations*
- *Raveling and weathering*
- *Water pumping*

Moisture increases the severity of the following already existing damages:

- *Potholes*
- *Premature Fatigue Cracking/Rutting*
Over more extensive areas, premature fatigue cracking or rutting may develop due to the reduced support strength of the overall pavement structure.

Some of the common moisture induced damages are shown in Figure 2.2.

Debonding is not always necessary in a moisture sensitive situation. Water in the pavement may simply weaken the asphalt mixture by softening or partially emulsifying the bitumen film without removing it from the aggregate surface. During this weakened state, the asphalt pavement layer is subjected to accelerated damage from applied traffic.



Fatigue Cracking



Stripping



Pothole



Rutting

Figure 2.2: Pavement Distresses

2.5 Effect of Moisture Damage

Probably the most damaging and often hidden effect of moisture damage is associated with reduced pavement strength. The higher vertical compressive stress in the moisture-damaged pavement can result in overstressing the underlying pavement layers and ultimately can create excessive permanent deformation or rutting in the wheel paths on the pavement surface. Higher tensile (bending) strains at the bottom of the treated pavement layer can translate into earlier than expected fatigue failure as

shown in Figure 2.3. The higher bending strain, ϵ_2 , associated with the moisture damaged pavement produces a much lower predicted fatigue life, N_2 , than the bending strain, ϵ_1 , associated with the dry asphalt pavement structure.

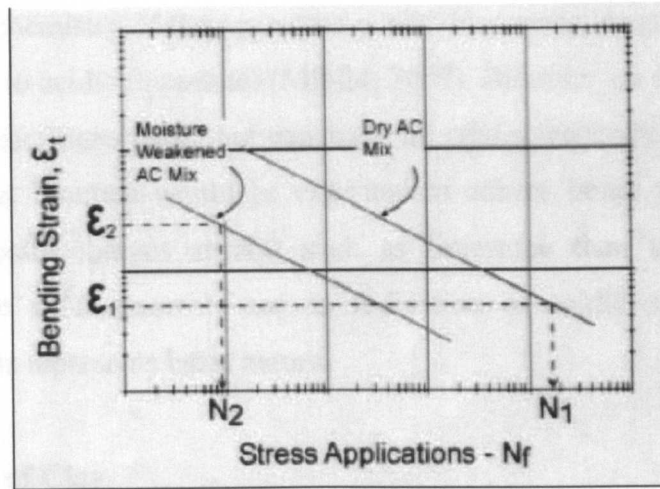


Figure 2.3: Moisture Effect on Fatigue Response (Santucci, 2002)

2.6 Factors Effecting Moisture Sensitivity

Bitumen and aggregates are the main constituents of an asphalt mixture. Aggregates make up roughly 95% by mass of a dense graded asphalt mixture with the binder being the remaining 5%. Thus the type/source of bitumen and aggregates used, and their surface characteristics play a significant role in an asphalt mixture's resistance to water action. Asphalt mixture moisture susceptibility can be influenced by factors like physical properties of the materials, design considerations and construction quality.

2.6.1 Aggregate physical properties

Physical properties of the aggregate, such as shape, surface texture and gradation, influence the bitumen content of the mixture and hence the bitumen film thickness. Thick films of bitumen resist the action of water better than thin films (Santucci, 2002). Rough surface textured aggregates help promote better mechanical adhesion at the bitumen-aggregate interface.

2.6.2 Aggregate Chemistry

Aggregates normally consist of inorganic (mineral origin) polar compounds and their properties vary depending upon the source and type of rock with which they are formed. Surface chemistry of the aggregate is also important. Aggregates range from basic (limestone) to acidic (quartzite) (MS-24, 2007). Bitumen, on the other hand, has relatively few basic ingredients, but can have an acidic tendency depending on the source. Therefore, bitumen would be expected to adhere better to alkaline (basic) aggregates (opposite charges attract) such as limestone than to acidic siliceous aggregates. More silica contents are an indication of acidic nature while more carbonate contents represents basic nature.

2.6.3 Presence of Clay

Clay, either in the form of fine aggregate or as a thin coating over the larger aggregate particles, can create a major problem with moisture sensitivity. Clay expands in the presence of moisture and acts as an effective barrier to the adhesion of bitumen to the aggregate surface.

2.6.4 Bitumen Properties

Bitumen consists of mostly hydrocarbons. They are non-polar materials (though a small percentage of hydrocarbons are also polar) but contain certain amount of polar organic compounds. These polar organic compounds can have an acidic or basic nature. The examples of acidic compound in bitumen are carboxylic acids. The acidic value of bitumen normally ranges from 1.5-5 mg KOH/g while the basic value ranges from 0-1 mg KOH/g (MS-24, 2007). This is an indication that bitumen is mostly acidic.

Bitumen properties also play a role in the moisture sensitivity of asphalt pavements. Complete coating of the aggregate surface during mixing is critical and is affected by the viscosity of the bitumen, which, in turn, is controlled by the mixing temperature used in a hot mix plant. Bitumen film thickness is influenced by bitumen viscosity as well as the use of additives such as polymers or rubber. The source of the bitumen (or

how it is produced in a refinery) can have some effect on its moisture sensitivity in an asphalt mixture.

2.6.5 Bitumen-Aggregate Interactions

As bitumen is mostly acidic in nature, it adheres well with the aggregates having basic characteristics like limestone. The calcium carbonate in the limestone reacts with carboxylic acid in bitumen and forms a strong bond. On the other hand, as siliceous aggregate also has acidic nature, no chemical bond is formed between the bitumen and aggregate. Water, being polar in nature, can easily replace the bitumen from the aggregate surface.

The above explanation, however, is not always true as the material surface properties may be different than its bulk chemistry (Kim, 2009). Also, because of the complex chemistry of the bitumen it is not possible to get similar results with even similar types of binders. In order to fully characterize the moisture susceptibility of a certain material, a lot of surface energy testing in conjunction with mechanical moisture sensitivity assessment is required to be done. It is also important to study the chemistry of the materials in detail.

2.6.6 Factors other than Material Properties

The primary construction issue that needs to be addressed in making asphalt pavements more moisture resistant is adequate compaction during construction. Better compaction of dense graded asphalt mixture leads to lower air void content and lower permeability of the completed pavement. Both factors reduce the ability of external moisture from entering the pavement.

2.7 Moisture Damage Mechanisms

Several theories have been proposed to describe the mechanisms of moisture damage. An asphalt pavement is exposed to moisture throughout its service life especially in the areas which have large amounts of rainfall throughout the year. Kringos and

Scarpas (2005) have explained the following three main phenomenon of moisture damage.

2.7.1 Advective flow through an Asphalt Mixture

This is a short term phenomenon in which the direct contact of moving water with an asphalt mixture causes desorption of the outer layer of bitumen film. Water washes away the bitumen film layer by layer.

2.7.2 Diffusion Leading to Bitumen-Aggregate Interface Failure

Diffusion is the homogenization of the chemical components of a phase at an atomic or molecular level. Water reaches the bitumen-aggregate interface through this phenomenon and replaces the bitumen film from the aggregate surface. This adhesive failure at bitumen-aggregate interface largely depends on the chemical characteristics of the two materials.

2.7.3 Diffusion causing Dispersion of the Bitumen Film

Amount of diffusion of water in the bitumen film increases with the passage of time until the bitumen particles loose cohesion and dispersion of the bitumen film occurs. This phenomenon largely depends on the individual properties of the bitumen and the level of exposure to water.

Following are some other mechanisms that cause the moisture damage to an asphalt pavement.

2.7.4 Emulsification of the bitumen film can occur in a pavement due to the presence of emulsifying agents in the aggregate such as clay particles. Traffic provides the action needed to promote emulsification. The resulting emulsion may migrate to the pavement surface and produce localized fat spots (MS-24, 2007).

2.7.5 Pore pressures can build up in an asphalt pavement due to the action of traffic in the presence of moisture. These pressures alternating between compression and tension can result in a debonding of the bitumen from the aggregate or raveling of the pavement surface. Freezing of water present in the pavement also has the same effect

as expansion of entrapped water and can seriously damage the pavement (MS-24, 2007).

2.8 Moisture Sensitivity Assessment

Durability of an asphalt pavement decreases with the passage of time because of ageing and moisture exposure. A moisture damaged pavement cannot efficiently support the traffic induced stresses and strains because of reduction in its strength. Numerous laboratory tests have been developed over the years in an effort to predict the moisture sensitivity of asphalt mixtures.

In order to avoid premature failure of road pavements, related to the bitumen-aggregate adhesion characteristics, it is very important to devise a laboratory test which could predict the moisture sensitivity of an asphalt mixture.

An extensive literature review on moisture sensitivity test methods for bituminous pavement materials has been carried out by Airey and Choi (2006). Moisture sensitivity tests are carried out on loose coated aggregates or asphalt mixtures. Different conditioning processes are used to simulate the field exposure conditions and the conditioned specimens are then inspected visually or mechanically for moisture sensitivity evaluation.

A summary of different bitumen-aggregates adhesion/moisture sensitivity assessment testing techniques is provided below.

2.8.1 Tests on Loose Coated Aggregate

These types of tests involve the following steps:

- i) Immersion of loose compacted mixture in water or chemical solution
- ii) Immersion is done for specified time at room or elevated temperature
- iii) Separation of bitumen from aggregate is assessed visually

Correlation with field: little information is available to correlate data with field performance.

Types of Tests

- i) Static Immersion Test (AASHTO T182, ASTM D1664)
- ii) Dynamic Immersion Test
- iii) Chemical Immersion Test (by use of sodium carbonate)
- iv) Rolling Bottle Method
- v) Boiling Water Test (ASTM D3625)
- vi) Ancona Stripping Test
- vii) Boiling Water Stripping Test
- viii) Ultrasonic Method
- ix) Net Adsorption Test (SHRP, M001)
- x) Modified Net Adsorption Test

Summary of some of the commonly used techniques is provided as follows;

Static immersion tests

In this test aggregates are coated with bitumen and are then immersed in water. After a certain period of time, visual inspection is made to assess the degree of stripping. It is considered as the simplest test. The example is AASHTO T182 (ASTM D1664); 'coating and stripping of bitumen-aggregate mixtures'.

Dynamic immersion tests

The only difference between a static and dynamic immersion test is that the sample is agitated mechanically by shaking or kneading in the later type.

Chemical immersion tests

Aggregates coated with bitumen, are boiled in solutions of sodium carbonate with varying concentrations of the chemical. The strength of solution which first causes stripping is related to the adhesion strength between the two materials.

Boiling water tests

This test involves the visual observation of the loss of adhesion in un-compacted bituminous coated aggregate mixtures due to the action of boiling water. The example is ASTM D3625; 'effect of water on bituminous-coated aggregate using boiling water'.

2.8.2 Tests on Compacted Asphalt Mixtures

These involve the following major steps:

- i) Samples are prepared in laboratory or cored from the field
- ii) Conditioning of samples to simulate in-situ condition
- iii) Tests are performed to calculate strength or stiffness
- iv) Assessment of moisture damage is made by calculating ratio of conditioned to unconditioned/wet to dry strength

Correlation with field: sometimes provides good correlation between laboratory tests and field results, but not always reliable (Airey and Choi, 2006).

These types of tests are further divided into three major categories;

(A) Immersion Mechanical Tests

Change in mechanical property of a mixture after immersion in water is measured. Measured mechanical properties are usually indirect tensile stiffness and indirect tensile strength.

Tests Types

- i) Texas Freeze-Thaw Pedestal Test
- ii) Immersion Compression Test (AASHTO T165, ASTM D1075)
- iii) Marshall Stability Test (AASHTO T245)
- iv) Duriez Test (NFP 98-251-1)
- v) Lottman Test
- vi) Tunncliff and Root Procedure
- vii) Modified Lottman Procedure (AASHTO T283)

viii) LINK Bitutest Water Sensitivity Protocol

(B) Immersion Wheel Tracking Tests

These tests incorporate aspects of repeated traffic loading in their procedures.

Tests Types

- i) Immersion Wheel Tracking Test
- ii) Hamburg Wheel Tracking

A summary of the above mentioned test techniques is provided below.

Immersion mechanical tests

A compacted asphalt mixture specimen is immersed in water and is tested for a specific mechanical property. The results are compared to the original mechanical property, in normal conditions. Any change in the mechanical property after immersion in water is related to the stripping potential of the material. The ratio of the two results, expressed in percentage, is used as an indirect measure of stripping.

The mechanical properties that can be measured include shear strength, flexural strength and compressive strength. The two most common are known as the retained Marshall Stability test (AASHTO T245) and the retained stiffness test using Nottingham Asphalt Tester (NAT). Other examples include AASHTO T165 (ASTM D1075); ‘immersion compression test’, ASTM D4867; ‘indirect tension test with moisture saturation only’ and AASHTO T283; ‘indirect tension test with moisture saturation and one freeze-thaw cycle’.

A new adhesion testing fixture has been developed by Fini et al. (2006) of the Illinois Center for Transportation to assess bituminous crack sealant-aggregate adhesion, utilizing the Direct Tension Tester (DTT). The briquette assembly consists of two half-cylinders of aggregates having 25mm diameter and 12mm length. The assembly (shown in Figure 2.4) has a half cylinder mold, open at the upper part. Prior to pouring the sealant, the assembly is heated to facilitate sealant flow and to ensure a uniform bonding area. The aspect ratio of the sealant is maintained as 1. After 1h of

curing, the specimen is trimmed and kept in the DTT cooling bath for 30 minutes before testing.

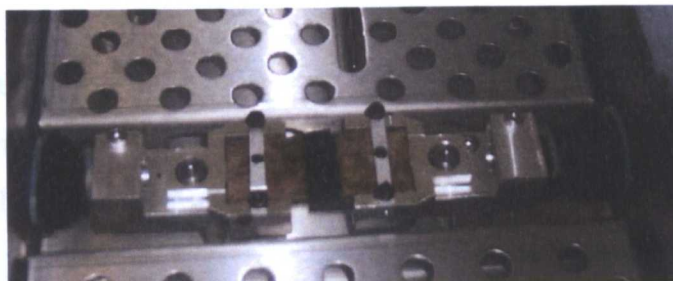


Figure 2.4: Adhesion Test Fixture (Fini et al., 2006)

Immersion trafficking tests

The main problem with most of the above mentioned tests is that they do not consider the effect of trafficking on stripping. Immersion wheel tracking test (AASHTO T324) has been developed to overcome this problem. In this test, a specimen is immersed in a water bath and is tested by a loaded solid rubber or steel tyre. The tyre forms a rut on the surface of specimen. Development of the rut is measured until stripping starts. The most popular type of wheel trafficking equipment is the Hamburg wheel tracking device and is shown in Figure 2.5.



Figure 2.5: Hamburg Wheel Tracker

(C) Environmental Conditioning System (AASHTO TP 34)

An environmental conditioning system consists of three main components;

- Fluid conditioning system
- Loading System
- Environmental conditioning system

Fluid conditioning system is used to condition the specimen and determine their permeability. The loading system consists of a tri-axial cell which serves as a loading frame and the samples are tested in an un-confined tri-axial configuration. The resilient modulus and permeability values obtained in dry conditions are compared to the values after conditioning. Results obtained from this test do not correlate well with the results obtained from field cores (Airey and Choi, 2006).

The shortcoming of most of the above mentioned methods is that only one discrete point/result is obtained from each test. In order to get a more realistic picture of the overall trend of failure, a large number of tests are required to be performed for a range of conditions. Conditioning of samples is done to get a desired saturation level for better field simulation. The freeze-thaw cycle method is used in some of the tests and, because of its severity, is considered to better simulate field conditions but it may cause film rupture damage and thus may not be a true representation of the original condition (Airey and Choi, 2006).

Some of the other popular bitumen-aggregate adhesion testing techniques are provided in the following sections.

Coating tests

This test is used to assess adhesion between aggregate chippings and bitumen. Examples are ASTM D5100; 'adhesion of mineral aggregate to hot bitumen' and 'immersion tray test' (<http://www.highwaysmaintenance.com/SDdata.html>, 2007). In the immersion tray test aggregate chippings are applied to a tray of bitumen covered

with a layer of water. Careful examination of chippings is carried out to check the effect of water on the adhesion.

Adsorption tests

These tests combine the measurement of bitumen-aggregate adhesion with a measure of moisture sensitivity. The examples are; 'net adsorption test' and 'modified net adsorption test' (Read and Whiteoak, 2003). Net adsorption test uses a screening procedure for selecting bitumen and aggregates, as well as determining the effectiveness of anti-stripping additives, as part of the Superpave mix design method. The test is based on the measurements of fundamental physical-chemical relationships of the amount of solute (bitumen) adsorbed from a solution onto the adsorbent (aggregate). This is accomplished by measuring the amount of bitumen dissolved in toluene that is adsorbed onto the aggregate surface followed by the amount which is desorbed (removed) by the addition of water to the system.

Impact tests

Two types of impact tests are used to assess the adhesive characteristics of bitumen, i.e. the Vialit pendulum test and the Vialit plate test.

In the Vialit plate test, shown in Figure 2.6, aggregate particles are pressed onto a tray of bitumen (<http://www.highwaysmaintenance.com/vialit.htm>, 2007). The tray is overturned and a steel ball is dropped on the inverted plate. The impact of the ball causes the removal of the aggregate particles from the bitumen tray. The number of detached aggregate particles in relation to the number of impacts may be used as an indication of bond strength. Detached aggregates are visually inspected to check the type of failure.



Figure 2.6: Vialit Plate Test

(<http://www.highwaysmaintenance.com/vialit.htm>, 2007)

Numerous testing techniques are being used by the adhesive manufacturing industries to determine the bond strength of adhesives. These techniques could also be considered to measure bitumen-aggregate adhesion. Some of the useful test techniques are identified as under:

Double Cantilever Beam

Double cantilever beam (ASTM D3433) is a widely used test in the area of structural adhesives and consists of two beams between which a film of bitumen is sandwiched (Figure 2.7). The force required to initiate a crack when the two beams are pulled apart is related to the strength of the bond, and fundamental fracture mechanics properties can be obtained from the test data (SHRP-A-369).

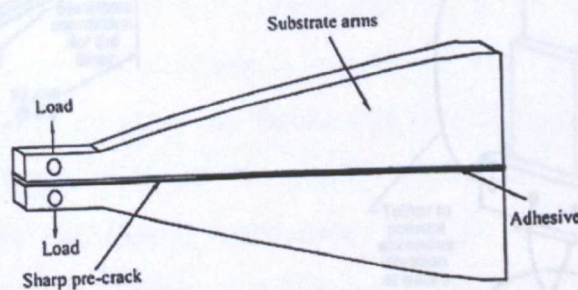
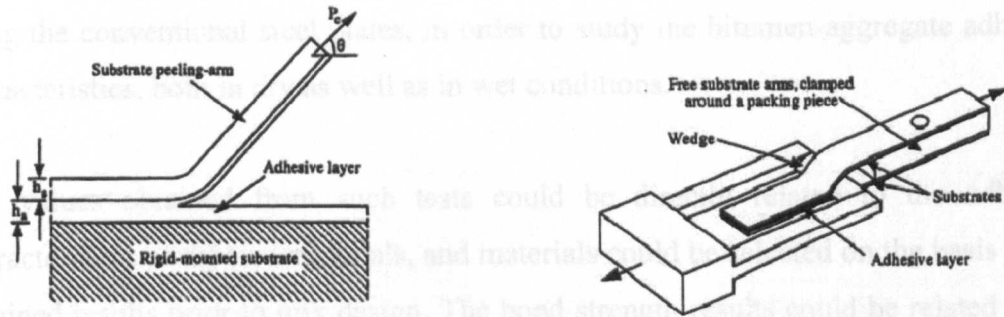


Figure 2.7: Sketch of the Tapered Double Cantilever Beam Specimen

(Kinloch, A.J. 2002)

Peel test

The peel test (ASTM D1876, D3330) is widely used in industry for measuring the adhesion of a very wide range of bonded joints and laminates (Kinloch, 1997). Schematic of a typical peel test and impact wedge peel joint specimen is shown in Figures 2.8(a) and 2.8(b) respectively.



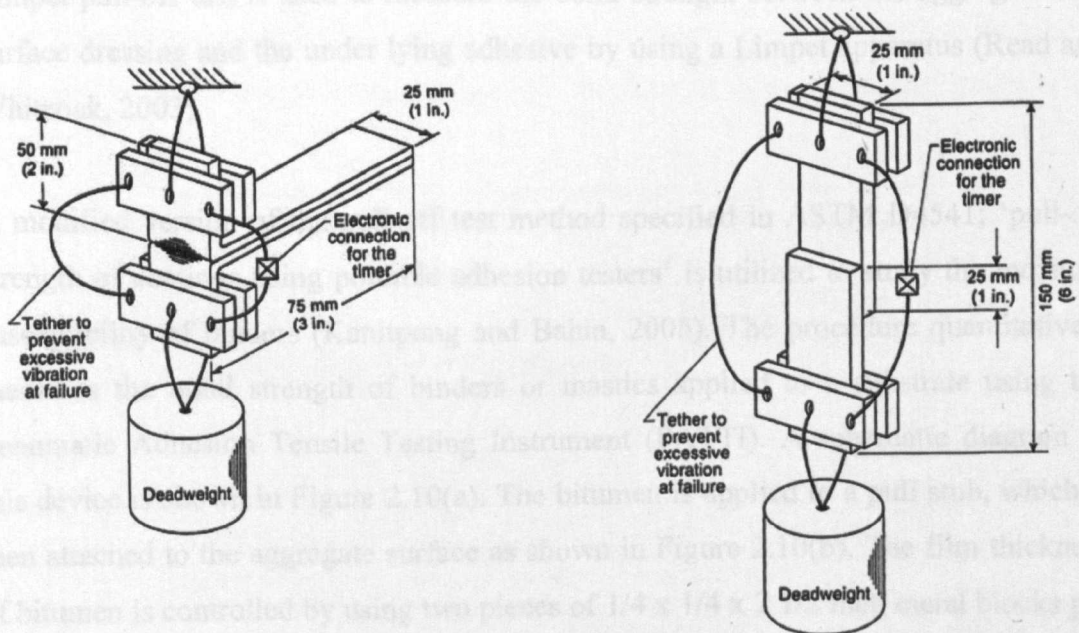
(a): Typical peel joint specimen (b): Impact wedge peel joint specimen

Figure 2.8: Peel Test (Kinloch, 1997)

2.8.3 Latest Advancements

Time-to-failure (creep-rupture) tests of joints (ASTM D-5405)

This test method covers laboratory determination of the time-to-failure (creep-rupture) of joints fabricated from non-bituminous organic roof membrane material. The test method covers both T-peel (Figure 2.9(a)) and lap-shear joints (Figure 2.9(b)) subjected to constant tensile load under controlled environmental conditions.



(a): Schematic of a T-Peel specimen (b): Schematic of a Lap-Shear specimen

Figure 2.9: Time-to-Failure (Creep-Rupture) Test (ASTM D-5405, 2004)

The above summary has been prepared to look into the possibility of developing an adhesion measurement technique which could directly give a bond strength value between bitumen and aggregate.

The technique developed by Fini et al. (2007) for a blister test could be used to prepare aggregate discs. The prepared discs could then be used in a DSR, instead of using the conventional steel plates, in order to study the bitumen-aggregate adhesion characteristics, both in dry as well as in wet conditions.

The values obtained from such tests could be directly related to the adhesion characteristics of the two materials, and materials could be selected on the basis of the obtained results prior to mix design. The bond strength results could be related to the surface energy characteristics of the bitumen and aggregate.

2.8.3 Latest Advancements

Pull-off tests

Bitumen adhesion is also assessed by using different types of pull-off tests. The Instron pull-off test is used to remove the aggregate specimens from the bitumen under controlled laboratory conditions by using an Instron apparatus. Similarly, the Limpet pull-off test is used to measure the bond strength between the aggregate of a surface dressing and the under lying adhesive by using a Limpet apparatus (Read and Whiteoak, 2003).

A modified version of the pull-off test method specified in ASTM D4541; 'pull-off strength of coatings using portable adhesion testers' is utilized to study the moisture susceptibility of binders (Kanitpong and Bahia, 2005). The procedure quantitatively measures the bond strength of binders or mastics applied to a substrate using the Pneumatic Adhesion Tensile Testing Instrument (PATTI). A schematic diagram of this device is shown in Figure 2.10(a). The bitumen is applied to a pull stub, which is then attached to the aggregate surface as shown in Figure 2.10(b). The film thickness of bitumen is controlled by using two pieces of 1/4 x 1/4 x 2 1/2 inch metal blocks put under the pull stub. The space underneath the pull-stub and aggregate surface is the film thickness of bitumen specimen. The PATTI transmits the air pressure to the

piston, which is placed over the pull stub and screwed on the reaction plate (Figure 2.10(a)). The air pressure induces an airtight seal formed between the piston gasket and the aggregate surface. When the pull stub is debonded from the aggregate surface, the pressure at which the cohesive or the adhesive failure occurs is measured and converted to the pull-off strength (kPa).

The pull-off strength can be used as an indicator of the adhesive bond strength of the bitumen.

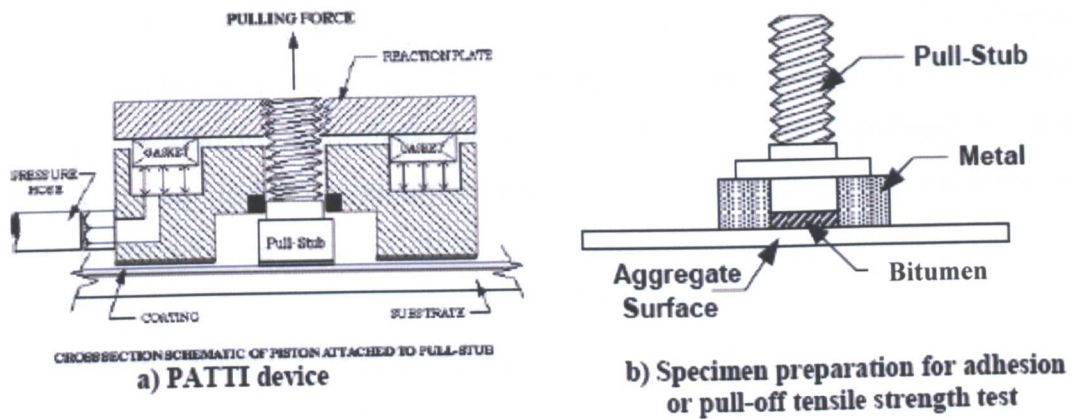


Figure 2.10: Pneumatic Adhesion Tensile Testing Instrument
(Kanitpong and Bahia, 2005)

Blister test

This test consists of a coating of bitumen over a flat aggregate surface. A hole, drilled through the aggregate under the coating, permits the application of steady or varying fluid pressure to the underside of the coating as shown in Figure 2.11. Adhesion is measured by the force required to displace the film from the aggregate (Fini et al., 2007).

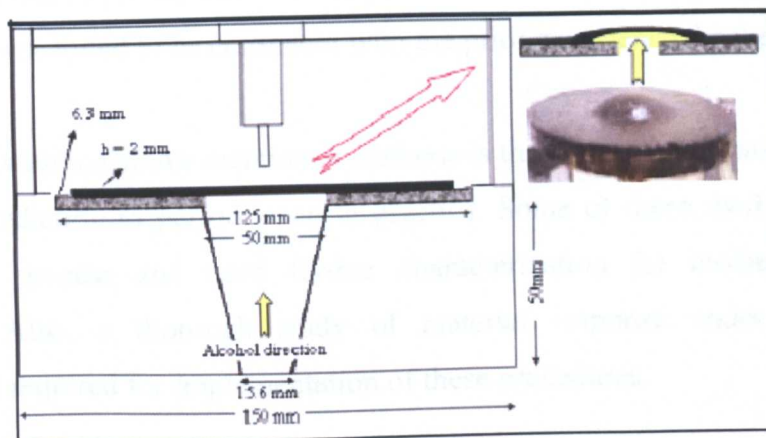


Figure 2.11: A Schematic of Blister Apparatus
(Fini et al. 2007)

It is not always possible to have the best bitumen-aggregate combinations, as it depends a lot on the availability of type of road aggregates on the site. Different treatment techniques are being used by the industry in order to improve the bitumen-aggregate adhesion characteristics. Irradiation is supposed to increase the wettability of the aggregates and could be used as an aggregate treatment technique in order to improve the bitumen-aggregate adhesion.

Beam Fatigue Test

Lu and Harvey (2007) developed a fatigue-based test procedure for moisture sensitivity assessment of different asphalt mixtures. A controlled-strain flexural beam fatigue test is used to study these moisture effects. Tests are performed at 10 Hz loading frequency, and 200 $\mu\epsilon$ strain level with specimens pre-saturated at 635 mm-Hg vacuum for 30 minutes.

The following parameters are used for sample preconditioning:

Moisture Content: low (20-30 percent saturation) and high (50-70 percent saturation).

Conditioning Temperature: 25°C and 60°C

Conditioning Duration: one day and ten days

Lu and Harvey compared the results from this fatigue test with the results obtained from both the TSR (Tensile Strength Ratio) test and the HWTD (Hamburg Wheel Tracking Device) test. Test results showed that the fatigue based test procedure can distinguish mixtures on the basis of their moisture sensitivities. The performance of the mixtures was found to be consistent with the prior experience for these mixtures.

The problem with the above mentioned methods is the lack of information relating the laboratory prediction to performance in practice. Some of these methods are in the development process and need further characterization for moisture sensitivity assessment. Also, a thorough study of material response under variable test parameters is required for implementation of these procedures.

Saturation Ageing Tensile Stiffness (SATS) Test

A new conditioning protocol and testing procedure has been developed by the Nottingham Transportation Engineering Centre (NTEC) known as the Saturation Ageing Tensile Stiffness (SATS) Test, shown in Figure 2.12, to measure the moisture sensitivity of asphalt mixtures.

Airey et al. (2006) used SATS and AASHTO T283 to test high modulus base (HMB) material samples. The relative performance of the two tests was compared in terms of measured retained stiffness modulus of the specimens. The values obtained from AASHTO T283 were approximately double than that produced from SATS for same saturation level. This gives an indication that SATS was more severe on the samples. The drop in the stiffness modulus for samples tested with SATS was due to the combined effect of moisture and air (ageing). The values obtained from SATS testing were comparable to the stiffness modulus values observed on a trial site where HMB material was placed. This gives an indication that SATS probably better simulates the field conditions as compared to AASHTO T283, at least for the set of mixtures that were analyzed.



Figure 2.12: SATS

SATS measures the combined effects of ageing and moisture using the following steps:

- i) Initial saturation of specimen
- ii) Ageing and saturation in a high temperature and pressure environment for extended period
- iii) Calculation of retained saturation
- iv) Calculation of retained stiffness modulus as:

$$\text{Retained stiffness modulus} = \frac{\text{Stiffness modulus after test}}{\text{Stiffness modulus before test}} \quad (1)$$

The SATS and AASHTO T283 procedures provide moisture sensitivity/susceptibility of different mixtures and can be used for correlation with field performance but as they do not assess the fundamental material properties like cohesion and adhesion, they cannot explain the cause of poor and good performance and do not provide any feedback for redesigning poorly performing mixtures (Airey et al., 2007).

In general, the following are desirable for an asphalt mixture to provide better resistance to moisture damage.

- a) Basic aggregate
- b) Low air voids
- c) High binder content to have greater film thickness
- d) Active filler

The above-mentioned properties and the mechanical properties like fracture, healing and viscoelastic properties are required for complete characterization of moisture damage (Airey et al., 2007). These mechanical properties are influenced by binder-aggregate adhesive bond energy along with physical properties like air voids, aggregate shape, etc.

2.9 Surface Energy and Moisture Sensitivity

2.9.1 Background

In an asphalt mixture the primary function of the bitumen is to provide an adhesive layer to bind aggregate particles together. A strong adhesive bond between the aggregate and the bitumen is very important in order to ensure good performance of a pavement.

The bond of bitumen with some aggregates is not strong enough even when they are dry and clean. However, all the aggregates are easily wetted by water, the presence of which results in stripping (Read and Whiteoak, 2003). The reasons for this are the surface/physico-chemical characteristics of both the bitumen and the aggregates and the individual chemical nature of these materials. Different types of aggregates have different chemical characteristics which influences their affinity for bitumen. Aggregates with high silicon oxide content, e.g. quartz and granite (i.e. acidic rocks) are classified as 'hydrophilic' (water loving) and are generally more difficult to coat with bitumen than basic rocks such as limestone.

Aggregates being high surface energy materials possess unbalanced surface charges (Bhasin, 2006). If the aggregate surface is coated with a liquid of opposite charge its surface energy demands are satisfied and the result is a strong adhesive bond. When two different liquids are present, e.g. bitumen and water, the liquid that will best satisfy the energy requirement will adhere more strongly to the aggregate. The stripping of bitumen, from the surface of aggregate in the presence of water, is due to the fact that water, being polar in nature, better satisfies the surface energy demands of aggregates which results in replacement of the bitumen from the aggregate surface (Read and Whiteoak, 2003). The bitumen on the other hand is non-polar in nature and hardly makes any chemical bond with the aggregates, except for having a small/weak acidic character because of the presence of carboxylic acid which makes it possible to bond well with the basic aggregates like limestone.

Because of the varying chemical nature between different bitumen (Read and Whiteoak, 2003), it is not always possible to get a similar type of adhesion even with the same aggregate. Similarly, the surface characteristics of the aggregates vary depending upon the source of the material even if they are made up of similar constituents. It is therefore important to study the surface characteristics of the bitumen and aggregate as well as the interfacial characteristics/adhesion between the two materials in order to predict the moisture susceptibility of the resultant asphalt mixture and/or recommend any material treatments or modifications.

According to thermodynamics, adhesive and cohesive bonds are directly related to surface energy characteristics of bitumen and aggregate. Binder and aggregate adhesive bond parameters, with and without the presence of water, can be studied/calculated for different bitumen, aggregate and filler combinations using the surface energy values of bitumen and aggregate (Cheng et al., 2002).

Using surface energy measurements we may also understand the mechanisms that effect adhesive or cohesive bonds.

2.9.2 Surface Energy Theory

Surface free energy is defined as the amount of energy/work required to create a unit surface area of a material in vacuum.

The presence of free energy on the material surface is the result of the differences in the intermolecular forces acting on the surface molecules as compared to forces acting on the molecules which are in the bulk of the material. The molecules at the surface of a material are attracted towards the bulk of the material. This can be explained with the example of a water droplet. The drop of water falling from a tap takes the shape of a sphere (minimum surface area shape) as the molecules from the surface are attracted inside the bulk of the liquid until the minimum possible surface area is achieved. The molecules at the surface are thus considered to have excess energy because of this difference in intermolecular forces between the surface and bulk of the material, and this energy is referred to as surface free energy. Work is required to be done to bring these molecules on the surface and increase the surface area of the material.

The term 'free energy' is used as it is related to the Gibbs free energy or work done, but not the total energy or enthalpy of the system (Bhasin, 2006). In case of liquids, the term '*surface free energy*' or '*surface energy*' is replaced by '*surface tension*'. In case of solids the reduction in surface area is not evident because of the limited mobility of the solid molecules, but the intermolecular forces still exist.

According to the Good, Van Oss and Chaudhury approach the forces that are responsible for surface energy are divided into two components namely, non polar (dispersive) component and polar component. The dispersive forces are termed as Lifshitz-van der Waals forces and the polar forces are divided into Lewis acid and Lewis base types of forces (Van Oss et al., 1988).

The surface energy, γ , can be given by the following equation:

$$\gamma^{\text{Total}} = \gamma^{\text{LW}} + \gamma^{\text{AB}} \quad (\text{Unit; erg/cm}^2) \quad (2)$$

where,

γ^{LW} = Lifshitz-Van der Waals component

γ^{AB} = Acid-Base component

A molecule is formed as a result of chemical bonding of atoms. In *polar molecules*, the arrangement of atoms is such that one end of the molecule possesses a positive charge while the other end has a negative charge. This is because of un-even distribution of electrons in the orbits or shells which makes them unstable and provides them with a tendency to interact with other polar molecules. While, in *non-polar molecules* the electrons are distributed more symmetrically and thus all the charges cancel out each other. Lifshitz-van der Waals forces are considered to be the non-polar or dispersive forces. These are believed to consist of three main components; London dispersion forces, Debye induction forces and Keesom orientation forces (Kim, 2009 & Rieke, 1997). All these forces represent different types of dipole/induced dipole interactions between neighbouring molecules and electronic shells. These forces between molecules in a material are viewed as residual electrostatic forces.

As mentioned earlier, water and aggregates are polar substances while bitumen is mostly a non-polar material. Thus water has greater attraction for aggregate surfaces than bitumen. Also, most liquids spread on a high energy surface like aggregates.

In polar components, the Acid-Base interactions include electron acceptor-electron donor interactions & hydrogen bonding (Morrison and Boyd, 1983).

According to acid-base theory (Van Oss et al., 1988), the acid-base component can be given as:

$$\gamma^{AB} = 2\left(\sqrt{\gamma^+ \gamma^-}\right) \quad (3)$$

where,

γ^+ = Lewis acid component of surface interaction

γ^- = Lewis base component of surface interaction

Surface free energy dimension corresponds to that of force per unit area i.e. mJ/m² or erg/cm².

In Transportation Engineering we are concerned about the surface energies of bitumen and aggregate, and the effect of these on bitumen-aggregate adhesion in dry and wet conditions.

2.9.3 General Principles

Several theories have been presented in the past in order to describe the adhesion forces between two materials. Thermodynamic theory is the most widely used theory to quantify adhesion between the two materials (Hefer, 2004). The intermolecular forces at the interface of materials are related to the surface energies of the material. As thermodynamic theory is a study of energy changes, the surface energy of a material is explained through Gibbs free energy. Gibbs free energy at constant temperature and pressure is given by the following equation:

Available energy = Gibbs free energy = Enthalpy - Entropy

$$\Delta G = \Delta H - T\Delta S \quad (4)$$

where; ΔH = Enthalpy of the system

T = Temperature

ΔS = Entropy

Enthalpy is the heat content of a system. The tendency of a system is to convert potential energy into work and heat. The amount of heat given off or absorbed during this process is called enthalpy and the increase in randomness of the system is called entropy. Entropy is also considered as amount of heat loss when work is done.

Gibbs free energy can be described as the excess energy of the system associated with the surface and interface and is also referred to as free energy of adhesion or cohesion (Hefer, 2004). As mentioned earlier, surface energy is described as the reversible work required to create a unit surface area of the material. In a reversible process the maximum useful work that can be obtained from a system is equal to the change in Gibbs free energy with a minus sign. So, the work of adhesion can be given by the following equation.

$$W^a = -\Delta G^a \quad (5)$$

In general, systems have a tendency to move towards the minimization of energy for stability. When two objects are strongly bonded to each other they tend to have lower energy (they are at a lower energy state, lower free energy) and more energy is required to separate them (Barton, 1997). In most of the industrial processes mixtures of materials are used (as bitumen-aggregate combination) rather than the single compounds. At the interface between two different materials, the adhesive properties are very important for the existence of that interface.

Adhesion between a solid and liquid can be given by *Dupre's equation* (Adam, 1941):

$$W_{SL} = \gamma_{SA} + \gamma_{LA} - \gamma_{SL} \quad (6)$$

Where S, L and A represents solid, liquid, and air respectively.

When two different types of materials/mediums are involved then surface energy can be referred as the Work of Adhesion while for identical or the same material the energy becomes the Work of Cohesion.

The *work of cohesion* for a material can be given by the following relation:

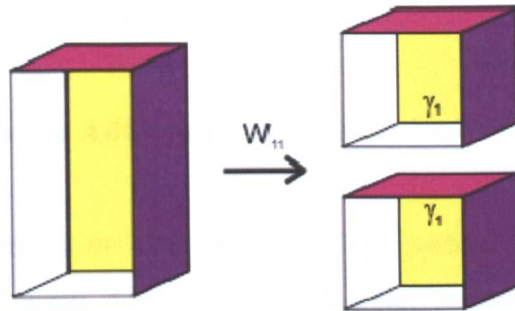


Figure 2.13: Work of Cohesion (Hansen, 2006)

$$\gamma_1 = (1/2)W_{11} \quad (7)$$

$$W_{11} = 2\gamma_1 \quad (8)$$

where; γ_1 = Surface Energy of the material

W_{11} = Work of Cohesion

When two different materials are separated, the energy required to increase the interfacial area between the two materials is given by:

$$\gamma_{12} = \gamma_1 + \gamma_2 - W_{12} \quad (9)$$

The *work of adhesion*, W_{12} , can be given by the following relationship:

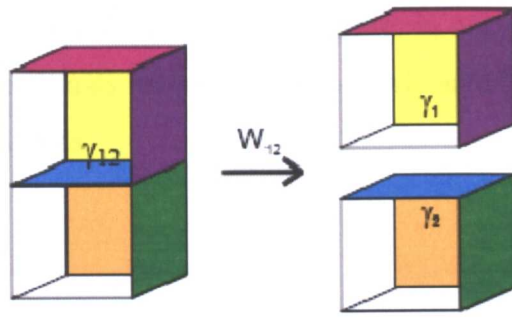


Figure 2.14: Work of Adhesion (Hansen, 2006)

$$W_{12} = \gamma_1 + \gamma_2 - \gamma_{12} \quad (\text{Dupre's equation}) \quad (10)$$

where; γ_1 = surface energy of material 1

γ_2 = surface energy of material 2

2.9.4 Bitumen-Aggregate Adhesion and Moisture Susceptibility

Moisture damage depends on the interaction of surface energy components of aggregate, bitumen and water. The adhesive and cohesive bond strength of a bitumen-aggregate system both in presence of water and without the presence of water on the interface can be calculated using the surface energy concept.

As mentioned earlier, according to Van Oss-Chaudhury-Good theory the surface free energy of a liquid or solid is composed of the Lifshitz van der Waals (LW) and Lewis acid/base (AB) forces and is given as:

$$\gamma = \gamma^{LW} + \gamma^{AB} \quad (11)$$

The acid/base components are further separated into Lewis acid, γ^+ , and Lewis base, γ^- , components.

$$\gamma^{AB} = 2\sqrt{\gamma^+\gamma^-} \quad (12)$$

The bond strength of a material (binder or aggregate; in our case) is the combination of these Lifshitz-van der Waals (non-polar) and Lewis acid/base forces and the total bond strength can be given as:

$$\Delta G = \Delta G^{LW} + \Delta G^{AB} \quad (13)$$

where; ΔG = total bond strength, Gibbs free energy of the material

ΔG^{LW} = Non-polar, Lifshitz-van der Waals component

ΔG^{AB} = Polar, Acid-Base component

The interfacial surface free energy can also be written as a sum of the Lifshitz-van der Waals and Lewis acid/base contributions.

$$\gamma_{BA} = \gamma_{BA}^{LW} + \gamma_{BA}^{AB} \quad (14)$$

The subscripts B and A represents bitumen and aggregate.

The adhesive non-polar bond strength can be determined by using the following equation:

$$\Delta G^{LW} = -\gamma_{BA}^{LW} + \gamma_B^{LW} + \gamma_A^{LW} \quad (15)$$

The adhesive polar strength is given as:

$$\Delta G^{AB} = -\gamma_{BA}^{AB} + \gamma_B^{AB} + \gamma_A^{AB} \quad (16)$$

By using geometric mean relationship the non-polar Lifshitz-van der Waals adhesive bond strength component, γ_{BA}^{LW} , is given as follows (Good-Girifalco-Fowkes combining rule) (Bhasin, 2006):

$$\gamma_{BA}^{LW} = \left(\sqrt{\gamma_B^{LW}} - \sqrt{\gamma_A^{LW}} \right)^2 \quad (17)$$

The polar acid/base adhesive surface energy component, γ_{BA}^{AB} , is given by the equation (Small's combining rule) (Erbil, 2006):

$$\gamma_{BA}^{AB} = 2\left(\sqrt{\gamma_B^+} - \sqrt{\gamma_A^+}\right)\left(\sqrt{\gamma_B^-} - \sqrt{\gamma_A^-}\right) \quad (18)$$

By combining the above two equations (17 & 18), the following relationship is obtained:

$$\Delta G_{BA}^a = 2\sqrt{\gamma_B^{LW} \gamma_A^{LW}} + 2\sqrt{\gamma_B^+ \gamma_A^-} + 2\sqrt{\gamma_B^- \gamma_A^+} \quad (19)$$

The above equation can be used to determine the adhesive bond strength in dry condition.

When there are three materials present on the same interface i.e. in the case of water being present at the bitumen-aggregate interface, then the general formula for the adhesive bond strength on the interface can be given by the following equation:

$$\Delta G_{BWA} = \gamma_{BW} + \gamma_{AW} - \gamma_{BA} \quad (20)$$

The subscripts, B, W and A, represents bitumen, water and aggregate respectively.

The equation for adhesive bond strength with water present on the interface can be given as (Cheng et al., 2002):

$$\begin{aligned} \Delta G_{BWA}^a &= \gamma_{BW} + \gamma_{AW} - \gamma_{BA} \\ &= 2\gamma_W^{LW} + 2\sqrt{\gamma_B^{LW} \gamma_A^{LW}} - 2\sqrt{\gamma_B^{LW} \gamma_W^{LW}} - 2\sqrt{\gamma_A^{LW} \gamma_W^{LW}} \\ &\quad + 4\sqrt{\gamma_W^+ \gamma_W^-} - 2\sqrt{\gamma_W^+}(\sqrt{\gamma_B^-} + \sqrt{\gamma_A^-}) - 2\sqrt{\gamma_W^-}(\sqrt{\gamma_B^+} + \sqrt{\gamma_A^+}) \\ &\quad + 2\sqrt{\gamma_B^+ \gamma_A^-} + 2\sqrt{\gamma_B^- \gamma_A^+} \end{aligned} \quad (21)$$

The above equation can also be written as follows; and is generally used for the calculation of wet bond strength (bitumen-aggregate adhesive bond strength in the presence of water).

$$\begin{aligned}
\Delta G_{BWA}^a = & \left\{ \left(\left(\sqrt{\gamma_A^{LW}} - \sqrt{\gamma_W^{LW}} \right)^2 \right) + \left(2 \times \left(\sqrt{\gamma_A^+} - \sqrt{\gamma_W^+} \right) \times \left(\sqrt{\gamma_A^-} - \sqrt{\gamma_W^-} \right) \right) \right\} \\
& + \left\{ \left(\left(\sqrt{\gamma_B^{LW}} - \sqrt{\gamma_W^{LW}} \right)^2 \right) + \left(2 \times \left(\sqrt{\gamma_B^+} - \sqrt{\gamma_W^+} \right) \times \left(\sqrt{\gamma_B^-} - \sqrt{\gamma_W^-} \right) \right) \right\} \\
& - \left\{ \left(\left(\sqrt{\gamma_B^{LW}} - \sqrt{\gamma_A^{LW}} \right)^2 \right) + \left(2 \times \left(\sqrt{\gamma_B^+} - \sqrt{\gamma_A^+} \right) \times \left(\sqrt{\gamma_B^-} - \sqrt{\gamma_A^-} \right) \right) \right\}
\end{aligned} \tag{22}$$

From the literature, the Lifshitz-Van der Waals component and the acid-base components for the water are given as:

$$\gamma_W^{LW} = 21.8 \tag{23}$$

$$\gamma_W^+ = \gamma_W^- = 25.5 \tag{24}$$

The square roots of these components are as follows:

$$\sqrt{\gamma_W^{LW}} = \sqrt{21.8} = 4.67 \tag{25}$$

$$\sqrt{\gamma_W^+} = \sqrt{\gamma_W^-} = \sqrt{25.5} = 5.05 \tag{26}$$

By replacing the values of surface energy components of water with the respective symbols in equation 22, the following relationship is obtained.

$$\begin{aligned}
\Delta G_{BWA}^a = & \left\{ \left(\left(\sqrt{\gamma_A^{LW}} - 4.67 \right)^2 \right) + \left(2 \times \left(\sqrt{\gamma_A^+} - 5.05 \right) \times \left(\sqrt{\gamma_A^-} - 5.05 \right) \right) \right\} \\
& + \left\{ \left(\left(\sqrt{\gamma_B^{LW}} - 4.67 \right)^2 \right) + \left(2 \times \left(\sqrt{\gamma_B^+} - 5.05 \right) \times \left(\sqrt{\gamma_B^-} - 5.05 \right) \right) \right\} \\
& - \left\{ \left(\left(\sqrt{\gamma_B^{LW}} - \sqrt{\gamma_A^{LW}} \right)^2 \right) + \left(2 \times \left(\sqrt{\gamma_B^+} - \sqrt{\gamma_A^+} \right) \times \left(\sqrt{\gamma_B^-} - \sqrt{\gamma_A^-} \right) \right) \right\}
\end{aligned} \tag{27}$$

The above equation is directly used to measure the bitumen-aggregate adhesion in the presence of water.

2.9.5 Bitumen-Aggregate Bond Energy Ratios

The ratio between the adhesive bond energy values in dry (ΔG_{BA}^a) condition and in the presence of water (ΔG_{BWA}^a) is used to predict the moisture sensitivity of asphalt mixtures. In order to represent the moisture damage by a single value, Bhasin et al. (2006) combined the two bond energy parameters as a dimensionless energy ratio.

$$R^{Total} = R_1 = \left| \frac{\Delta G_{BA}^a}{\Delta G_{BWA}^a} \right| \quad (28)$$

A higher value of energy ratio, R, indicates better resistance to moisture damage for that bitumen-aggregate combination. The energy ratio was then used to study different types of asphalt mixtures and it was concluded that mixtures with a ratio higher than 1.5 were more moisture resistant than the ones with ratios lower than 0.8.

Aggregates with higher surface roughness and greater surface area are supposed to bond well with bitumen by providing more bond area and better interlocking. In order to accommodate this effect, Bhasin (2006) multiplied the bond energy ratio (R_1) with specific surface area (SSA) of aggregates.

Wetting/coating of an aggregate with bitumen is not only affected by the surface properties of the two materials but the viscosity or cohesion of the bitumen itself plays a very important role. Bitumen with lesser cohesion and greater affinity for the aggregates will have a higher wetability property and will coat the aggregate surface more than bitumen having lesser wetability characteristics. However, a softer bitumen having less cohesion may be more prone to emulsification (decrease in cohesion) in the presence of water. Bhasin (2006) modified the above mentioned bond energy ratio by replacing the bond strength in dry condition (ΔG_{BA}) with a wetability relationship ($\Delta G_{BA} - \Delta G_{BB}$). This new moisture sensitivity assessment parameter can be given as:

$$R_2 = \left| \frac{\Delta G_{BA} - \Delta G_{BB}}{\Delta G_{BWA}} \right| \quad (29)$$

where;

ΔG_{BA} & ΔG_{BB} represents bitumen-aggregate dry bond strength and bitumen cohesion respectively.

This bond energy ratio was then multiplied with the square root of the specific surface area of the aggregates in order to accommodate the effects of aggregate micro-texture on the final bitumen-aggregate bond strength (Bhasin, 2006).

These four bitumen-aggregate bond energy parameters (R_1 , $R_1 \times SSA$, R_2 and $R_2 \times \sqrt{SSA}$) are used to assess the moisture susceptibility of the asphalt mixtures. Bhasin (2006) compared the results from these parameters with the laboratory test results for different mixtures. It was concluded that the fourth parameter ($R_2 \times \sqrt{SSA}$) provided best correlation with moisture sensitivity of the mixtures estimated by laboratory testing.

Dupre's relationship (equation 6) and the relationship for the adhesive bond strength in dry condition (equation 19) have been used frequently in the following chapters for the calculation of surface energy parameters of solids (bitumen and aggregates). The bond energy ratio parameters (equations 28 and 29) have been used to assess the moisture susceptibility for different bitumen-aggregate combinations. SATS is the latest and arguably the best mechanical moisture sensitivity assessment technique and therefore has been chosen for this study.

CHAPTER 3

SURFACE ENERGY TESTING OF BINDERS

3.1 Background

As mentioned in the previous chapter, the word ‘*surface tension*’ is used for liquids in place of ‘*surface energy*’. It is a phenomenon referred to as related to liquids. Liquid molecules slide past each other and easily flow throughout the liquid body. The cohesive/intermolecular forces keep the molecules in close proximity. The molecules within a liquid body are attracted from all the sides thus pulling themselves towards each other while the molecules at the top surface of a liquid are attracted by the molecules from inside the liquid body only. As there is no force acting on the top of these molecules an imbalance is created which results in the net movement of top surface molecules inside the liquid body. The result of this is that the top surface of liquid behaves like an elastic stretched layer as shown in Figure 3.1 below.

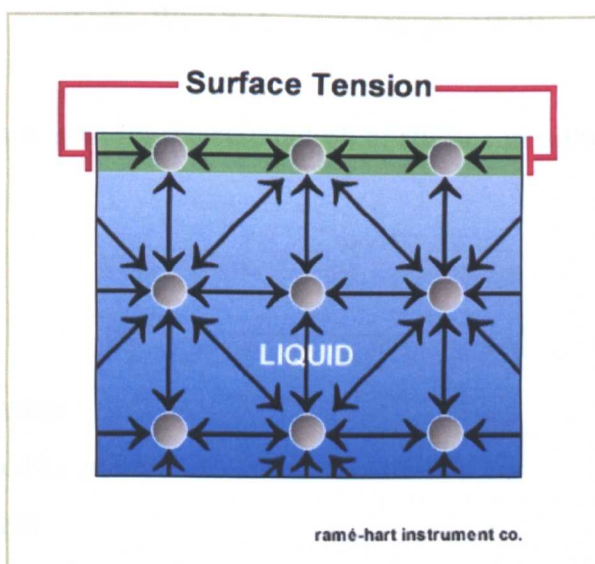


Figure 3.1: Surface Tension

(http://www.ramehart.com/goniometers/surface_tension.htm, 2008)

Surface tension for a liquid can be directly measured with the help of the Wilhelmy Plate Device or Du-Nouy ring method.

Wilhelmy Plate Method

A small rectangular plate of solid (glass or platinum) with known dimensions and thickness is attached with a balance and is immersed vertically in the test liquid, as shown in Figure 3.2, and the related force is measured.

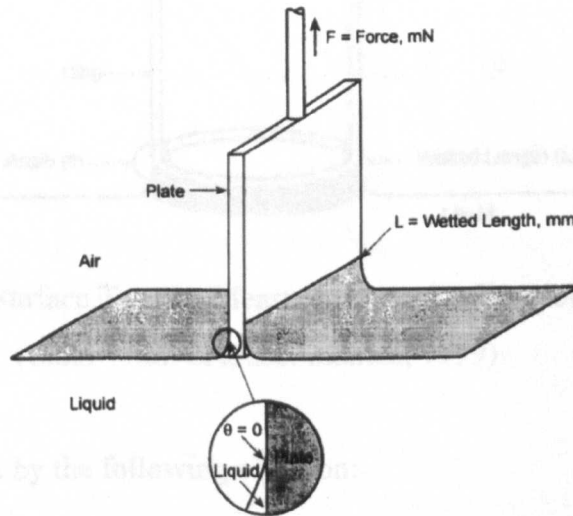


Figure 3.2: Surface Tension Measurement using Wilhelmy Plate
(Cahn WinDCA, user manual, 1999)

The following equation is used for the calculation of surface tension:

$$\sigma = \frac{F}{L \cdot \cos \theta} \quad (30)$$

where; σ = Surface Tension

F = Force exerted by plate

L = Wetted length

θ = Contact angle of liquid with plate

Du-Nouy Ring Method

A platinum wire ring is immersed and then pulled out from the test liquid. When the ring is pulled out from the pool of test liquid, it stretches the surface of the liquid and a force is exerted on the ring by the test liquid, shown in Figure 3.3. A correction factor is used to take into account the small amount of liquid that is lifted up with the ring.

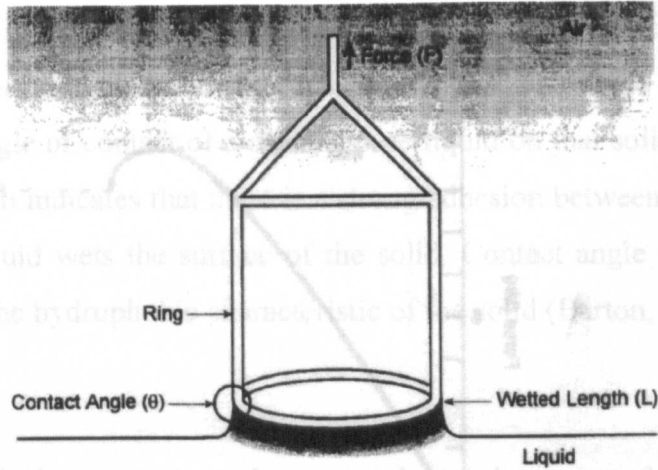


Figure 3.3: Surface Tension Measurement using Du-Nouy Ring

(Cahn WinDCA, user manual, 1999)

Surface tension is given by the following equation:

$$\sigma = \frac{F_{measured} \times F}{2C} \quad (31)$$

where; σ = Surface Tension

$F_{measured}$ = Maximum pull exerted on the ring

F = Correction factor

C = Circumference of the ring

The determination of the surface energy parameters of a solid is not that straight forward. Surface energy values for a solid are very difficult to measure directly. The work of adhesion of a solid with different liquids is measured which is then used to calculate the surface energy components of the solid. The two most popular techniques for measurement of interaction of a solid with the probe liquid are the contact angle approach and the vapour/gas adsorption technique.

3.2 Contact Angle Technique

Contact angle is used to determine the wettability characteristics of a solid surface, by measuring the angle of contact of a drop of pure liquid on that solid. A contact angle value close to zero indicates that there is a strong adhesion between the liquid and the solid, and the liquid wets the surface of the solid. Contact angle value greater than ninety indicates the hydrophobic characteristic of the solid (Barton, 1997), also shown in Figure 3.7.

Young described the contact angle approach to determine the surface energy properties of a solid. The definition of contact angle is given by the three surface tensions (solid, liquid and vapour/air) and is summarised by the Young's equation as shown in Figure 3.4 below:

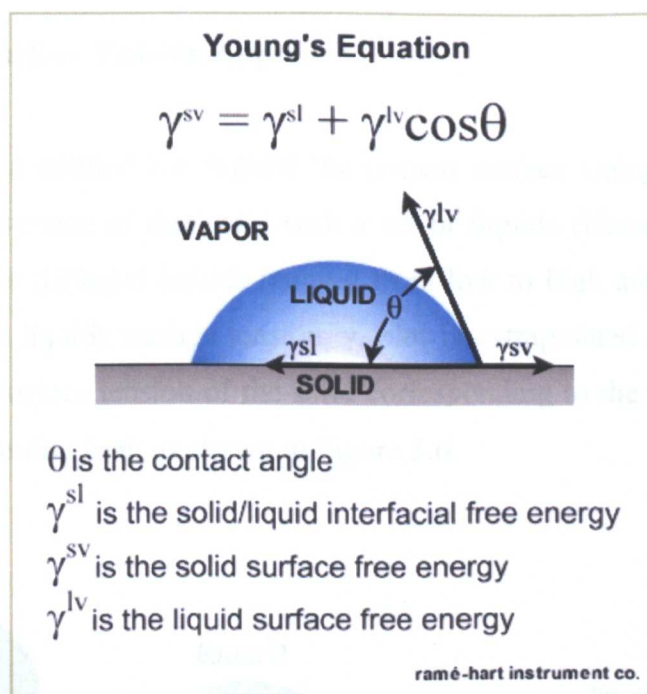


Figure 3.4: Young's Contact Angle Formula

(<http://www.ramehart.com/goniometers/contactangle.htm>, 2008)

The equation can be written as:

$$\gamma_{LA} \cos\theta + \gamma_{SL} = \gamma_{SA} \tag{32}$$

where L, S and A represents liquid, solid and air respectively.

By substituting the Dupre's equation (6) with the above mentioned Young's equation, work of adhesion between the two materials can be obtained through the following Young-Dupre's equation:

$$W_{SL} = \gamma_{LA}(1 + \cos \theta) \quad (33)$$

3.3 Theories for Surface Energy Calculation from Contact Angle Data

The calculation of surface energy of a solid or a solid-liquid interface is not that simple. Different techniques have been used in the past in order to measure reliable values for solid surface energy (Hansen, 2006).

3.3.1 Critical Surface Tension Approach

Zisman proposed a method for finding the critical surface energy of the solid, by testing a smooth surface of that solid with a set of liquids (Hansen, 2006). Contact angle values, θ , for different liquids ranging from low to high are measured (Figure 3.5). $\cos \theta$ versus liquids surface tension, γ , plot is extrapolated to $\cos \theta = 1$. This gives the critical surface tension of the solid corresponding to the zero contact angle, or the complete wetting limit as shown in Figure 3.6.

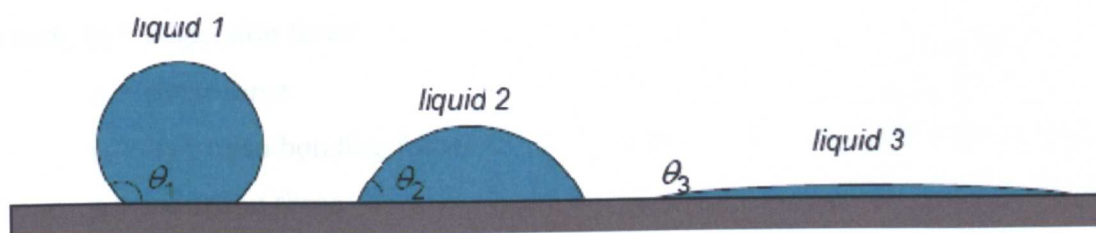


Figure 3.5: Contact Angle-Sessile Drop Technique
(KSV Instruments, Ltd. Application Note No. 108)

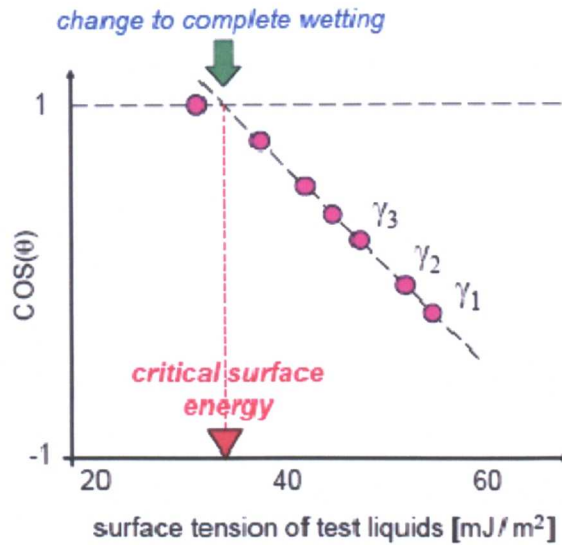


Figure 3.6: Critical Surface Energy of Solid
(KSV Instruments, Ltd. Application Note No. 108)

The critical surface energy in this case is not really surface energy but rather wettability benchmark.

3.3.2 Geometric Mean Approach

Fowkes proposed that surface forces/energies, γ , are the sum of several forces that are acting on the surface (Hansen, 2006).

According to Fowkes, these forces are additive i.e. $\gamma = \gamma_d + \gamma_p + \gamma_h + \gamma_i + \gamma_{ab}$

where; γ_d = dispersion force

γ_p = polar force

γ_h = hydrogen bonding force

γ_i = induction force

γ_{ab} = acid-base force

Fowkes also proposed the Geometric Mean Method for determination of Work of Adhesion for each type of energy.

The same approach was then used by *Owens and Wendt* (Erbil, 2006). They proposed that surface energy of a system consists of dispersive and polar interactions and through geometric mean the work of adhesion can be expressed as:

$$W_{SL} = 2\left(\sqrt{\gamma_S^d \gamma_L^d}\right) + 2\left(\sqrt{\gamma_S^p \gamma_L^p}\right) \quad (34)$$

Where; S = Solid, L = Liquid, d = dispersive component, and p = polar component

This theory was based on the assumption that all the polar materials interact with each other as a function of their internal polar cohesive forces but later it was identified as incorrect by researchers because polar interactions are mostly electron acceptor (acid) and electron donor (base) type interactions and strong interaction can only occur when one material has an acidic character and the other has a basic character (Erbil, 2006).

3.3.3 Harmonic Mean Approach

Wu suggested a harmonic mean approach to sum the dispersive and polar components of surface energy but the technique was based on the same wrong assumption as the Owens-Wendt approach and was rejected. Even if these types of relationships fit for the dispersion forces, and possibly also for some polar forces, they are not so good for acid/base and hydrogen bonding (Rieke, 1997). For this reason, Van Oss et al. (1988) proposed an alternative combination of surface energies.

3.3.4 Acid-Base Approach

Good, Van Oss and Chaudhury suggested (Erbil, 2006) that the surface energy components of a solid consists of two main interactions namely Lifshitz-van der Waals interactions and acid-base interactions. They divided the polar components into Lewis acid and base components, comprised of all the electron donor and electron acceptor type interactions. This theory has already been explained in the previous chapter.

Based on acid-base theory, the work of adhesion between the solid and the probe liquid is determined by using the following equation (Bhasin, 2006) which is dry adhesive bond strength as given in Equation 19:

$$W_{SL} = 2\sqrt{\gamma_S^{LW} \gamma_L^{LW}} + 2\sqrt{\gamma_S^+ \gamma_L^-} + 2\sqrt{\gamma_S^- \gamma_L^+} \quad (35)$$

where; W_{SL} = Work of adhesion between the solid and the probe liquid

S and L represents solid and liquid respectively

The solid should be tested with at least three different types of probe liquids in order to get three linear equations. The obtained equations are then used to calculate the three unknown surface energy components ($\gamma_S^{LW}, \gamma_S^+, \gamma_S^-$) of the solid. A combination of at least two to four polar and one non-polar liquid is generally used for the purpose.

Contact angle approach is suitable for solids having slightly lower surface free energy, like bitumen (generally 20 to 40mJ/m²). Static/Sessile Contact Angle measurement method or Dynamic Contact Angle/Wilhelmy Plate method is used for the measurement of contact angle values of different probe liquids on the required bitumen sample.

3.4 Sessile Drop/Static Contact Angle Technique

‘*Sessile Drop*’ term is used for the drops of liquids that permanently rest on the surface of substrate and are not free to move about. ‘Sessile Drop Method’ is a method of measuring the contact angle of this drop at the liquid-substrate interface. Angle between the baseline of the drop and the tangent at drop boundary is measured, as shown in Figure 3.7, which is then used to estimate the wetting properties of the substrate. This is also known as the ‘Static Drop’ or ‘Static Contact Angle Method’.

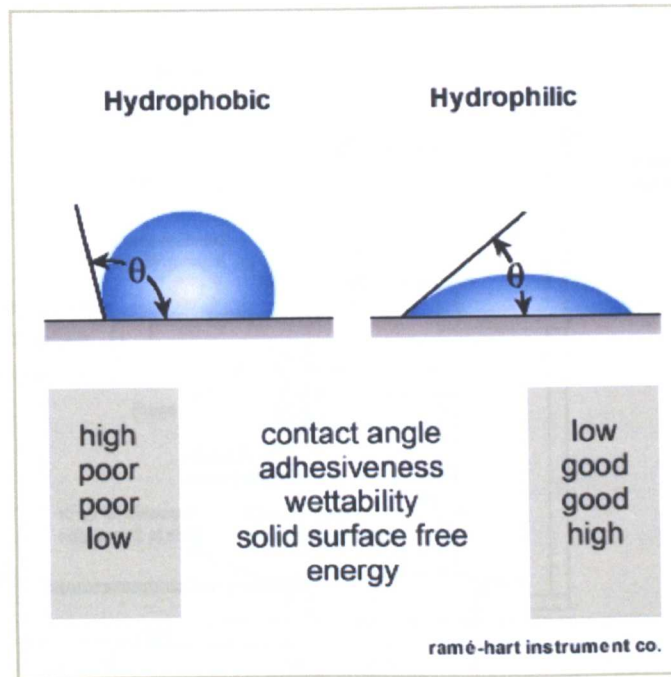


Figure 3.7: Contact Angles

(<http://www.ramehart.com/goniometers/contactangle.htm>, 2008)

A goniometer is used to measure the static contact angle of probe liquids on the bitumen surface. A schematic of the test equipment is shown in Figure 3.8. Small drops of liquid are dispensed on the bitumen sample glass slide, as shown in Figure 3.9. Images of the drops are captured and the contact angle values are measured with the help of inbuilt software. Young-Dupre's Equation 33 and Equation 35 are combined together as follows:

$$\gamma_L(1 + \cos \theta) = 2\sqrt{\gamma_S^{LW} \gamma_L^{LW}} + 2\sqrt{\gamma_S^- \gamma_L^+} + 2\sqrt{\gamma_S^+ \gamma_L^-} \quad (36)$$

where; γ_L , is the total surface energy of the probe liquid.

The obtained contact angle values are related to the surface energy components of the liquid.

An experimental technique for the measurement of contact angles of different probe liquids on bitumen samples with the Goniometer was developed and the detailed protocol is provided in Appendix A.

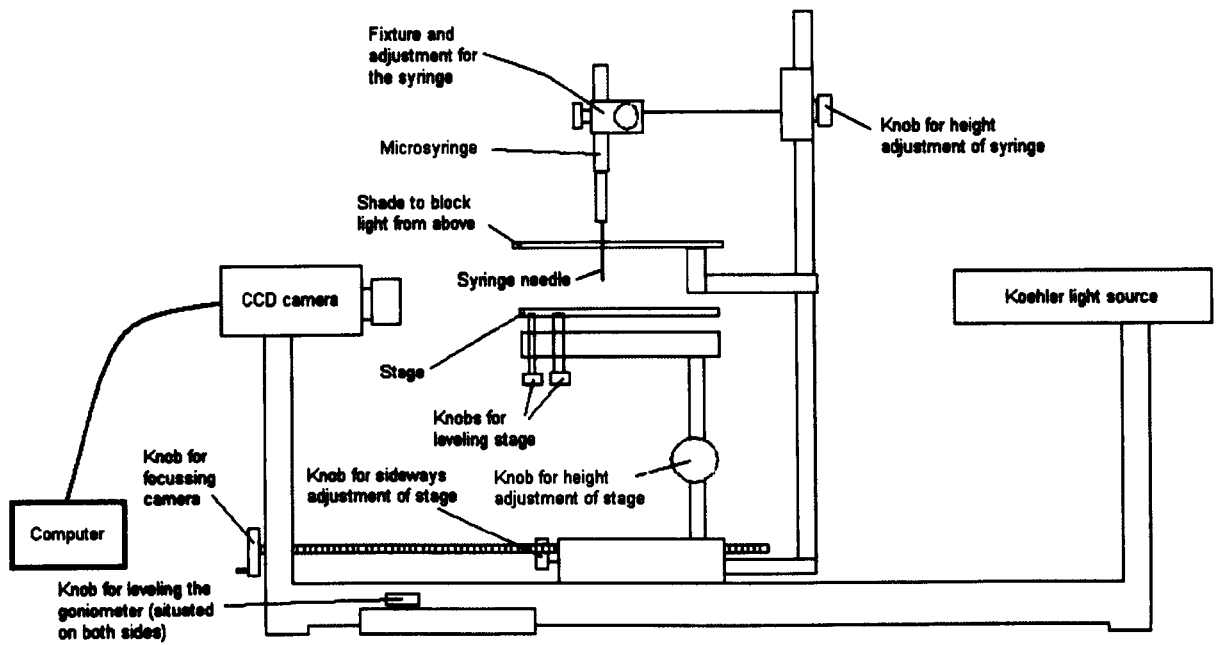


Figure 3.8: Goniometer Schematic

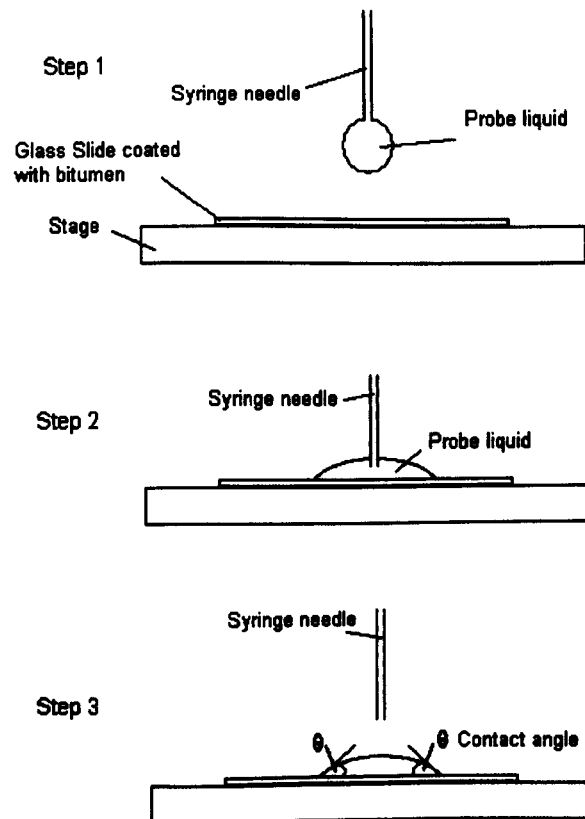


Figure 3.9: Static Contact Angle; Process Steps

3.5 Dynamic Contact Angle-DCA Technique

A dynamic contact angle analyser (*Wilhelmy plate device*) is used to measure the contact angle of probe liquid with the substrate/bitumen under dynamic conditions. This technique is also referred to as the *tensiometric contact angle technique*. A schematic of the test equipment is shown in Figure 3.10. A clean glass slide is coated with the bitumen to be tested and hung from the balance of the equipment with the help of a crocodile clip. A beaker containing the test liquid is placed under the glass slide. The bottom edge of the slide is kept parallel with the surface of the probe liquid. The slide is immersed and then withdrawn from the liquid at a constant speed, as shown in Figures 3.11 & 3.12, and the force involved is continuously measured. The value of force F applied during the immersion and withdrawal process is measured from the automatically controlled DCA analyzer balance and the contact angle is calculated. A detailed test protocol for the measurement of contact angle of chemicals with bitumen slides was produced and is provided in Appendix B of the dissertation.

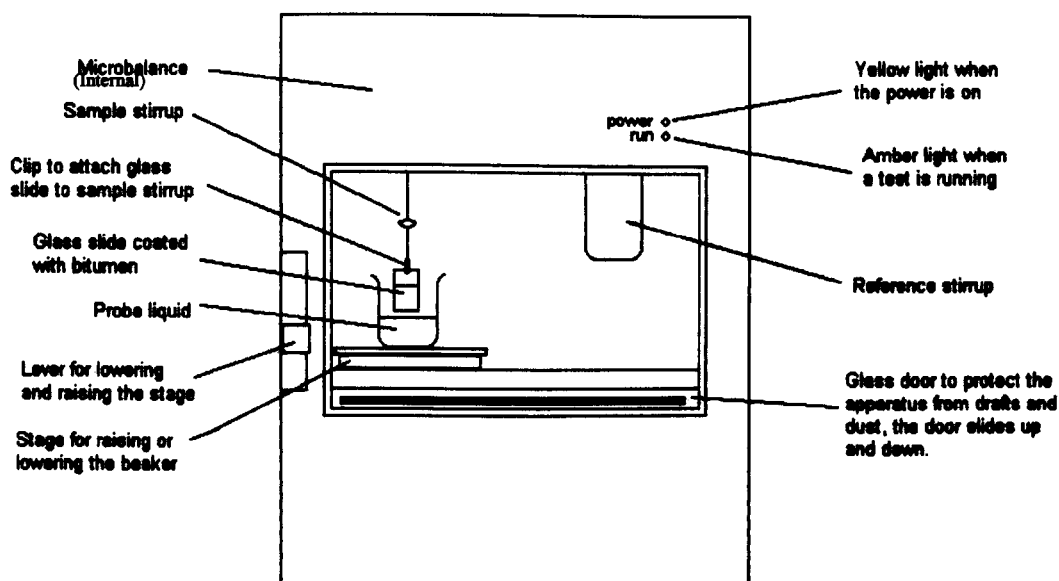


Figure 3.10: Schematic of Dynamic Contact Angle Analyser

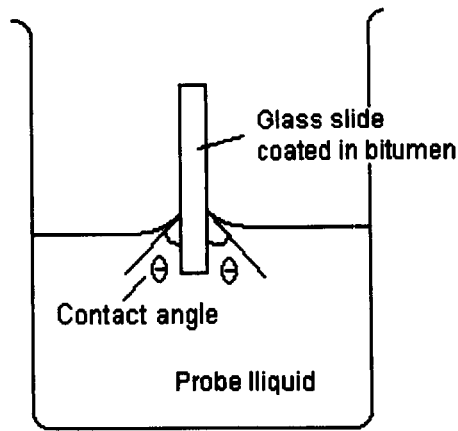


Figure 3.11: Contact Angle Measurement; Wilhelmy Plate Technique

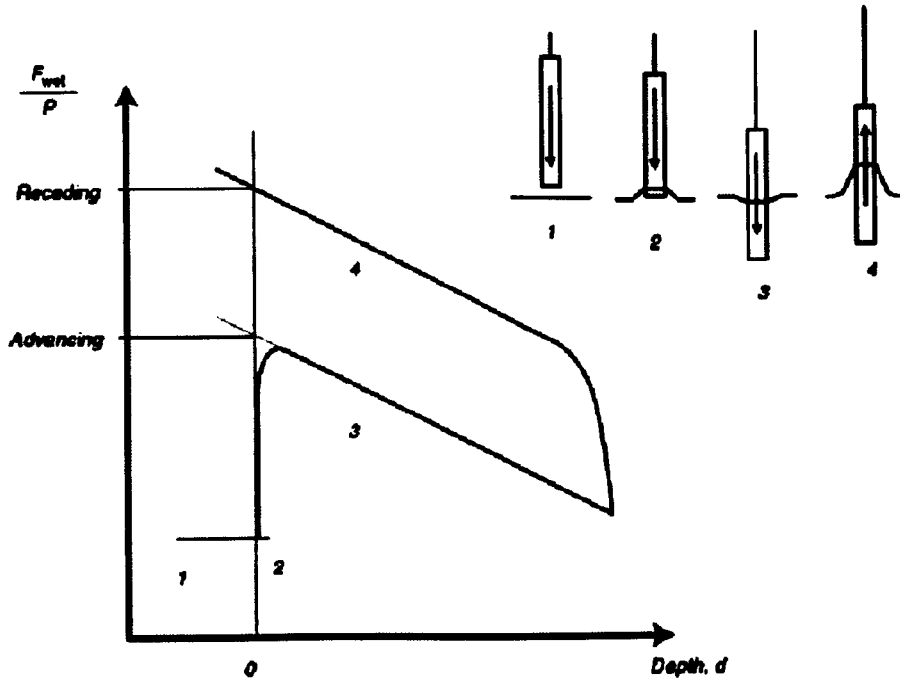


Figure 3.12: Variation of Wetting Force versus Depth of Immersion during a DCA Test (Erbil, 2006)

The contact angle value measured during the immersion of glass slide is referred to as the *advancing contact angle* while the value measured during the withdrawal of substrate is called the *receding contact angle*. As during the advancing movement the substrate is wetted by the probe liquid, the receding contact angle values are always

less than the advancing ones. The contact angle (θ) values are obtained by using the following equation (Bhasin, 2006):

$$\cos\theta = \frac{\Delta F + V_{im}(\rho_L - \rho_{air}g)}{P_i\gamma_L} \quad (37)$$

where; P_i = perimeter of the bitumen coated plate

γ_L = total surface energy of the probe liquid

ΔF = difference between weight of plate in air and partially submerged in probe liquid

V_{im} = volume of solid immersed in the liquid

ρ_L = density of the liquid

ρ_{air} = air density

g = gravitational force

Contact angle values for at least three probe liquids are measured and are applied to Equation 33 for the measurement of three surface energy components ($\gamma^{LW}, \gamma^+, \gamma^-$) of the bitumen. Three equations are produced using the known surface energy components of the three probe liquids. The equations are then written in a matrix form in order to obtain the unknowns.

3.6 Calculation of Surface Energy Parameters - Example Solution

An example solution is provided here in order to explain the steps that are generally followed to calculate the surface energy components of the solids from the obtained contact angle values.

As we are using bitumen as the solid in equation 36, the abbreviation S is replaced by b to represent bitumen.

$$\gamma_L(1 + \cos\theta) = 2(\sqrt{\gamma_b^{LW}\gamma_L^{LW}} + \sqrt{\gamma_b^-\gamma_L^+} + \sqrt{\gamma_b^+\gamma_L^-}) \quad (38)$$

The above equation is rearranged as;

$$(1 + \cos \theta) = 2\sqrt{\gamma_b^{LW}} \frac{\sqrt{\gamma_L^{LW}}}{\gamma_L} + 2\sqrt{\gamma_b^-} \frac{\sqrt{\gamma_L^+}}{\gamma_L} + 2\sqrt{\gamma_b^+} \frac{\sqrt{\gamma_L^-}}{\gamma_L} \quad (39)$$

The equation is then divided into known and unknown components as follows:

$$1 + \cos \theta = Y_i, 2\sqrt{\gamma_b^{LW}} = X_1, 2\sqrt{\gamma_b^-} = X_2, 2\sqrt{\gamma_b^+} = X_3 \quad (40)$$

Where; 'i' represents the values obtained for probe liquid 1, 2 or 3 which, for this example, are water, glycerol and diiodomethane.

$$\text{Similarly, for any liquid } i, A_{1i} = \frac{\sqrt{\gamma_L^{LW}}}{\gamma_L}, A_{2i} = \frac{\sqrt{\gamma_L^+}}{\gamma_L}, A_{3i} = \frac{\sqrt{\gamma_L^-}}{\gamma_L} \quad (41)$$

The divided components are then written as three separate matrices of the form;

$$Ax = y \quad (42)$$

where, 'x' matrix represents the three unknowns.

A three by three matrix is used in order to obtain the three unknown surface energy parameters of the bitumen as shown below:

$$\begin{bmatrix} A_{11} & A_{21} & A_{31} \\ A_{12} & A_{22} & A_{32} \\ A_{13} & A_{23} & A_{33} \end{bmatrix} \begin{bmatrix} X_1 \\ X_2 \\ X_3 \end{bmatrix} = \begin{bmatrix} Y_1 \\ Y_2 \\ Y_3 \end{bmatrix} \quad (43)$$

The surface energy components of the probe liquids are as shown in Table 3.1. These probe liquids have been used for almost all the testing that has been done using the contact angle technique.

Table 3.1: Surface Energy Components of the Probes (Example Solution)

No.	Probe Liquid	γ^{LW}	γ^+	γ^-	γ^{TOTAL}	SQRT γ^{LW}	SQRT γ^+	SQRT γ^-
1	Water	21.8	25.5	25.5	72.8	4.67	5.05	5.05
2	Glycerol	34.0	3.92	57.4	64.0	5.83	1.98	7.57
3	Diiodomethane	50.8	0	0	50.8	7.13	0	0

The contact angle values obtained with each probe liquid are provided in Table 3.2:

Table 3.2: Contact Angle Results (Example Solution)

No.	Probe Liquid	Contact Angle Values (Degrees)
1	Water	75
2	Glycerol	68
3	Diiodomethane	57

Now;

$$Y_1 = 1 + \cos \theta_1 \tag{44}$$

where; $\theta_1, \theta_2, \text{ and } \theta_3$ represents the contact angle values for water, glycerol and diiodomethane respectively.

By substituting the contact angle for water in the above equation;

$$Y_1 = 1 + \cos 75.29$$

$$Y_1 = 1.254$$

Similarly values for glycerol and diiodomethane are;

$$Y_2 = 1.378$$

and

$$Y_3 = 1.542$$

Also, as we know that for any liquid i , $A_{1i} = \frac{\sqrt{\gamma_L^{LW}}}{\gamma_L}$, $A_{2i} = \frac{\sqrt{\gamma_L^+}}{\gamma_L}$, $A_{3i} = \frac{\sqrt{\gamma_L^-}}{\gamma_L}$

The following values are obtained by substituting the surface energy components of water (liquid number 1) from Table 3.1 into the above equations;

$$A_{11} = \frac{\sqrt{\gamma_L^{LW}}}{\gamma_L} = \frac{4.67}{72.8} = 0.0641$$

$$A_{21} = \frac{\sqrt{\gamma_L^+}}{\gamma_L} = \frac{5.05}{72.8} = 0.0694$$

$$A_{31} = \frac{\sqrt{\gamma_L^-}}{\gamma_L} = \frac{5.05}{72.8} = 0.0694$$

Similar procedure is followed for glycerol (liquid no. 2) and diiodomethane (liquid no. 3). The obtained results are:

For glycerol;

$$A_{12} = 0.0911$$

$$A_{22} = 0.0309$$

$$A_{32} = 0.1184$$

For diiodomethane;

$$A_{13} = 0.1403$$

$$A_{23} = 0.0$$

$$A_{33} = 0.0$$

By substituting the values of Y's and A's in the matrices below, the unknowns are obtained.

$$\begin{bmatrix} A_{11} & A_{21} & A_{31} \\ A_{12} & A_{22} & A_{32} \\ A_{13} & A_{23} & A_{33} \end{bmatrix} \begin{bmatrix} X_1 \\ X_2 \\ X_3 \end{bmatrix} = \begin{bmatrix} Y_1 \\ Y_2 \\ Y_3 \end{bmatrix}$$

Here the 'A' matrix comprises the known surface energy components of the three liquid solvents. The 'X' matrix comprises the required unknown surface energy components of the binder and 'Y' matrix is a known function of the measured contact angles of the binder with the three liquid solvents (θ_{water} , $\theta_{Methylene\ Iodide}$, $\theta_{Glycerol}$).

The following results are obtained by solving the matrix.

$$2\sqrt{\gamma_b^{LW}} = X_1 = 10.990734,$$

$$2\sqrt{\gamma_b^-} = X_2 = 6.408241,$$

$$2\sqrt{\gamma_b^+} = X_3 = 1.509540$$

Above equations are then solved to obtain the surface energy components of the solid/bitumen under consideration.

$$\gamma_b^{LW} = 30.2$$

$$\gamma_b^- = 10.3$$

$$\gamma_b^+ = 0.57$$

If five probe liquids are used then this system of linear equations becomes an overdetermined system as the numbers of unknowns are still three but the numbers of

equations have increased to five. A system of linear equations can be written as a matrix equation as mentioned above but for an overdetermined system this technique no longer works. Method of least squares is used to find an approximate solution to an overdetermined system. In our case it falls into the category of non-linear least squares problem and is solved by iterative refinement using solver in excel.

3.7 Results and Discussion

This section discusses the experimental work that has been carried out using the Goniometer and the Wilhelmy plate devices.

3.7.1 Test/Probe Liquids

Selection of suitable probe liquids is very important for the determination of reliable/correct surface energy characteristics of a material. Combinations of polar and non-polar probe liquids are used for the purpose.

Bhasin (2006) shortlisted five liquids namely distilled water, glycerol, diiodomethane, formamide and ethylene glycol for testing bitumen samples. Because of restrictions on use of certain chemicals at NTEC, like formamide (due to their harmful or toxic nature), a number of other liquids were identified from the literature, but most of them dissolved bitumen. For instance, bromonaphthalene was initially tried as a non-polar liquid to replace diiodomethane but it was almost impossible to take readings as it readily dissolved bitumen samples. Diiodomethane is a light sensitive liquid. When exposed to light, it becomes unstable and changes in colour. This suggests that a change in chemical composition takes place which probably alters its surface energy properties. Diiodomethane also has the tendency to dissolve bitumen but not as quickly as other non-polar probes. This was taken into account during the contact angle measurements and fresh liquid was used for each replicate during the testing. Liquid syringe was covered with black tape for testing with Goniometer and a dark beaker was used for testing with the Wilhelmy plate device.

For initial testing of binders only three probe liquids namely distilled water, glycerol and diiodomethane were used. Later, COSHH assessments were carried out and

material safety data sheets were produced for each chemical in order to get permission for their use. An example of a COSHH assessment record is provided in Appendix F for reference.

As mentioned earlier, the Goniometer and Wilhelmy Plate devices are used to measure the surface energy components of the bitumen by using the contact angle technique. The angle of contact of a probe liquid is measured with the bitumen. The known surface properties of the liquid and the contact angle values are then used to calculate the surface energy components of the bitumen. In order to get the three unknown surface energy parameters, at-least three probe liquids are used. The liquids that are used with bitumen are provided in Table 3.3 along with their physico-chemical properties. The following factors are considered for the selection of probe liquids:

- The liquid must not dissolve or chemically react with bitumen at test temperature
- The surface energy components of the liquid must be known
- The liquid must be pure and homogeneous
- The surface energy value for probe liquid should be more than that of the solid for contact angle measurements. As a solvent with low surface energy/surface tension will readily spread on the substrate and it would be difficult to get an accurate angle measurement.
- The substrate should be tested with a combination of at-least one non-polar and two polar liquids. Out of the two polar probes one should be acid and the other should be base, or they may have a combination of acid-base character. This is required to fully characterize the surface properties of the substrate and to remove errors that may occur if liquids with very similar surface energy properties are used.

A complete list of probe liquids that have been used for this research along with their supplier codes is provided in Appendix E.

Table 3.3: Probes for the Analysis of Bitumen

S. No.	Probe Liquid	Liquid Surface Tension (erg/cm ²)	Angle of Contact with Bitumen (Degrees)	Liquid Density (g/cc)	Molecular Weight (g/mol)
1	Water	72.8	102	1.000	18
2	Glycerol	64.0	92	1.262	92
3	Formamide	58.0	85	1.133	45
4	Diiodomethane	50.8	68	3.325	268
5	Ethylene Glycol	48.0	78	1.113	62

In Table 3.3 above, the liquids are arranged in the descending order of their surface tension values. The above mentioned contact angle values (Table 3.3) were obtained with one bitumen only and are provided to show the general trend.

It has been observed that diiodomethane gives the lowest contact angle values, generally with both Goniometer and Wilhelmy plate device but specifically very low values when static contact angle technique is used, despite having high surface tension as compared to that of ethylene glycol. The reason for this is its non-polar nature like bitumen (non-polar substances are miscible in non-polar solutions) and the higher density and molecular weight as compared to the other liquids.

3.7.2 Sample Preparation Techniques and Test Parameters

Surface energy equipment is generally used by the chemical industry to test different types of paints, polishes and waxes. This is the first time in UK, that this equipment is being used for testing road material. Initial testing was done with the equipment and different trials were carried out to decide sample preparation techniques and testing procedures for road material. Sample preparation techniques and test procedures for all the equipments are provided in detail in Appendices.

The test parameters which can significantly affect the results are discussed below.

Time of Reading of Contact Angle (Goniometer)

In case of testing with the goniometer, the time at which the contact angle reading of the probe liquid on a binder sample is taken can have significant impact on the final obtained results. It is observed that the drops of the probe liquids start evaporating after a certain amount of time. Also, drops of almost all the probes start spreading on the surface of the bitumen. This is more profound in case of diiodomethane which readily spreads on the surface of bitumen. It is therefore important that the contact angle readings are obtained immediately after the drop is dispensed on the bitumen, especially in case of diiodomethane. This parameter is further discussed later in this chapter.

Probe Liquid Drop Volume (Goniometer)

Volume of the drop of probe liquid can also effect the contact angle results when testing with goniometer. Theoretically, drop volume should not have any effect on the contact angle results but it is observed that a drop volume of 5 μ l gives consistent results for most of the probe liquids. Drop volume beyond 6.5 μ l suffers from the gravitational effects and readily spreads/flow on the solid/bitumen surface. Again, in case of diiodomethane drop volume is further reduced to around 3.5 μ l in order to be able to take correct readings.

Depth of Immersion of Bitumen Slide in Test Liquid (DCA)

As explained in section 3.5, a glass slide coated with bitumen is immersed into the test liquid in order to measure the angle of contact of the test liquid with the bitumen sample with a DCA system. Initially, a 15mm depth of immersion was chosen for the tests in order to cover larger area of bitumen surface. Theoretically, depth of immersion should not have an effect on the contact angle readings. However, it was observed that when the slides are prepared with very stiff or aged binders the bitumen does not flow down the slide (when the slide is inverted and placed on the stand after dipping it in the molten bitumen, see appendix B) as a normal binder would. Lesser area of the slide is covered by an aged binder and hence smaller area of uniform binder thickness is obtained. The slide should be immersed into the liquid only up to

the point where the bitumen thickness is consistent or in other words only the uniform thickness portion of the slide/bitumen should be immersed in to the test liquid. An immersion depth of 5mm is found to be suitable in most of the cases.

Advancing versus Receding Contact Angle Values (DCA)

During dynamic contact angle analysis the advancing contact angle is measured when the bitumen coated slide is immersed in the probe liquid while the receding contact angle is measured when the slide is taken out from the liquid. The advancing contact angle values are always higher than the receding ones. The main reason for this hysteresis is the microscopic chemical heterogeneity of the solid (bitumen) surface (Erbil, 2006). The other reason could be that the probe liquid has already wetted the surface of the bitumen during the advancing movement, hence resulting in reduction of the receding contact angle values. This is especially true when the binder samples are tested with a non polar (diiodomethane) liquid. It appears that diiodomethane starts dissolving the binder sample during the receding movement of the slide, as by that time the sample is in the liquid for quite a while. This means that receding contact angle values obtained with diiodomethane could be quite inaccurate. For the above mentioned reasons the advancing contact angle values are only used for the calculation of surface energy parameters of bitumen.

3.7.3 Contact Angle Data Selection

As mentioned above, in a static contact angle measurement technique the drops of probe liquids spread on the surface of binder. In the case of diiodomethane this spread is quite quick and instantaneous. For this reason, the readings taken during the initial few seconds after dispensing the drop are only used for the analysis. It is recommended that the first reading should be used wherever possible. Multiple drops of a liquid are dispensed on a slide of the binder sample to check the consistency of the contact angle values. At least three slides of a given sample are analysed with one probe liquid. The average of these readings is then used as the final contact angle value for that specific probe liquid.

For analysis with Wilhelmy plate device, at least four sample slides are tested with one probe liquid and the average of the four obtained contact angle values is then used for surface energy determinations.

Neumann (2011) recommends that a plot of $\gamma_L \cos \theta$ versus γ_L should be produced for the contact angle values obtained with each probe liquid. γ_L is the surface tension of the probe liquid and θ is the angle of contact of that probe with the bitumen. Contact angle values of all the probe liquids for a given solid should lie on a smooth curve when $\gamma_L \cos \theta$ is plotted versus γ_L . If a value falls far from the curve, it should not be included in the final data for the calculation of surface energy properties. Contact angle data for three different types of binders and a ($\gamma_L \cos \theta$) versus (γ_L) plot are provided in Table 3.4 and Figure 3.13 respectively.

Table 3.4: Contact Angle Data (Neumann Plot)

Probe Liquid	γ_L	Contact Angle (θ)			$\gamma_L \cos \theta$		
		15pen	50pen	100pen	15pen	50pen	100pen
Water	72.8	95.05	93.04	93.88	-6.41	-3.86	-4.93
Glycerol	64	80.18	82.58	84.23	10.92	8.26	6.43
Formamide	58	75.02	80.35	82.1	15	9.72	7.97
Ethylene Glycol	48	65.72	72.77	76.22	19.74	14.22	11.43
Diiodomethane	50.8	58.3	66.99	68.93	26.7	19.86	18.26

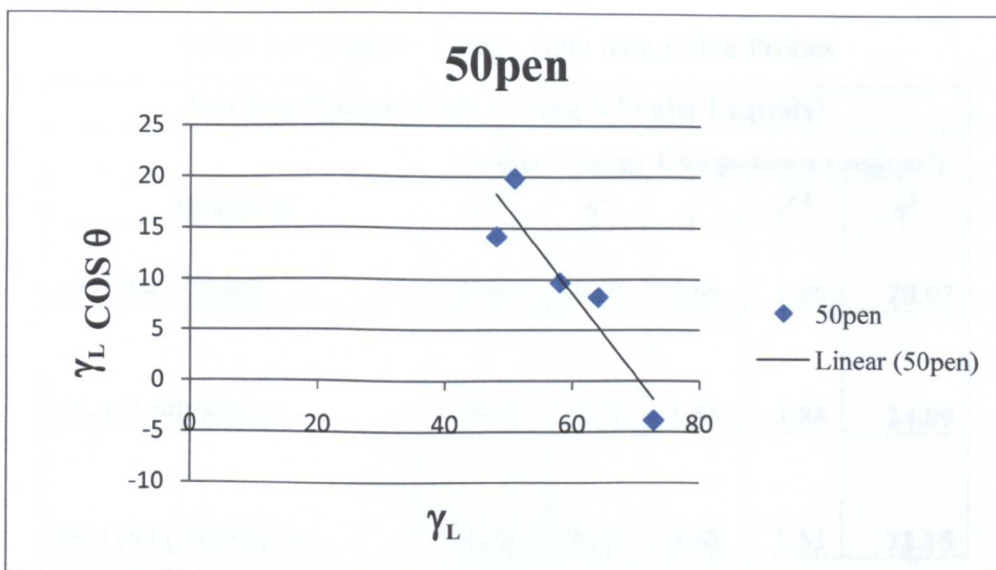


Figure 3.13: Neumann Plot

It can be seen from Figure 3.13 that the data points for almost all the probe liquids lie very close to the trend line which means that for this scenario the contact angle values from all the probe liquids can be used for the surface energy calculation of the binder sample.

3.7.4 SFE Using Different Number of Probe Liquids

Bhasin (2006) recommends use of five probe liquids as it reduces the chance of getting a negative number from the square root of the surface energy components. Negative values are obtained if fewer probe liquids having similar surface energy components are used for the tests, as in that case even small errors in contact angle readings obtained by using these liquids are magnified and result in inaccurate surface energy properties of the binder.

Surface energy properties of three different binders have been obtained by using contact angle data from a combination of five and three probe liquids. For five liquid combination contact angle data from water, glycerol, formamide, ethylene glycol and diiodomethane was used while for the three liquid combination data from water glycerol and diiodomethane was selected. The binders surface energy properties for five and three liquid combinations are provided in Table 3.5 and Table 3.6 respectively.

Table 3.5: Surface Energy Data using Five Probes

Surface Energy Data (Using 5 Probe Liquids)					
Bitumen	Surface Energy Components (erg/cm²)				
	γ^{LW}	γ^+	γ^-	γ^{AB}	γ^T
01-1794 (15pen)	27.97	0.15	1.66	1.00	28.97
05-473 (40/60pen)	23.01	0.23	3.83	1.88	24.89
06-1164 (70/100pen)	20.62	0.12	4.88	1.53	22.15

Table 3.6: Surface Energy Data using Three Probes

Surface Energy Data (Using 3 Probe Liquids)					
Bitumen	Surface Energy Components (erg/cm²)				
	γ^{LW}	γ^+	γ^-	γ^{AB}	γ^T
01-1794 (15pen)	29.48	0.24	1.14	1.05	30.53
05-473 (40/60pen)	24.57	0.25	3.04	1.74	26.31
06-1164 (70/100pen)	23.48	0.20	3.20	1.60	25.08

It has been observed that for a good set of contact angle data surface energy properties for a given binder remains quite similar for both three and five sets of liquids. However, wherever possible five probe liquids should be used to avoid inaccuracies. Diiodomethane should always be used as it is the only non-polar probe.

3.7.5 Goniometer versus DCA

Different types of bitumen samples have been tested by using the Goniometer and the Wilhelmy plate device. A comparison of the contact angle data for some of the samples tested by using these equipments is provided in Table 3.7 below.

Table 3.7: Comparison of Goniometer and DCA Contact Angle Data

Bitumen	Probe Liquid	DCA Contact Angle Values (Average)	Goniometer Contact Angle Values (Average)
15pen 07-1394	Water	91.0	97.2
	Glycerol	81.3	85.6
	Diiodomethane	55.7	47.9
50pen 08-3336	Water	94.3	101.3
	Glycerol	84.2	86.2
	Diiodomethane	56.2	45.4
50pen 08-2602	Water	96.67	103.03
	Glycerol	91.74	99.76
	Diiodomethane	55.08	58.23
94pen 09-243	Water	99.29	103.12
	Glycerol	87.88	91.25
	Diiodomethane	52.33	34.37

Following are the conclusions from the tests:

- Polar liquid contact angle values obtained by using the Goniometer are slightly higher than the ones obtained by DCA. The reason for this may be the higher surface tension of these liquids and the polarity which doesn't allow them to spread or wet the non-polar substrate (bitumen).
- With most of the bitumen samples it is very difficult to get a consistent contact angle value for diiodomethane, when tested by using Goniometer. For explanation, the change of contact angle and width of drop with respect to time is plotted for diiodomethane and glycerol for the same bitumen and is shown in Figures 3.14, 3.15, 3.16 and 3.17. It can be seen that the contact angle values for diiodomethane collapse rapidly while the values for glycerol remains more or less constant. The reasons for this are:
 - High density and molecular weight of diiodomethane
 - Low surface tension
 - Diiodomethane being non-polar in nature dissolves the non-polar substrate (bitumen) and spreads readily on its surface

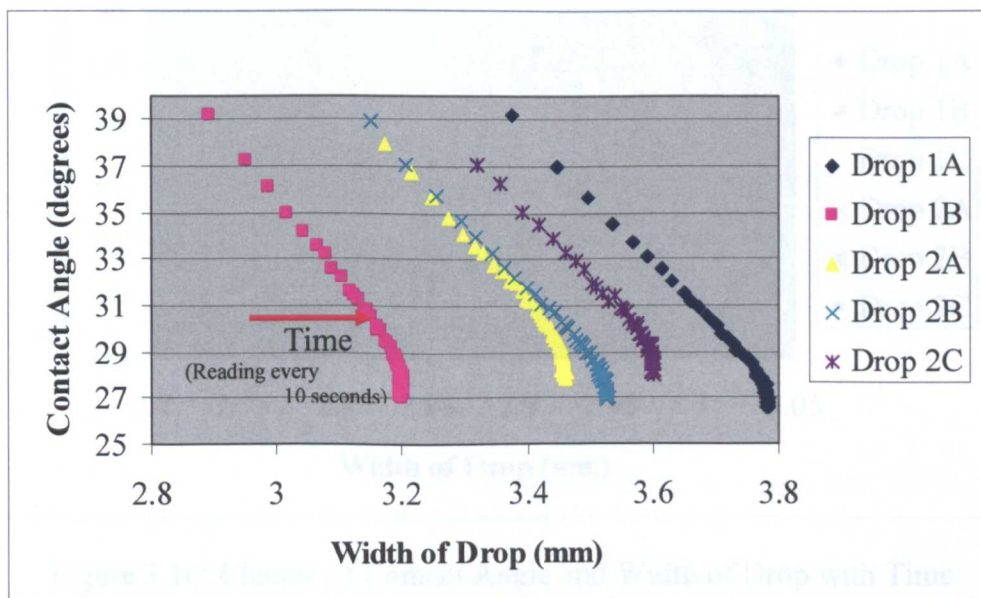


Figure 3.14: Change of Contact Angle and Width of Drop with Time
(Diiodomethane on Sample 07-1215)

Here, in legend 'Drop 1A', '1' represents the number of sample/bitumen slide while 'A' represents the drop of probe liquid. Similarly, 'Drop 2B' means the second drop of the probe liquid that was used to take the readings on sample slide number 2.

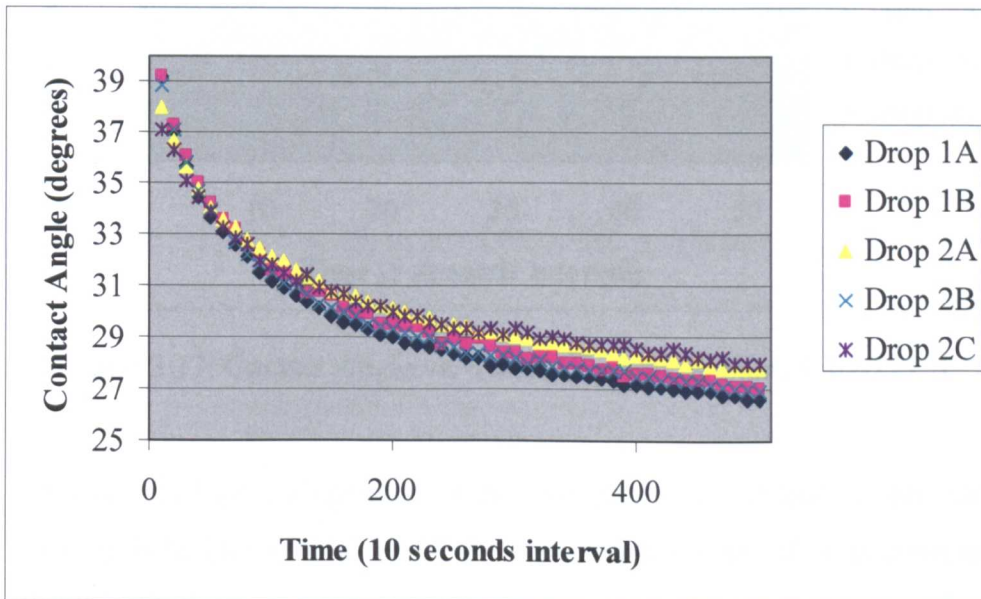


Figure 3.15: Contact Angle vs. Time (Diiodomethane on Sample 07-1215)

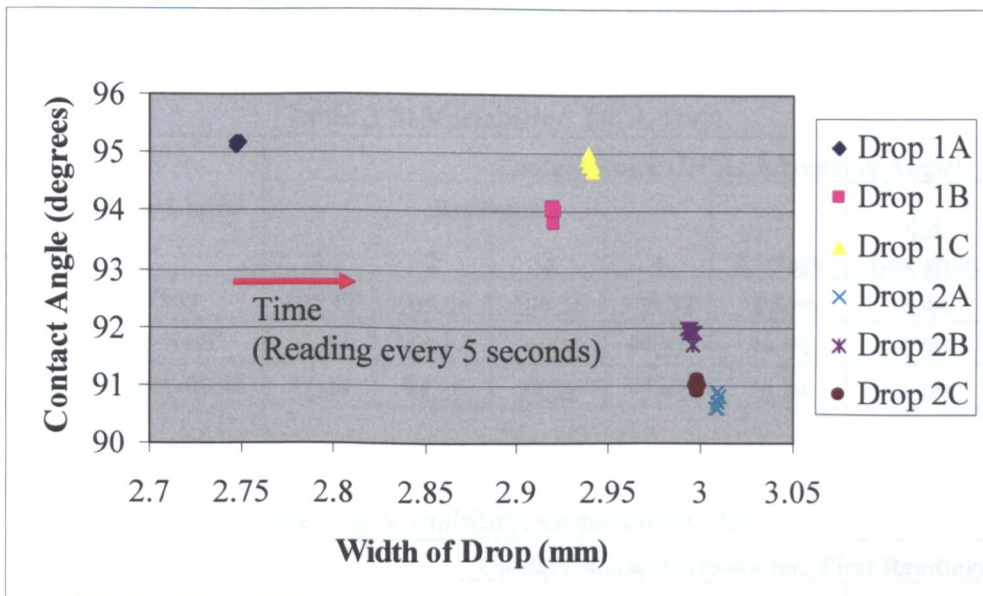


Figure 3.16: Change of Contact Angle and Width of Drop with Time

(Glycerol on Sample 07-1215)

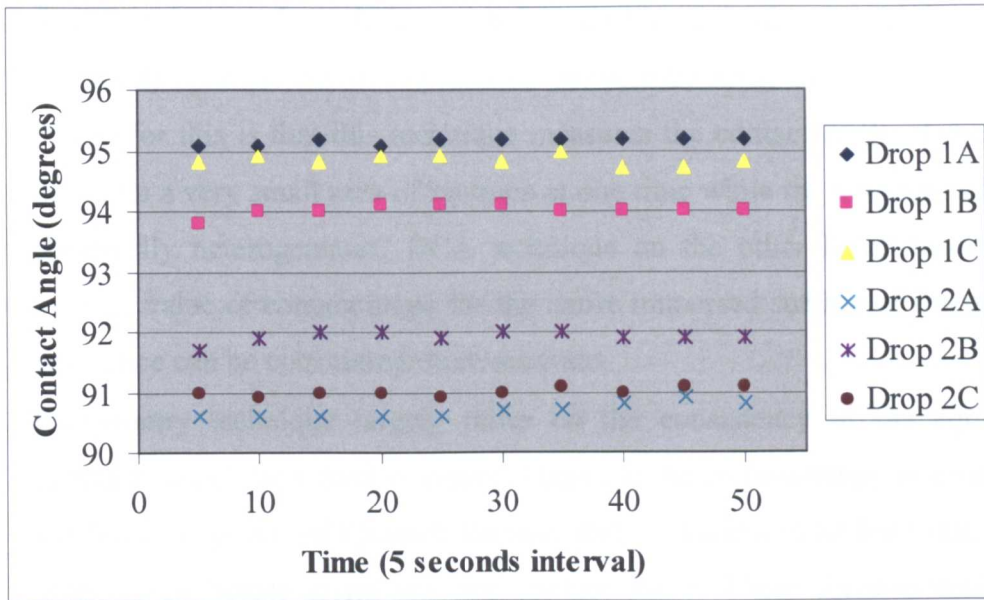


Figure 3.17: Contact Angle vs. Time (Glycerol on Sample 07-1215)

- It was observed during most of the tests that it is difficult to get consistent results with Goniometer while the repeatability with DCA is comparatively better. Similarly, a large number of replicates are required to be done with Goniometer than that with DCA and this is especially true if the probe liquid is diiodomethane. Some of the results along with their coefficients of variability are provided in Tables 3.8 and 3.9 below for comparison.

Table 3.8: Variability; DCA Data

Bitumen (09-268)	Probe Liquid	Contact Angle (DCA; Advancing Angle)						
		Replicate				Average	Std. Deviation	Coefficient of Variability (%)
		1	2	3	4			
Water	106.18	105.56	106.58	105.82	106.04	0.44	0.42	
Glycerol	99.24	100.04	99.3	99.81	99.60	0.39	0.39	
Diiodomethane	72.09	74.21	72.32	73.94	73.14	1.09	1.49	

Table 3.9: Variability; Goniometer Data

Bitumen (07-1394)	Probe Liquid	Contact Angle (Goniometer; First Readings)						
		Replicate				Average	Std. Deviation	Coefficient of Variability (%)
		1	2	3	4			
Water	101.2	97.1	98.0	97.80	98.53	1.82	1.85	
Glycerol	84.4	86.0	86.6	87.0	86.00	1.14	1.33	
Diiodomethane	37.3	42.5	52.6	51.0	45.85	7.22	15.75	

- Static contact angle technique can be considered inadequate as it may not accurately characterise the interactions between bitumen and probe liquid. The reason for this is that this technique measures the contact angle of the probe liquid on a very small area of bitumen at one time while the bitumen is largely chemically heterogeneous. DCA technique on the other hand measures an average value of contact angle for the entire immersed surface of the bitumen and hence can be considered more accurate.
- Goniometry technique largely relies on the consistency of the equipment operator, which may lead to errors. There can be inconsistency in dispensing the liquid drop on the bitumen surface, and in placement of base line on the drop image before measuring the contact angle. These inconsistencies are removed in case of testing with DCA as it is a more automated technique.

Dynamic contact angle technique appears to be better than the Goniometer one as far as bitumen testing is concerned and therefore, wherever possible, should be used for the testing of binders.

CHAPTER 4

SURFACE ENERGY TESTING OF AGGREGATES

4.1 Background

Aggregates are high surface energy materials. The contact angle technique cannot be used in case of aggregates as the liquids readily spread on a high energy surface and the contact angles approach to zero. Equation 36 is used for calculation of surface energy components of solids whose surface energies are not that high (less than the surface tension of probes), the spreading pressure, Π_e , of the probes in this case is very small and is ignored in the calculations. In case of high energy surfaces, the contact angle approaches to zero while the spreading pressure has a high value. Therefore the work of adhesion is related to the spreading pressure of the probe vapour on the solid, rather than the contact angle of the probe liquid.

4.2 Dynamic Vapour Sorption-DVS Technique

As mentioned above, it is difficult to use the contact angle technique on high surface energy materials like aggregates (SE values generally $> 60\text{mJ/m}^2$) as the liquids readily spread on high energy surfaces and it is difficult to obtain correct angle values. Vapour sorption techniques are normally used for high surface energy materials. For this study a dynamic vapour sorption (DVS) system has been used to measure the surface energy components of the aggregate. Probe vapours with known surface energy components are passed through the aggregate sample, under controlled temperature and pressure conditions, with the help of an inert carrier gas. Normally dry nitrogen is used as the carrier gas. On the basis of the surface characteristics of the aggregate, vapour probes get adsorbed at their surfaces which results in an increase in the mass of the aggregate sample. This technique is termed as gravimetric adsorption technique. The vapour mass adsorbed on the aggregate surface is measured for each solvent with the help of a sensitive balance. The probe liquids that have been used for the DVS testing are octane, ethyl acetate and chloroform.

The aggregates to be tested are first washed with deionised water and then dried in an oven. Aggregate fraction passing 5mm and retained on 2.36mm is generally used for the tests however, smaller size fraction can also be used. The upper limit on aggregate size is because of the material holding capacity of the sample chamber. The solvent/probe liquid vapours are passed through the aggregate. The balance measures the quantity of solvent adsorbed onto the surface of the aggregates/sample chamber. This method is comparatively suitable because it considers the irregularity in shape, and surface texture of the aggregates.

An adsorption isotherm is plotted between the partial vapour pressure of the probe vapour at x-axis and the adsorbed mass at y-axis, which is then used to calculate the spreading pressure and the specific surface area of the solid. A schematic of the test equipment along with the detailed procedure is provided in Appendix C.

Here, the term adsorption means the adhesion of the liquid/vapour molecules on the surface of the aggregate and the specific surface area refers to the surface area per unit mass of the solid. The specific surface area of the solid is determined by using the Brunauer-Emmett-Teller (BET) approach and is given by Equation 45.

$$A = \left(\frac{n_m N_o}{M} \right) \alpha \quad (45)$$

where; A = specific surface area of solid, m^2

n_m = monolayer specific amount of vapour adsorbed on the surface of aggregate, mg (monolayer capacity of the adsorbed solute on the adsorbent)

N_o = Avogadro's number, $6.022 \times 10^{23} \text{ mol}^{-1}$

M = molecular weight of the vapour, g/mol

α = projected or cross-sectional area of the vapour single molecule, m^2

The number of vapour molecules adsorbed and required to form a monolayer on the solid surface is determined by using the Langmuir approach and is given by Equation 46.

$$\frac{P}{n(P_0 - P)} = \left(\frac{c-1}{n_m c} \right) \frac{P}{P_0} + \frac{1}{n_m c} \quad (46)$$

where; P = partial vapour pressure, Pa

P_0 = saturated vapour pressure of solvent, Pa

n = specific amount adsorbed on the surface of the absorbent, mg; and

c = BET constant (parameter theoretically related to the net molar enthalpy of the adsorption)

Adsorption of vapour molecules on the aggregate surface reduces its surface energy. So, spreading pressure as a result of adsorption of the vapour molecules can be expressed as:

$$\Pi_e = \gamma_S - \gamma_{SV} \quad (47)$$

where; Π_e = spreading pressure at maximum saturated vapour pressure or equilibrium spreading pressure, ergs/cm²

γ_S = aggregate surface energy in vacuum

γ_{SV} = aggregate surface energy after exposure to vapour

Spreading pressure at maximum saturation vapour pressure, Π_e for each solvent, is calculated by using the following Gibbs free energy equation:

$$\Pi_e = \frac{RT}{A} \int_0^{P_0} \frac{n}{P} dP \quad (48)$$

where; R = universal gas constant, 83.14 cm³ bar/mol.K

T = absolute temperature, K

By introducing spreading pressure, Π_e , in Young-Dupres's relation, Equation 33, the following relationship is obtained:

$$W_{SL} = \Pi_e + \gamma_{LV}(1 + \cos \theta) \quad (49)$$

As mentioned earlier, the contact angle value for high energy solids is zero, Equation 49 can be re-written as:

$$W_{SL} = \Pi_e + 2\gamma_{LV} \quad (50)$$

By substituting the above relation in Equation 35, the following equation is obtained;

$$2\gamma_L + \Pi_e = 2\sqrt{\gamma_S^{LW}\gamma_L^{LW}} + 2\sqrt{\gamma_S^+\gamma_L^-} + 2\sqrt{\gamma_S^-\gamma_L^+} \quad (51)$$

Spreading pressures from three different probe vapours are measured in order to get the three surface energy components of the solid. It can be seen that irrespective of the test method, the basic principle of calculation of surface energy components is the same.

4.3 Microcalorimeter Technique

Microcalorimeter is used to measure the heat of immersion when aggregates are immersed in the probe liquids. Detailed experimental protocol for testing the aggregate materials with microcalorimeter is provided in Appendix D. The amount of heat measured using this technique is actually the enthalpy of immersion and is given by the Gibbs free energy, as mentioned in Equation 4.

$$\Delta G_{imm} = \Delta H_{imm} - T\Delta S_{imm} \quad (52)$$

where; ΔG_{imm} = change in free energy of system due to immersion

ΔH_{imm} = enthalpy of immersion

$T\Delta S_{imm}$ = product of temperature and entropy of immersion

When a solid is immersed in a liquid, a new solid-liquid interface is formed which results in the reduction of the total energy of the system. If γ_{SL} is the interfacial surface energy between the two material and γ_S is the surface free energy of the solid, then the change in free energy of system due to immersion, ΔG_{imm} is given by the following equation (Bhasin, 2006):

$$\frac{\Delta G_{imm}}{A} = \gamma_{SL} - \gamma_S \quad (53)$$

where, A is the specific surface area of the aggregate material.

According to Dupres's Equation (6) work of adhesion between a solid and liquid is given by:

$$W_{SL} = \gamma_S + \gamma_L - \gamma_{SL} \quad (54)$$

$$\text{or } \gamma_{SL} - \gamma_S = \gamma_L - W_{SL} \quad (55)$$

By substituting the value of W_{SL} from Equation 35, above equation can be written as:

$$\gamma_{SL} - \gamma_S = \gamma_L - 2\sqrt{\gamma_S^{LW} \gamma_L^{LW}} - 2\sqrt{\gamma_S^+ \gamma_L^-} - 2\sqrt{\gamma_S^- \gamma_L^+} \quad (56)$$

Substituting the values from Equation 52 and 56, Equation 53 can be written as:

$$\frac{\Delta H_{imm} - T\Delta S_{imm}}{A} = \gamma_L - 2\sqrt{\gamma_S^{LW} \gamma_L^{LW}} - 2\sqrt{\gamma_S^+ \gamma_L^-} - 2\sqrt{\gamma_S^- \gamma_L^+} \quad (57)$$

Doullaard postulated that the entropy term ($T\Delta S_{imm}$) for various minerals is approximately the half of their enthalpy (ΔH_{imm}) (Bhasin, 2006). The above equation can then be written as:

$$\frac{\Delta H_{imm}}{2A} = \gamma_L - 2\sqrt{\gamma_S^{LW} \gamma_L^{LW}} - 2\sqrt{\gamma_S^+ \gamma_L^-} - 2\sqrt{\gamma_S^- \gamma_L^+} \quad (58)$$

ΔH_{imm} for aggregates is measured with the help of microcalorimeter, by using three probe liquids with known surface energy components. The surface energy components of the aggregates are then calculated by using Equation 58.

Glass vials containing the preconditioned aggregate sample are placed in the thermal wells of calorimeter, the probe liquid is injected with the help of syringes and the heat of immersion is directly measured with the help of integrated software. Microcalorimeter can also be used for direct measurement of heat of adhesion between bitumen and aggregate.

4.4 Determination of Surface Energy Parameters - Example Solution

The steps that are generally followed to calculate the surface energy components of the aggregates, from the results obtained through a DVS test, are provided here. An aggregate sample is tested by using a combination of three probe liquids. The surface energy parameters of these three probe liquids are provided in Table 4.1 below.

Table 4.1: Surface Energy Parameters of the Test Liquids (Example Solution)

No.	Probe Liquid	γ^{LW}	γ^+	γ^-	γ^{TOTAL}	SQRT γ^{LW}	SQRT γ^+	SQRT γ^-
1	Octane	21.62	0	0	21.62	4.65	0	0
2	Ethyl Acetate	23.9	0	19.2	23.9	4.89	0	4.38
3	Chloroform	27.15	3.8	0	27.15	5.21	1.95	0

The values of spreading pressures of the probes on the aggregate sample are obtained from the DVS software. These values are then substituted in Equation 51. The obtained equations for three probe liquids are then solved by using the following matrix solution.

$$Ax = y \quad (59)$$

$$\begin{bmatrix} A_{11} & A_{21} & A_{31} \\ A_{12} & A_{22} & A_{32} \\ A_{13} & A_{23} & A_{33} \end{bmatrix} \begin{bmatrix} X_1 \\ X_2 \\ X_3 \end{bmatrix} = \begin{bmatrix} Y_1 \\ Y_2 \\ Y_3 \end{bmatrix} \quad (60)$$

A three by three matrix is used in order to obtain the three unknown surface energy parameters of the aggregate material.

The obtained spreading pressure values are provided in Table 4.2 below.

Table 4.2: Obtained Spreading Pressures (DVS Test Results)

No.	Probe Liquid	Spreading Pressure (mJ/m ²)
1	Octane	33.95
2	Ethyl Acetate	119.3
3	Chloroform	46.39

Equation 51 can be then be separated into the known and unknown components as three separate matrices.

$$2\sqrt{\gamma_S^{LW} \gamma_L^{LW}} + 2\sqrt{\gamma_S^+ \gamma_L^-} + 2\sqrt{\gamma_S^- \gamma_L^+} = 2\gamma_L + \Pi_e \quad (61)$$

$$Ax=y$$

Now,

$$Y_i = 2\gamma_{Li} + \pi_{ei}$$

Substituting the values of spreading pressure and surface tension for Octane from Tables 4.1 and 4.2 above:

$$Y_1 = 2(21.62) + 33.95 = 77.19$$

Similarly for ethyl acetate and chloroform;

$$Y_2 = 2(23.9) + 119.3 = 167.1$$

&

$$Y_3 = 2(27.15) + 46.39 = 100.69$$

The known surface energy components of the probes are written as a separate matrix 'A'.

$$A_{1i} = \sqrt{\gamma_L^{LW}}$$

$$A_{2i} = \sqrt{\gamma_L^+}$$

$$A_{3i} = \sqrt{\gamma_L^-}$$

The values for Octane are:

$$A_{11} = 4.65$$

$$A_{21} = 0$$

$$A_{31} = 0$$

Similarly, the values for ethyl acetate and chloroform are obtained. The values are obtained directly from the Table 4.1.

By substituting the values of A's and Y's into the respective matrices (Equation 60), the following results are obtained:

$$X_1 = 2\sqrt{\gamma_S^{LW}} = 16.60$$

$$X_2 = 2\sqrt{\gamma_S^-} = 7.28$$

$$X_3 = 2\sqrt{\gamma_S^+} = 19.61$$

The above equations are solved for the surface energy components of the aggregate material and the following results are obtained:

$$\gamma_S^{LW} = 68.898$$

$$\gamma_S^- = 13.246$$

$$\gamma_S^+ = 96.172$$

4.5 Results and Discussion

This section provides the summary of the results that have been obtained by using both the vapour sorption and microcalorimeter testing techniques. A range of aggregate material has been tested by using both the techniques. Aggregate fractions of the following sizes are used;

- Fraction passing 5mm and retaining on 2.36mm sieve
- Fraction passing 150 μ m and retaining on 75 μ m sieve
- Fraction passing 75 μ m sieve

4.5.1 Probe Liquids

Set of three probe liquids are used for testing with both the equipment. Benzene, chloroform and heptane are used with microcalorimeter while octane, ethyl acetate and chloroform are used for testing with the DVS system. The details of the probe liquids are provided in the following table:

Table 4.3: Probes for Aggregate Analysis

Probe Liquid	γ^{LW} (erg/cm ²)	γ^+ (erg/cm ²)	γ^- (erg/cm ²)	Liquid Surface Tension, γ^T (erg/cm ²)	Liquid Density (g/cc)	Molecular Weight (g/mol)
Benzene	28.85	0	2.7	28.85	0.8765	78.11
Chloroform	27.15	3.8	0	27.15	1.492	119.38
Ethyl Acetate	23.9	0	19.2	23.9	0.90	88.11
Octane	21.62	0	0	21.62	0.703	114.23
Heptane	20.14	0	0	20.14	0.68	100.21

Probes that are chosen for aggregate analysis generally possess lower surface tension values as compared to the ones that are used for testing the bitumen. This helps in getting a uniform adsorption/monolayer of the probe on the aggregate surface. It is recommended that water may not be used with DVS as it tends to form clusters because of its high surface tension/high surface energy/high cohesion (Williams and Levoguer, SMS Application Note No. 18).

4.5.2 DVS Results

Initial trials were carried out with the dynamic vapour sorption (DVS) system to determine the surface energy parameters of the aggregates. The material is tested by using a non-polar (Octane), an acid (chloroform) and a base (ethyl acetate). The aggregate material is exposed to different concentrations/vapour pressures of the probe liquids (shown in Figure 4.1) and the increase in mass of the aggregates because of adsorption of the probe vapours on the aggregate surface is measured. The test is performed at a temperature of 25°C. The change in mass of an aggregate sample is plotted against the increasing vapour pressure values. A typical adsorption isotherm is

shown in Figure 4.2 below. BET-Brunauer-Emmett-Teller technique is used to calculate the specific surface area of the aggregate sample (Shaw, 1991 and Sing, 1969). A BET line fit plot and a plot showing change in mass of aggregate during the sorption and desorption cycle are shown in Figures 4.3 and 4.4 respectively.

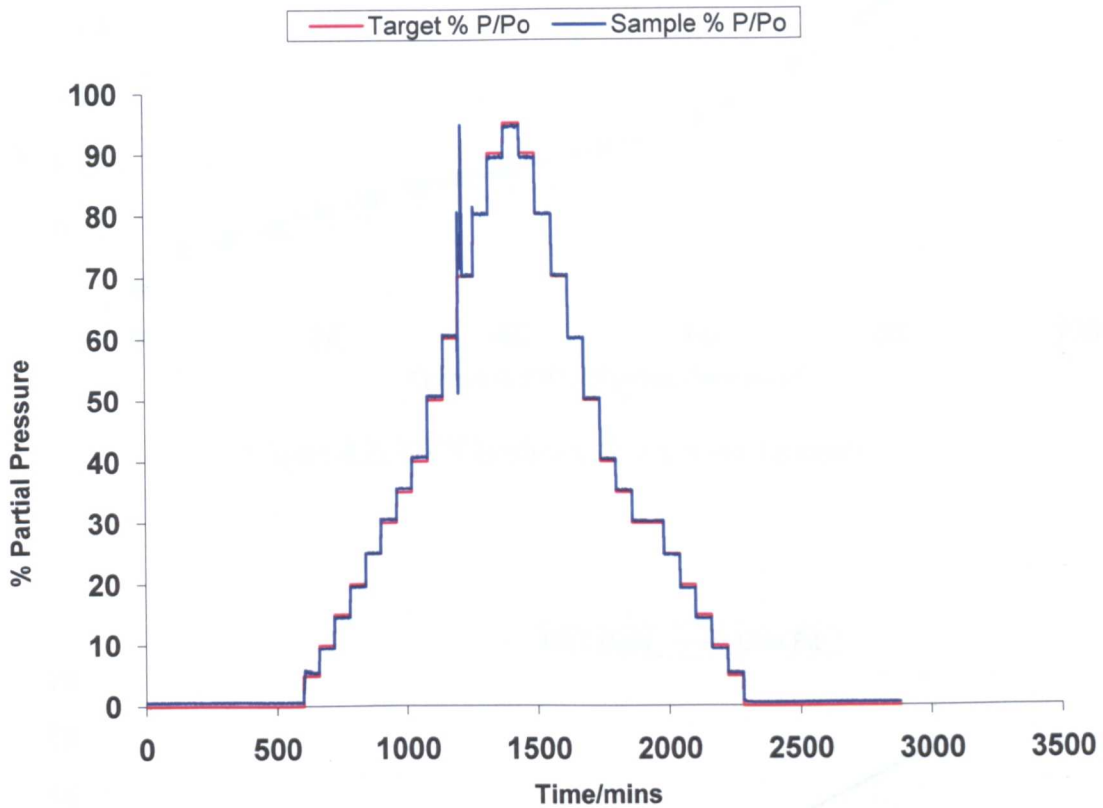


Figure 4.1: DVS Partial Pressure Plot (Limestone-Octane)



Figure 4.3: BET Line-Fit Plot

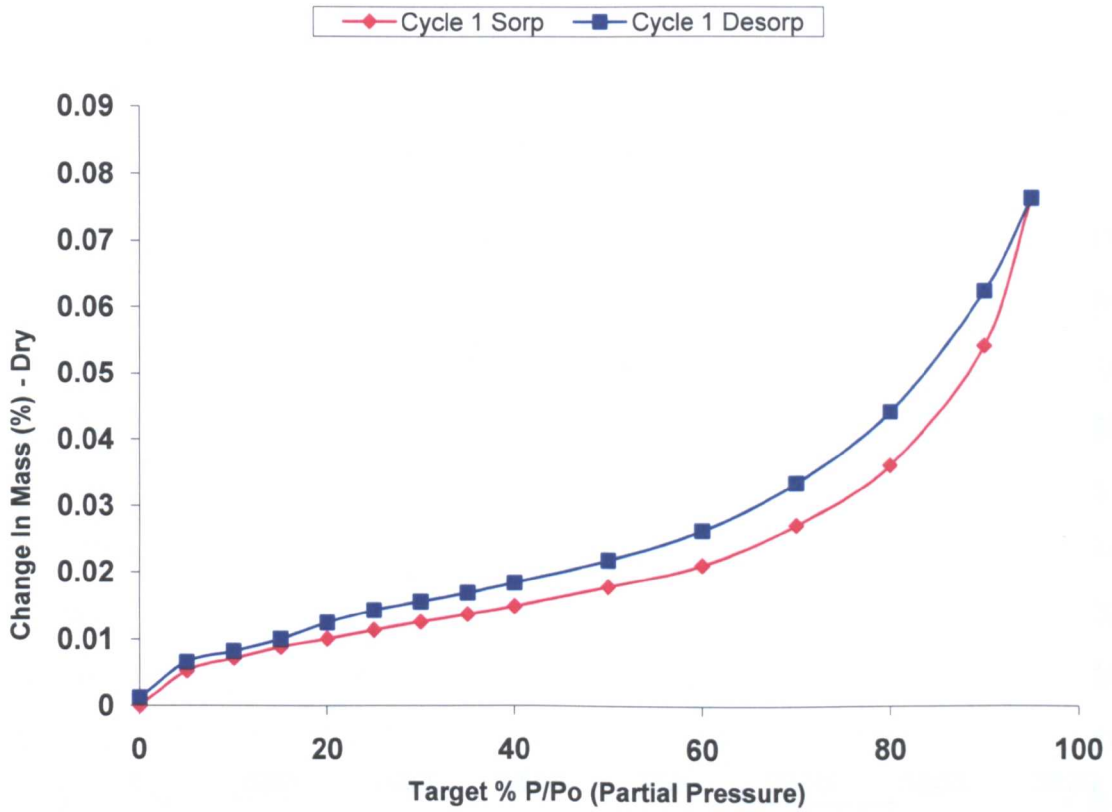


Figure 4.2: DVS Isotherm (Limestone-Octane)

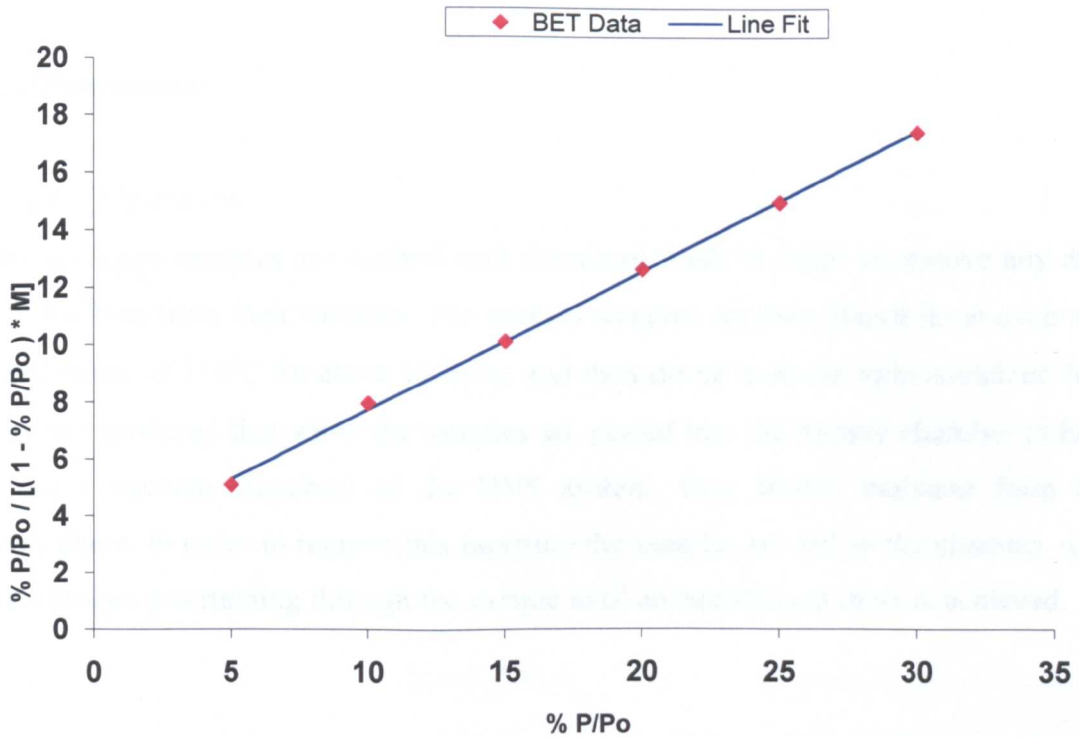


Figure 4.3: BET Line-Fit Plot

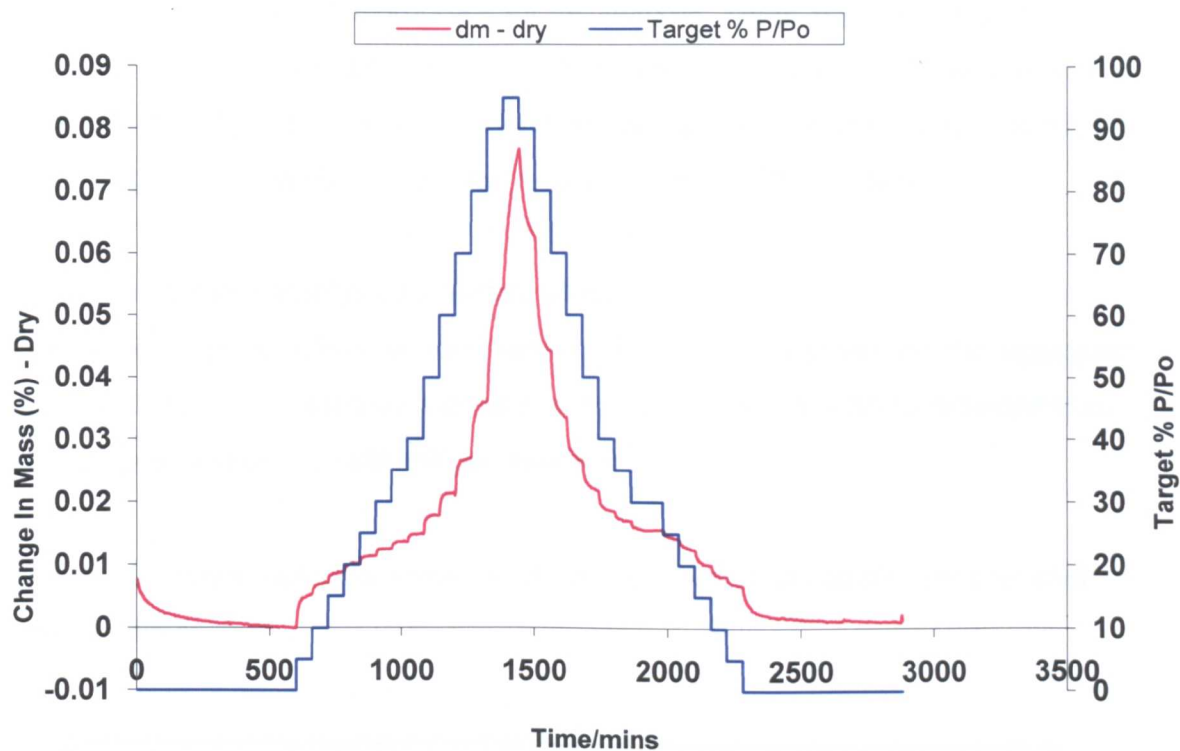


Figure 4.4: Partial Pressure and Aggregate Change in Mass

Test Parameters

Sample Preparation

The aggregate samples are washed with deionised water in order to remove any dust or impurities from their surfaces. The washed samples are then placed in an oven at a temperature of 110°C for about 16 hours and then stored in an air tight container. It is however observed that while the samples are placed into the sample chamber (which is not a vacuum chamber) of the DVS system, they absorb moisture from the atmosphere. In order to remove this moisture the samples are left in the chamber with dry nitrogen gas running through the sample until an equilibrium mass is achieved.

Sample Size

Bhasin (2006) suggested that the aggregate fractions passing 5mm sieve and retained on 2.36mm sieve are most appropriate for the analysis. These aggregate fractions have mostly been used for the analysis. The other reason for selection of this size is the limitation to the size of DVS sample chamber and sample container. A maximum of 3 grams of aggregate sample can be used for a test with the DVS system.

Adsorption Isotherm and Specific Surface Area

If the increase in adsorbed amount (mass) of the probe vapours on the aggregate surface with varying adsorptive vapour pressure is plotted for a constant temperature, an adsorption isotherm is obtained (as shown in Figure 4.2).

Typical adsorption isotherm plots for different types of materials are provided in Figure 4.5 below.

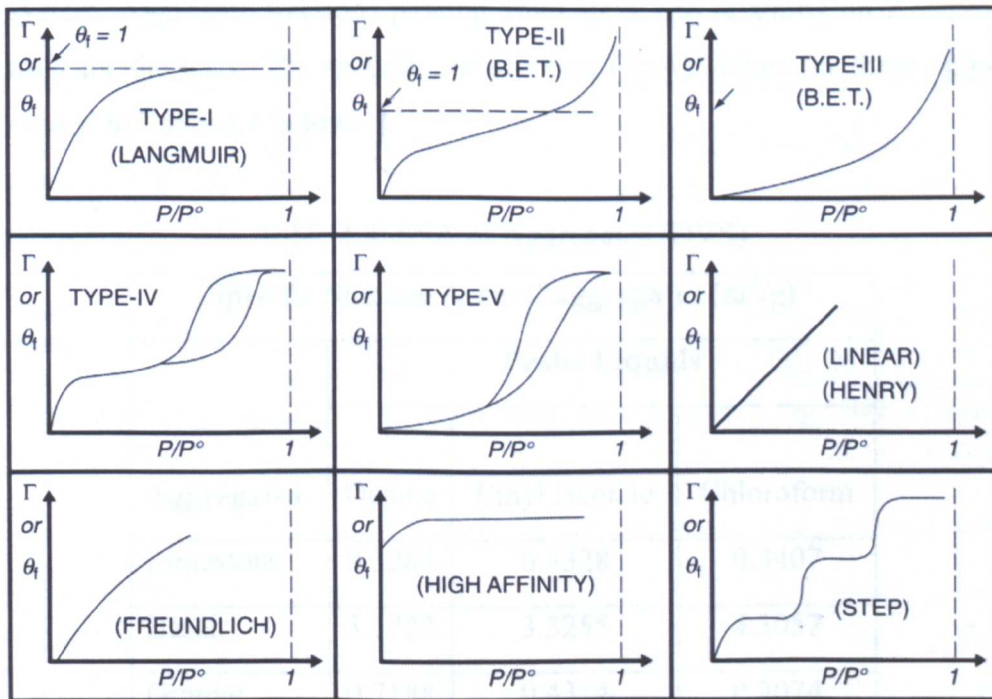


Figure 4.5: Typical Adsorption Isotherm Plots (Erbil, 2006)

Adsorption Isotherm

Type-II adsorption isotherm is always obtained for the aggregate material (shown in Figure 4.2). Adsorption isotherm from the non polar liquid (octane) is used to measure the aggregate surface area for all the three probes. Octane being non-polar in

calculate the specific surface area of a given aggregate material by using the BET technique.

Length of Sorption Cycle

It has been observed during the tests that time required for an adsorbed mass value to reach equilibrium for a given increase in adsorptive vapour pressure varies significantly between aggregates. It is important to get an equilibrium mass value for each set of increase in vapour pressure in order to get an accurate BET line fit (shown in Figure 4.3) and hence a precise value of specific surface area for the material under study. Length of sorption cycle for each increment of vapour pressure is adjusted for each type of material to obtain accurate specific surface area values.

Specific Surface Area

Three different types of aggregate materials were tested for initial analysis with the DVS system. Aggregate fractions passing 5mm sieve and retaining on 2.36mm sieve were used for the tests. The specific surface area (SSA) values for these aggregates are provided in Table 4.4 below.

Table 4.4: SSA of Aggregates (DVS)

Specific Surface Area of aggregates (m²/g)			
Aggregates	Probe Liquids		
	Octane	Ethyl Acetate	Chloroform
Limestone	0.3286	0.5328	0.3407
Basalt	3.1722	3.5255	4.3057
Granite	0.7188	0.4314	0.3074

Spreading pressures

SSA values obtained by using the Octane are then used to calculate the spreading pressures on the aggregate surfaces for all the three probes. Octane being non-polar in

nature is supposed to give true values of surface area (non-polar substances do not have affinity for the polar ones). The obtained spreading pressures are provided in Table 4.5.

Table 4.5: Aggregates Spreading Pressure Values (DVS)

Spreading Pressures (mJ/m²)			
Aggregates	Probe Liquids		
	Octane	Ethyl Acetate	Chloroform
Limestone	33.95	120.6	46.93
Basalt	23.83	55.42	50.77
Granite	26.87	36.73	18.69

Surface Energy Components

The obtained spreading pressure values are then used to calculate the surface energy components of the aggregate samples by using the calculation steps as provided in section 4.4. The final surface energy components for the three aggregates are provided in Table 4.6 below.

Table 4.6: Aggregates SE Parameters; DVS Analysis

Surface Energy Characteristics of Aggregates						
No.	Aggregate	Surface Energy Components (erg/cm²)				
		γ^{LW}	γ^+	γ^-	γ^{AB}	γ^T
1	Limestone	68.72	99.34	14.49	75.88	144.60
2	Basalt	51.68	14.12	59.82	58.13	109.81
3	Granite	56.55	1.58	1.90	3.46	60.01

Discussion

The test results indicate that there is not a big difference between the van der Waals components of the aggregates though limestone has a value slightly higher than the other two types of aggregates. The total surface energy of the limestone is also higher as compared to the others. The acid component of the limestone is higher than its base component though limestone is considered a basic material. Similarly, granite has a slightly higher basic component. The reason for these may be that the surface chemistry of the material does not always correspond to the bulk chemistry (Kim, 2009). Granite on the other hand has very small polar components and thus has a very low final surface energy value.

It was postulated that the reason for a very low total surface energy value (less than the surface tension of water) of granite could be the presence of moisture in the sample at the time of test, and that the purging of sample with dry nitrogen was not effective in removing any adsorbed moisture from the sample surface. In order to get rid of this discrepancy a sample pre-heater was installed inside the sample chamber so that the samples can be dried just before the commencement of a test and used without exposing them to the atmosphere.

The samples from the three above mentioned materials were tested again. Samples were prepared by using the same protocol as discussed earlier except that they were reheated in the sample chamber at a temperature of 110°C by using the pre-heater. The reduction in sample mass was monitored during the heating process and it was found that five hours of heating was sufficient to dry the sample and attain an equilibrium mass. The surface energy properties of the pre-heated samples are provided in Table 4.7 below.

Table 4.7: Aggregates SE Parameters (Pre-heated)

Surface Energy Characteristics of Aggregates					
Aggregate	Surface Energy Components (erg/cm²)				
	γ^{LW}	γ^+	γ^-	γ^{AB}	γ^T
Limestone	75.18	109.07	49.91	147.56	222.74
Basalt	66.66	176.03	214.92	389.01	455.67
Granite	67.78	164.22	123.37	284.67	352.45

It can be clearly seen from the table above that the values for the surface energy components have increased when the sample is completely dry. It is therefore recommended that the samples should be reheated (dried) within the sample chamber and tested immediately without removing them from the chamber in order to get accurate surface energy values.

Surface energy properties for some of the other materials which were analysed by using the DVS system are provided in Table 4.8 below.

Table 4.8: Aggregates SE Parameters (DVS)

Aggregate	Surface Energy Components (erg/cm²)				
	γ^{LW}	γ^+	γ^-	γ^{AB}	γ^T
Limestone Filler	55.27	51.57	178.07	191.66	246.93
Gritstone	40.00	5.00	131.00	51.19	91.19
Limestone	45.00	8.00	214.00	82.75	127.75
Hydrated Lime Filler	70.00	18.00	28.00	44.90	114.90

4.5.3 Microcalorimeter Results

Dynamic vapour sorption technique only accounts for the physical adsorption of probes vapours on the surface of aggregate samples. However in case of materials like limestone and other active fillers like hydrated lime filler, chemical interactions may take place. Also, the adhesion of these materials with the bitumen samples can be a

combination of both physical and chemical interactions. Bhasin (2006) proposed the use of microcalorimeter to quantify these adhesions. The enthalpy of immersion of an aggregate sample with different probe liquids is measured with the help of a microcalorimeter which is then used to calculate the surface energy properties of the aggregates. The ratio of number of atoms on a solid (aggregate) surface to the number of atoms in the bulk of the material can be quite small. Also aggregates can be quite heterogeneous chemically because of the presence of different mineral crystals and impurities on the surface (Erbil, 2006). As the aggregate samples are immersed in the probe liquid during the enthalpy of immersion measurements in a calorimeter test, this technique is supposed to produce true surface energy properties of the materials. Fine/crushed aggregate samples may give higher exothermic heat when immersed in probe liquids and probably a true value for interaction with the probes. However, it may be argued that a powdered sample is not a true representation of the aggregates in an asphalt mixture.

A typical heat flow curve that is obtained during a microcalorimeter test is shown in Figure 4.6. It can be seen from the figure that the heat flow is constant before the injection of probe liquids into the system. It increases rapidly when the probes are injected and decreases slowly until the equilibrium is reached again. The total heat is calculated by integrating the area under the heat flow curve.

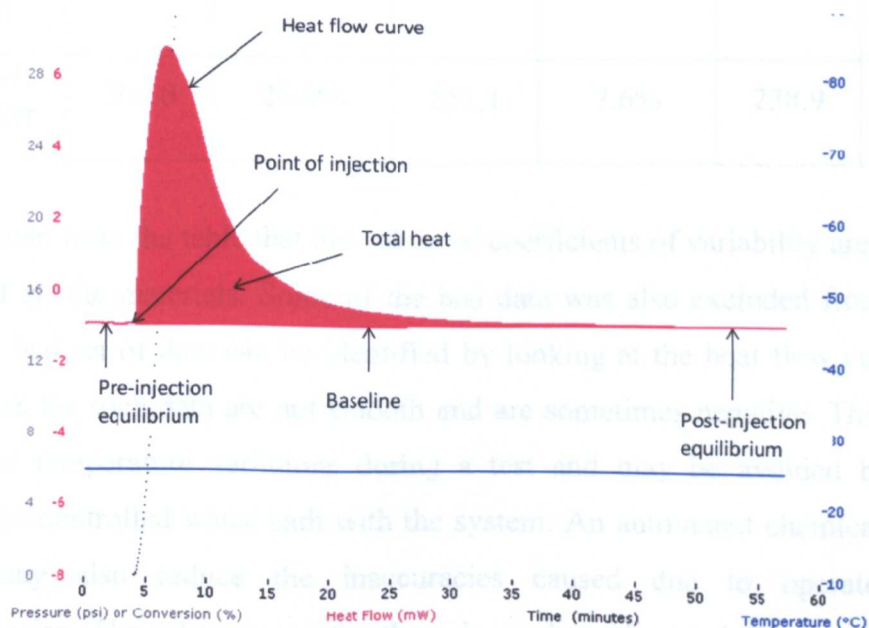


Figure 4.6: A Typical Heat Flow Curve

Different size fractions of three different types of materials were tested by using three probe liquids (chloroform, benzene and heptane). The values for enthalpy of immersion along with the coefficients of variability for the tested materials are provided in Table 4.9 below.

Table 4.9: Heat of Immersion (ergs/g)

Aggregate	Chloroform		Benzene		Heptane	
	Average	Coefficient of Variability	Average	Coefficient of Variability	Average	Coefficient of Variability
Gritstone (2.36-5mm)	101.2	10.0%	127.4	6.8%	64.1	14.2%
Gritstone (75-150 μ m)	363.0	28.3%	426.7	3.1%	161.5	42.8%
Gritstone passing (75 μ m)	53.0	33.6%	108.0	7.8%	63.7	1.6%
Limestone (2.36-5mm)	87.4	26.3%	125.4	36.4%	52.9	136.7%
Limestone (75-150 μ m)	24.1	126.6%	85.5	16.4%	50.4	48.2%
Limestone passing (75 μ m)	111.4	28.1%	86.9	17.4%	90.7	10.3%
Hydrated Lime Filler	200.0	26.4%	251.1	7.6%	238.9	20.3%

It can be seen from the table that the values of coefficients of variability are quite high for almost all the materials. Some of the bad data was also excluded from the final results. A bad set of data can be identified by looking at the heat flow curves. Heat flow curves for such data are not smooth and are sometimes negative. This could be because of temperature variations during a test and may be avoided by using a temperature controlled water bath with the system. An automated chemical injection system may also reduce the inaccuracies caused due to operator related inconsistencies. The other reason for these inconsistencies could be the presence of moisture in the samples.

These discrepancies were more profound for coarse aggregates probably because of smaller surface area of the samples and smaller heat of immersion values. Smaller size fractions with higher surface areas were less sensitive to these variations. For the above mentioned reasons, dynamic vapour sorption system has been used for measuring the surface energy properties of the aggregates for the rest of this research. It is however recommended that the microcalorimeter test procedure is improved on the basis of the suggestions made earlier in this section in order to get consistent data with the equipment, as it is quite a quick technique to obtain the surface energy properties of the aggregates as compared to the vapour sorption method.

CHAPTER 5

BITUMEN-AGGREGATE ADHESION AND MOISTURE SENSITIVITY

5.1 Introduction

The surface energy properties of the bitumen and the aggregates on their own have very little significance. However, when combined thermodynamically they help compute the interfacial work of adhesion between the two materials. Effect of water or moisture on the interfacial work of adhesion (intrinsic adhesion) can also be studied by using these parameters. These parameters can therefore be used to assess the moisture sensitivity of an asphalt mixture.

This chapter discusses the parameters that are used to assess the moisture sensitivity of a bitumen-aggregate combination.

5.2 Bond Energy Parameters

Surface energy properties of the bitumen and the aggregates are used to determine the following parameters:

Binder Cohesion: It is the cohesive bond strength of the binder material and is twice the total surface energy of the material.

Dry Bond Strength: It is the interfacial work of adhesion between the bitumen and aggregate. A bigger value of this parameter means greater adhesion between the two materials and hence more resistance against debonding. Equation for calculation of dry bond strength is provided in chapter 2 (see section 2.9.4, equation 19).

Work of Debonding: It is the reduction in bond strength of a bitumen-aggregate system when water is introduced into the system or in other words, when water displaces the bitumen from the aggregate surface. A smaller value of this parameter for a given bitumen-aggregate system is indicative of a better moisture damage performance of that system. Mathematical interpretation of this parameter is provided in chapter 2 (see section 2.9.4, equation 27).

A combination of these parameters can be used to assess the moisture susceptibility of a given bitumen-aggregate system.

5.3 Moisture Sensitivity Parameters

In addition to the above mentioned parameters, adsorption of bitumen into the aggregate may depend on several other factors including the total volume of permeable pore space, the size of the pore openings and surface texture of the aggregates. Rougher aggregate surfaces provide a good lock with bitumen and can have better adhesion characteristics. These factors can be slotted into the equation by including surface area of the aggregate material with the above mentioned parameters.

Bhasin (2006) incorporated and arranged the above mentioned parameters into four different types of ratios referred to as bond energy ratios, for moisture sensitivity analysis of different bitumen-aggregate combinations. These four types of moisture sensitivity analysis parameters are given as follows:

Parameter No. 1:

$$R_1 = \left| \frac{\Delta G_{BA}}{\Delta G_{BWA}} \right|$$

It is the ratio of dry to wet bond strength of the bitumen-aggregate combination. This is equation 28, explained earlier in chapter 2 (section 2.9.5). It is also referred as the compatibility ratio for a bitumen-aggregate system.

Parameter No. 2:

$$\left| \frac{\Delta G_{BA}}{\Delta G_{BWA}} \right| \times SSA(\text{Aggregate} \cdot \text{Surface} \cdot \text{Area})$$

Parameter No. 1 is multiplied with the specific surface area of the aggregates in order to accommodate the effects of aggregate surface roughness on the final adhesion.

A rougher aggregate surface will have a higher specific surface area and will provide good interlocking spaces for the bitumen.

Parameter No. 3:

$$R_2 = \left| \frac{\Delta G_{BA} - \Delta G_{BB}}{\Delta G_{BWA}} \right|$$

Bitumen cohesive bond strength (ΔG_{BB}) is used in the parameter in order to account for the wettability ($\Delta G_{BA} - \Delta G_{BB}$) of the binder. For a given aggregate surface, bitumen with greater wettability will better coat the aggregate surface leaving fewer weak places for the water to penetrate and cause stripping.

Parameter No. 4:

$$\left| \frac{\Delta G_{BA} - \Delta G_{BB}}{\Delta G_{BWA}} \right| \times \sqrt{SSA}$$

Aggregate specific surface area is again introduced giving a fourth parameter. Square root of the surface area is taken on the basis of the principle of catalysis. According to this principle the rate of diffusion in micro porous materials is proportional to the square root of the specific surface area (Bhasin, 2006). It is believed that this parameter best simulates the moisture sensitivity results obtained through other laboratory tests (Bhasin, 2006).

Individual or combinations of these parameters are used to assess the moisture sensitivity of asphalt mixtures.

5.4 Bitumen-Aggregate Combinations and Moisture Sensitivity

The bitumen and the aggregates surface energy data is combined in order to assess the moisture damage performance of a given combination by using the above mentioned four parameters. The analysis gives an insight into the compatibility between different set of materials.

The surface energy parameters for three different types of bitumen samples that have been used for the comparability analysis are provided in Table 5.1 below. The values for the aggregates have already been provided in Table 4.7.

Table 5.1: Binder Surface Energy (Compatibility Analysis)

Bitumen	Surface Energy Components (mJ/m ²)					Cohesive Bond Strength (mJ/m ²)
	γ^{LW}	γ^+	γ^-	γ^{AB}	γ^T	
15pen	31.05	0.01	3.37	0.37	31.42	62.80
50pen	30.61	0.00	2.40	0.00	30.61	61.20
100pen	19.06	0.00	0.78	0.00	19.06	38.10

The adhesive bond strengths for both the dry and the wet conditions have been calculated as explained in section 2.9.4. The compatibility ratios (ratio of dry to wet bond strength) of the material combinations are calculated and provided in Table 5.2 below.

Table 5.2: Bitumen-Aggregate Compatibility Ratios

Adhesive Bond Strength in Dry and Wet conditions and Compatibility Ratio									
Bitumen	Aggregate								
	Limestone			Basalt			Granite		
	Dry	Wet	Compatibility Ratio	Dry	Wet	Compatibility Ratio	Dry	Wet	Compatibility Ratio
	(ΔG_{BA})	(ΔG_{BWA})	$\left \frac{\Delta G_{BA}}{\Delta G_{BWA}} \right $	(ΔG_{BA})	(ΔG_{BWA})	$\left \frac{\Delta G_{BA}}{\Delta G_{BWA}} \right $	(ΔG_{BA})	(ΔG_{BWA})	$\left \frac{\Delta G_{BA}}{\Delta G_{BWA}} \right $
15pen	136	-47	2.89	143	-141	1.01	141	-103	1.37
50pen	128	-51	2.52	131	-148	0.89	131	-109	1.20
100pen	94	-68	1.39	95	-168	0.57	95	-128	0.74

Table 5.3 provides the moisture sensitivity analysis parameters obtained for all the bitumen-aggregate combinations. A higher value of the parameter is indicative of a better moisture damage performance of that bitumen-aggregate combination.

Table 5.3: Parameters to Predict the Moisture Susceptibility of a Bitumen-Aggregate System

Moisture Sensitivity Analysis Parameters					
Bitumen	Aggregates				
	Limestone				
	1	2	3	4	
	R_1	$R_1 \times SSA$	R_2	$R_2 \times \sqrt{SSA}$	
	$ \Delta G_{BA}/\Delta G_{BWA} $	$ \Delta G_{BA}/\Delta G_{BWA} \times SSA$	$ \Delta G_{BA}-\Delta G_{BB})/\Delta G_{BWA} $	$ \Delta G_{BA}-\Delta G_{BB})/\Delta G_{BWA} \times \sqrt{SSA}$	
	15pen	2.89	0.49	1.56	0.64
50pen	2.52	0.43	1.31	0.54	
100pen	1.39	0.24	0.82	0.34	
	Basalt				
	1	2	3	4	
	R_1	$R_1 \times SSA$	R_2	$R_2 \times \sqrt{SSA}$	
	$ \Delta G_{BA}/\Delta G_{BWA} $	$ \Delta G_{BA}/\Delta G_{BWA} \times SSA$	$ \Delta G_{BA}-\Delta G_{BB})/\Delta G_{BWA} $	$ \Delta G_{BA}-\Delta G_{BB})/\Delta G_{BWA} \times \sqrt{SSA}$	
	15pen	1.01	1.80	0.57	0.76
	50pen	0.89	1.59	0.47	0.63
100pen	0.57	1.02	0.34	0.45	
	Granite				
	1	2	3	4	
	R_1	$R_1 \times SSA$	R_2	$R_2 \times \sqrt{SSA}$	
	$ \Delta G_{BA}/\Delta G_{BWA} $	$ \Delta G_{BA}/\Delta G_{BWA} \times SSA$	$ \Delta G_{BA}-\Delta G_{BB})/\Delta G_{BWA} $	$ \Delta G_{BA}-\Delta G_{BB})/\Delta G_{BWA} \times \sqrt{SSA}$	
	15pen	1.37	0.61	0.76	0.51
	50pen	1.2	0.53	0.64	0.43
100pen	0.74	0.33	0.44	0.29	

It is concluded from the results that for the combination of materials under study the stiffer binders would perform well under moisture as they exhibit higher compatibility values with aggregates as compared to the softer binders. This can also be seen from Figures 5.1 and 5.2 below.

Values obtained from bond ratio parameter 3 shows that limestone would perform far better as compared to the other two aggregates, as shown in Figure 5.1. However, when the surface area parameter is introduced into the equation the basalt because of its high surface area moves up on the plot, as shown in Figure 5.2.

Results show that granite is probably more susceptible to moisture damage as compared to the limestone and basalt. This is in accordance with the general perception for this material regarding its moisture damage performance.

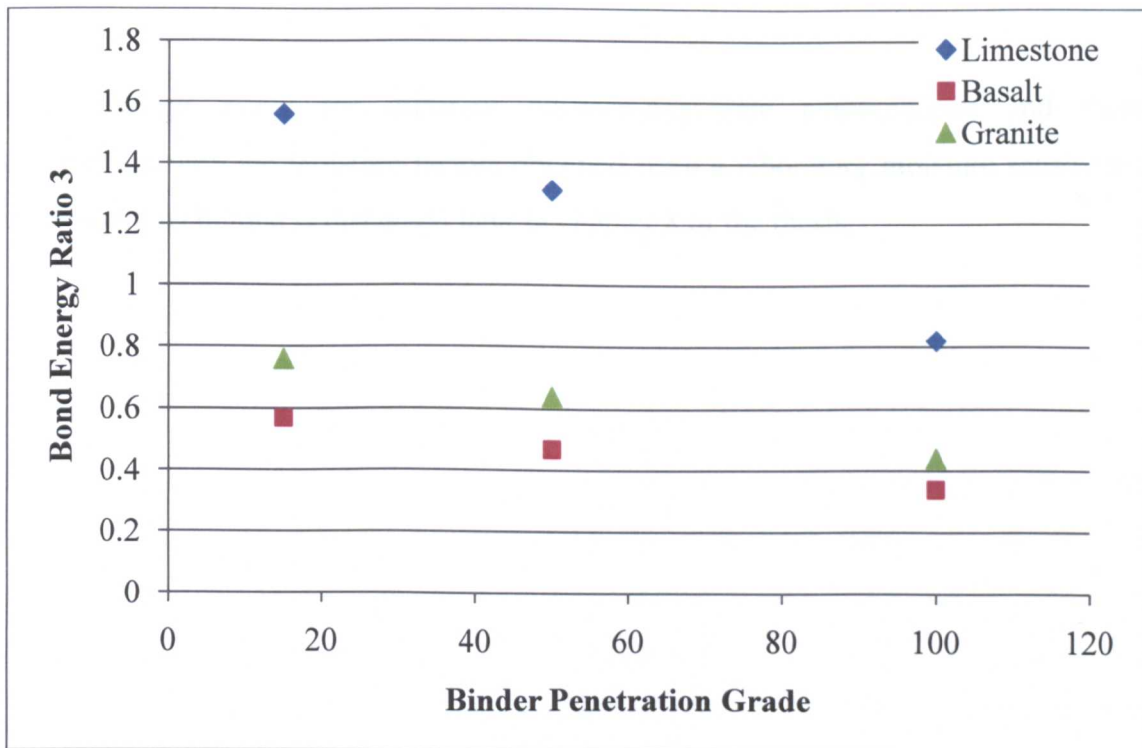


Figure 5.1: Bitumen-Aggregate Compatibility Ratio 3

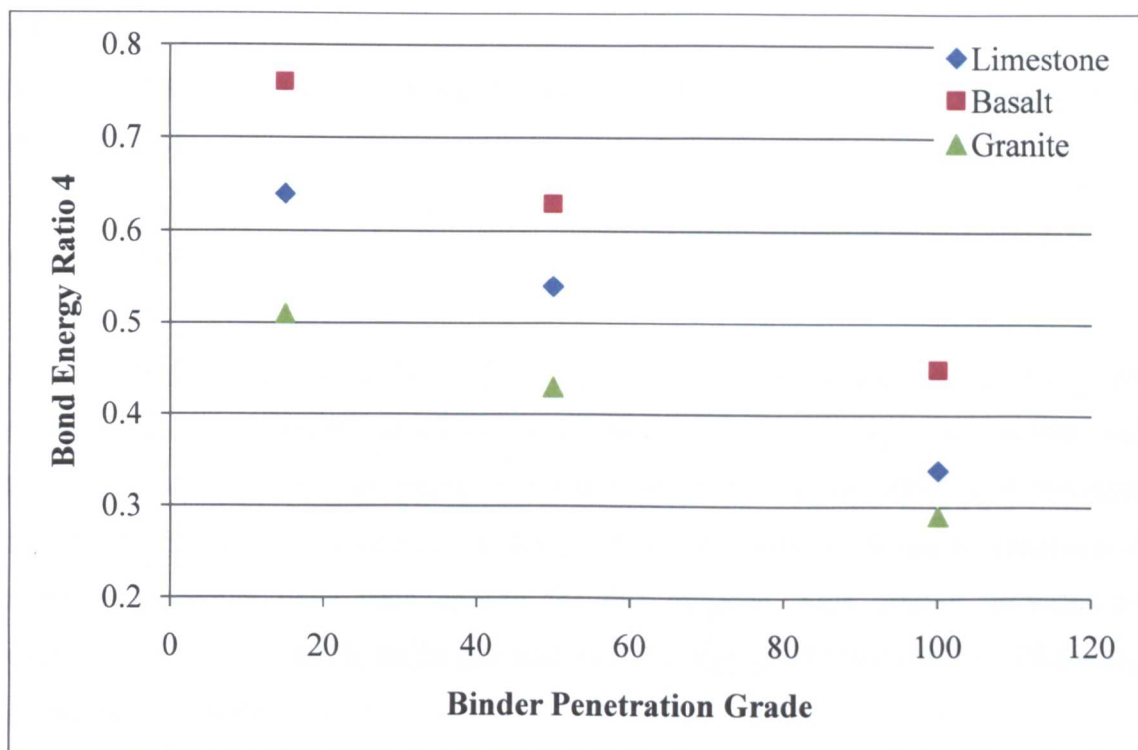


Figure 5.2: Bitumen-Aggregate Compatibility Ratio 4

Bond energy ratios for different bitumen-aggregate combinations and their comparison with the moisture factors obtained from a laboratory moisture sensitivity assessment technique is discussed later in chapter 8 of the thesis.

CHAPTER 6

MOISTURE DAMAGE PERFORMANCE OF ASPHALT USING SATS PROTOCOL

6.1 Introduction

It is important to correlate the surface energy results with ones obtained by using some mechanical moisture sensitivity assessment technique in order to validate and fully characterise the surface energy method of material analysis. The SATS moisture sensitivity protocol and testing technique together with a dynamic mechanical analysis procedure have been chosen for this purpose. This section provides an overview of the SATS test technique and includes the results from the SATS testing of asphalt materials.

The Saturation Ageing Tensile Stiffness (SATS) test is the first procedure of its kind that combines the ageing and water damage mechanisms to which an asphalt pavement is subjected in service within a single laboratory test. SATS makes use of tried and tested methods of assessment (based on mixture stiffness) that have been developed to meet the specific objectives.

The SATS procedure involves conditioning five pre-saturated specimens simultaneously in a pressure vessel under 2.1MPa air pressure at a temperature of 85 °C for a period of 65 hours. This conditioning is followed by a cooling period of 24 hours before the air pressure is released and the vessel opened to remove the specimens for stiffness testing. This procedure has been found to successfully reproduce the loss in stiffness observed with high modulus asphalt material laid on a trial site at TRL (Collop et al. 2004a), and to distinguish between this poor performing material and an alternative mixture incorporating aggregate with a good durability track record, when manufactured at 4 % binder content and 8 % air voids (Choi et al, 2002, Airey et al. 2003, Collop et al. 2004b and Choi, 2005).

It has also been shown that the SATS test ranked mixtures in terms of moisture sensitivity, in the same order as the AASHTO T283 procedure (Anon, 2000), although the relative performance of a mixture containing a moisture sensitive

aggregate was significantly lower in the SATS test (Airey et al., 2006). As a result of these and further studies, the SATS test was adopted by the Highways Agency in the UK as a “type test” to assess the likelihood of moisture-induced damage for different aggregate types (Anon, 2004).

Experimental work was carried out using 15 and 50pen binders and 4 different aggregate types, referenced to as A, B, C and D. Aggregate type A is basic and is believed to perform well in moisture sensitivity tests. Aggregate type B is acidic, and was not expected to perform as well. Aggregate type C was also acidic, but with a track record of successful use in surface course material, and was expected to have intermediate behaviour. The final material used (Aggregate type D) had been found to perform poorly in previous moisture sensitivity work and was used as a benchmark for identification of ‘poor’ aggregates.

6.2 SATS Protocol

Figures 6.1a & 6.1b show the SATS pressure vessel and the tray used in the test. The main features of the test are as follows:

- A well insulated heated pressure vessel capable of holding 5 compacted asphalt specimens (100mm diameter × 60mm height) is used (BSI 2003a).
- The set-up allows simultaneous pressure & temperature control.
- Asphalt specimens which have been pre-saturated with water (under vacuum) are located on a purpose built tray.
- A pre-determined quantity of water is placed in the vessel so that the bottom specimen is fully immersed during the test.
- Five specimens are tested simultaneously under 2.1MPa air pressure at a temperature of 85°C for a duration of 65hrs. This is followed by a cooling down period of 24hrs before the pressure is released and the vessel opened to remove the specimens for stiffness testing.
- The SATS test conditions were specifically selected to be similar to the HiPAT bitumen ageing protocol.



Figure 6.1a: SATS Pressure Vessel

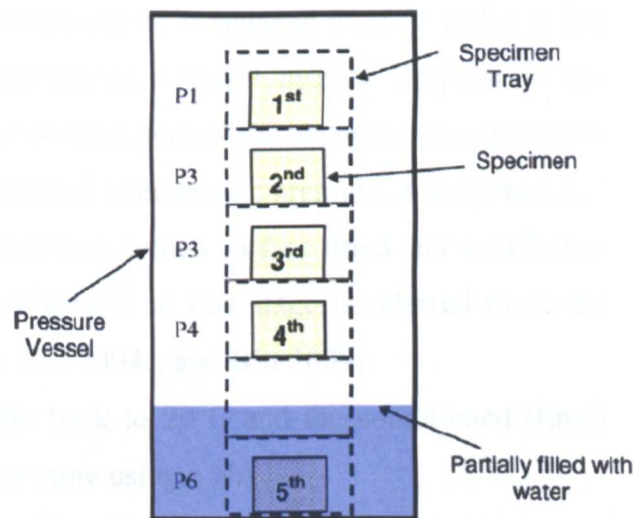


Figure 6.1b: SATS Specimen Tray

6.2.1 Summary of Test Procedure

- 1) The unconditioned (initial) indirect tensile stiffness modulus of each asphalt specimen is determined at 20°C using a Nottingham Asphalt Tester (NAT) in accordance with BS EN 12697-26 Annex C (124msec rise time, 5µm peak transient horizontal diametric deformation) (BSI 2004b).

- 2) The dry mass of each specimen is next determined by weighing.
- 3) The specimens are subsequently immersed in distilled water at 20°C and saturated using a residual pressure of 33kPa (i.e. 68kPa below atmospheric pressure) for 30 minutes.
- 4) The wet mass of each specimen is next determined by weighing, and the percentage saturation of each specimen calculated, referred to as “initial saturation”.
- 5) The SATS pressure vessel is partly filled with distilled water (water level between sample positions P4 and P5). The pressure vessel and water are maintained at the target temperature of 85°C for at least 2 hours prior to introducing the specimens.
- 6) The saturated asphalt specimens are then placed into the pressure vessel, the vessel is sealed and the air pressure is gradually raised to 2.1MPa.
- 7) The specimens are maintained at the testing conditions, i.e. 2.1MPa and 85°C, for 65 hours.
- 8) After 65 hours, the target vessel temperature is reduced to 30°C and it is left for 24 hours to cool. When the pressure vessel display temperature has reduced to 30°C (after the 24 hour cooling period) the air pressure is gradually released. When the vessel has achieved atmospheric pressure, it is opened and the specimens removed. Each specimen is then surface dried and weighed in air. The percentage saturation calculated at this stage is referred to as the “retained saturation” (BSI 2003b, BSI 2004c, and BSI 2009).
- 9) The specimens are finally brought back to 20°C and the conditioned (final) stiffness modulus determined once more using a NAT.
- 10) The ratio of the final stiffness modulus / initial stiffness modulus can thus be calculated, and is referred to as the “retained stiffness modulus”.

6.3 Testing and Material Variables

There are three testing variables that can be altered in the SATS protocol. These are pressure, temperature and duration. In order to establish a reference for comparison, control tests were firstly carried out using the standard protocol of 65 hours, 85°C and 2.1MPa pressure.

Tested Combinations

- Pressure: 2.1MPa, 1.0MPa, 0.5MPa and 0MPa
- Temperature: 85°C, 60°C and 30°C
- Duration: 65 hours, 24 hours and 4 hours
- Aggregate type: Limestone, Granite, Porphyritic Andesite (Granite) and
a
'poor' Granite
- Binder type: 15pen and 50pen
- Binder Content: 4% by mass and 5% by mass
- Air void content: 8-10% air voids and 4-6% air voids

A total of 48 combinations were tested by varying different parameters. Some of these combinations were then selected for the recovery of binder from the respective cores and the determination of the surface energy properties. The surface energy results of these materials and their correlation with the SATS results are provided and discussed in the proceeding chapters.

During the SATS testing exercise, four different aggregate types were tested. Table 6.1 shows a summary of the expected properties of the different aggregate types.

Table 6.1: Aggregate Properties

Aggregate Source	General Classification	Acid/Base	Adhesion with Bitumen	Road Performance
A	Limestone	Basic	Very good	Best
B	Granite	Acidic	Fair	Ok
C	Granite	Acidic	Fair	Ok
D	Granite	Acidic	Poor	Poor

Material was obtained from each source and characterised in terms of its size fractions. Mixture designs were then made in order to manufacture a 0/32 mm Dense Base material (BSI 2005), which is the material that was used during this testing. The grading curves for the four different aggregate types are given in Figure 6.2.

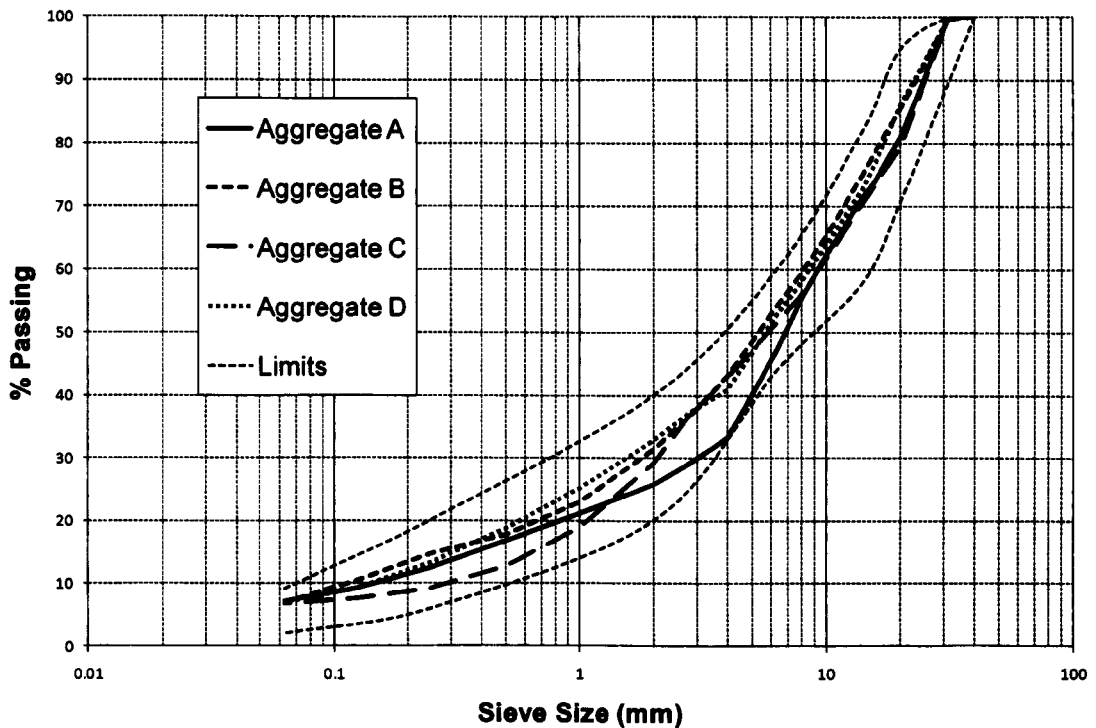


Figure 6.2: Gradation Curves for All Aggregate Types

Roller compacted slabs manufactured with 4% binder content for the SATS investigation were compacted to achieve air void contents in subsequently recovered cores of between 8 and 10 % by volume. Only cores that achieved this target were selected for SATS runs in this investigation. However, in order to investigate the effect of air void content on SATS performance, slabs manufactured with 5% binder content were compacted to achieve both 8-10% and 4-6% air voids by volume and both conditions were subsequently tested (BSI 2003b, BSI 2003c and BSI 2009).

6.3.1 Effect of Changing Individual Parameters

During this SATS investigation, the effects of many variables were studied. In the following sections, each of the variables will be dealt with in turn and, where the effect of more than one variable has been investigated simultaneously, analysis will be included in the most appropriate section. This has been done to try to discuss the results in the most logical order.

The initial part of this SATS investigation involved a series of tests carried out using the standard conditions that were selected for the previous research, based on

specimens made using a 15pen binder. Initial tests were carried out on 15 and 50pen bitumen specimens made from the four different aggregate types. This was done to firstly check that the same results would be obtained with the materials used, to those obtained from the previous investigation with the 15pen binder. This was then repeated with specimens made using 50pen binder to see the effect that the standard SATS parameters would have, as they were expected to be too harsh.

Binder Type

As can be seen from Figure 6.3, the specimens from Aggregates A, B and C all performed well under the standard conditions, all having retained stiffness values of 0.7 or higher for specimens above water in the pressure vessel. The specimens from Aggregate D, however, had retained stiffnesses generally less than 0.5 of their original values, most being 0.3 or lower.

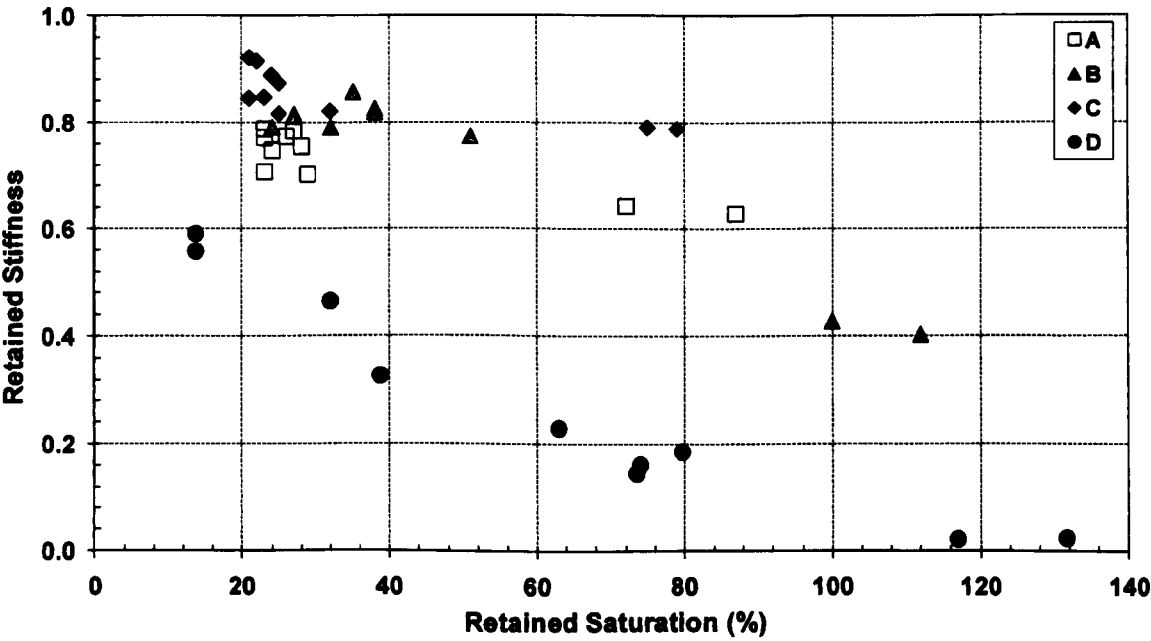


Figure 6.3: SATS results for specimens from different aggregate type made using 15pen binder and tested under standard conditions (85°C, 65 hours and 2.1MPa)

The 50pen specimens tested under the standard conditions all performed much worse, with the retained stiffness values ranging from 0.6 to 0.3 for Aggregate B specimens and 0.5 to 0.2 for Aggregate D specimens (see Figure 6.4). The other thing to notice

from the figure is that the Aggregate B and D specimens have much higher retained saturation values than the Aggregate A and C material.

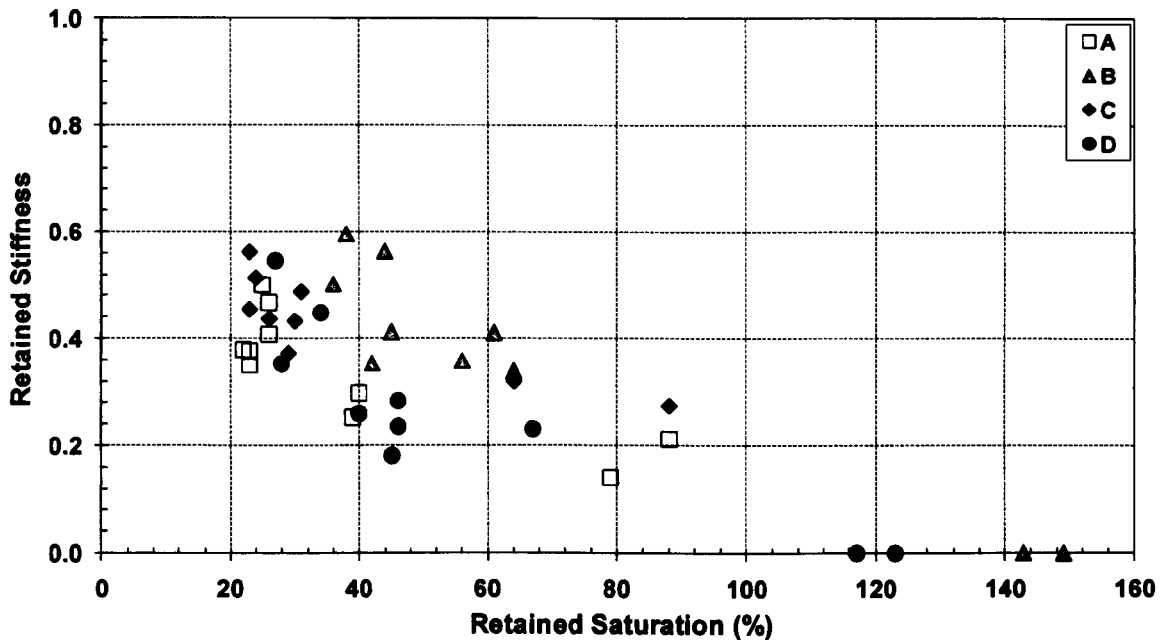


Figure 6.4: SATS results for specimens from different aggregate type made using 50pen binder and tested under standard conditions (85°C, 65 hours and 2.1MPa)

Figure 6.5 shows the reduction in retained stiffness for Aggregate A material when changing the binder from 15 to 50pen: the retained stiffness values fall from a range of 0.7-0.8 to 0.3-0.5. This figure illustrates the scope of the investigation: specifically, to find conditions which are less harsh, to bring values of retained stiffness for 50pen specimens up to comparable values for the 15pen specimens, under the standard conditions, and still be able to distinguish between a good and poor quality aggregate in terms of sensitivity to moisture damage.

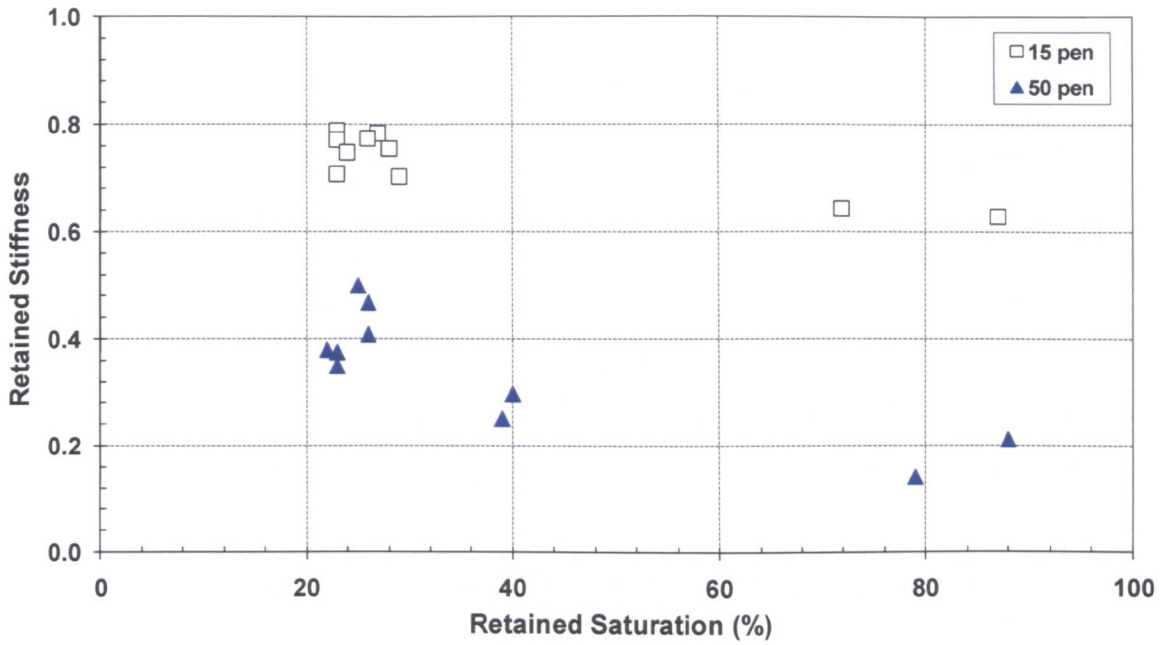


Figure 6.5: SATS results for Aggregate A specimens made using 15 and 50pen binders and tested under standard conditions (85°C, 65 hours and 2.1MPa)

Pressure

The first parameter to be altered was pressure. It was thought that a reduction of pressure was the obvious choice to make the conditions less harsh. Figure 6.6 shows 50pen Aggregate A specimens tested under standard conditions of both temperature and duration, but reducing the pressure from 2.1MPa, to 1.0MPa, 0.5MPa and then atmospheric pressure. It can be seen that the retained stiffness increases with decreasing pressure, with the specimens tested at atmospheric pressure having retained stiffness values of the order of 0.7. It can also be seen that there is no significant difference between specimens tested at 1.0MPa, 0.5MPa or atmospheric pressure.

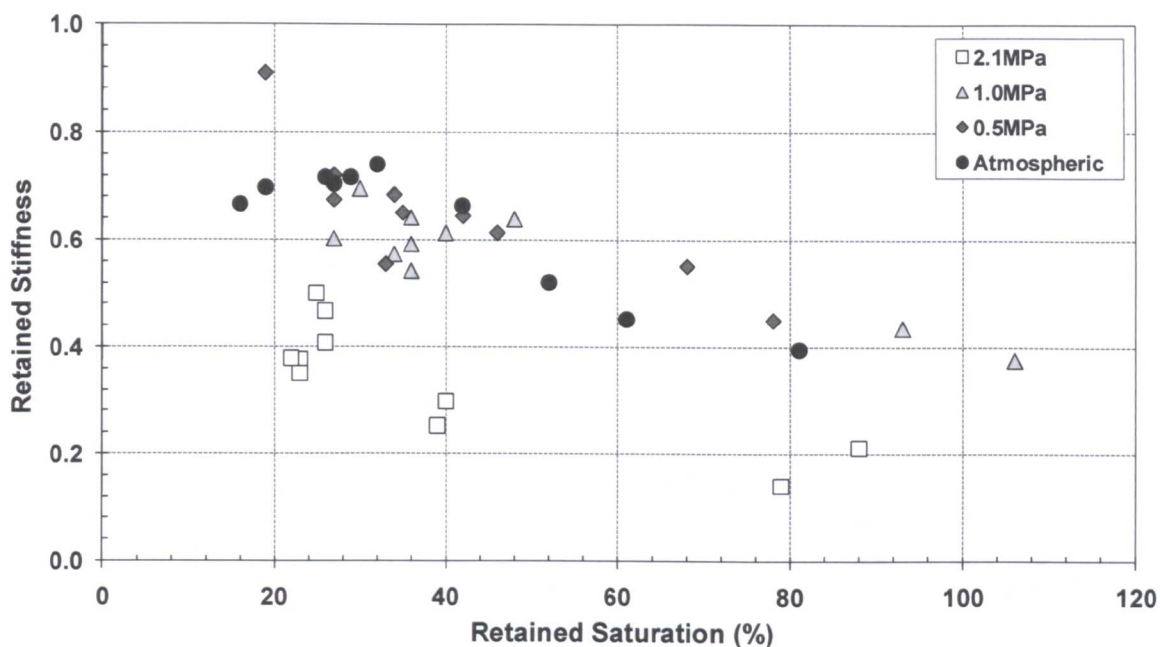


Figure 6.6: SATS results for 50pen Aggregate A specimens tested under different pressures for 65 hours at 85°C

To see how the reduction of the pressure influenced different aggregate types, Aggregate B material was also subjected to a reduction in pressure (see Figure 6.7). It was decided that only 0.5MPa and atmospheric pressure would be tested. The specimens tested at 0.5MPa showed higher retained stiffness compared with specimens tested under standard conditions, as would be expected; however the specimens tested at atmospheric pressure actually exhibited similar retained stiffness to those tested at 2.1MPa.

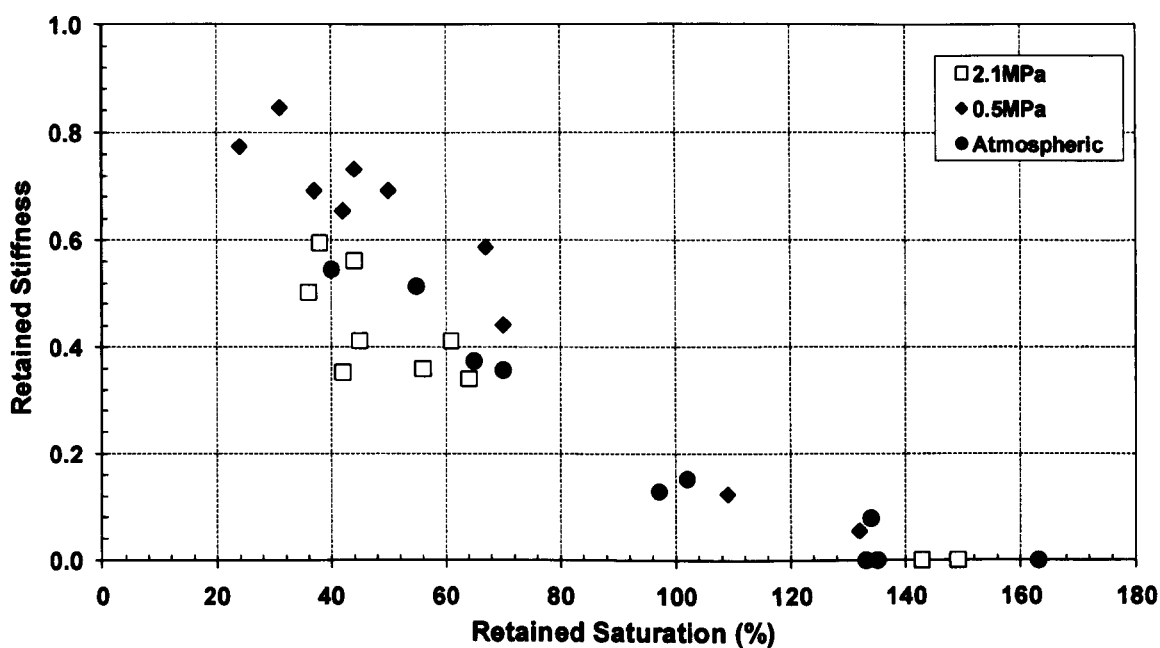


Figure 6.7: SATS results for 50pen Aggregate B specimens tested under different pressures for 65 hours at 85°C

Aggregate D specimens were also subjected to testing at different pressures. It is interesting to note that there is no significant increase in the retained stiffness values for the specimens tested at 0.5MPa as compared with those tested at 2.1MPa, as was seen for the other aggregate types. Aggregate D was expected to behave badly as it was considered to be a moisture susceptible aggregate from the previous SATS research. It seems that this is the case here as the reduction in pressure has not led to an increase in retained stiffness.

Temperature

The effect of temperature was investigated by using the standard conditions of 65 hours and 2.1MPa pressure, but reducing the temperature from 85°C to 60°C and 30°C. It can be seen from Figure 6.8 that specimens tested at 60°C and 30°C have slightly lower retained stiffnesses, but it can also be seen that the retained saturations of these specimens is also reduced slightly. It would appear that although less damage would be expected at the lower temperatures, the dominant factor is that due to the reduced temperature, less ageing of the binder occurs and therefore the stiffness of the binder and consequently the stiffness of the mixtures is lower compared to

those tested at 85°C. Conversely, for the submerged specimens, it can be seen that greater damage occurs at higher temperature as the influence of ageing is less significant.

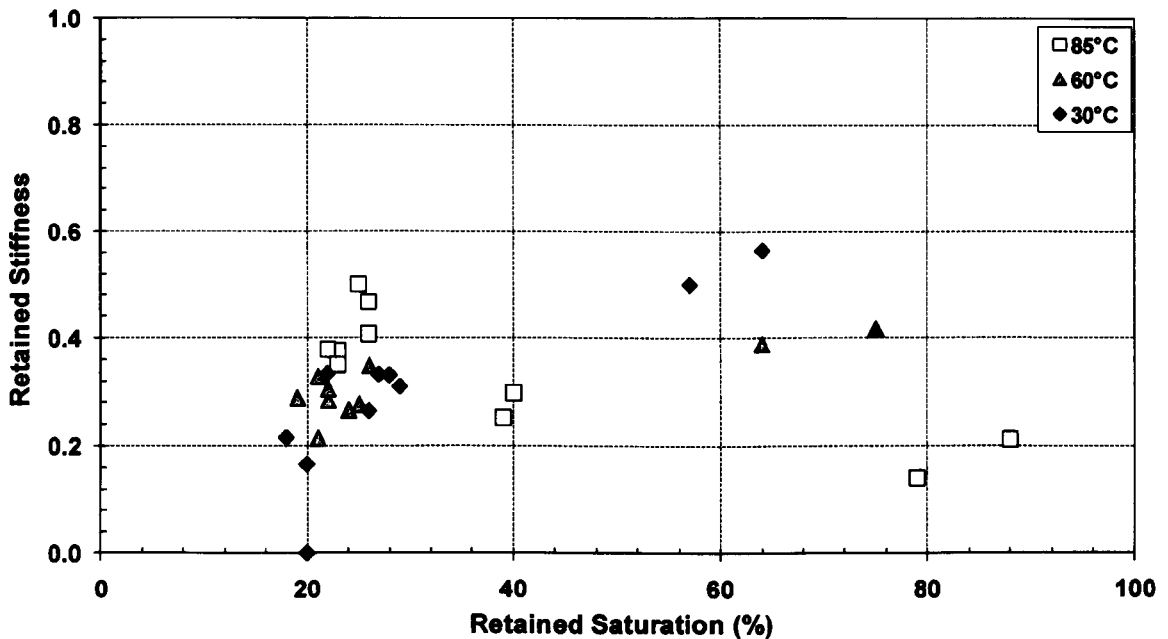
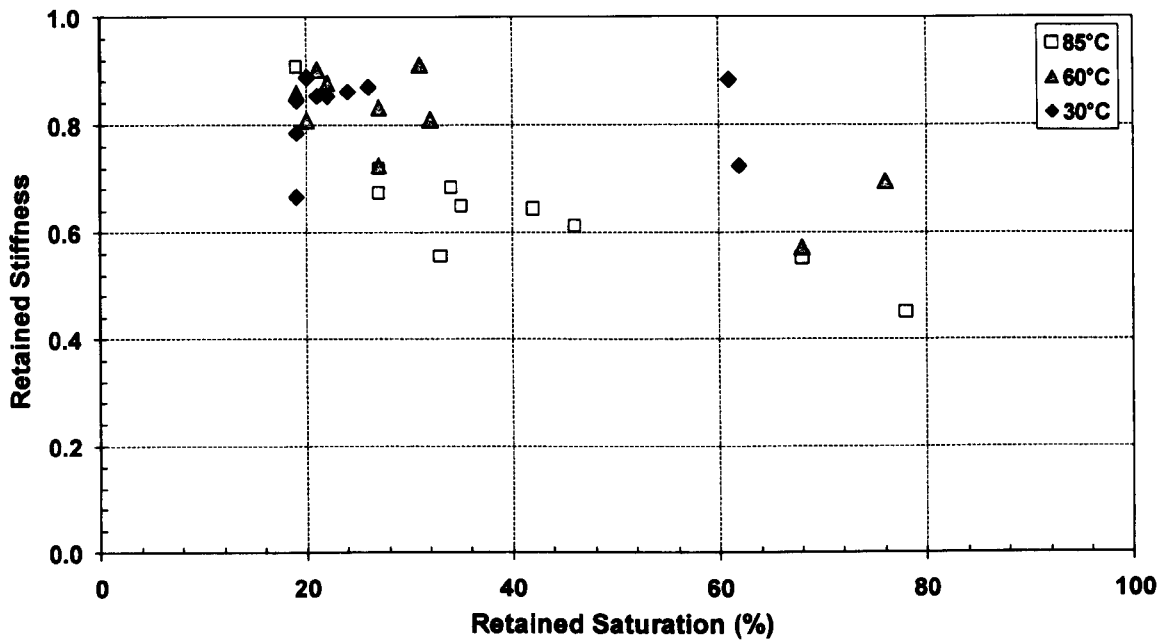


Figure 6.8: SATS results for 50pen Aggregate A specimens tested at different temperatures for 65 hours at 2.1MPa

The same effect can also be seen for the specimens made from Aggregate B. Again, the reduction of temperature leads to a reduction in the retained stiffness, but also to a reduction in the retained saturation of the specimens.

The effect of temperature was also looked at on specimens tested at 0.5MPa for 65 hours. Again three temperatures were looked at; 85°C, 60°C and 30°C (see Figure 6.9). At the lower pressure the trends that were seen at 2.1MPa were reversed. The specimens tested at 85°C exhibited the lowest retained stiffness and those tested at 30°C the highest. This is what was expected at the higher pressure. The specimens at the higher temperature were damaged more by the pressure than those at lower temperatures. In the case of 0.5MPa, the same trend was followed by the specimens tested under water as those above water, the higher the temperature, the less the retained stiffness.



similar to the effect of temperature discussed above). It seems that the duration parameter is more significant for the Aggregate B material as the reduction is more significant, but it is still not a large effect.

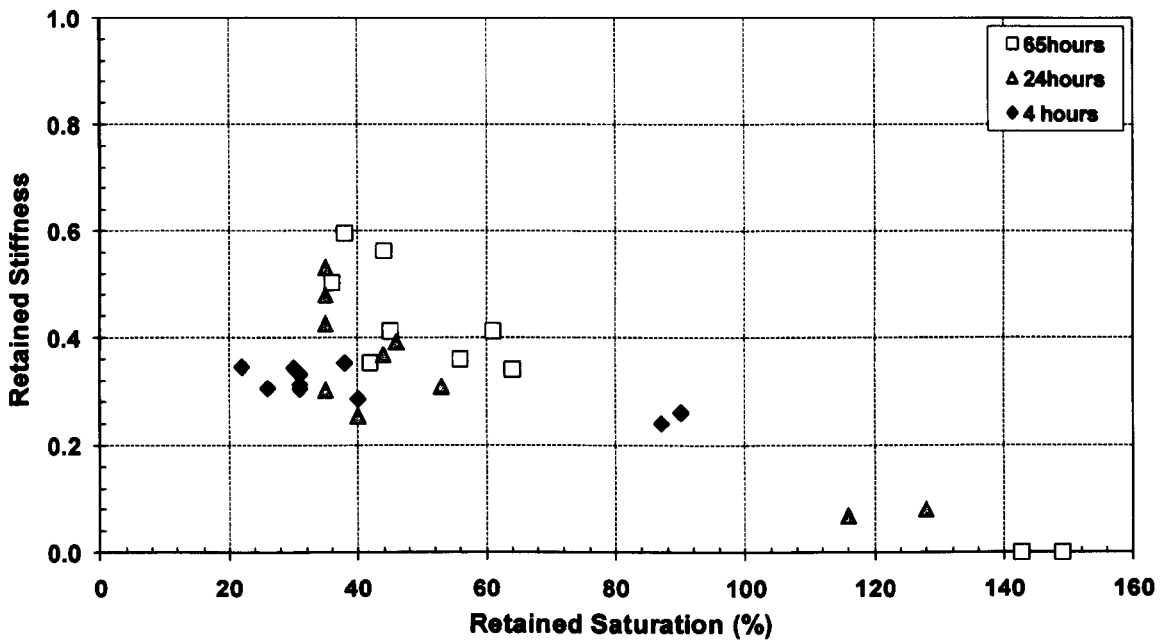


Figure 6.10: SATS results for 50pen Aggregate B specimens tested at different durations at 85°C and 2.1MPa

Binder Content

Figure 6.11 shows the effect of binder content on the retained stiffness and saturation values of specimens after SATS tests carried out under the standard conditions. Similar effects are seen for both Aggregate types A and B. In each case, it is seen that specimens containing 5% binder have lower retained stiffness and lower retained saturation. Two different mechanisms could be acting here, which should be competing. Firstly, due to the higher binder content, the bitumen or mastic film thickness will be greater and this will mean more time would be needed for the binder to be aged all the way through. This would mean the binder would be less aged after testing and therefore less stiff leading to the lower retained stiffnesses. Secondly, the thicker bitumen or mastic film should provide more protection from moisture damage. Due to the reduction in the retained stiffness, it appears that the former mechanism is the dominant one.

Figure 6.11 also shows the effect of temperature and binder content on the retained stiffness and saturation values of Aggregate A specimens after SATS tests carried out at 0.5MPa pressure and 24 hours duration. Similar effects in terms of retained saturation are seen as for Aggregate A and B specimens tested under standard conditions, although the differences are small. In each case, it can be seen that specimens containing 5% binder have lower retained stiffness. Again, the same two mechanisms could be acting here, with the ageing effect dominating.

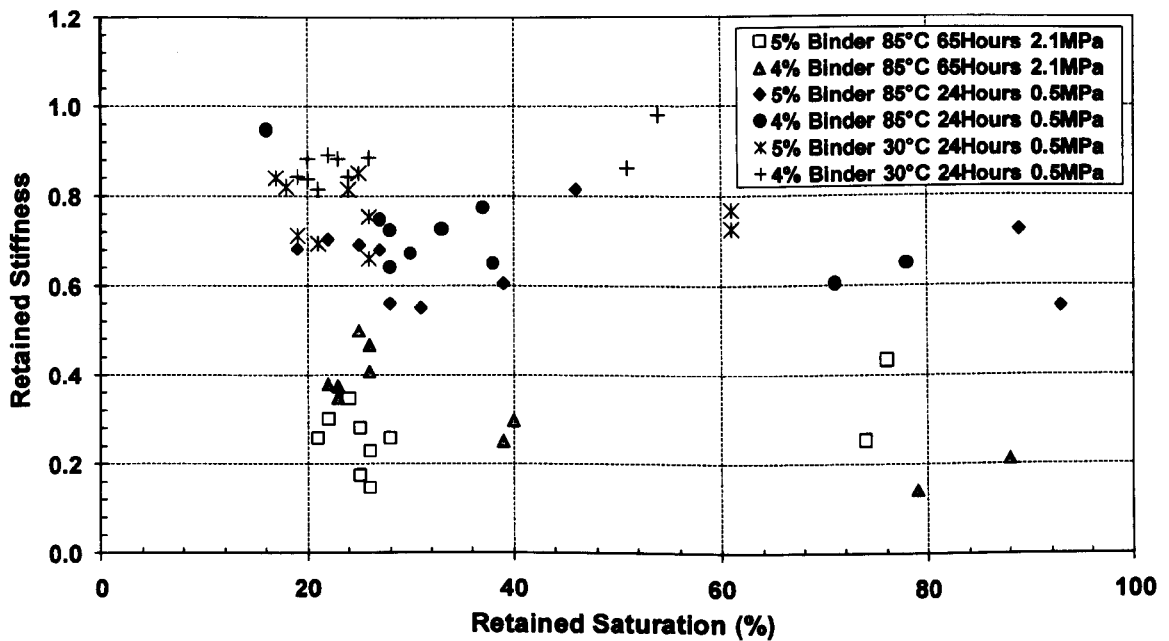


Figure 6.11: SATS results for 50pen Aggregate A specimens made with different binder contents tested at different temperatures and durations under 0.5MPa and 2.1MPa pressure

Figure 6.12 shows the effect of binder content on the retained stiffness and saturation values of Aggregate A and D specimens after SATS tests carried out at 85°C, 0.5MPa and 24 hours. (It should be noted that the two average retained stiffness points for the Aggregate D material with 5% binder actually overlap on the figure). It appears that in the case of the Aggregate A material, the ageing effect is the dominant effect, with higher binder content specimens having lower retained stiffnesses after testing. However, in the case of the Aggregate D material, it appears that the protective nature of the thicker binder film is the dominant effect, as the higher binder content specimens have higher retained stiffnesses. Intuitively, this seems sensible due to the much higher moisture susceptibility of this aggregate type.

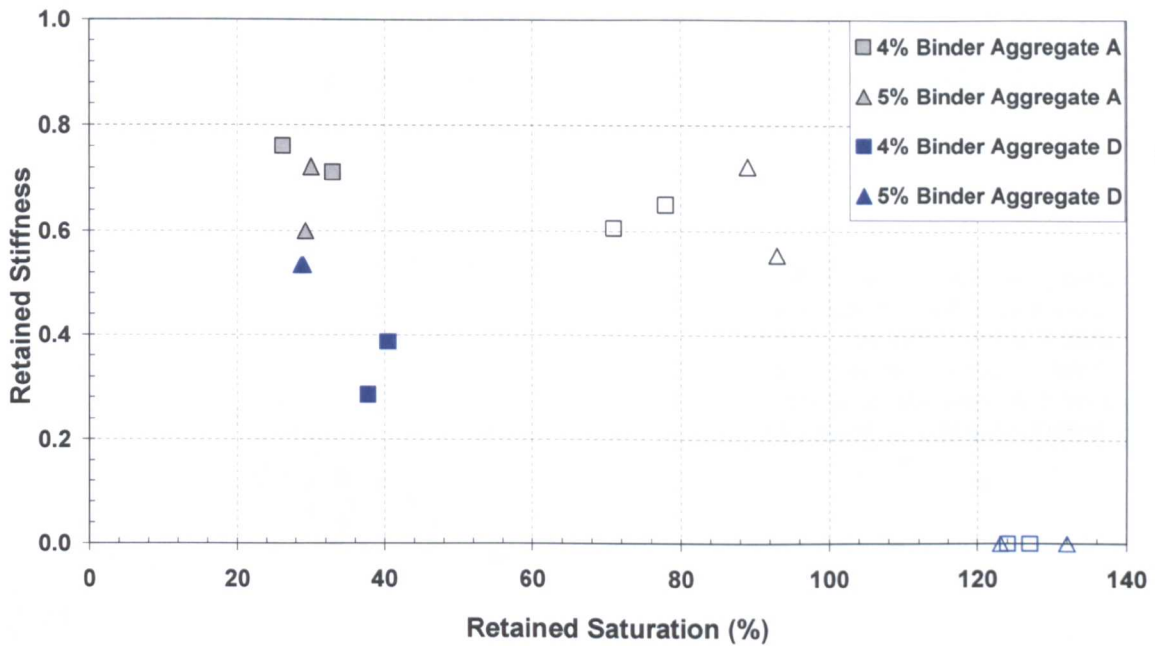


Figure 6.12: SATS results for 50pen Aggregate A and D specimens made with 4% and 5% binder, tested at 85°C, 0.5MPa and 24 hours

Air Void Content

Figure 6.13 shows the effect of air void content on the retained stiffness and saturation values of specimens after SATS tests carried out under the standard conditions. Similar effects are seen for both the Aggregate A and B specimens. In each case, it is seen that specimens containing 4-6% air voids have lower retained stiffness and higher retained saturation. It appears that the increased retained saturation could be due to there being less void volume for the water to fill up, so any voids filled with water have a larger effect on the saturation level. The decrease in retained stiffness of the lower air void content specimens could again be due to the effect of ageing, as the lower air void content would leave reduced surface area to allow the ageing of the binder in the mastic to occur. This reduction of ageing is believed to be the reason for this reduction in retained stiffness.

Figure 6.13 also shows the effect of temperature and air void content on the retained stiffness and saturation values of Aggregate A specimens after SATS tests carried out at 0.5MPa pressure and 24 hours duration. It appears that at 30°C, the lower void content specimens have a higher retained stiffness; however, as the temperature increases, the retained stiffnesses become similar. This could probably be explained

by the fact that at 30°C very little ageing occurs, but as the temperature is increased the ageing effect gets larger and starts to counteract the effect of having reduced air void content.

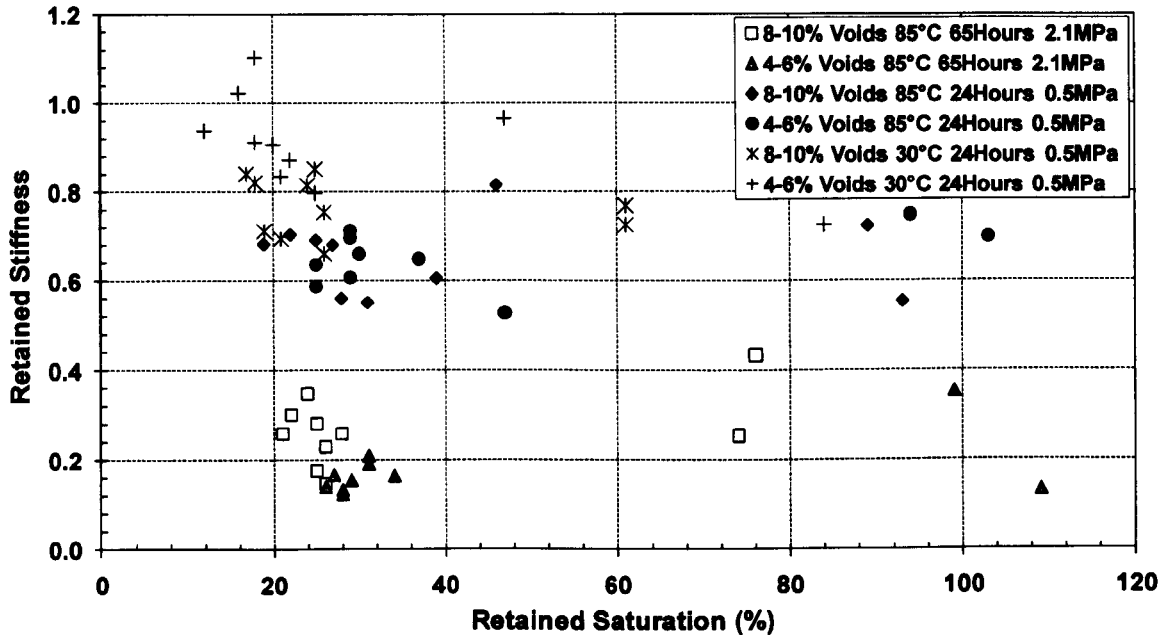


Figure 6.13: SATS results for 50pen Aggregate A specimens made with different air void contents tested at different temperatures and durations under 0.5MPa and 2.1MPa pressure

Figure 6.14 shows the effect of air void content on the retained stiffness and saturation values of Aggregate A and D specimens after SATS tests carried out at 85°C, 0.5MPa and 24 hours. In both aggregate types, it appears that the average retained stiffness for both materials are similar irrespective of air void content. In the case of the Aggregate A material, the retained saturations are similar for both air void contents. However, the 4-6 % air void content Aggregate D specimens have a higher retained saturation than those with the higher air void content. This may again be due to the smaller volume that is needed to be filled with water to increase the saturation level significantly in low air void specimens.

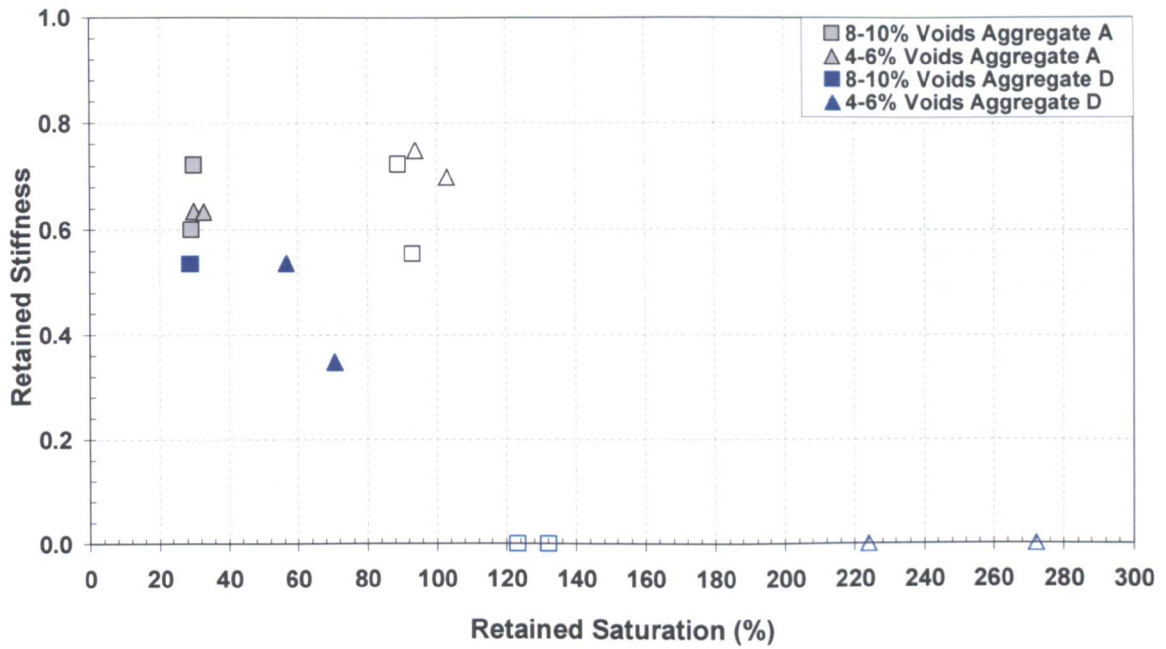


Figure 6.14: SATS results for 50pen Aggregate A and D specimens made with different air void contents tested at 85°C, 0.5MPa and 24 hours

6.3.2 Effect of Changing Multiple Parameters

After each of the parameters was considered separately, the next step was to study the effects of combining changes in two of the parameters simultaneously. The first two parameters assessed at the same time were pressure and temperature. The details of the effect of changing multiple parameters are in report TRL, RPN570 2/462_080 (Nicholls et. al., 2009). This section summarises the work presented in the report.

Pressure and Temperature

Figure 6.15 shows the effect of reducing both the temperature to 60°C and the pressure to 0.5MPa. The first thing to notice is that the retained stiffnesses of these specimens are all in the region of 0.7 to 0.9. So it can be seen that this set of parameters gives a condition that reduces the harshness of the test so that the retained stiffnesses are of a similar order to the retained stiffnesses of 15pen specimens tested under the standard conditions. However, it can also be seen that there is no significant difference in the results for the different aggregate types. This is a problem, since it

means that this combination of parameters is unable to distinguish between the good aggregates (A and B) and the poor aggregate (D).

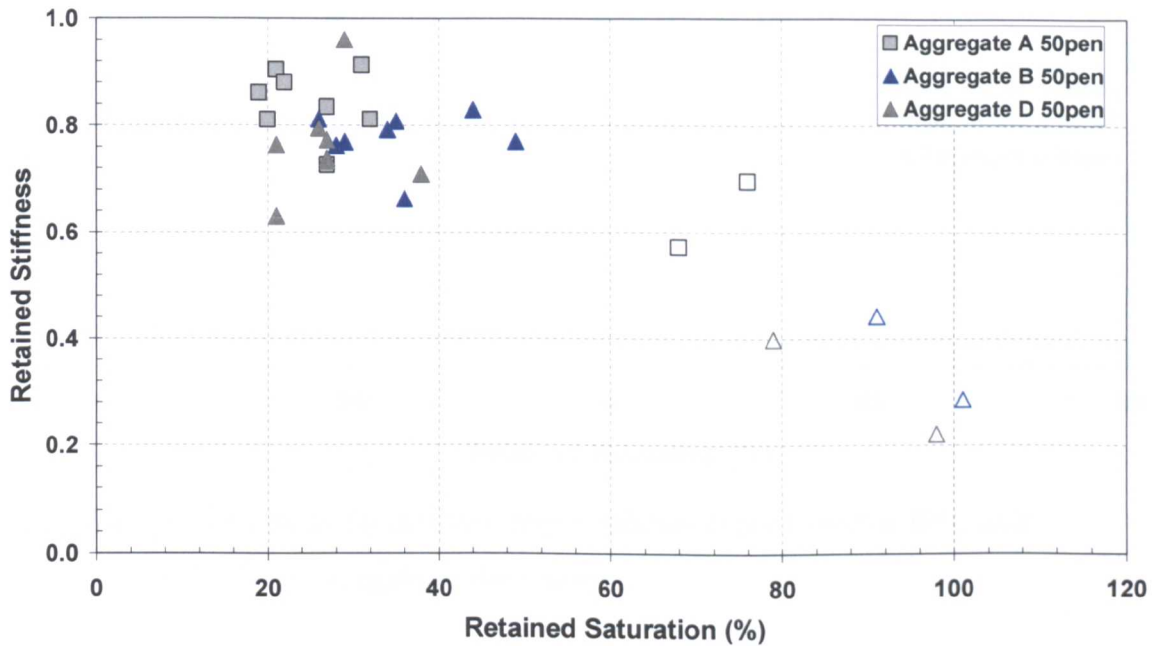


Figure 6.15: SATS results for different 50pen mixture types tested at 60°C and 0.5MPa for a duration of 65 hours

In Figure 6.16 a similar response to a reduction in both temperature, this time 30°C, and pressure can be seen. Again, all the retained stiffness values are high, but there is also no distinction between the ‘good’ and ‘poor’ aggregates.

Figure 6.16: SATS results for three Aggregate A mixture types tested at 30, 40 and 50°C at 0.5, 1.0 and 2.0 MPa for a duration of 65 hours

Figure 6.17 shows a summary of the influence of both temperature and pressure on Aggregate A specimens tested for 65 hours. The standard SATS conditions of 85°C, 0.5 MPa and 65 hours duration are marked with the white squares, with an average

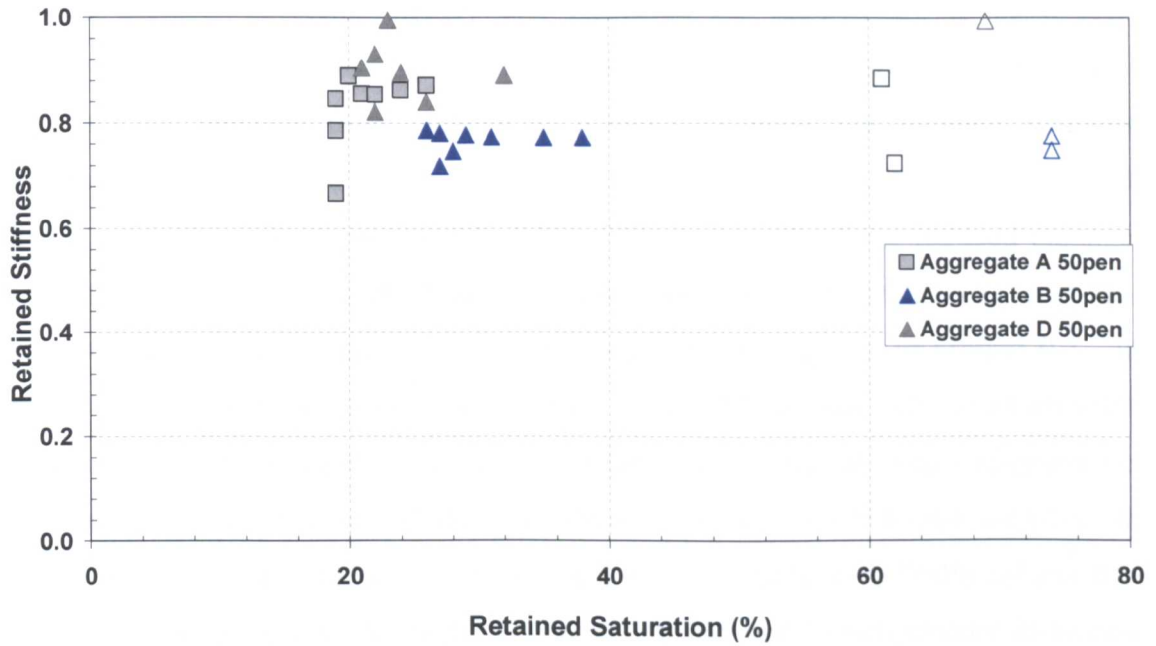


Figure 6.16: SATS results for different 50pen mixture types tested at 30°C and 0.5MPa for a duration of 65 hours

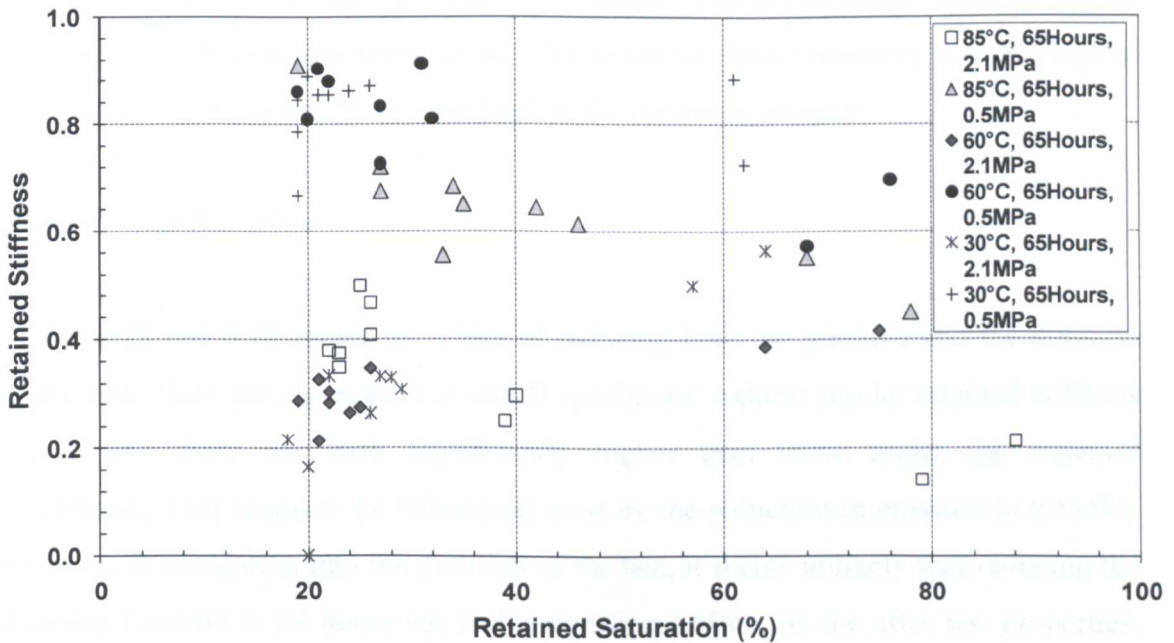


Figure 6.17: SATS results for 50pen Aggregate A mixture types tested at 30, 60 and 85°C at either 0.5 or 2.1MPa for a duration of 65 hours

Figure 6.17 shows a summary of the influence of both temperature and pressure on Aggregate A specimens tested for 65 hours. The standard SATS conditions of 85°C, 2.1MPa and 65 hours duration are marked with the white squares, with an average

retained stiffness of approximately 0.4. Reducing the temperature to 60°C also reduces the retained stiffness, presumably due to the reduced ageing taking place. Reducing the pressure from 2.1MPa to 0.5MPa increases the retained stiffness dramatically. In the case of the test carried out at 60°C and 0.5MPa, the retained stiffness values rise to approximately 0.85. This is a result of the reduced damage associated with the lower applied pressure. Increasing the temperature to 85°C at this pressure reduces the average values of retained stiffness slightly, to around 0.7. It appears that the increase in temperature at the lower pressure has been more affected by the increase in damage occurring due to the softer binder at higher temperature than the ageing effect which would be expected to increase the retained stiffness. It follows from this that reducing the pressure from 2.1MPa to 0.5MPa affects the influence of temperature. At higher pressures, an increase in temperature increases retained stiffness, presumably through increased ageing. However, at lower pressures, the increase in temperature lowers retained stiffness. It appears that the dominant effect of temperature at higher pressure is due to its ageing effect, whereas at lower pressure, it is the fact that the damage process can occur faster at higher temperatures. This theory needs to be fully tested by binder recovery and rheological testing for which the results are provided in the following chapter.

Pressure and Duration

Figure 6.18 and 6.19 shows the effect of reducing both the pressure and the duration of the test. Both the Aggregates A and B specimens' exhibit similar retained stiffness values and these are both significantly higher than those under the standard conditions. This seems to be influenced most by the reduction in pressure to 0.5MPa. From the investigation into the duration of the test, it seems unlikely that reducing the duration from 65 to 24 hours has had a significant effect on the after test properties. Any reduction in the properties as seen from the 0.5MPa, 60°C, 65 hour results that were shown in Figure 6.15 appear to have come from the increased temperature of 85°C. It also appears that these parameters are able to distinguish between 'good' and 'poor' aggregates, as the retained stiffness values of the Aggregate D specimens are significantly lower than those of the other two aggregate types.

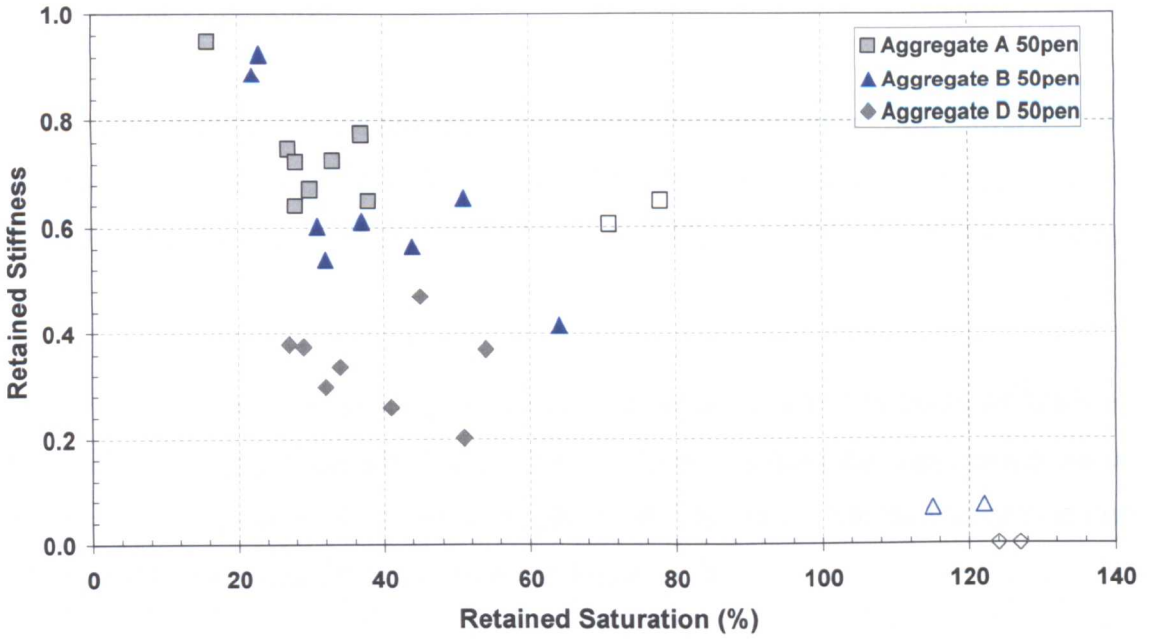


Figure 6.18: SATS results for different 50pen mixture types tested at 85°C and 0.5MPa for a duration of 24 hours

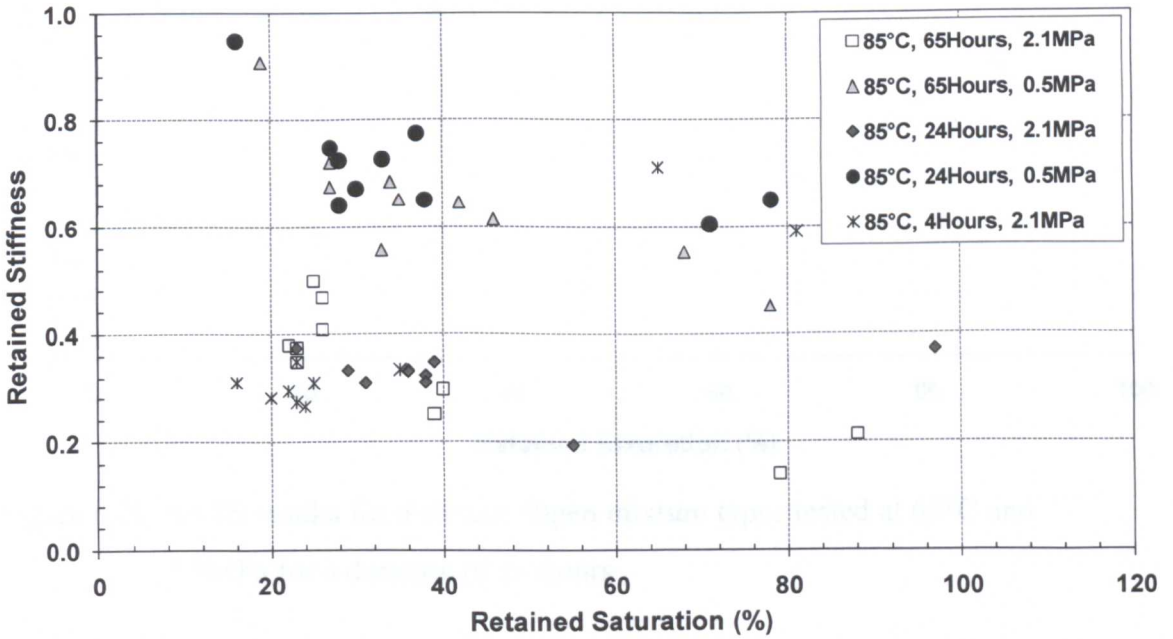


Figure 6.19: SATS results for 50pen Aggregate A mixture types tested at 85°C at either 0.5 or 2.1MPa for different durations

Duration and Temperature

Reducing the duration of the test from 65 hours to 24 hours shows little difference in results from the tests carried out at 65 hours, 0.5MPa and 60°C shown in Figure 6.15. The results for the test carried out at 24 hours, 0.5MPa and 60°C are shown in Figure 6.20.

The same can be said for reducing the duration of the test from 65 hours to 24 hours at 30°C and 0.5MPa pressure, with little difference in results from the tests carried out at 65 hours, 0.5MPa and 30°C shown in Figure 6.16. The results for the test carried out at 24 hours, 0.5MPa and 30°C are shown in Figure 6.21.

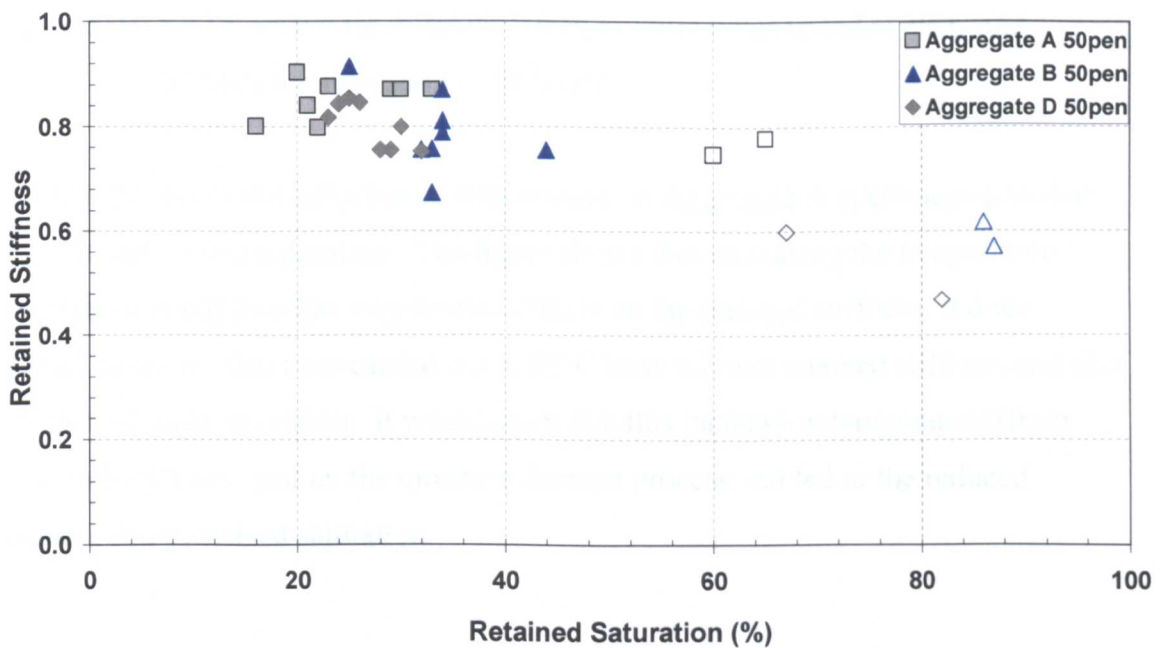


Figure 6.20: SATS results for different 50pen mixture types tested at 60°C and 0.5MPa for a duration of 24 hours

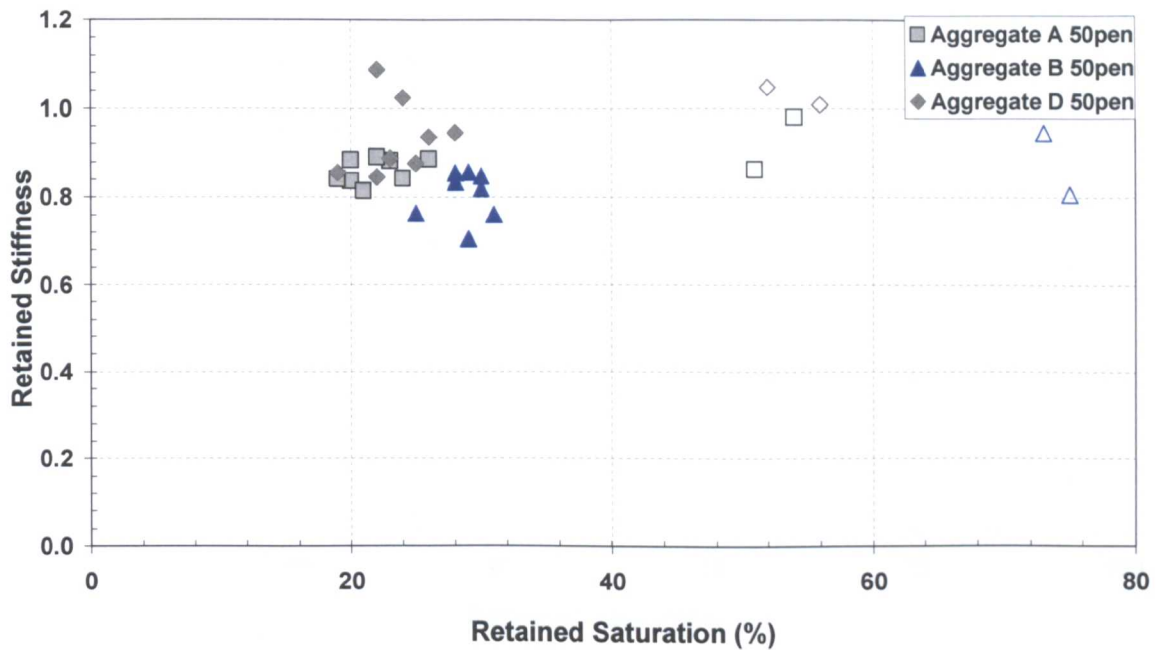


Figure 6.21: SATS results for different 50pen mixture types tested at 30°C and 0.5MPa for a duration of 24 hours

Figure 6.22 shows the influence of temperature on Aggregate A specimens tested at 0.5MPa and 65 hours duration. The figure shows that increasing the temperature under these conditions has very limited effects on the retained stiffness. It does appear, however, that tests carried out at 85°C have a lower retained stiffness and also a higher retained saturation. It would seem that this increase in temperature (from 60°C to 85°C) has sped up the moisture damage process and led to the reduced stiffness and increased saturation.

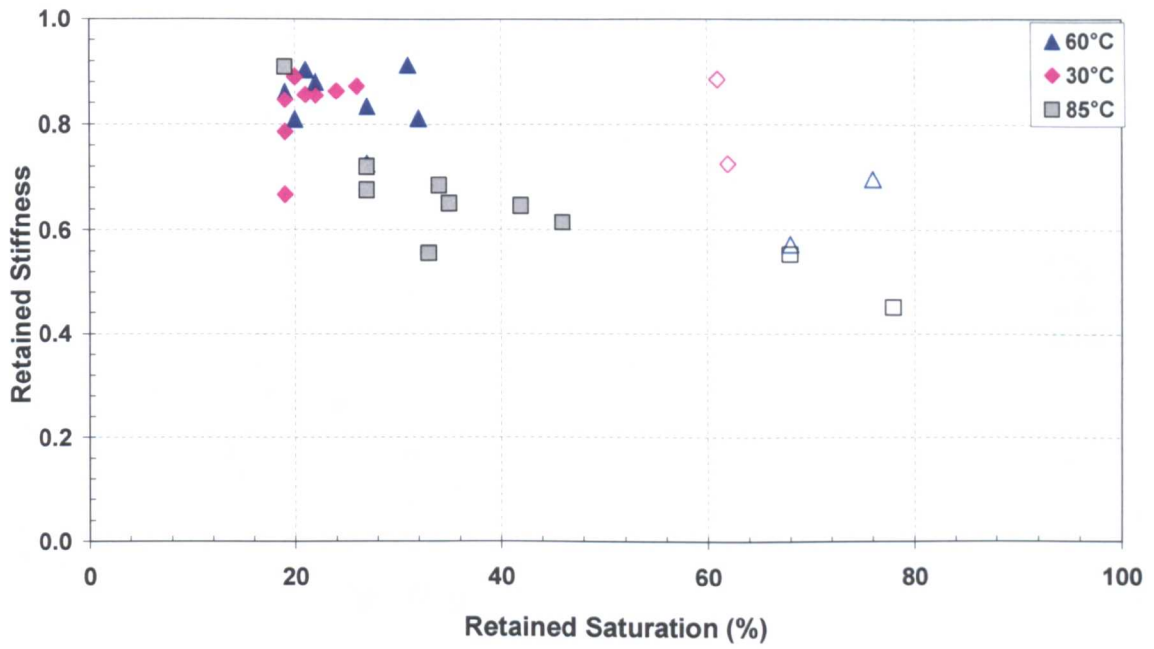


Figure 6.22: SATS results for 50pen Aggregate A specimens tested at different temperatures under 0.5MPa pressure for a duration of 65 hours

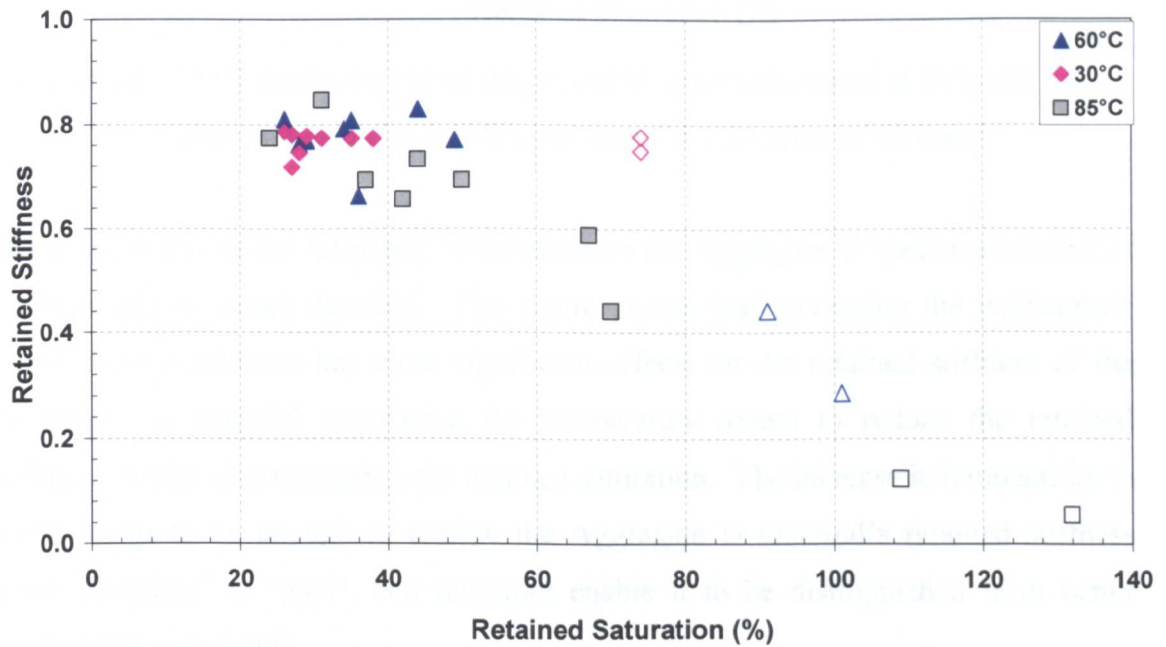
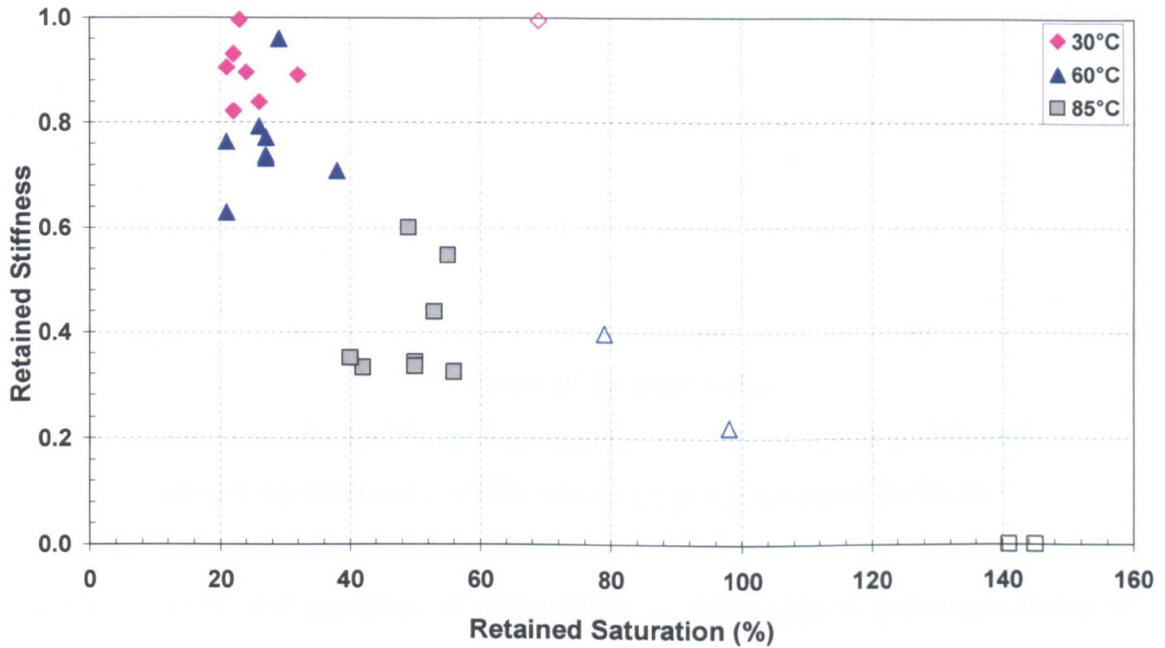


Figure 6.23: SATS results for 50pen Aggregate B specimens tested at different temperatures under 0.5MPa pressure for a duration of 65 hours

Figure 6.23 shows the influence of temperature on Aggregate B specimens tested at 0.5MPa and 65 hours duration. The figure shows that increasing the temperature under these conditions has very limited effects on the retained stiffness, as also shown by the Aggregate A material. It is possible to argue that tests carried out at 85°C have

a lower retained stiffness and also a higher retained saturation, but the effects are small. It would again appear that this increase in temperature has sped up the moisture damage process and led to the reduced stiffness and increased saturation.



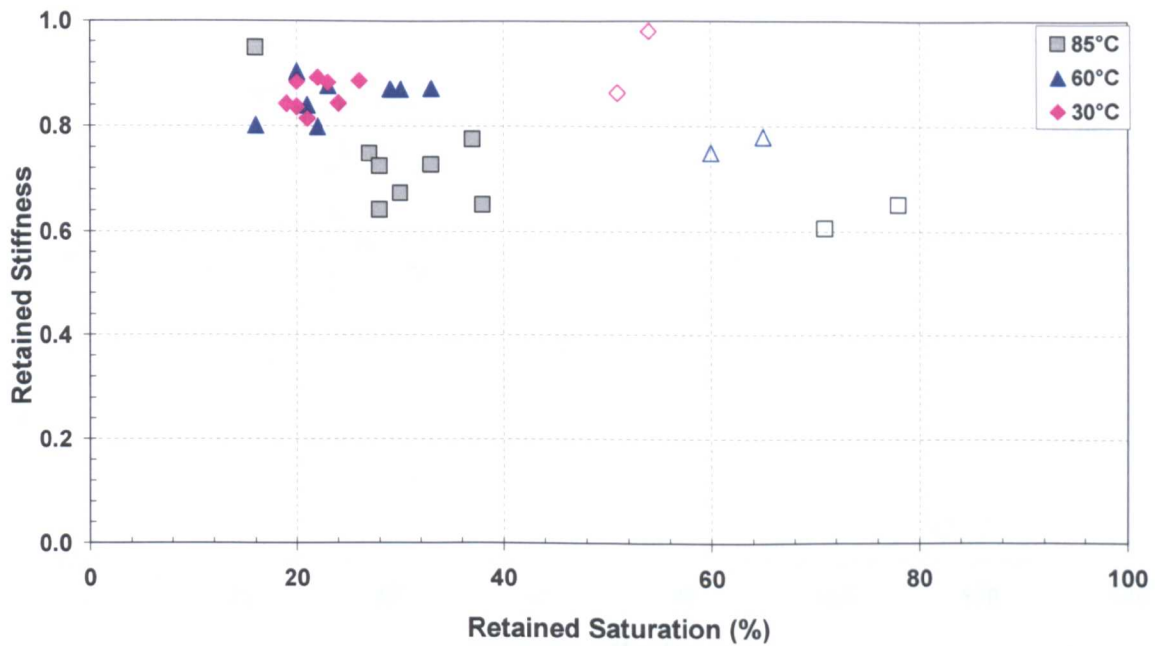


Figure 6.25: SATS results for 50pen Aggregate A specimens tested at different temperatures under 0.5MPa pressure for a duration of 24 hours

Figure 6.25 shows the influence of temperature on Aggregate A specimens tested at 0.5MPa and 24 hours duration. The figure shows that increasing the temperature under these conditions again has very limited effects on the retained stiffness. It appears that the tests carried out at 85°C have a lower retained stiffness and also a higher retained saturation. It would seem that this increase in temperature has again sped up the moisture damage process and led to the reduced stiffness and increased saturation, as seen at the longer duration of 65 hours.



Figure 6.27: SATS results for 50pen Aggregate D specimens tested at different temperatures under 0.5MPa pressure for a duration of 24 hours

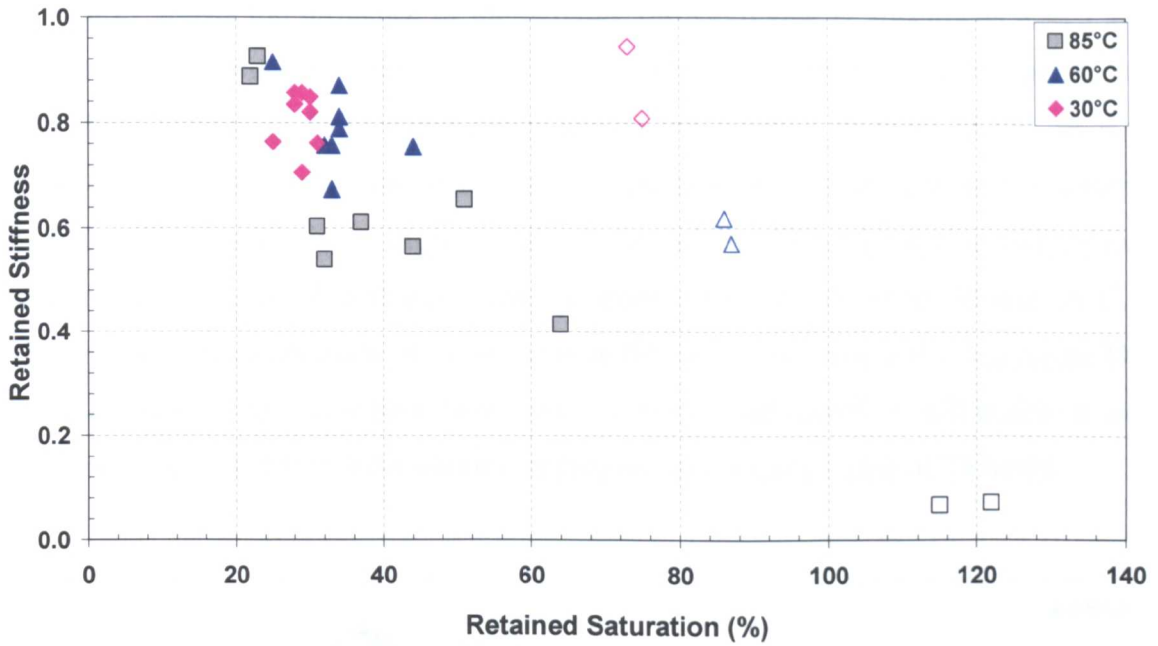


Figure 6.26: SATS results for 50pen Aggregate B specimens tested at different temperatures under 0.5MPa pressure for a duration of 24 hours

Figure 6.26 shows the influence of temperature on Aggregate B specimens tested at 0.5MPa and 24 hours duration. It seems that the temperature changes under these conditions have the same effect as seen for the Aggregate A aggregate.

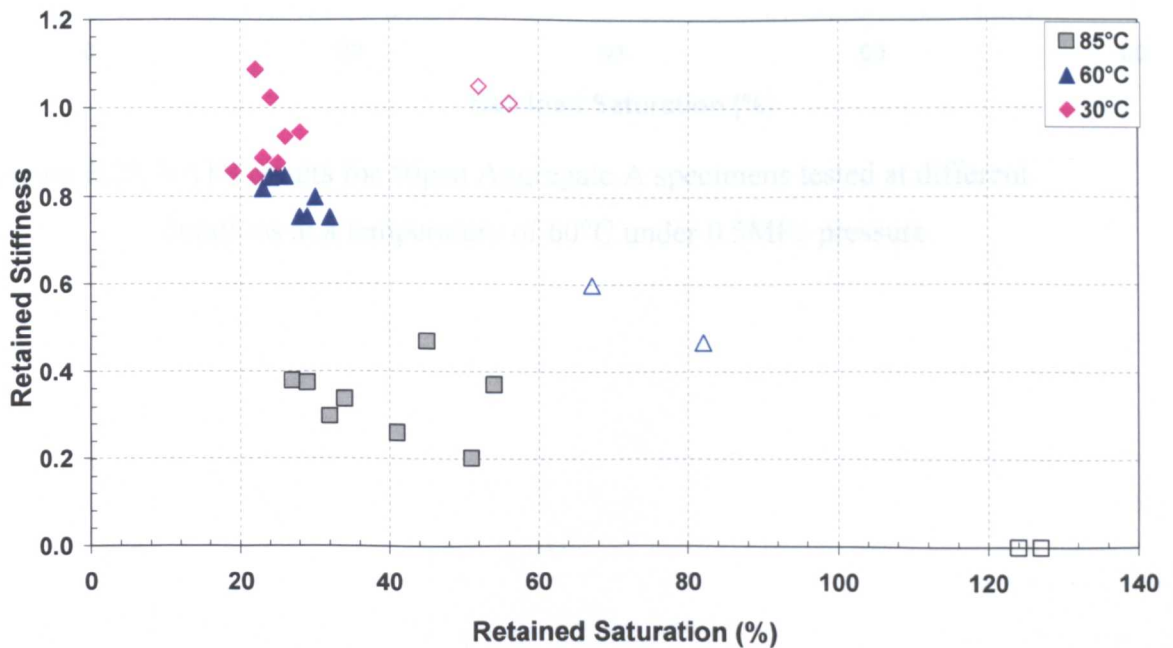


Figure 6.27: SATS results for 50pen Aggregate D specimens tested at different temperatures under 0.5MPa pressure for a duration of 24 hours

Figure 6.27 shows the influence of temperature on Aggregate D specimens tested at 0.5MPa and 24 hours duration. The figure shows that increasing the temperature under these conditions more significantly affects the retained stiffness of the 'poor' quality aggregate. It seems that the tests carried out at 85°C have a significantly lower retained stiffness and also a higher retained saturation. There is also a noticeable reduction in the retained stiffness values between tests carried out at 30 and 60°C. The increase in temperature to 85°C appears to be enough to change the Aggregate D material's retained stiffness from 'adequate' to 'poor', and therefore still enable it to be distinguished from better performing aggregates at a reduced time of 24 hours.

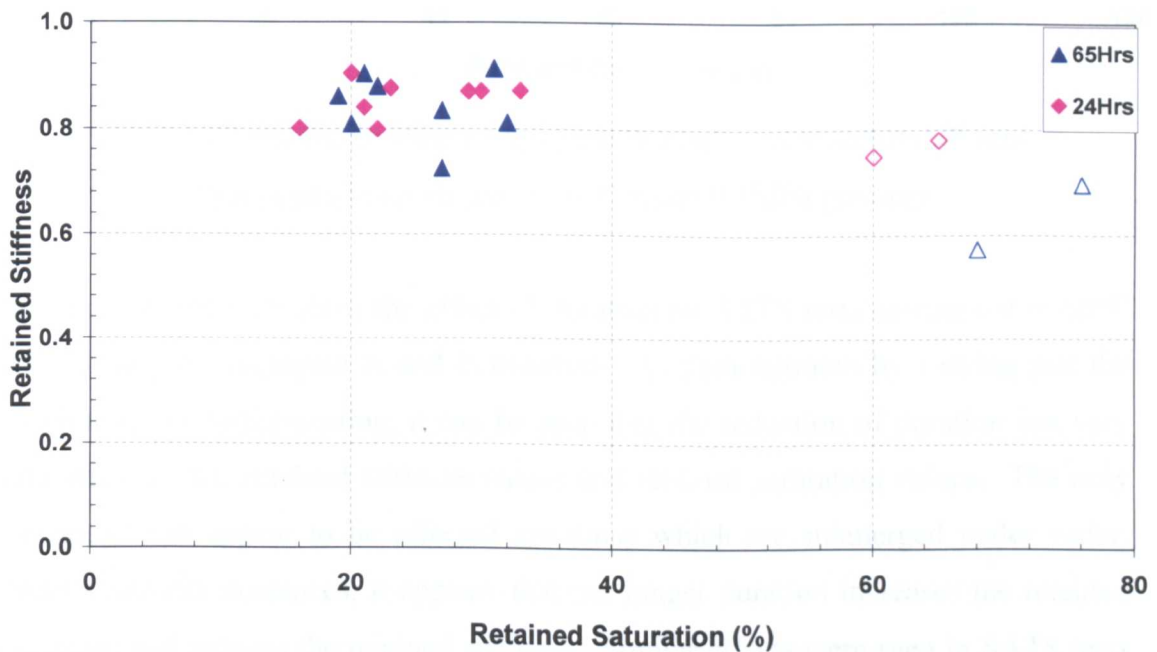


Figure 6.28: SATS results for 50pen Aggregate A specimens tested at different durations at a temperature of 60°C under 0.5MPa pressure

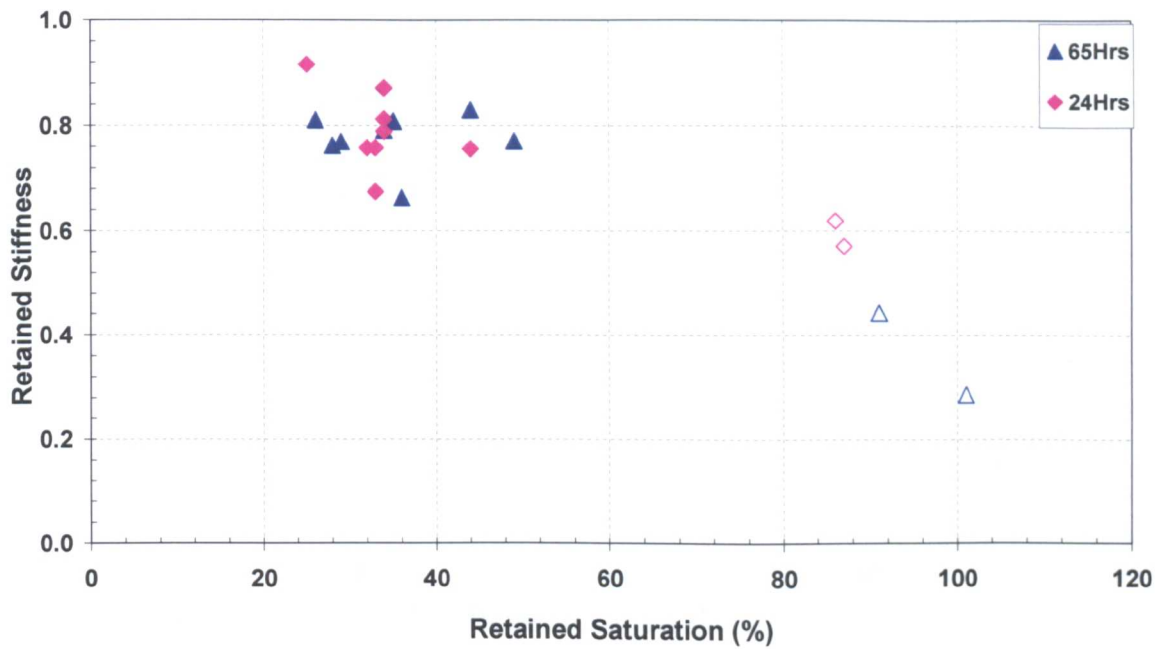


Figure 6.29: SATS results for 50pen Aggregate B specimens tested at different durations at a temperature of 60°C under 0.5MPa pressure

Figures 6.28 and 6.29 show the effect of duration on SATS tests carried out at 60°C and 0.5MPa on Aggregate A and B material. As demonstrated by varying just the duration in the earlier section, it can be seen that the reduction of duration has very little effect on the retained stiffness values and retained saturation values. The only specimens that appear to be affected are those which are submerged under water. Under these circumstances, it appears that the longer duration increases the retained saturation and reduces the retained stiffness. Similar effects were seen in SATS tests carried out for different durations at 30°C and 0.5MPa (see Figures 6.30 and 6.31).

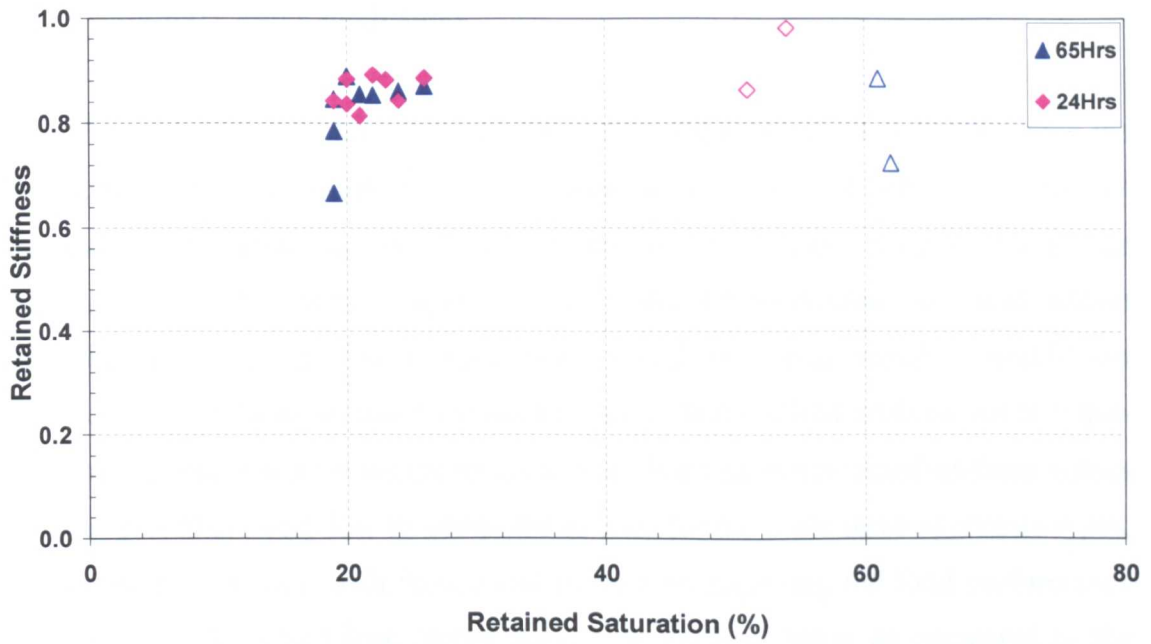


Figure 6.30: SATS results for 50pen Aggregate A specimens tested at different durations at a temperature of 30°C under 0.5MPa pressure

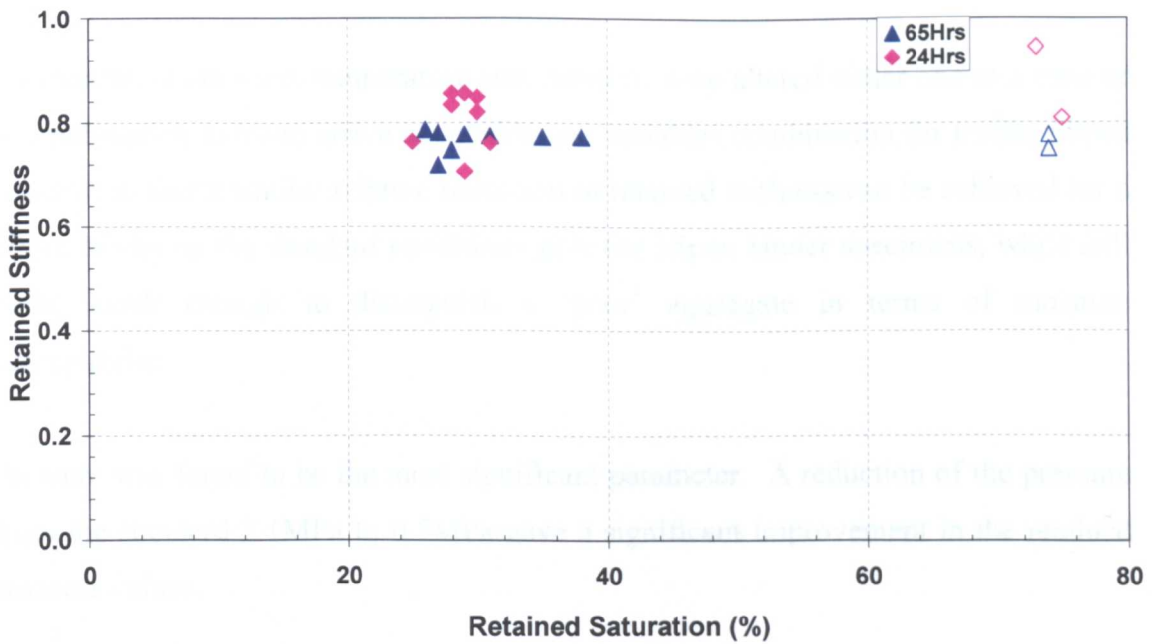


Figure 6.31: SATS results for 50pen Aggregate B specimens tested at different durations at a temperature of 30°C under 0.5MPa pressure

6.4 Summary and Conclusions

A number of SATS tests have been performed by the researchers at NTEC since the development of this equipment. Researchers have used four different types of sources/quarries obtaining two main types of aggregates namely Limestone (Aggregate A) and Granites (Aggregates B, C and D) to produce different asphalt specimens and the specimens have been tested by using variable SATS test conditions. 15pen bitumen had been used for most of the initial analysis while 50pen binder was mainly used for the recent tests. It is observed that retained stiffness values for aggregate D are very low as compared to ones for the other three aggregate types, which corroborates well with the general perception regarding the field performance of these materials. The 15pen binder appears to perform better as compared to the 50pen, or in other words the standard SATS conditions that were used for 15pen binder specimens (2.1MPa, 85°C, 65h) have been found to be too harsh for specimens made with 50pen binder.

Parameters of pressure, temperature and duration were altered either one at a time or in combination to try to arrive at suitable test variables combination for testing 50pen material so that a similar relative reduction in retained stiffness can be achieved for a 50pen binder as the standard conditions give for 15pen binder specimens, while still being harsh enough to distinguish a 'poor' aggregate in terms of moisture susceptibility.

Pressure was found to be the most significant parameter. A reduction of the pressure from the standard 2.1MPa to 0.5MPa gave a significant improvement in the retained stiffness values.

A reduction in temperature was also found to increase the retained stiffness values. However, it was not such a significant parameter as pressure. When in combination with other parameters, it was found that a temperature of 85°C was needed to distinguish between the 'good' and 'poor' aggregates in terms of moisture susceptibility.

Duration was not found to have any significant effect on the SATS results. As this was the case, it was decided that test duration of 24 hours was favourable due to the shorter time and therefore smaller expense.

The best parameter combination for a Saturation Ageing Tensile Stiffness test for specimens made from 50pen binder was found to be 85°C temperature, 0.5MPa pressure and 24 hours duration.

SATS tests were also carried out under dry conditions to try to factor out the effect of moisture in the system.

Some of the SATS tested specimens/cores that have gone through different test parameter combinations are then selected for the measurement of rheological and surface energy parameters of the tested binder. This is done by carrying out binder recovery tests on the specimens and then testing them for the required properties.

The surface energy and rheology results for the recovered binders are then correlated and compared to the retained stiffness and saturation values obtained from the SATS tests for these materials in order to isolate the effects of each of the different parameters and their influence on the ageing of the binder. This analysis is provided in the following two chapters.

CHAPTER 7

MOISTURE SENSITIVITY INTERPRETATION FOR SATS TESTED ASPHALT MIXTURES

7.1 Introduction

As mentioned in the previous chapter, the SATS protocol measures the combined effect of ageing, pressure and moisture on an asphalt mixture. The ageing of binder tested under the SATS protocol can be defined as hardening of material under high temperature and pressure which results in an increase in the stiffness modulus of the asphalt mixture. The presence of moisture on the other hand results in a reduction of the stiffness modulus. It has been seen that the increase in pressure also causes a drop in stiffness modulus which is not related to the moisture damage. In other words, keeping all the above factors in mind, stiffness modulus of a SATS tested specimen is basically a combination of ageing (hardening of mixture), pressure and moisture damage. Choi (2005) developed a procedure to separately investigate the effects of ageing, pressure and moisture on the results from the SATS test. A moisture factor is determined at the end of the procedure which is considered as a true measure of the moisture sensitivity (moisture damage) of the asphalt mixture under consideration (Collop et al, 2007).

The procedure developed by Choi (2005) has been used to determine the moisture factors for the material combinations under investigation. The first step towards this study is the recovery of bitumen from the SATS tested cores. The recovered binder is then tested for its rheological properties. The details of the selected material combinations, rheological properties of the recovered binder and the effects of ageing pressure and moisture are provided in the following sections.

7.2 Material Combinations

A number of SATS tested cores (see Chapter 6 for material details) were selected for the binder recovery. The aim was to study enough material combinations in order to be able to have the following main comparisons:

- 15pen versus 50pen binder with at least one aggregate type. Aggregate ‘A’ (limestone) was selected for the purpose.
- Effect of aggregate types on the moisture sensitivity of the resulting asphalt mixtures. All the aggregate types A, B, C and D (B, C and D are generally classified as granites) with 50pen binder mixes were selected.
- Effect of different SATS test conditions on the resulting moisture sensitivity and retained stiffness. Asphalt mixture with 50pen binder and aggregate ‘A’ was selected.

A summary of the material combinations and SATS test conditions that were used for the analysis are provided in the following table.

Table 7.1: Material Combinations for Binder Recovery and Analysis

SATS Test Conditions (4% binder, 9% air voids)	Aggregate	SATS with Moisture Conditioning (Water in the chamber)		Dry SATS (No Water)
		Binder (penetration grade)	Specimen Position	Binder (penetration grade)
2.1MPa, 85°C, 65Hrs	A	15 & 50	1, 2, 3, 4, 6	15 & 50
	B	50	1	50
	C	50	1, 2, 3, 4, 6	50
	D	50	1, 2, 3, 4, 6	50
0.5MPa, 85°C, 65Hrs	A	50	1, 2, 3, 4, 6	50
0MPa, 85°C, 65Hrs	A	50	1, 4, 6	50
2.1MPa, 60°C, 65Hrs	A	50	1, 4, 6	50
2.1MPa, 30°C, 65Hrs	A	50	1, 4, 6	50
2.1MPa, 85°C, 24Hrs	A	50	1, 4, 6	50
2.1MPa, 85°C, 4Hrs	A	50	1, 4, 6	50
0.5MPa, 60°C, 65Hrs	A	50	1, 4, 6	50
0.5MPa, 30°C, 65Hrs	A	50	1, 4, 6	50
0.5MPa, 85°C, 24Hrs	A	50	1, 4, 6	50

Test Conditions (5% Binder, 9% air voids)	Aggregate	SATS with Moisture Conditioning (Water in the chamber)		Dry
		Binder	Position	Binder
2.1MPa, 85°C, 65Hrs	A	50	1, 4, 6	50
Test Conditions (5% Binder, 5% air voids)	Aggregate	SATS with Moisture Conditioning (Water in the chamber)		Dry
		Binder	Position	Binder
2.1MPa, 85°C, 65Hrs	A	50	1, 4, 6	50

Position '6' (also referred '5') represents those specimens that are submerged in water

7.3 Binder Recovery and Rheological Testing

The selected SATS cores are passed through a material recovery process/technique (BS EN 12697-4:2005). This is a fractionating column technique where dichloromethane is used as the solvent for the distillation process. The recovered binder was then tested for its rheological properties with the help of a Dynamic Shear Rheometer (DSR).

This section provides results from the dynamic mechanical analysis of all the un-aged/virgin and aged (RTFOT, PAV and SATS) binders.

7.3.1 Rheology Testing of Control and SATS Recovered Binders

All the above mentioned binder specimens were tested for their rheological properties by using a Dynamic Shear Rheometer (DSR). The equipment that was used for the tests is shown in Figure 7.1 below.



Figure 7.1: Dynamic Shear Rheometer

The silicone mould method (Airey and Hunter, 2003), shown in Figure 7.2, was used to prepare the samples.



Figure 7.2: DSR Test; Sample Preparation

The prepared samples are placed on the equipment plates and the test parameters are entered by using the equipment software. An image of the DSR test control software is shown in Figure 7.3 below.

Figure 7.4: DSR-Result Analysis

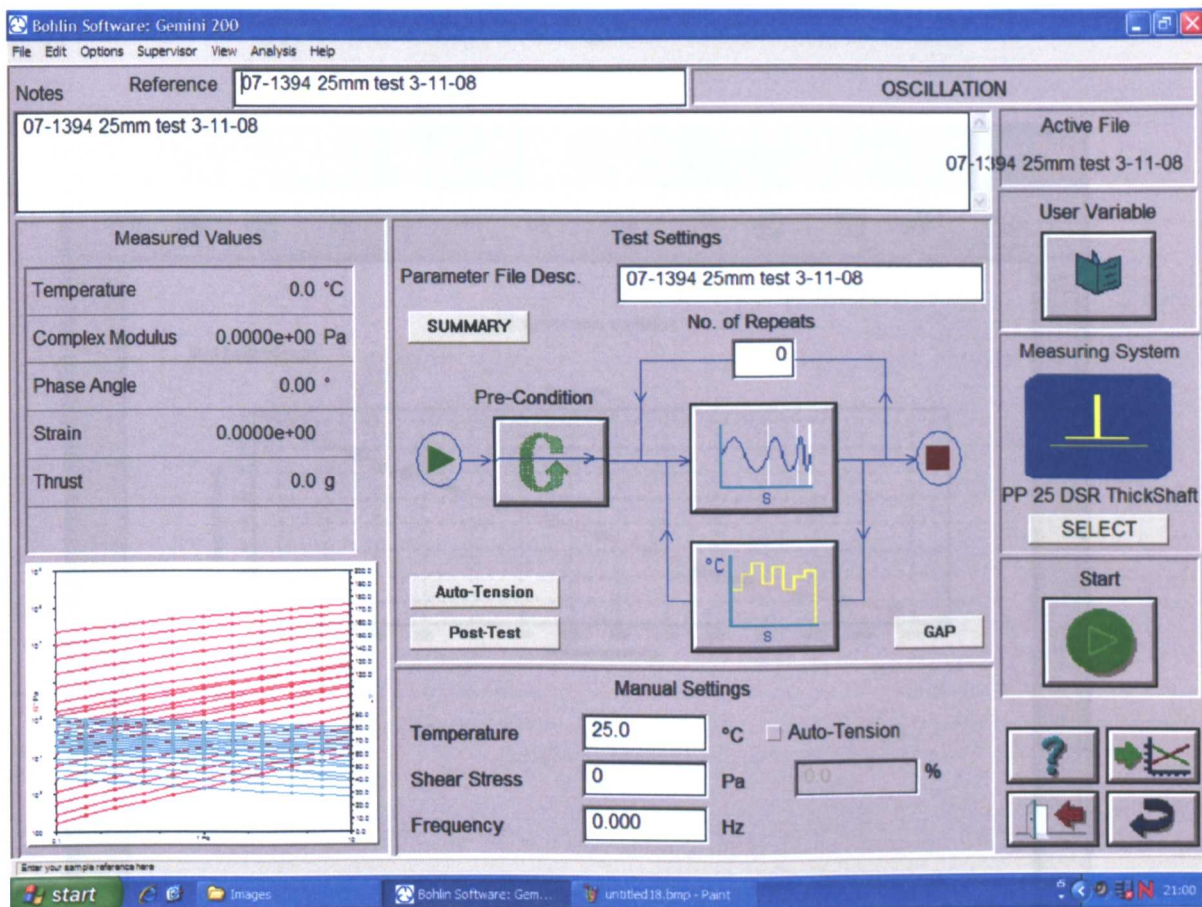


Figure 7.3: DSR-Control Software

At the end of the test, the data is saved and the time-temperature superposition analysis facility (shown in Figure 7.4) present in the software is used for plotting the master curves and shift factors.

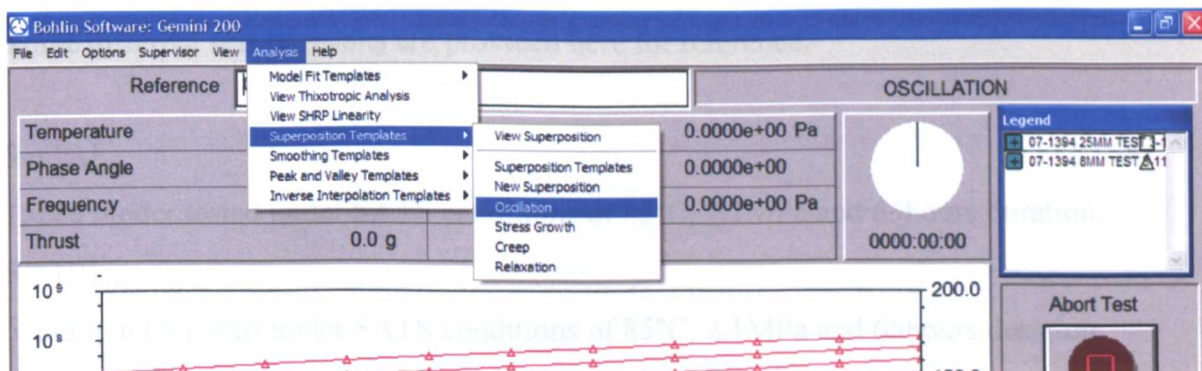


Figure 7.4: DSR-Result Analysis

A typical shift factor plot is also shown in Figure 7.5 below.

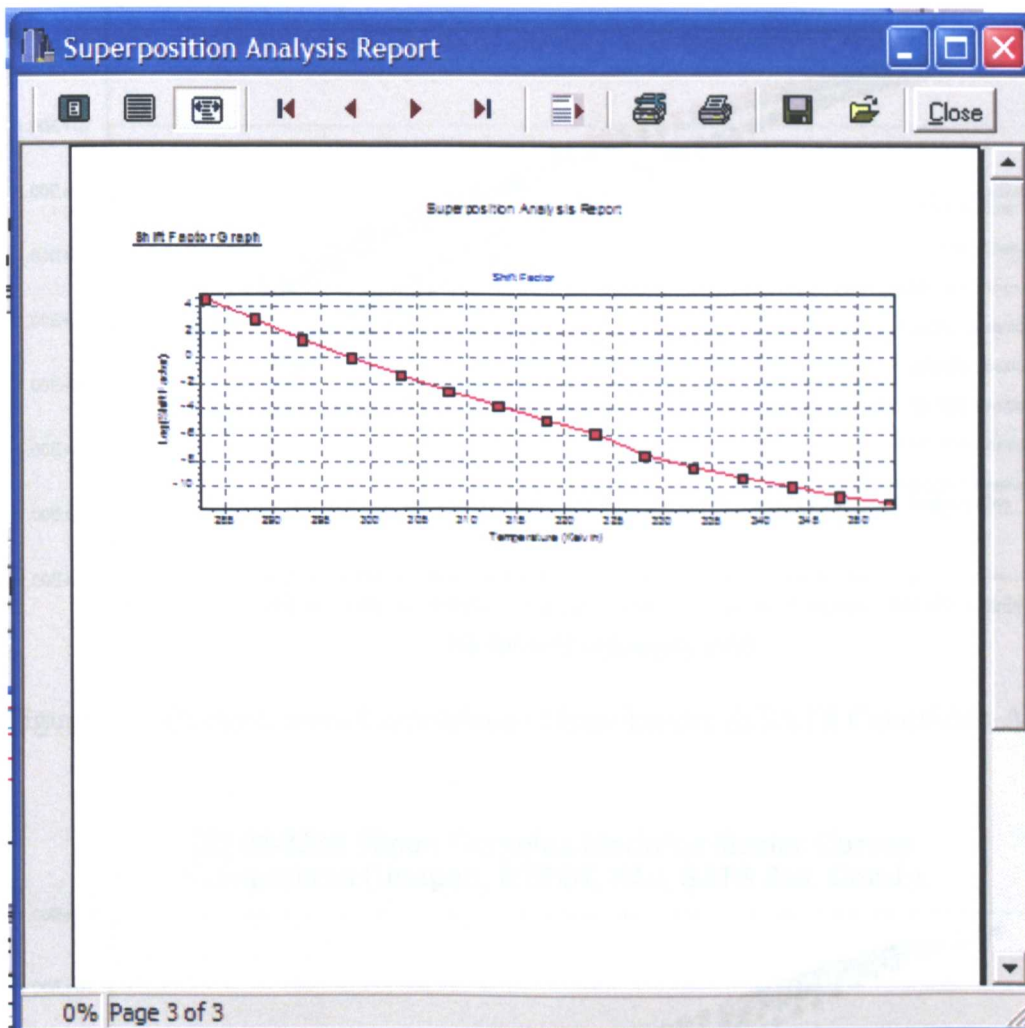


Figure 7.5: Typical Shift Factor Plot

Three different sets of results are provided here for reference:

Set [A]

15pen binder tested under SATS conditions of 85°C, 2.1MPa and 65hours duration.

Set [B]

50pen binder tested under SATS conditions of 85°C, 2.1MPa and 65hours duration.

Set [C]

50pen binder tested under SATS conditions of 85°C, 0.5MPa and 65hours duration.

The master curves for each set along with the curves for un-aged, RTFOT and PAV aged samples are shown in Figures 7.6, 7.7 and 7.8 respectively.

[A] 07-1394 15pen Complex Modulus Master Curves Comparison (Unaged, RTFOT, PAV, SATS Std. Cond.)

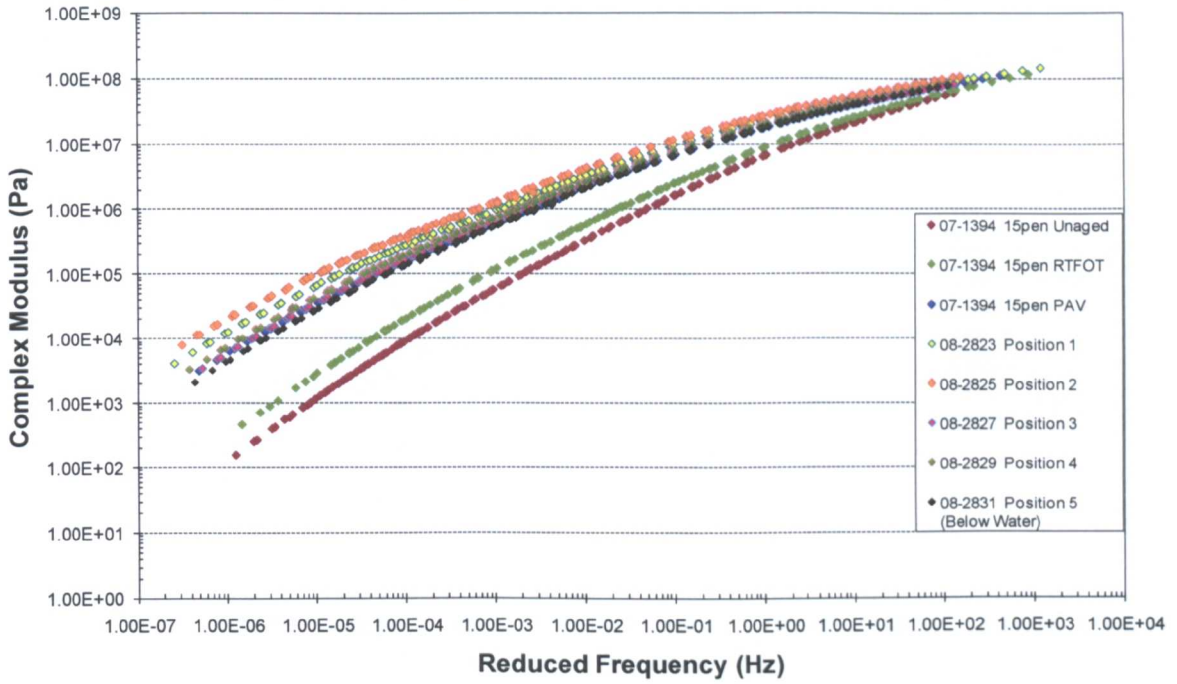


Figure 7.6: Master Curves Comparison (15pen Binder & SATS Conditions-A)

[B] 08-3336 50pen Complex Modulus Master Curves Comparison (Unaged, RTFOT, PAV, SATS Std. Cond.)

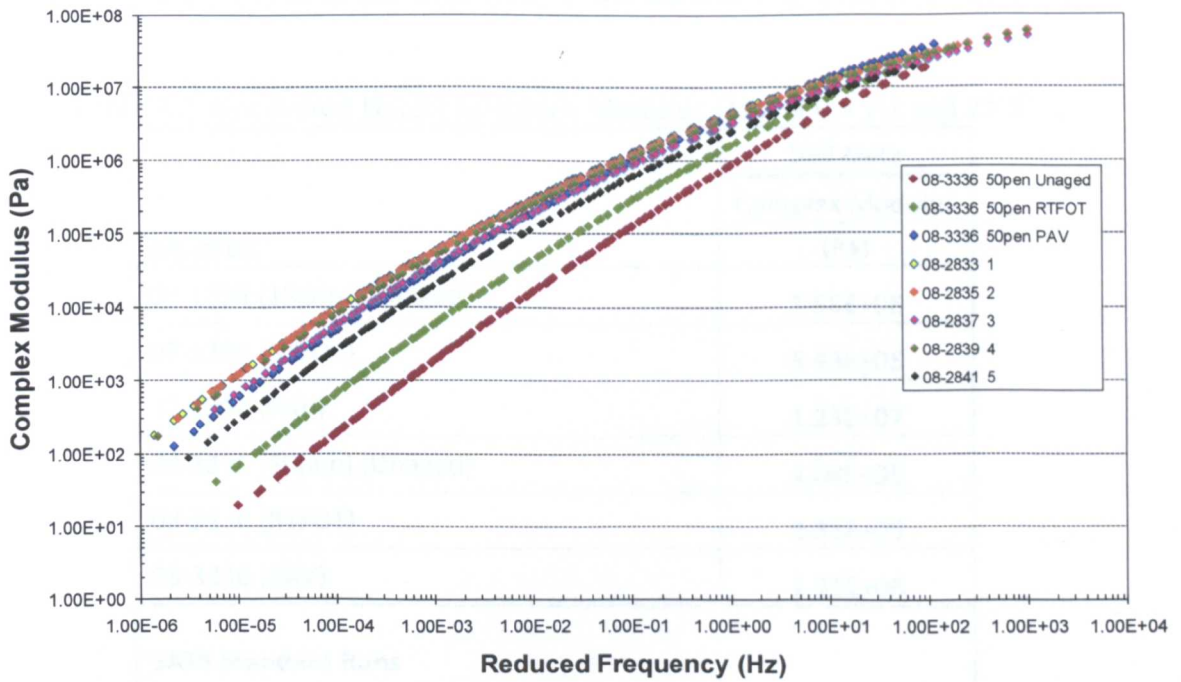


Figure 7.7: Master Curves Comparison (50pen Binder & SATS Conditions-B)

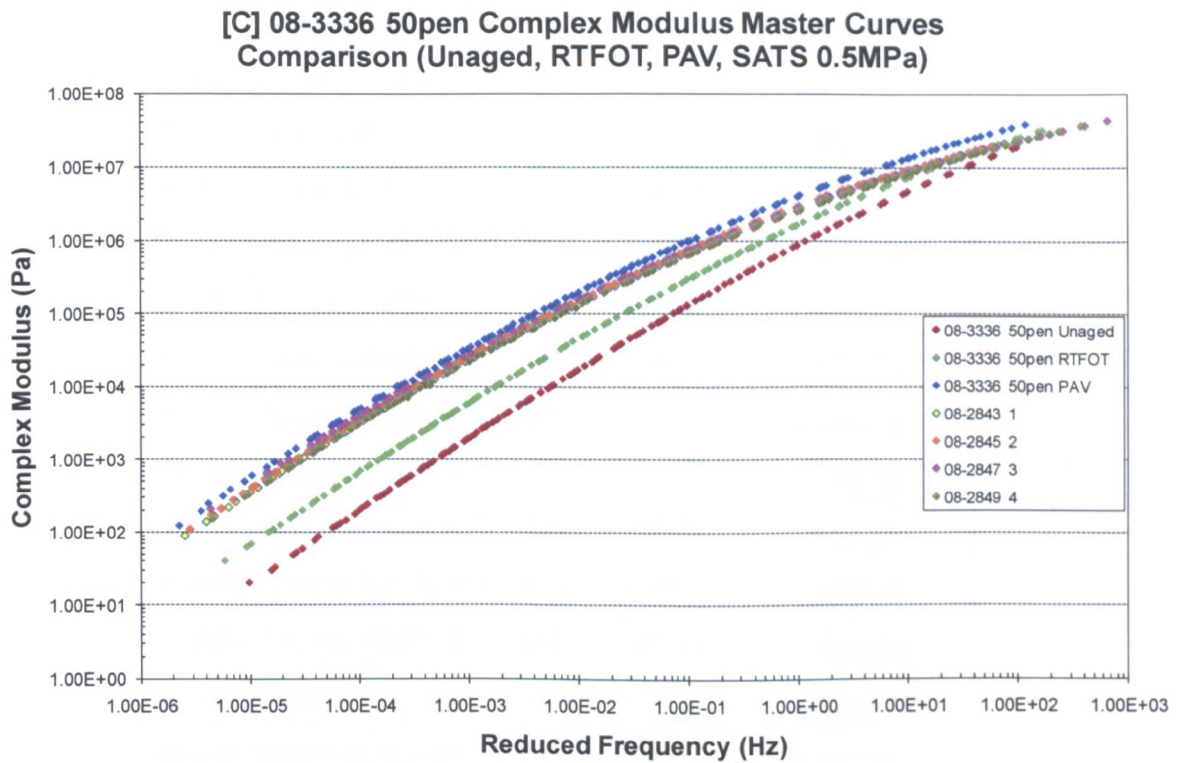


Figure 7.8: Master Curves Comparison (50pen Binder & SATS Conditions-C)

A list of recovered binder complex modulus data (at a frequency of 0.4 hertz and temperature of 25°C) which has been used for the analysis is provided in Table 7.2.

Table 7.2: Recovered Binder Complex Modulus Data at 0.4 Hz and 25°C

Bitumen	DSR Data
	Complex Modulus (Pa)
07-1394 (15pen) (Unaged)	3.86E+06
07-1394 (RTFOT)	5.43E+06
07-1394 (PAV)	1.23E+07
08-3336 (50pen) (Unaged)	4.08E+05
08-3336 (RTFOT)	8.31E+05
08-3336 (PAV)	2.31E+06
SATS Standard Runs	
08-2823 (15pen) (SATS; 85°C, 65Hrs, 2.1MPa)	1.61E+07
08-2825 (15pen) (SATS; 85°C, 65Hrs, 2.1MPa)	1.90E+07
08-2827 (15pen) (SATS; 85°C, 65Hrs, 2.1MPa)	1.28E+07

08-2829 (15pen) (SATS; 85°C, 65Hrs, 2.1MPa)	1.39E+07
08-2831 (15pen) (SATS; 85°C, 65Hrs, 2.1MPa)	1.21E+07
08-2833 (50pen) (SATS; 85°C, 65Hrs, 2.1MPa)	2.80E+06
08-2835 (50pen) (SATS; 85°C, 65Hrs, 2.1MPa)	2.54E+06
08-2837 (50pen) (SATS; 85°C, 65Hrs, 2.1MPa)	1.97E+06
08-2839 (50pen) (SATS; 85°C, 65Hrs, 2.1MPa)	2.40E+06
08-2841 (50pen) (SATS; 85°C, 65Hrs, 2.1MPa)	1.42E+06
08-2843 (50pen) (SATS; 85°C, 65Hrs, 0.5MPa)	1.63E+06
08-2845 (50pen) (SATS; 85°C, 65Hrs, 0.5MPa)	1.67E+06
08-2847 (50pen) (SATS; 85°C, 65Hrs, 0.5MPa)	1.64E+06
08-2849 (50pen) (SATS; 85°C, 65Hrs, 0.5MPa)	1.48E+06
08-2851 (50pen) (SATS; 85°C, 65Hrs, 0.5MPa)	5.95E+04
09-648 (50pen) (SATS; 85°C, 65Hrs, 2.1MPa)	1.82E+06
09-654 (50pen) (SATS; 85°C, 65Hrs, 2.1MPa)	1.47E+06
09-664 (50pen) (SATS; 85°C, 65Hrs, 2.1MPa)	9.82E+05
09-692 (50pen) (SATS; 85°C, 24Hrs, 0.5MPa)	7.78E+05
SATS Dry Runs	
09-3092 (15pen) (SATS; 85°C, 65Hrs, 2.1MPa)	1.66E+07
09-3022 (50pen) (SATS; 85°C, 65Hrs, 2.1MPa)	3.31E+06
09-3024 (50pen) (SATS; 85°C, 65Hrs, 0.5MPa)	2.66E+06
09-3040 (50pen) (SATS; 60°C, 65Hrs, 0.5MPa)	1.14E+06
09-3052 (50pen) (SATS; 30°C, 65Hrs, 0.5MPa)	7.49E+05
09-3044 (50pen) (SATS; 85°C, 24Hrs, 0.5MPa)	1.57E+06
09-3048 (50pen) (SATS; 85°C, 65Hrs, 2.1MPa)	2.45E+06
09-3028 (50pen) (SATS; 85°C, 65Hrs, 2.1MPa)	4.67E+06
09-3060 (50pen) (SATS; 85°C, 65Hrs, 2.1MPa)	1.32E+06
SATS Standard Runs	
10-1120 (50pen) (SATS; 30°C, 65Hrs, 2.1MPa)	4.15E+05
10-1180 (50pen) (SATS; 85°C, 65Hrs, 0MPa)	5.71E+05
10-1182 (50pen) (SATS; 85°C, 24Hrs, 2.1MPa)	9.78E+05
10-1186 (50pen) (SATS; 60°C, 65Hrs, 2.1MPa)	7.47E+05
10-1190 (50pen) (SATS; 85°C, 4Hrs, 2.1MPa)	4.94E+05
10-3292 (50pen) (SATS; 85°C, 65Hrs, 2.1MPa)	5.45E+05

SATS Dry Runs	
10-1124 (50pen) (SATS; 85°C, 24Hrs, 2.1MPa)	7.01E+05
10-1194 (50pen) (SATS; 85°C, 65Hrs, 0MPa)	5.73E+05
10-1196 (50pen) (SATS; 85°C, 4Hrs, 2.1MPa)	4.45E+05
10-1200 (50pen) (SATS; 60°C, 65Hrs, 2.1MPa)	8.22E+05
10-1204 (50pen) (SATS; 30°C, 65Hrs, 2.1MPa)	3.63E+05
SATS Standard Runs	
10-3294 (50pen) (SATS; 85°C, 65Hrs, 0MPa)	6.84E+05
10-3296 (50pen) (SATS; 85°C, 65Hrs, 0MPa)	9.92E+05
10-3319 (50pen) (SATS; 85°C, 24Hrs, 2.1MPa)	6.55E+05
10-3321 (50pen) (SATS; 85°C, 24Hrs, 2.1MPa)	1.13E+06
10-3343 (50pen) (SATS; 30°C, 65Hrs, 2.1MPa)	6.53E+05
10-3345 (50pen) (SATS; 30°C, 65Hrs, 2.1MPa)	6.24E+05
10-3298 (50pen) (SATS; 60°C, 65Hrs, 2.1MPa)	8.25E+05
10-3478 (50pen) (SATS; 60°C, 65Hrs, 2.1MPa)	5.26E+05
10-3347 (50pen) (SATS; 85°C, 4Hrs, 2.1MPa)	5.19E+05
10-3349 (50pen) (SATS; 85°C, 4Hrs, 2.1MPa)	5.55E+05
10-3355 (50pen) (SATS; 85°C, 24Hrs, 0.5MPa)	6.89E+05
10-3357 (50pen) (SATS; 85°C, 24Hrs, 0.5MPa)	8.08E+05
10-3483 (50pen) (SATS; 85°C, 65Hrs, 2.1MPa)	6.83E+05
10-3485 (50pen) (SATS; 85°C, 65Hrs, 2.1MPa)	8.51E+05
10-3498 (50pen) (SATS; 85°C, 65Hrs, 2.1MPa)	6.24E+05
11-3 (50pen) (SATS; 85°C, 65Hrs, 2.1MPa)	3.38E+05
11-5 (50pen) (SATS; 85°C, 65Hrs, 2.1MPa)	4.98E+05
11-7 (50pen) (SATS; 85°C, 65Hrs, 2.1MPa)	5.84E+05
10-3278 (50pen) (SATS; 85°C, 65Hrs, 2.1MPa)	1.30E+06
10-3280 (50pen) (SATS; 85°C, 65Hrs, 2.1MPa)	1.90E+06
10-3282 (50pen) (SATS; 85°C, 65Hrs, 2.1MPa)	1.89E+06
10-3284 (50pen) (SATS; 85°C, 65Hrs, 2.1MPa)	1.19E+06
10-3286 (50pen) (SATS; 85°C, 65Hrs, 2.1MPa)	1.13E+06
10-3288 (50pen) (SATS; 85°C, 65Hrs, 2.1MPa)	2.04E+06
10-3290 (50pen) (SATS; 85°C, 65Hrs, 2.1MPa)	1.08E+06
10-3292 (50pen) (SATS; 85°C, 65Hrs, 2.1MPa)	5.49E+05

SATS Dry Runs	
10-3500 (50pen) (SATS; 85°C, 65Hrs, 2.1MPa)	8.91E+05
11-9 (50pen) (SATS; 85°C, 65Hrs, 2.1MPa)	8.58E+05

7.3.2 Results

It has been observed that the binder becomes stiffer with increased ageing. The SATS specimen aged the most because of the comparatively harsh protocol while the RTFOT aged binders were the least stiff (lower complex modulus). The master curves for SATS aged binder hover around the PAV master curve. The specimen taken from below water/submerged position was the least aged. The reason for this is that the specimen below water undergoes a lesser amount of oxidative ageing (hardening of the material) because of the presence of comparatively smaller amounts of free oxygen. Instead it is water aged/damaged.

7.4 Data Analysis for Moisture Sensitivity Determination

As mentioned in Section 7.1, the main objective of this analysis is to determine the moisture factor for the selected set of material combinations. The data that is mainly used for the analysis includes the following:

- Retained saturation values for the SATS tested specimens
- Retained stiffness values (initial ITSM and SATS conditioned ITSM)
- Recovered binder data for both dry and conditioned SATS tested specimens

7.4.1 SATS Retained Stiffness Modulus and Moisture Damage

SATS retained stiffness modulus is obtained by dividing the stiffness modulus of SATS conditioned specimen by the stiffness modulus of the unconditioned specimen as follows (Choi, 2005):

$$RS = \frac{S_{conditioned}}{S_{initial}} \quad (62)$$

where;

RS = Retained stiffness of a specimen (MPa/MPa)

$S_{conditioned}$ = Stiffness modulus of conditioned specimen (MPa); and

$S_{initial}$ = Stiffness modulus of unconditioned specimen (MPa)

The stiffness modulus of the SATS conditioned specimen is not only affected by moisture induced damage but it is a result of a number of factors. The stiffness modulus of the SATS tested specimen can be described by the following equation (Choi, 2005):

$$S_{conditioned} = S_{initial} \times f_{ageing} \times f_{pressure} \times f_{moisture} \quad (63)$$

where;

f_{ageing} = Ageing factor (age hardening of mixture)

$f_{pressure}$ = Pressure factor (damage/loss of stiffness due to pressure)

$f_{moisture}$ = Moisture factor (moisture damage)

As per Choi (2005), once the ageing and pressure factors are determined the moisture sensitivity of the specimen can be obtained as follows:

$$f_{moisture} = \frac{RS}{f_{ageing} \times f_{pressure}} \quad (64)$$

The procedure for the determination of ageing, pressure and the moisture factors is provided in the following sections. For simplicity, the resulting plots and data for only one combination of material (50pen binder and Aggregate type 'A' tested under standard SATS conditions of 85°C, 65Hrs and 2.1MPa) are provided in the explained procedure. However, comparisons between different binders, aggregate types and SATS test conditions are provided at the end of the analysis.

7.4.2 Age Hardening (Ageing Factor)

First of all, the effect of ageing (increase in stiffness) in the SATS test without the presence of water (dry ageing) is determined. The following steps are followed for this purpose.

1. The penetration grade and softening point (ring and ball-R&B apparatus) values for the unaged, RTFOT and PAV aged binders are determined. All this material is also tested with a dynamic shear rheometer (DSR) for its rheological properties. The complex shear modulus values for the material at temperature of 25°C and at frequency of 0.4 Hz are determined.
2. The dynamic shear modulus values for all the binders are normalised to the PAV (HiPAT-long term ageing) aged modulus values.
3. The penetration grade and softening point values are then plotted as a function of normalised DSR data at 0.4Hz and 25°C, as shown in Figure 7.9.

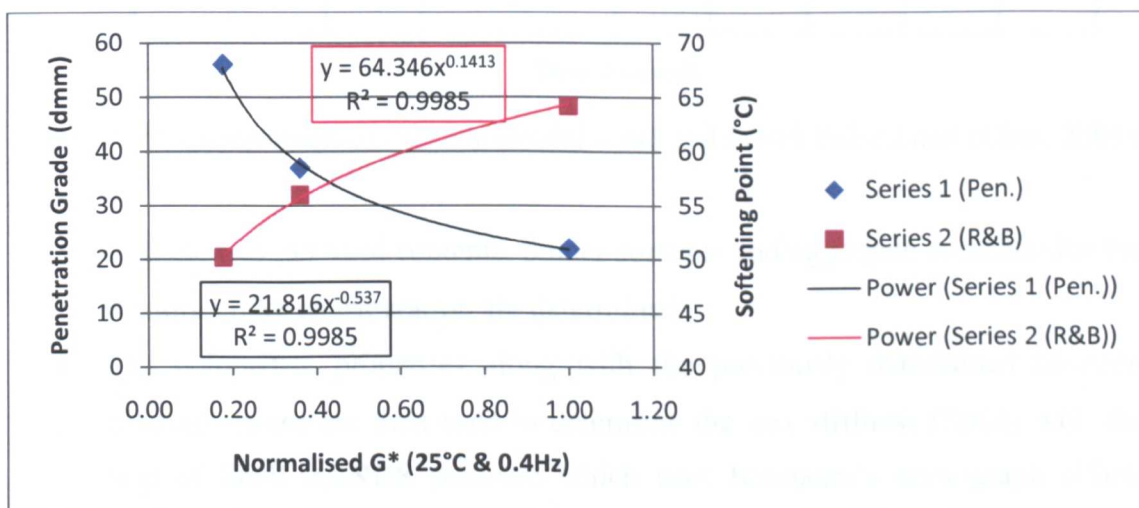


Figure 7.9: Penetration and Softening Point vs. Normalised Shear Complex Modulus

4. Power law functions are fitted to the curves in the plot.
5. The fitted power law functions are then used to determine the values of penetration grade and softening points as a function of normalised DSR data at 0.4Hz and 25°C for increments of 0.1 values.
6. The Shell BANDS 2.0 software is used to determine the stiffness of bitumen (Sbit) from the predicted penetration grade and softening point values. The software uses the Van der Poel nomograph (Choi, 2005) to predict the bitumen stiffness. A frequency of 2Hz is considered to be comparable to the ITSM testing condition, as in Figure 7.10 below and is used in the software.

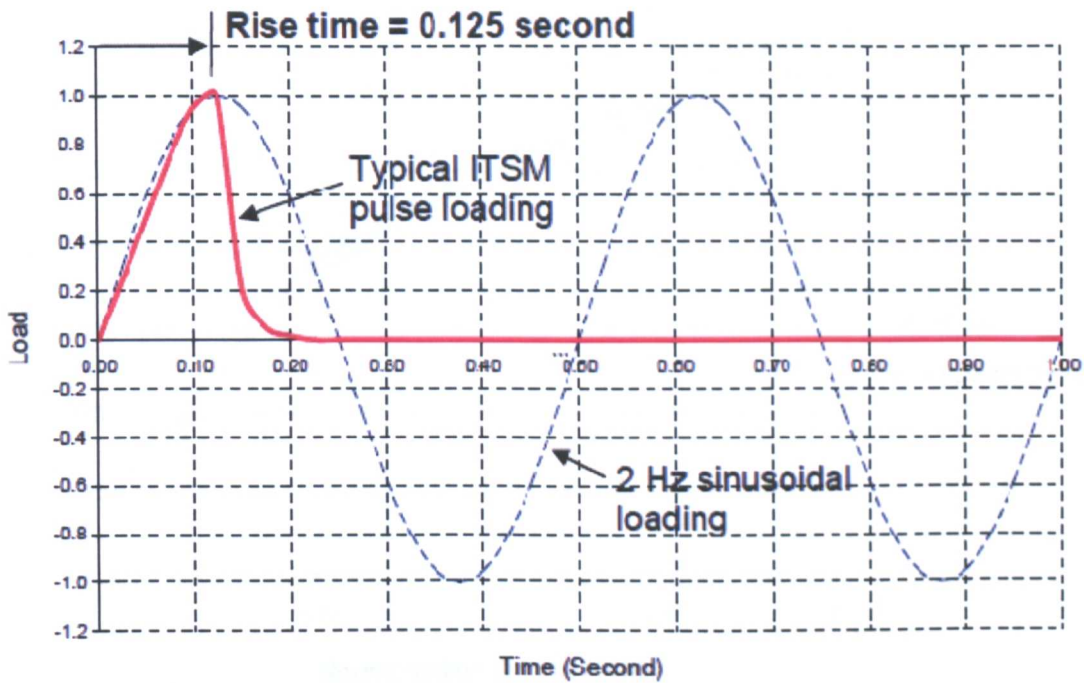


Figure 7.10: Comparison of 2Hz Sinusoidal Load and ITSM Pulse Load (Choi, 2005)

7. Volumetrics (air void contents, binder contents and aggregate contents) for the mixture under consideration are determined.
8. The volumetric properties along with the previously determined bitumen stiffness values are then used to determine the mix stiffness (S_{mix}) with the help of Shell BANDS software which uses Bonnaure's nomograph (Choi, 2005).
9. The mixture stiffness is plotted as a function of normalised DSR G^* data at 25°C and 0.4Hz, shown in Figure 7.11. A power law equation is fitted to the data.

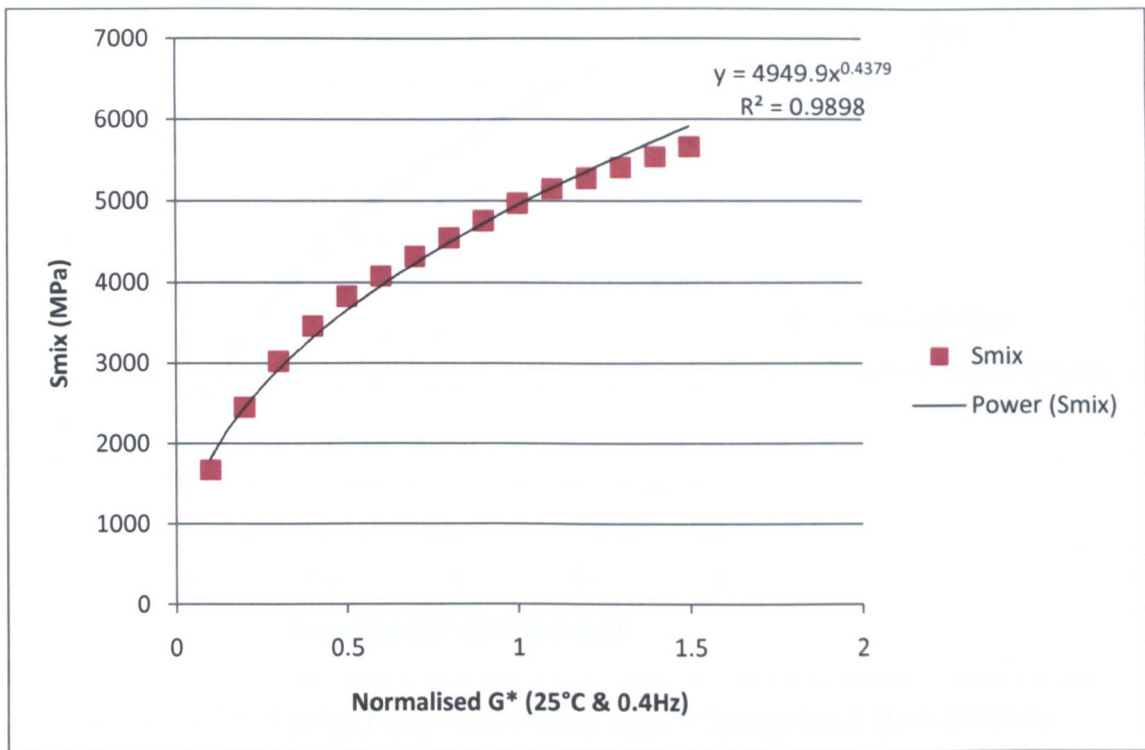


Figure 7.11: Predicted Asphalt Mixture Stiffness Moduli

10. The power law equation is then used to determine the Smix at values of normalised DSR G* at increments of 0.1. This is referred to as predicted Smix.
11. The Smix that corresponds to the normalised DSR G* that corresponds to RTFOT aged bitumen is then determined.
12. The predicted Smix results at various normalised DSR G* values is then divided by the value of Smix at RTFOT aged binder conditions. This is referred to as normalised Smix.
13. The normalised Smix data is then plotted against the normalised DSR G* data and a power law equation is fitted to the data as shown in Figure 7.12 below.

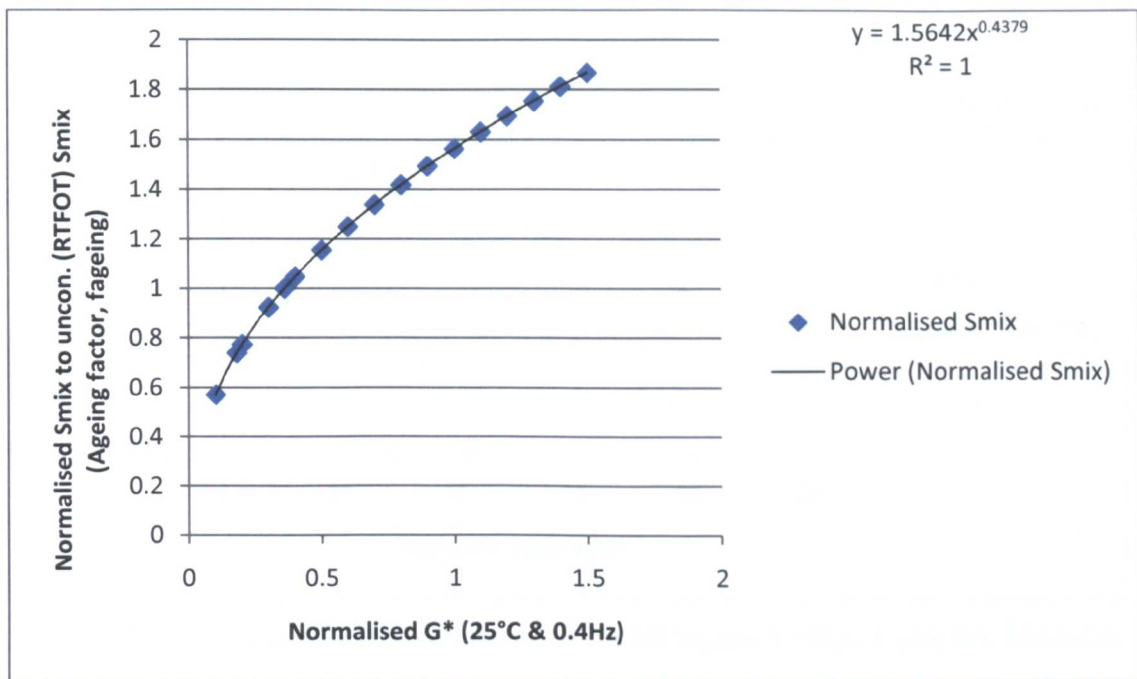


Figure 7.12: Ageing Factor of Mixture against Normalised DSR G* Data

In order to study the effect of moisture content on the ageing of the binder the following steps are followed.

1. Binder is recovered from each of the SATS tested specimens.
2. The DSR G* data at 0.4Hz and 25°C is determined for all the recovered binders.
3. The obtained results are then normalised to the PAV DSR G* values at 25°C and 0.4Hz.
4. The calculated normalised DSR G* values for the recovered binders are then plotted versus the retained saturation values obtained from the SATS tests for the respective specimens. The recovered binder data from the dry SATS test is also included. A linear function is then fitted to the data as shown in Figure 7.13.
5. The obtained linear function is then used to determine the normalised DSR G* values as a function of 10% increments of retained saturation.

Figure 7.13: Predicted Ageing Factor Plotted as a Function of Retained Saturation

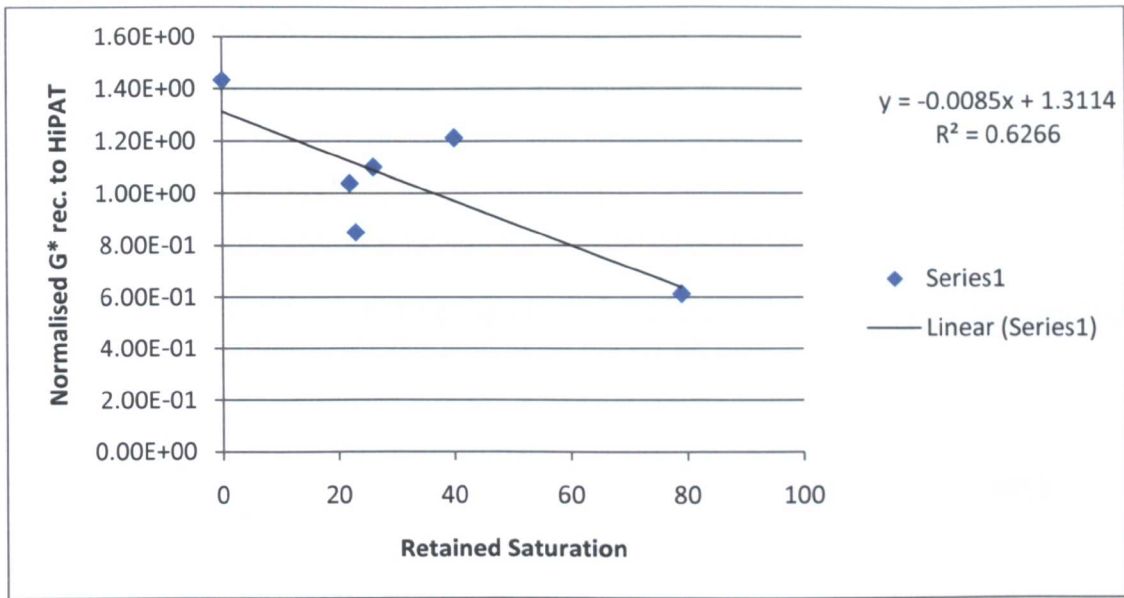


Figure 7.13: Effect of Retained Saturation on Normalised Shear Complex Modulus

The ageing factor for the combined effect of moisture and dry ageing is now determined by combining the data from Figures 7.12 and 7.13. The normalised DSR G^* values obtained by using the linear function from Figure 7.13 are used in the power law function obtained from Figure 7.12 to determine the ageing factor relative to retained saturation levels, shown in Figure 7.14 below.

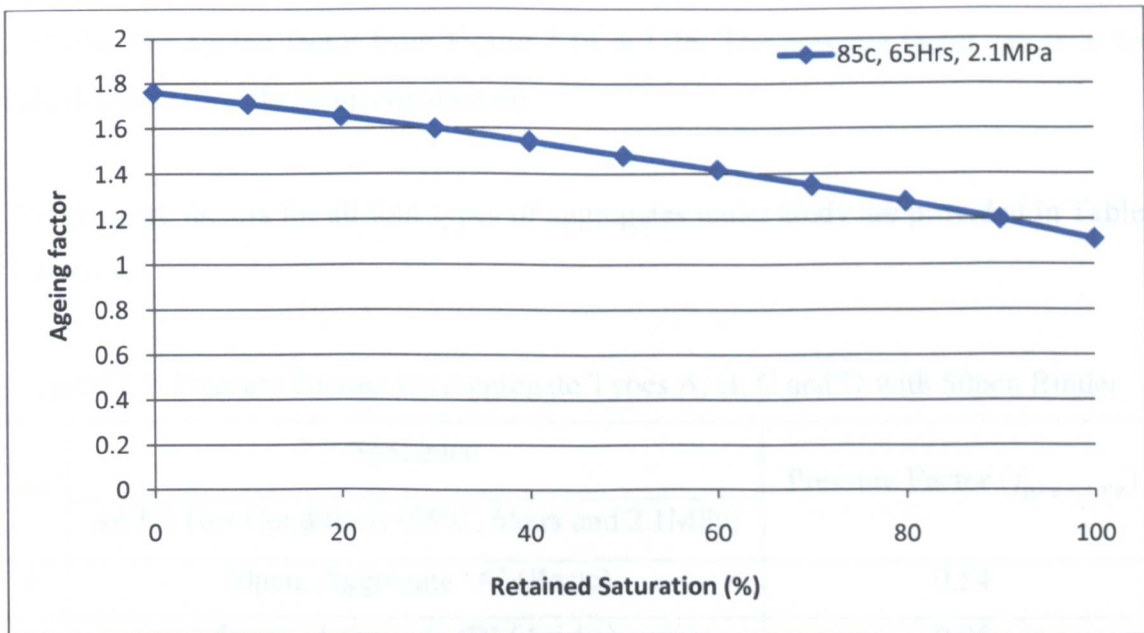


Figure 7.14: Predicted Ageing Factor Plotted as a Function of Retained Saturation

It can be seen from the figure that the ageing factor decreases with an increase in the retained saturation because there is less air available to age the binder.

7.4.3 Pressure Factor

For a dry SATS test the moisture factor can be taken as 1 which means that equation 64 can be written as:

$$1 = \frac{RS}{f_{ageing} \times f_{pressure}} \quad (65)$$

Pressure factor can then be written as:

$$f_{pressure} = \frac{RS}{f_{ageing}} \quad (66)$$

The ageing factors for different mixture combinations and sets of conditions can be determined by producing plots as in Figure 7.14 above. As mentioned earlier, Figure 7.14 has been produced for an asphalt mixture produced by using 50pen binder and aggregate type 'A', and tested under standard SATS conditions of 85°C, 65hrs and 2.1MPa. The ageing factor from Figure 7.14 is 1.76. The pressure factor can then be calculated by directly using equation 66.

The pressure factors for all four types of aggregates under study are provided in Table 7.3 below.

Table 7.3: Pressure Factors for Aggregate Types A, B, C and D with 50pen Binder

No.	Specimen	Pressure Factor ($f_{pressure}$)
	SATS Test Conditions (85°C, 65hrs and 2.1MPa)	
1	50pen, Aggregate 'A' (Basic)	0.54
2	50pen, Aggregate 'B' (Acidic)	0.98
3	50pen, Aggregate 'C' (Acidic)	0.97
4	50pen, Aggregate 'D' (Acidic)	0.96

It can be seen from the above table that the pressure factor for the mixture containing basic aggregate is quite low as compared to the mixtures containing acidic aggregates which indicates that the basic aggregate mixture is more sensitive to the effects of pressure.

7.4.4 Moisture Factor

The moisture factor for a material combination is determined as follows:

1. Multiply the pressure factor (which is a constant and doesn't change with the retained saturation value) with the calculated ageing factor (which does change with retained saturation).
2. Plot the values obtained above in step 1 versus the retained saturation and fit a linear function to the data (pressure x ageing factors as a function of retained saturation) as shown in Figure 7.15.

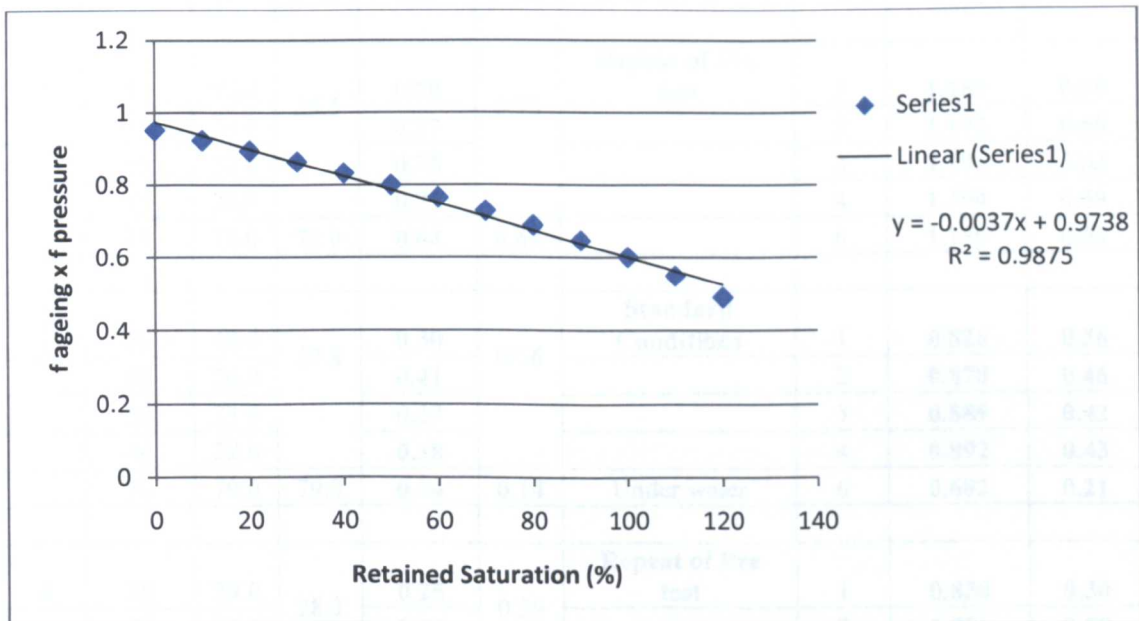


Figure 7.15: Chart showing $f_{ageing} \times f_{pressure}$ of Standard SATS

3. Then use the retained saturation from any SATS test specimen (using the correct SATS testing conditions and materials) to determine the pressure x ageing factors using the linear function.

4. The retained stiffness values (again for any specimens but for the correct conditions and materials) are then used with the pressure x ageing factor parameter to determine the moisture factor.

Moisture factor values for aggregate 'A' for the specimens tested under standard SATS test conditions are provided in Table 7.4 below for reference.

Table 7.4: Moisture Factors for Aggregate Type 'A'

Test No.	Binder (Pen.)	Ret. Sat. (%)	Avg.	Stiff. Ratio	Avg.	Comments	Place	Standard $F_{ageing} \times F_{pressure}$	$F_{moisture}$
						Standard Conditions			
1	15	28.0	25.3	0.76	0.77	Temperature = 85°C	1	1.190	0.63
	15	27.0		0.78		Duration = 65Hrs	2	1.191	0.66
	15	23.0		0.79		Pressure = 2.1Mpa	3	1.194	0.66
	15	23.0		0.77			4	1.194	0.65
	15	87.0	87.0	0.63	0.63	Below water position	6	1.143	0.55
2	15	29.0	25.5	0.70	0.73	Repeat of Pre test	1	1.189	0.59
	15	26.0		0.77			2	1.192	0.65
	15	24.0		0.75			3	1.193	0.63
	15	23.0		0.71			4	1.194	0.59
	15	72.0	72.0	0.64	0.64		6	1.155	0.56
3	50	40.0	27.8	0.30	0.36	Standard Conditions	1	0.826	0.36
	50	26.0		0.41			2	0.878	0.46
	50	23.0		0.37			3	0.889	0.42
	50	22.0		0.38			4	0.892	0.43
	50	79.0	79.0	0.14	0.14	Under water	6	0.682	0.21
4	50	39.0	28.3	0.25	0.39	Repeat of Pre test	1	0.830	0.30
	50	25.0		0.50			2	0.881	0.57
	50	23.0		0.35			3	0.889	0.39
	50	26.0		0.47			4	0.878	0.53
	50	88.0	88.0	0.21	0.21	Under water	6	0.648	0.33

7.5 Results and Conclusions

As mentioned in Section 7.2, different sets of material combinations and test conditions were selected for the study. Figure 7.16 shows a comparison of moisture factors of 15pen versus the 50pen binder. Both were tested with aggregate 'A' under standard SATS test conditions (85°C, 65Hrs, 2.1MPa).

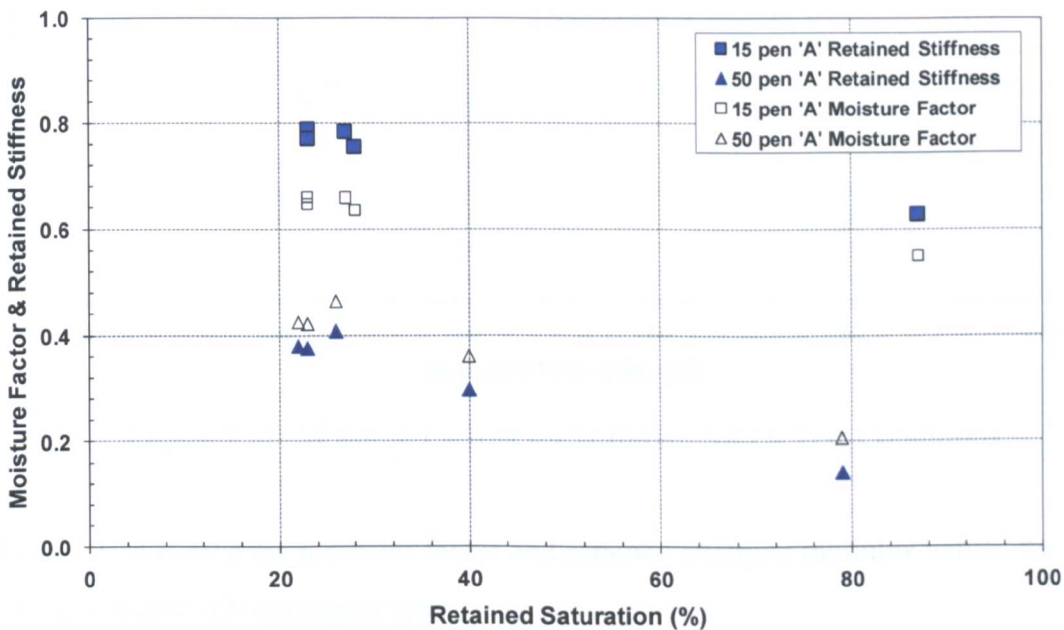


Figure 7.16: Moisture Factors for 15 and 50pen Binders with Basic Aggregate

Moisture factor is determined in order to get a parameter that is independent of the ageing and pressure factors and can solely assess the moisture sensitivity of the material. It can be seen from Figure 7.16 that the moisture factor for the 50pen binder has values higher than its retain stiffness values which indicates that this parameter has factored out the effect of high pressure damage on the softer binder. The 15pen binder however still has a higher moisture factor and hence more resistance to moisture damage. A similar effect can be seen in Figure 7.17 where the moisture factor and retained stiffness values for the specimens tested under high pressure and longer duration are compared with the specimens tested under low pressure and shorter duration. The moisture factor values for less harsh test conditions are quite comparable to their retained stiffness values while the moisture factor values for the high pressure test are more than their retained stiffness values. This means that the

moisture factor compensates for the pressure and ageing effects and the resulting moisture factor values lies in a comparatively narrower band.

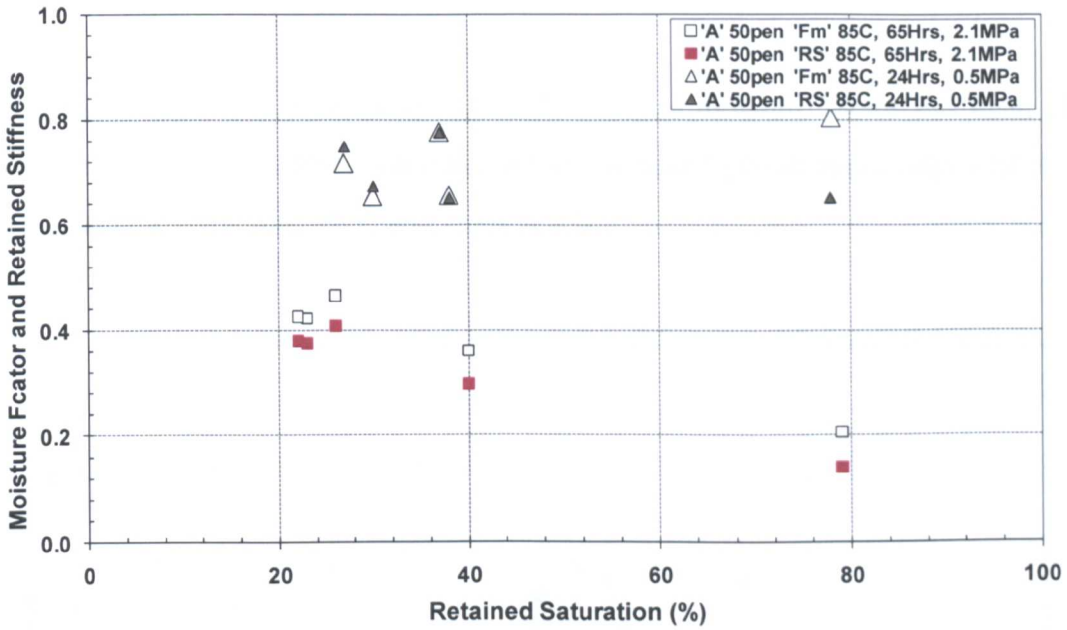


Figure 7.17: Moisture Factors for Different SATS Test Conditions

Figure 7.18 shows the moisture factor and retained stiffness modulus values for basic (A) and Acidic (D) aggregate types.

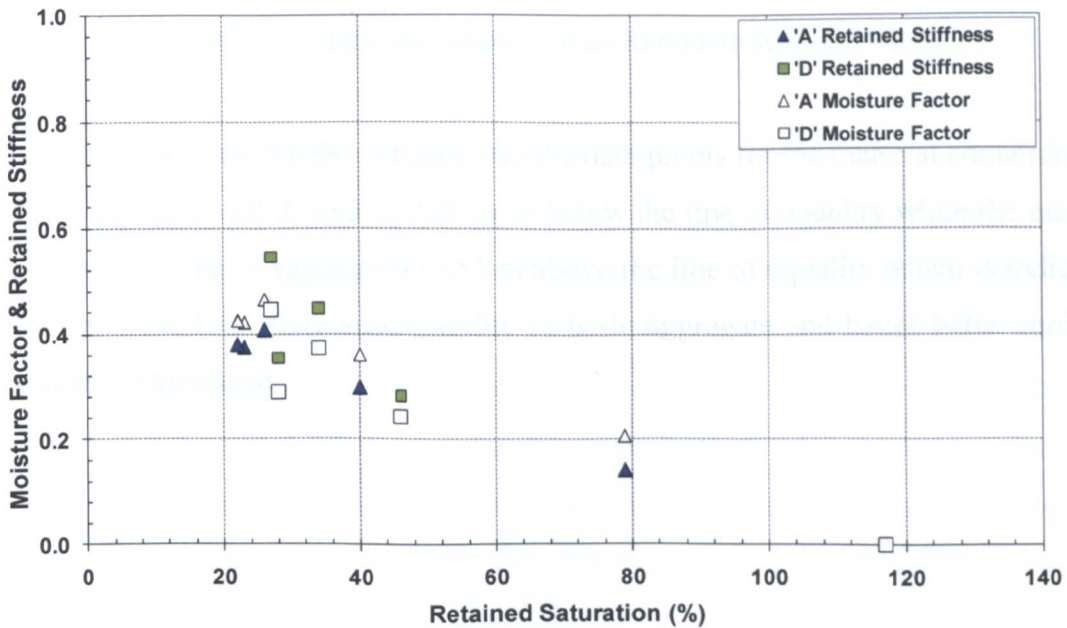


Figure 7.18: Moisture Factors for Basic (A) and Acidic (D) Aggregates

It can be seen from the figure that the moisture factors for the basic aggregate mixtures have increased indicating improved moisture damage performance while they have decreased for the mixtures containing acidic aggregates indicating increased moisture susceptibility.

A similar effect can be seen in Figure 7.19 where moisture factor has been plotted against the retained stiffness modulus for all the four types of aggregates with A being basic and the remaining B, C and D are acidic.

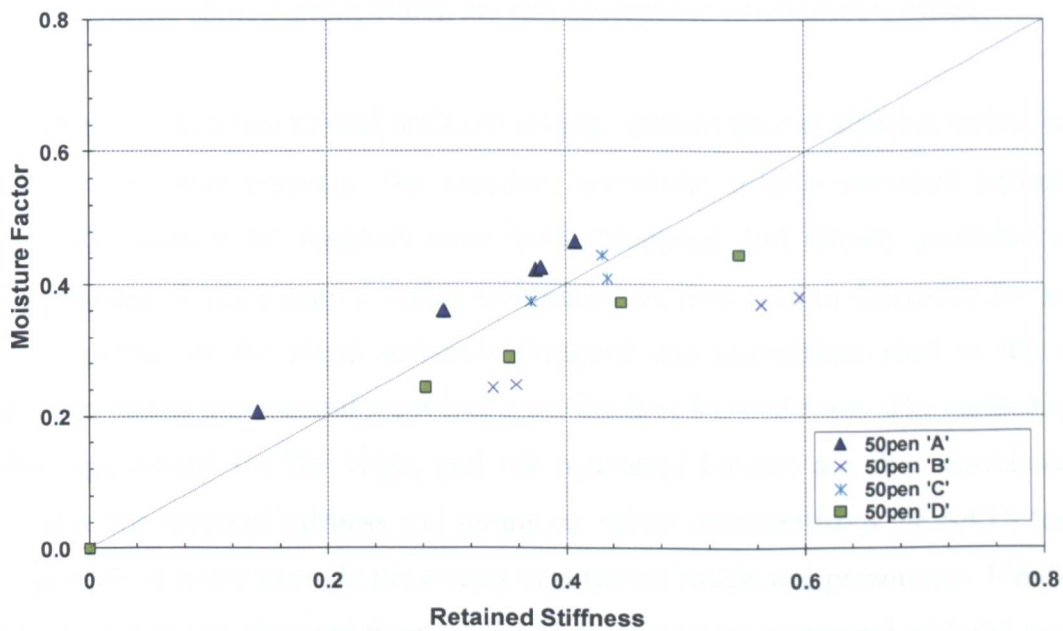


Figure 7.19: Moisture Factor versus Retained Stiffness Modulus

It can be seen from the above figure that the data points for the material containing the acidic aggregates (B, C and D) fall on or below the line of equality while the material containing the basic aggregates (A) lies above the line of equality which is indicative of an improved moisture susceptibility of basic aggregate and hence better moisture damage performance.

CHAPTER 8

SURFACE ENERGY AND SATS PROTOCOL

8.1 Introduction

One of the main objectives of this research is to combine a surface energy testing technique with a mechanical moisture sensitivity assessment technique in order to study the correlation between the moisture damage performance parameters obtained from both the techniques and to see if surface energy parameters can be used to identify compatible bitumen-aggregate combinations which are less susceptible to moisture damage.

The SATS protocol, a mechanical moisture damage performance evaluation technique, has been chosen for this purpose. The moisture sensitivity results (moisture factors) for different combination of materials have been calculated and already provided in the previous chapter. Surface energy testing techniques are then used to determine the surface energy properties of the virgin materials (bitumen and aggregates) used in the SATS protocol and that of the material recovered from the SATS tested cores. The surface energy and rheology results for the virgin and the recovered binders are then correlated and compared to the retained stiffness and saturation values obtained from the SATS tests for these materials in order to study the effects of different SATS test parameters. Finally, the moisture factor values obtained from the SATS technique are compared with the moisture sensitivity assessment ratios determined from the surface energy parameters.

8.2 Surface Energy Testing of SATS Material

The material combinations that were chosen for the study have already been provided in Section 7.2 of Chapter 7 (see Table 7.1). Two different penetration grade binders i.e. 15pen and 50pen were used. In order to cover a good spectrum of material that is being used in the UK for road construction, aggregates from four different sources were selected. They are divided into two major groups namely limestone (aggregate A) and granites (aggregates B, C and D). Different sets of SATS test conditions were also selected in order to study their effects.

8.2.1 Surface Energy Properties of Binders

As mentioned above 15pen and 50pen binders were used for the production of asphalt mixtures with different aggregate types.

In order to compare the SATS test results with the surface energy properties of the same material, the SATS tested cores were passed through a material recovery process (BS EN 12697-4:2005). The control/virgin material and the material recovered from the SATS cores were then tested for their surface energy properties. The testing and calculation procedures are the same as discussed in earlier chapters of this thesis.

The control binder was also aged by using the rolling thin film oven test-RTFOT (BS EN 12607-1:2007) and pressure ageing vessel-PAV (BS EN 14769:2005). The surface energy properties of the un-aged (virgin binder) and all the aged (RTFOT, PAV and SATS aged) material were compared and analysed.

The surface energy components of the unaged and the recovered/aged binders are provided in Table 8.1 below.

Table 8.1: SATS Binder, SE Parameters

Bitumen	Aggregate	Surface Energy Components (erg/cm ²)				
		γ^{LW}	γ^+	γ^-	γ^{AB}	γ^T
07-1394 (15pen) Unaged	A	34.66	0.00	0.59	0.0	34.7
07-1394 RTFOT		35.63	0.00	0.48	0.0	35.6
07-1394 PAV		35.21	0.00	0.22	0.0	35.2
09-3092 (15pen) (SATS; Std.; Dry)		20.63	0.01	2.11	0.3	20.9
08-2823 (15pen) (SATS; Std.; 1)		30.59	0.00	0.22	0.0	30.6
08-2825 (SATS; Std.; 2)		32.67	0.00	0.29	0.0	32.7
08-2827 (SATS; Std.; 3)		32.21	0.00	0.48	0.0	32.2
08-2829 (SATS; Std.; 4)		32.88	0.00	0.22	0.0	32.9
08-2831 (SATS; Std.; 6)		30.02	0.00	0.34	0.0	30.0
08-3336 (50pen) Unaged		A	36.15	0.00	0.04	0.0
08-3336 RTFOT	35.39		0.00	0.09	0.0	35.4
08-3336 PAV	35.65		0.00	0.15	0.0	35.7
09-3022 (50pen) (SATS; Std.; Dry)	27.52		0.00	2.78	0.0	27.5
08-2833 (50pen) (SATS; Std.; 1)	32.65		0.00	0.39	0.0	32.7

08-2835 (50pen) (SATS; Std.; 2)		32.81	0.00	0.55	0.0	32.8
08-2837 (50pen) (SATS; Std.; 3)		32.52	0.00	0.51	0.0	32.5
08-2839 (50pen) (SATS; Std.; 4)		28.81	0.00	0.36	0.0	28.8
08-2841 (50pen) (SATS; Std.; 6)		27.56	0.00	0.72	0.0	27.6
09-3024 (50pen) (SATS; 0.5MPa; Dry)	A	27.86	0.02	1.51	0.3	28.2
08-2843 (50pen) (SATS; 0.5MPa; 1)		29.93	0.00	0.66	0.0	29.9
08-2845 (50pen) (SATS; 0.5MPa; 2)		30.38	0.00	0.41	0.0	30.4
08-2847 (50pen) (SATS; 0.5MPa; 3)		31.14	0.00	0.55	0.0	31.1
08-2849 (50pen) (SATS; 0.5MPa; 4)		30.75	0.00	0.45	0.0	30.8
09-3048 (50pen) (SATS; Std.; Dry)	C	26.53	0.00	2.97	0.0	26.5
09-664 (50pen) (SATS; Std.; 1)		26.41	0.13	1.73	0.9	27.4
09-3028 (50pen) (SATS; Std.; Dry)	B	25.08	0.00	3.78	0.0	25.1
09-654 (50pen) (SATS; Std.; 1)		24.51	0.09	2.22	0.9	25.4
10-3278 (50pen) (SATS; Std.; 2)		23.72	0.25	2.79	1.7	25.4
10-3280 (50pen) (SATS; Std.; 3)		23.52	0.27	2.20	1.5	25.1
10-3282 (50pen) (SATS; Std.; 4)		23.37	0.21	2.84	1.5	24.9
10-3284 (50pen) (SATS; Std.; 6)		26.36	0.10	1.85	0.9	27.2
09-3060 (50pen) (SATS; Std.; Dry)	D	25.21	0.02	2.54	0.5	25.7
09-648 (50pen) (SATS; Std.; 1)		35.34	0.00	0.32	0.0	35.3
10-3286 (50pen) (SATS; Std.; 2)		29.63	0.01	1.74	0.3	29.9
10-3288 (50pen) (SATS; Std.; 3)		25.70	0.00	3.34	0.0	25.7
10-3290 (50pen) (SATS; Std.; 4)		28.94	0.03	1.59	0.4	29.4
10-3292 (50pen) (SATS; Std.; 6)		30.23	0.00	2.23	0.0	30.2
09-3044 (50pen) (SATS; 24Hrs, 0.5MPa; Dry)	A	23.52	0.03	2.13	0.5	24.0
09-692 (50pen) (SATS; 24Hrs, 0.5MPa; 1)		23.09	0.04	2.46	0.6	23.7
10-3355 (50pen) (SATS; 24Hrs, 0.5MPa; 4)		24.78	0.04	1.52	0.5	25.3
10-3357 (50pen) (SATS; 24Hrs, 0.5MPa; 6)		25.99	0.00	2.38	0.0	26.0
10-1186 (50pen) (SATS; 60C; 1)		24.96	0.00	2.26	0.0	25.0
10-1200 (50pen) (SATS; 60C; 2)		26.30	0.01	1.66	0.3	26.6
10-3298 (50pen) (SATS; 60C; 4)		25.05	0.00	2.18	0.0	25.1
10-3478 (50pen) (SATS; 60C; 6)		25.89	0.00	2.09	0.0	25.9

where;

‘SATS Std.’ corresponds to standard test conditions and the numbers 1 to 6 represent the specimen position in the SATS stand.

In order to study the effects of SATS ageing and moisture damage, a set of binder surface energy data was selected and is provided in Table 8.2.

Table 8.2: Binder Cohesion

SATS Project; Effect of Ageing and Moisture on Binder Cohesion						
No	Bitumen	Contact Angle Values (Degrees)			Surface Energy (erg/cm ²)	Cohesive Bond Strength (erg/cm ²)
		Water	Glycerol	Diiodomethane		
1	07-1394 (15pen) Unaged	97.2	85.6	47.9	34.7	69.3
2	07-1394 RTFOT	97.6	84.8	44.8	35.6	71.3
3	07-1394 PAV	98.5	84.7	45.2	35.2	70.4
4	08-2823 (15pen) (SATS; Std.; 1)	101.4	88.8	52.3	30.6	61.2
5	08-2825 (SATS; Std.; 2)	100.5	87.6	52.6	32.7	65.3
6	08-2827 (SATS; Std.; 3)	100.1	87.3	51.4	32.2	64.4
7	08-2829 (SATS; Std.; 4)	101.4	86.9	52.1	32.9	65.8
8	08-2831 (SATS; Std.; 6)	102.4	89.3	57.0	30.0	60.0
9	08-3336 (50pen) Unaged	101.3	86.2	45.4	36.2	72.3
10	08-3336 RTFOT	101.0	87.7	46.9	35.4	70.8
11	08-3336 PAV	99.8	85.7	46.3	35.7	71.3
12	08-2833 (50pen) (SATS; Std.; 1)	100.4	85.9	52.3	32.7	65.3
13	08-2835 (SATS; Std.; 2)	99.2	85.6	52.0	32.8	65.6
14	08-2837 (SATS; Std.; 3)	99.7	85.9	53.0	32.5	65.0
15	08-2839 (SATS; Std.; 4)	100.8	90.2	58.1	28.8	57.6
16	08-2841 (SATS; Std.; 6)	101.7	90.5	59.2	27.6	55.1
17	08-2843(50pen) (SATS; 0.5MPa; 1)	100.6	87.5	56.8	29.9	59.9
18	08-2845 (SATS; 0.5MPa; 2)	100.7	91.5	53.8	30.4	60.8
19	08-2847 (SATS; 0.5MPa; 3)	100.4	87.0	55.1	31.1	62.3
20	08-2849 (SATS; 0.5MPa; 4)	100.7	87.7	55.8	30.8	61.5

Results and Discussion

The contact angle and surface energy results have been plotted against the SATS test conditions to study the effect of ageing, moisture and binder penetration on the material properties. The plots are provided in Figures 8.1, 8.2 and 8.3.

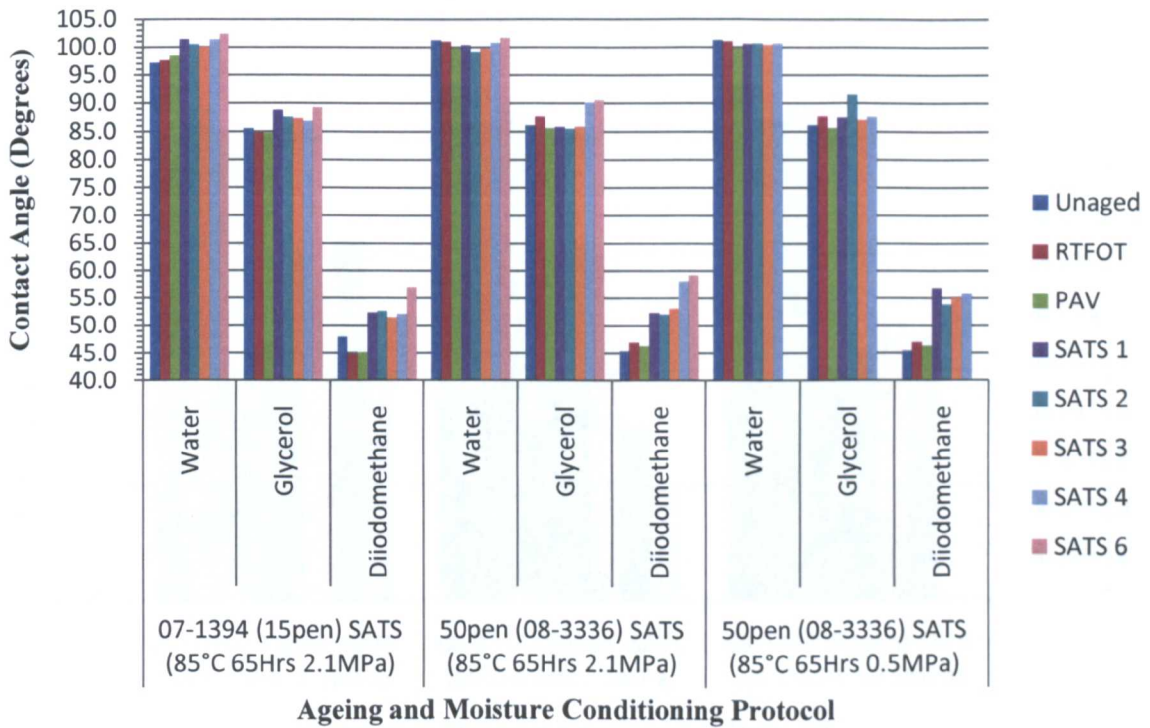


Figure 8.1: Effect of Ageing and Moisture on Contact Angle

- 07-1394 (15pen) SATS (85°C 65Hrs 2.1MPa) Water
- 07-1394 (15pen) SATS (85°C 65Hrs 2.1MPa) Glycerol
- 07-1394 (15pen) SATS (85°C 65Hrs 2.1MPa) Diiodomethane
- 50pen (08-3336) SATS (85°C 65Hrs 2.1MPa) Water
- 50pen (08-3336) SATS (85°C 65Hrs 2.1MPa) Glycerol
- 50pen (08-3336) SATS (85°C 65Hrs 2.1MPa) Diiodomethane
- 50pen (08-3336) SATS (85°C 65Hrs 0.5MPa) Water
- 50pen (08-3336) SATS (85°C 65Hrs 0.5MPa) Glycerol
- 50pen (08-3336) SATS (85°C 65Hrs 0.5MPa) Diiodomethane

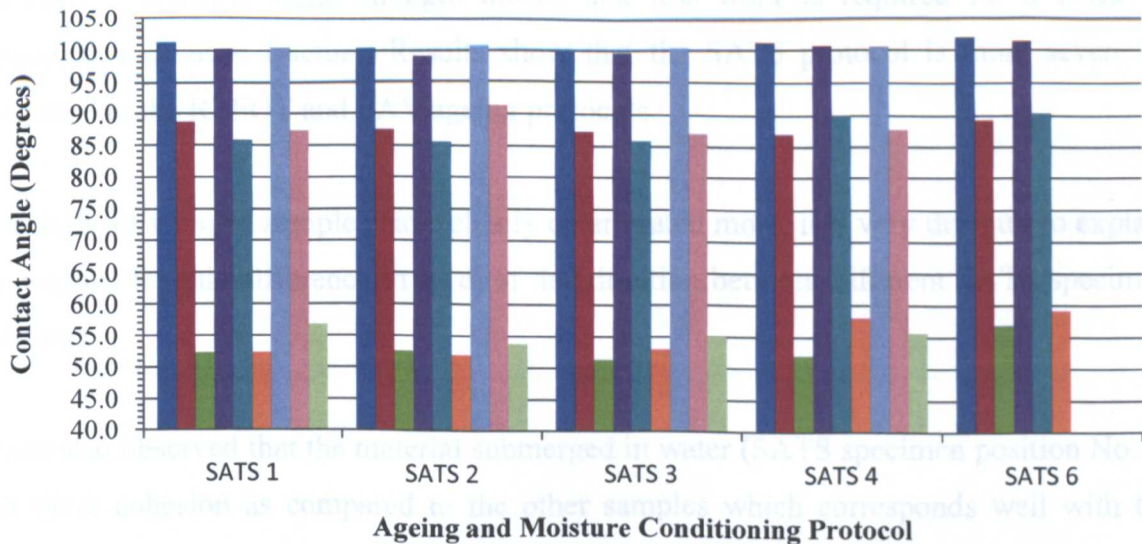


Figure 8.2: Effect of Binder Grade and SATS Conditions on Contact Angle

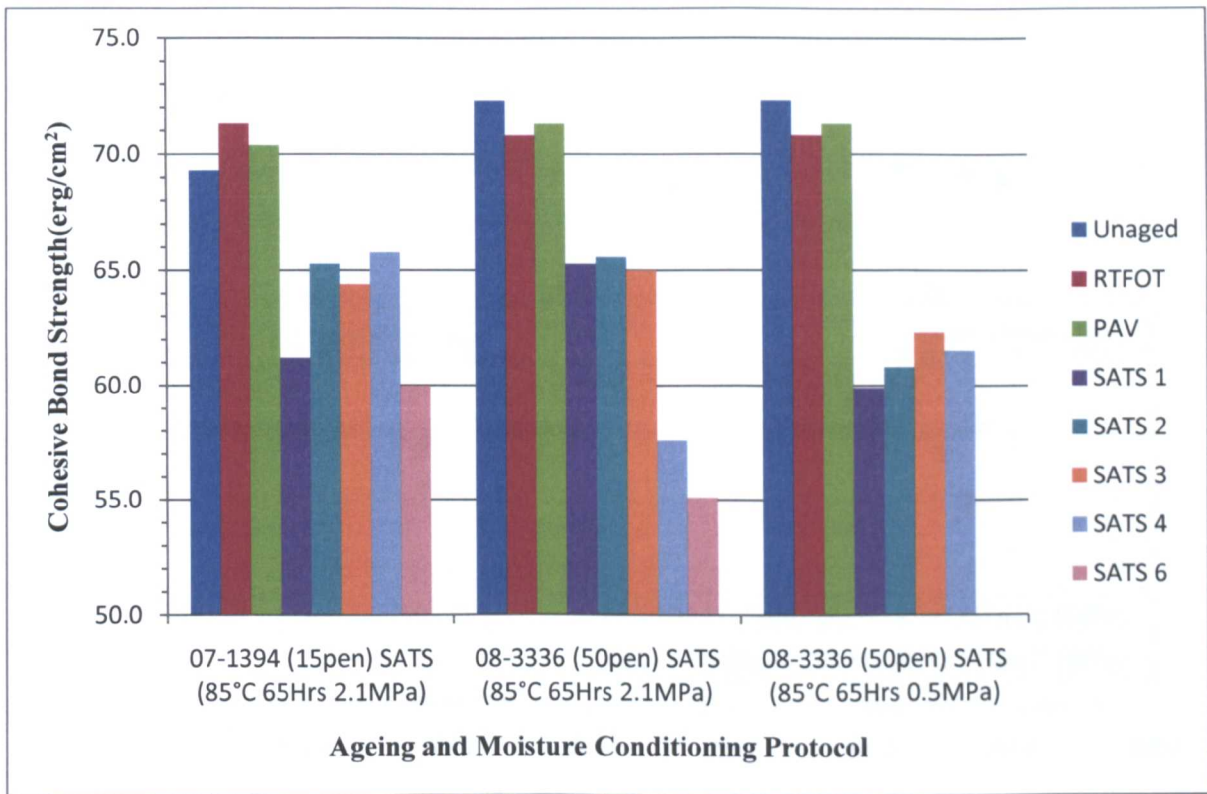


Figure 8.3: Effect of Ageing and Moisture on Cohesive Bond Strength

No big difference has been observed between different binders and different SATS conditions. All three sets of conditions follow the same trend as shown in Figure 8.3. The RTFOT and PAV have a very small effect on the cohesion of the binder while ageing by SATS considerably decreases the binder surface energy/cohesion. Decrease in the work of cohesion due to long term ageing is consistent with the literature (Bhasin et al., 2007). A decrease in cohesive bond strength means that less work is required for a crack to propagate and cause fracture. Results show that the SATS protocol is more severe as compared to the RTFOT and PAV ageing protocols.

Although SATS aged samples have clearly deteriorated more, it is very difficult to explain the reasons for this difference in level of deterioration between different SATS specimen positions.

It was also observed that the material submerged in water (SATS specimen position No. 6) lost more cohesion as compared to the other samples which corresponds well with the results obtained through the ITSM test, as shown in Figure 8.4.

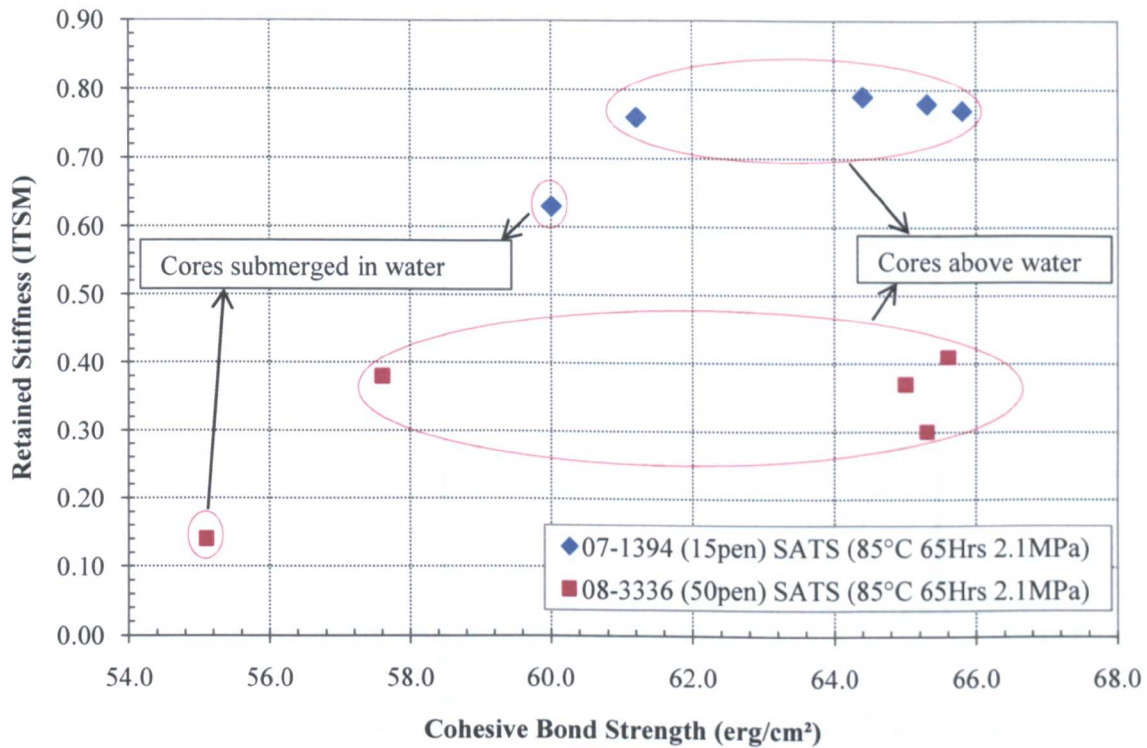


Figure 8.4: Cores above Water versus Cores Submerged in Water

Binder from the SATS tested cores was recovered by using dichloromethane (DCM). The presence of any residual DCM from the recovery process can have a significant effect on the surface energy properties of the recovered binder.

A nuclear magnetic resonance (NMR) technique was therefore used to check the presence of DCM in the recovered material. Presence of DCM in the binder gives a signature value of 5.30ppm. This can be seen in the Figure 8.5, where a small amount of DCM was added to the 50pen binder before testing using the NMR.

Some of the SATS recovered binder samples were tested with the NMR technique and no DCM was found in the recovered binders. The result for one of the recovered binder is provided for reference in Figure 8.6.



Figure 8.6: ¹H NMR (400 MHz, CDCl₃, 25°C) of SATS Recovered Binder

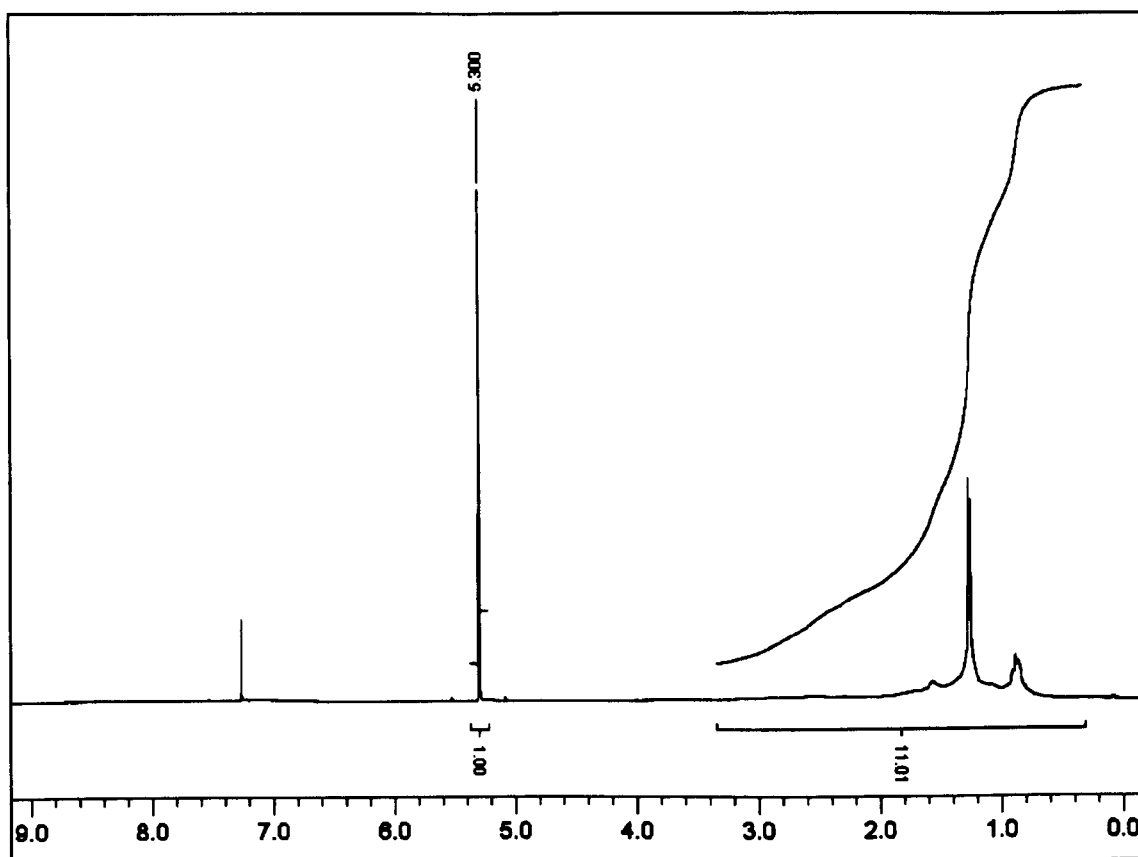


Figure 8.5: ¹H NMR (400 MHz, CDCl₃, 25°C) of 50pen binder with added DCM

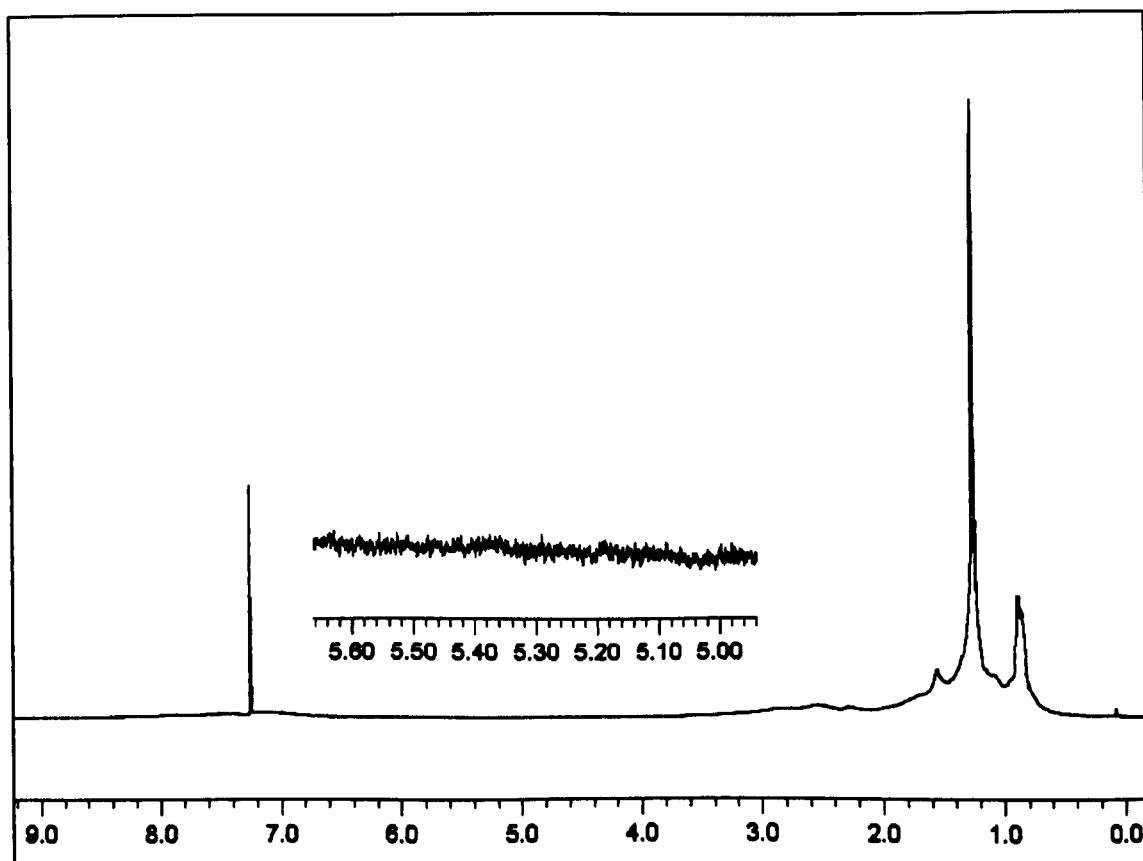


Figure 8.6: ¹H NMR (400 MHz, CDCl₃, 25°C) of SATS Recovered Binder

8.2.2 Binder Rheology and Surface Energy

The results from the dynamic mechanical analysis of all the unaged/virgin and aged (RTFOT, PAV and SATS) binders have been provided in section 7.3 of Chapter 7 (see table 7.2). This section provides a comparison of the rheology of the binders with their surface energy properties and SATS results.

A comprehensive comparison of all the test data is provided in Table 8.3. The amount of free air in the specimens was calculated on the basis of their retained saturations. Ageing indices for complex modulus were obtained for a frequency of 0.4 Hz at temperatures of 25 and 60°C. Ageing indices, percentage free air, cohesive bond strength and retained stiffness of the specimens were plotted and compared. The plots are provided in Figures 8.7, 8.8 and 8.9.

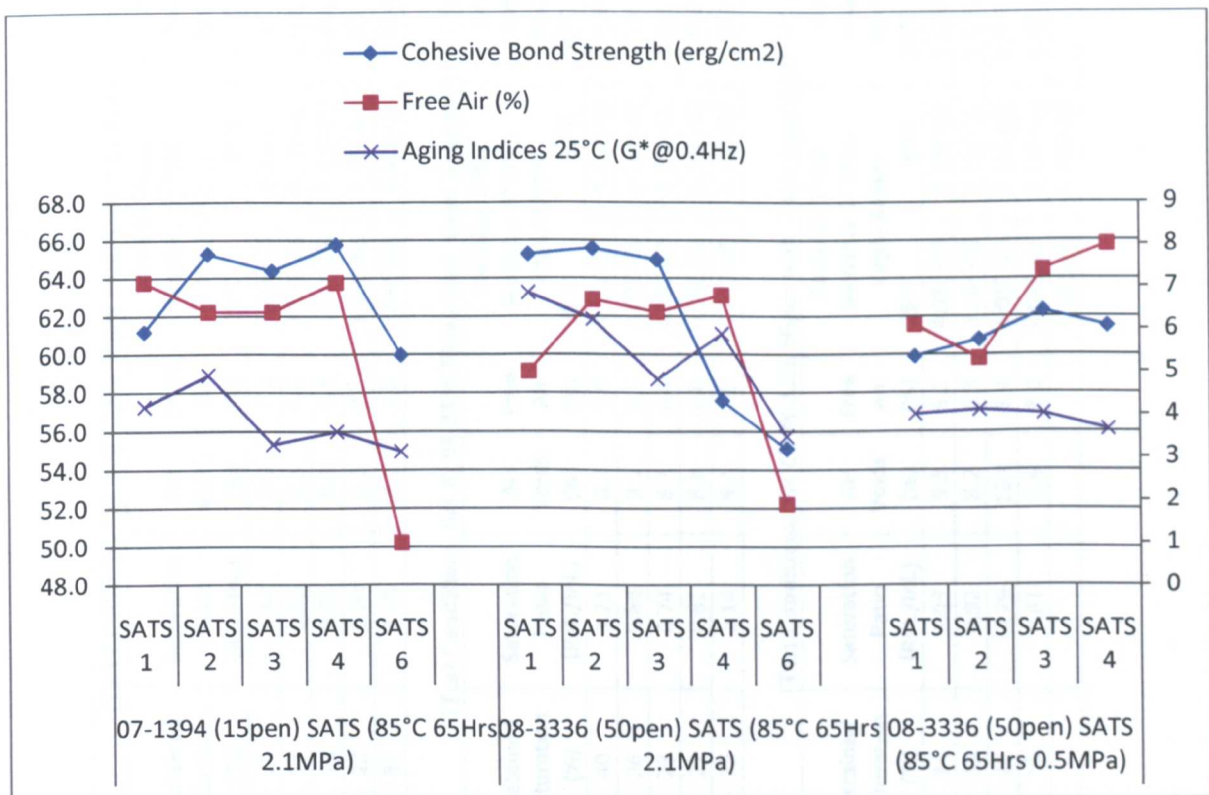


Figure 8.7: Effect of Presence of Air on Binder Rheology and SE

Table 8.3: Test Results; Executive Summary

[Test Conditions, Set A] 07-1394 15pen with Basic Aggregate 'A', SATS Std. Conds. (85°C 65Hrs 2.1Mpa)													
SATS Position	Initial Saturation (%)	Retained Saturation (%)	Saturation Ratio (Ret./ini.)	Air Voids (%)	Free Air (%)	Complex Shear Modulus G* (Pa), Virgin Binder		Complex Shear Modulus G* (Pa) Recovered Binder		Ageing Indices (G* @ 0.4Hz)		Retained Stiffness (ITSM)	Cohesive Bond Strength Recovered Binder (erg/cm ²)
						25°C	60°C	25°C	60°C	25°C	60°C		
1	25	28	1.12	9.9	7.1	3.86E+06	8.51E+03	1.61E+07	1.72E+05	4.18	20.18	0.76	61.2
2	28	27	0.96	8.8	6.4	3.86E+06	8.51E+03	1.90E+07	2.13E+05	4.91	25.02	0.78	65.3
3	29	23	0.79	8.3	6.4	3.86E+06	8.51E+03	1.28E+07	1.11E+05	3.30	13.05	0.79	64.4
4	29	23	0.79	9.2	7.1	3.86E+06	8.51E+03	1.39E+07	1.44E+05	3.60	16.90	0.77	65.8
6	25	87	3.48	8.1	1.0	3.86E+06	8.51E+03	1.21E+07	9.90E+04	3.14	11.64	0.63	60.0

[Test Conditions, Set B] 08-3336 50pen with Basic Aggregate 'A', SATS Std. Conds. (85°C 65Hrs 2.1Mpa)													
SATS Position	Initial Saturation (%)	Retained Saturation (%)	Saturation Ratio (Ret./ini.)	Air Voids (%)	Free Air (%)	Complex Shear Modulus G* (Pa), Virgin Binder		Complex Shear Modulus G* (Pa) Recovered Binder		Ageing Indices (G* @ 0.4Hz)		Retained Stiffness	Cohesive Bond Strength Recovered Binder (erg/cm ²)
						25°C	60°C	25°C	60°C	25°C	60°C		
1	33	40	1.21	8.4	5.0	4.08E+05	9.16E+02	2.80E+06	1.08E+04	6.87	11.77	0.30	65.3
2	31	26	0.84	9.1	6.7	4.08E+05	9.16E+02	2.54E+06	1.04E+04	6.24	11.36	0.41	65.6
3	31	23	0.74	8.3	6.4	4.08E+05	9.16E+02	1.97E+06	8.54E+03	4.82	9.32	0.37	65.0
4	36	22	0.61	8.8	6.8	4.08E+05	9.16E+02	2.40E+06	8.63E+03	5.89	9.42	0.38	57.6
6	37	79	2.14	9.4	1.9	4.08E+05	9.16E+02	1.42E+06	5.17E+03	3.48	5.65	0.14	55.1

[Test Conditions, Set C] 08-3336 50pen with Basic Aggregate 'A', SATS Conds. (85°C 65Hrs 0.5Mpa)													
SATS Position	Initial Saturation (%)	Retained Saturation (%)	Saturation Ratio (Ret./ini.)	Air Voids (%)	Free Air (%)	Complex Shear Modulus G* (Pa), Virgin Binder		Complex Shear Modulus G* (Pa) Recovered Binder		Ageing Indices (G* @ 0.4Hz)		Retained Stiffness	Cohesive Bond Strength Recovered Binder (erg/cm ²)
						25°C	60°C	25°C	60°C	25°C	60°C		
1	33	34	1.03	9.3	6.1	4.08E+05	9.16E+02	1.63E+06	5.19E+03	4.00	5.66	0.68	59.9
2	38	35	0.92	8.2	5.3	4.08E+05	9.16E+02	1.67E+06	6.33E+03	4.10	6.91	0.65	60.8
3	34	27	0.79	10.1	7.4	4.08E+05	9.16E+02	1.64E+06	6.38E+03	4.01	6.96	0.72	62.3
4	31	19	0.61	9.9	8.0	4.08E+05	9.16E+02	1.48E+06	4.77E+03	3.64	5.20	0.91	61.5

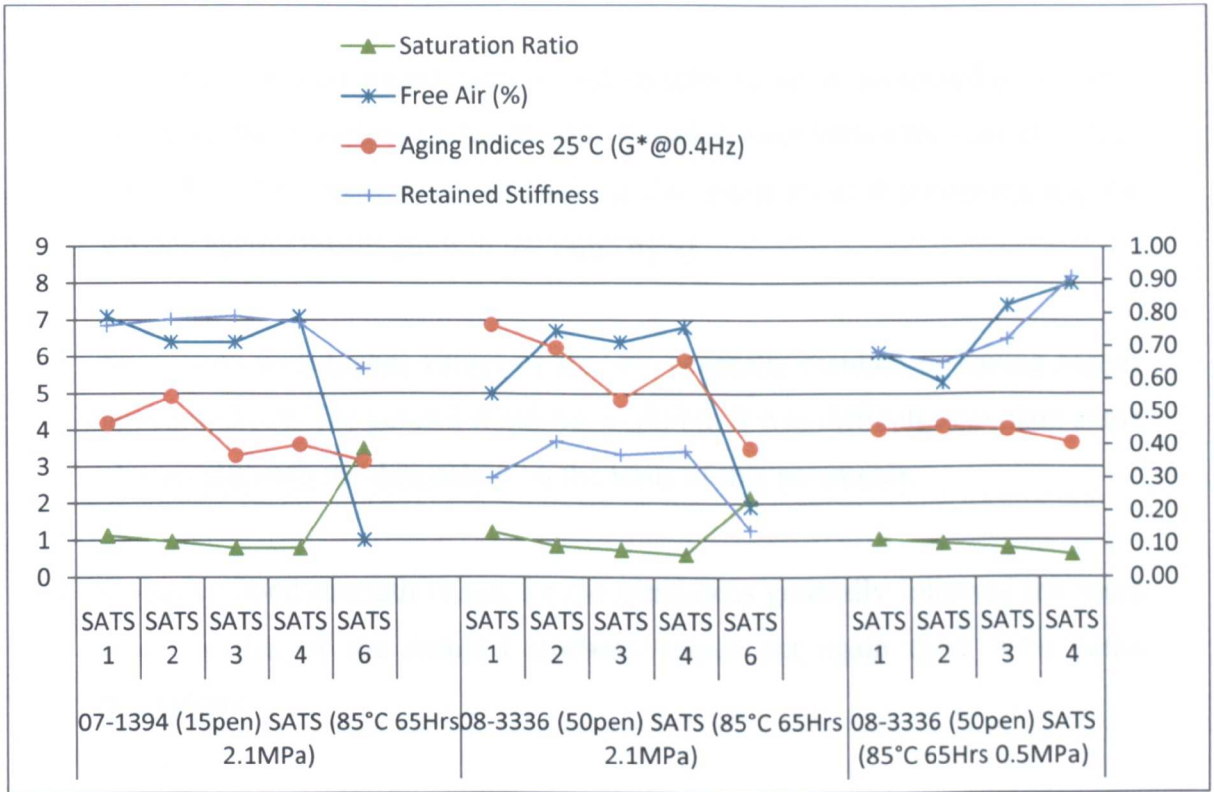


Figure 8.8: SATS Results and Binder Rheology

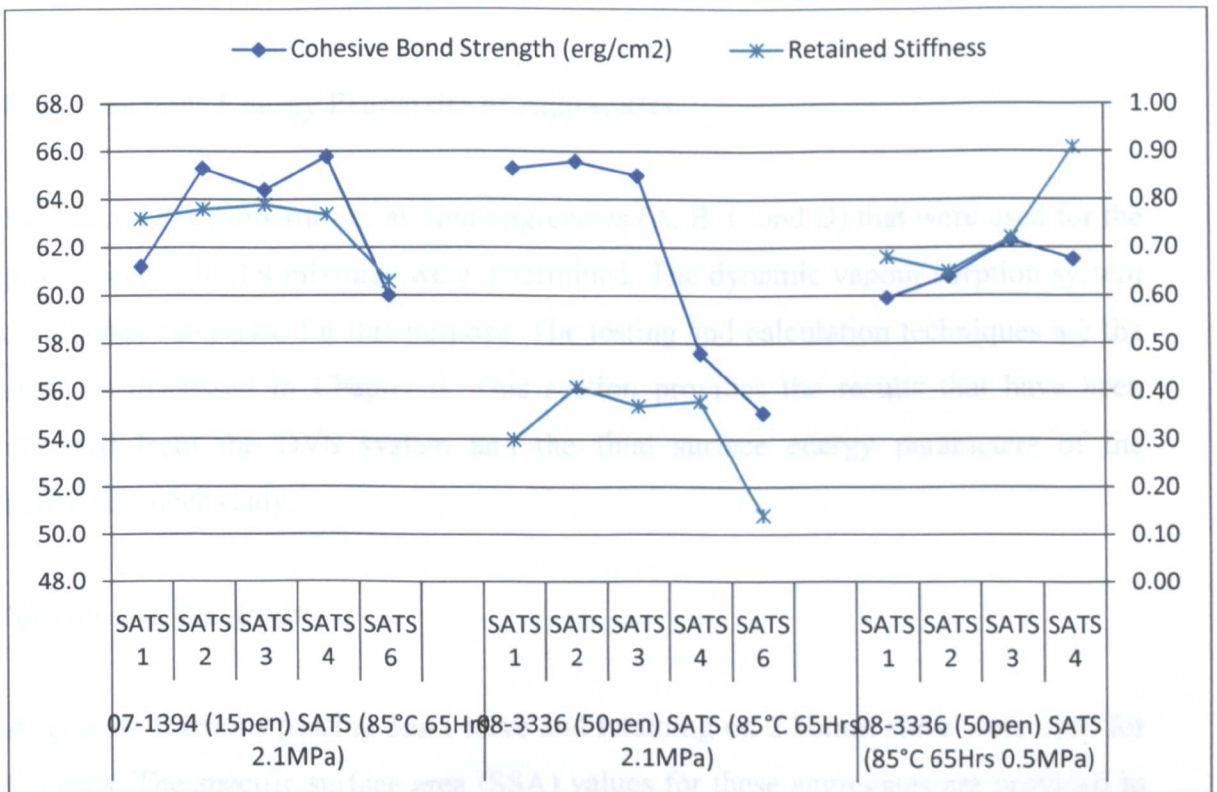


Figure 8.9: SATS Results and Binder SE

The following results can be shown from the comparison:

- The specimen submerged in water deteriorates more as compared to the ones above the water surface in the pressure vessel. Lower values for ageing indices and retained stiffness were obtained for the specimen at this position and the surface energy results showed the same trend.
- Specimens with higher values of free air generally resulted in having higher ageing indices. The general trend was right but it was difficult to explain some abnormalities in the data solely on the basis of this parameter.
- Cohesive bond strength values for the specimens generally followed the same trend as that of the retained stiffness values but again there were some exceptions.
- The results from all the three types of tests (SE, rheology and SATS) generally followed the same trend or somewhat expected trend but it was difficult to characterise the materials exactly on the basis of the obtained results.

8.2.3 Surface Energy Properties of Aggregates

Surface energy properties of all four aggregates (A, B, C and D) that were used for the production of SATS mixtures were determined. The dynamic vapour sorption system (DVS) has been used for this purpose. The testing and calculation techniques are the same as discussed in Chapter 4. This section provides the results that have been obtained from the DVS system and the final surface energy parameters of the materials under study.

Specific Surface Areas

Aggregate fractions passing 5mm sieve and retaining on 2.36mm sieve were used for the tests. The specific surface area (SSA) values for these aggregates are provided in Table 8.4.

Table 8.4: SSA of Aggregates (SATS)

Specific Surface Area of Aggregates (m²/g)			
Aggregates	Probe Liquids		
	Octane	Ethyl Acetate	Chloroform
A	0.7863	0.5526	0.7274
C	0.3819	0.4551	1.1655
B	0.3807	0.4251	0.6208
D	0.4420	0.9872	0.8237

Spreading pressures

SSA values obtained by using the Octane liquid were then used to calculate the spreading pressures on the aggregate surfaces for all the three probe liquids. Octane being non-polar in nature is supposed to give true values of specific surface area. The obtained spreading pressure results are provided in Table 8.5.

Table 8.5: Aggregates Spreading Pressure Values (SATS)

Spreading Pressures (mJ/m²)			
Aggregates	Probe Liquids		
	Octane	Ethyl Acetate	Chloroform
A	32.49	46.64	39.19
C	34.09	69.97	125.3
B	33.60	68.47	56.72
D	33.42	145	74.80

Surface Energy Components

The obtained spreading pressure values were then used to calculate the surface energy components of the aggregate samples. The final surface energy components for the four aggregate types are provided in Table 8.6 below.

Table 8.6: Aggregates SE Parameters (SATS)

Surface Energy Characteristics of Aggregates						
No.	Aggregate	Surface Energy Components (erg/cm²)				
		γ^{LW}	γ^+	γ^-	γ^{AB}	γ^T
1	A	66.12	2.90	5.04	7.65	73.77
2	C	68.97	17.41	569.68	199.18	268.15
3	B	68.10	16.49	41.19	52.12	120.22
4	D	67.78	164.22	123.37	284.67	352.45

The test results indicate that there is not a big difference between the van der Waals components of the aggregates. The total surface energy of the basic aggregate (A) is quite low as compared to the others. Two of the acidic aggregates (C and D) on the other hand have very high final surface energy values. Aggregate D has a higher acidic component but the other two acidic aggregates (B and C) have higher basic components. The reason for these may be that the surface chemistry of the material does not always correspond to the bulk chemistry (Kim, 2009). Also, the nature of probes and the initial preparation of the test material (storage conditions, weathering, washing/drying etc.) may also have an effect on the final results.

8.3 Bitumen-Aggregate Bond Energies and Moisture Sensitivity

The surface energy results for all the above mentioned four aggregate types and the binders were combined together in order to obtain the adhesive bond characteristics between the two materials in dry and wet conditions. The analysis gives an indication of the compatibility between different sets of materials and their moisture damage performance.

The surface energy values for all the binders have already been provided in Table 8.1. It can be seen from the table that the surface energy properties for almost all the recovered binders were very similar. Therefore, it was decided that the surface energy characteristics of only the virgin/unaged material will be used for the analysis. It should also be noted that the surface energy properties for the unaged binder mentioned above were obtained by using Goniometer test technique. The unaged

binder was also tested with the Wilhelmy plate device (DCA) and the results are provided in Table 8.7 below. The binder surface energy properties obtained by using DCA technique have been used for the compatibility analysis.

Table 8.7: Binder Surface Energy (SATS Material)

Surface Energy Characteristics of Binder						
No.	Bitumen	Surface Energy Components (mJ/m ²)				
		γ^{LW}	γ^+	γ^-	γ^{AB}	γ^T
1	Unaged 15pen (DCA)	31.05	0.01	3.37	0.37	31.42
2	Unaged 50pen (DCA)	30.61	0.00	2.40	0.00	30.61
3	Unaged 15pen (Goniometer)	34.66	0.00	0.59	0.00	34.66
4	Unaged 50pen (Goniometer)	36.15	0.00	0.04	0.00	36.15

The cohesive bond strength values for the binders tested by using DCA technique are also provided in Table 8.8 below.

Table 8.8: Binder Cohesion (SATS Material)

Cohesive Bond Strength of Bitumen						
No.	Bitumen	Contact Angle Values (Degrees)			Surface Energy (mJ/m ²)	Cohesive Bond Strength (mJ/m ²)
		Water	Glycerol	Diiodomethane		
1	Unaged 15pen	91.02	81.25	55.73	31.42	62.8
2	Unaged 50pen	94.30	84.15	56.17	30.61	61.2

The adhesive bond strengths for both dry and wet conditions have been calculated as explained in Chapter 5. The compatibility ratios (ratio of dry to wet bond strength) of the material combinations are calculated and are provided in Tables 8.9 and 8.10.

Table 8.9: Bitumen-Aggregate Compatibility Ratios (Aggregates 'A' & 'C')

Adhesive Bond Strength in Dry and Wet Conditions and Compatibility Ratios						
Bitumen	Aggregates					
	A			C		
	Dry (ΔG_{BA})	Wet (ΔG_{BWA})	Compatibility Ratio $\left \frac{\Delta G_{BA}}{\Delta G_{BWA}} \right $	Dry (ΔG_{BA})	Wet (ΔG_{BWA})	Compatibility Ratio $\left \frac{\Delta G_{BA}}{\Delta G_{BWA}} \right $
Unaged 15pen	97	56	1.75	113	-174	0.65
Unaged 50pen	95	58	1.64	105	-177	0.59

Table 8.10: Bitumen-Aggregate Compatibility Ratios (Aggregates 'B' & 'D')

Adhesive Bond Strength in Dry and Wet Conditions and Compatibility Ratios						
Bitumen	Aggregates					
	B			D		
	Dry (ΔG_{BA})	Wet (ΔG_{BWA})	Compatibility Ratio $\left \frac{\Delta G_{BA}}{\Delta G_{BWA}} \right $	Dry (ΔG_{BA})	Wet (ΔG_{BWA})	Compatibility Ratio $\left \frac{\Delta G_{BA}}{\Delta G_{BWA}} \right $
Unaged 15pen	108	-0.520	207.59	141	-103	1.37
Unaged 50pen	104	-0.514	202.32	131	-109	1.2

Moisture Sensitivity Analysis

The following four types of moisture sensitivity analysis parameters have been used for each combination of material.

$$R_1 = \left| \frac{\Delta G_{BA}}{\Delta G_{BWA}} \right| \quad (67)$$

It is the ratio of dry to wet bond strength of the bitumen-aggregate combination. These ratios have been shown in Tables 8.9 and 8.10.

$$\left| \frac{\Delta G_{BA}}{\Delta G_{BWA}} \right| \times SSA(\text{Aggregate} \cdot \text{Surface} \cdot \text{Area}) \quad (68)$$

Specific surface area of the aggregate is used to account for the individual aggregate surface characteristics/roughness.

$$R_2 = \left| \frac{\Delta G_{BA} - \Delta G_{BB}}{\Delta G_{BWA}} \right| \quad (69)$$

Bitumen cohesive bond strength (ΔG_{BB}) is used in the parameter in order to account for the wettability property ($\Delta G_{BA} - \Delta G_{BB}$) of the binder.

$$\left| \frac{\Delta G_{BA} - \Delta G_{BB}}{\Delta G_{BWA}} \right| \times SSA \quad (70)$$

Aggregate specific surface area is introduced in the third bond ratio parameter. It is supposed to better simulate the moisture sensitivity results obtained through other laboratory tests (Bhasin and Little, 2007).

Table 8.11 provides the results for the above mentioned four moisture sensitivity analysis parameters obtained for all the bitumen-aggregate combinations. A higher value of the parameter indicates a better moisture damage performance of the bitumen-aggregate mixture under consideration.

Table 8.11: Prediction of Moisture Susceptibility of a Bitumen-Aggregate System

Moisture Sensitivity Analysis Parameters				
Bitumen	Aggregates			
	A (Basic)			
	1	2	3	4
	R ₁	R ₁ x SSA	R ₂	R ₂ x SSA
	$ \Delta G_{BA}/\Delta G_{BWA} $	$ \Delta G_{BA}/\Delta G_{BWA} $ x SSA	$ \Delta G_{BA}-\Delta G_{BB})/\Delta G_{BWA} $	$ \Delta G_{BA}-\Delta G_{BB})/\Delta G_{BWA} $ x SSA
15pen	1.75	1.38	0.61	0.48
50pen	1.64	1.29	0.58	0.46
50pen	C (Acidic)			
	1	2	3	4
	R ₁	R ₁ x SSA	R ₂	R ₂ x SSA
	$ \Delta G_{BA}/\Delta G_{BWA} $	$ \Delta G_{BA}/\Delta G_{BWA} $ x SSA	$ \Delta G_{BA}-\Delta G_{BB})/\Delta G_{BWA} $	$ \Delta G_{BA}-\Delta G_{BB})/\Delta G_{BWA} $ x SSA
	0.59	0.23	0.25	0.10
50pen	B (Acidic)			
	1	2	3	4
	R ₁	R ₁ x SSA	R ₂	R ₂ x SSA
	$ \Delta G_{BA}/\Delta G_{BWA} $	$ \Delta G_{BA}/\Delta G_{BWA} $ x SSA	$ \Delta G_{BA}-\Delta G_{BB})/\Delta G_{BWA} $	$ \Delta G_{BA}-\Delta G_{BB})/\Delta G_{BWA} $ x SSA
	202.32	77.02	42.8	16.29
50pen	D (Acidic)			
	1	2	3	4
	R ₁	R ₁ x SSA	R ₂	R ₂ x SSA
	$ \Delta G_{BA}/\Delta G_{BWA} $	$ \Delta G_{BA}/\Delta G_{BWA} $ x SSA	$ \Delta G_{BA}-\Delta G_{BB})/\Delta G_{BWA} $	$ \Delta G_{BA}-\Delta G_{BB})/\Delta G_{BWA} $ x SSA
	1.2	0.53	0.64	0.28

The values for the moisture sensitivity analysis parameter number 4 from the above table are used to assess the moisture sensitivity of the material (bitumen-aggregate)

combinations. It is concluded from the results that stiffer binder would perform better under moisture as it has a slightly higher bond ratio as compared to the 50pen binder. The aggregate 'A' (basic) has a higher energy ratio value as compared to the aggregates 'C' and 'D' (both acidic) which is in accordance with the general perception that a basic aggregate should have a better moisture damage performance as compared to the acidic aggregates. The anomaly is the energy ratio value of aggregate 'B' (acidic) which is quite high as compared to the other three aggregates.

8.4 SATS Moisture Factors versus SE Moisture Sensitivity Ratios

As mentioned earlier in this chapter, the main objective of this comparative study is to check if the moisture sensitivity assessment parameters for different bitumen-aggregate combinations obtained by using surface energy parameters of the individual materials can identify good and poor performing asphalt mixtures, and to see if these parameters can be correlated with the moisture factors for the same mixtures obtained by using the SATS protocol.

A comparison of SATS moisture factors versus the bond energy ratios obtained from surface energy parameters is provided in Figure 8.10.

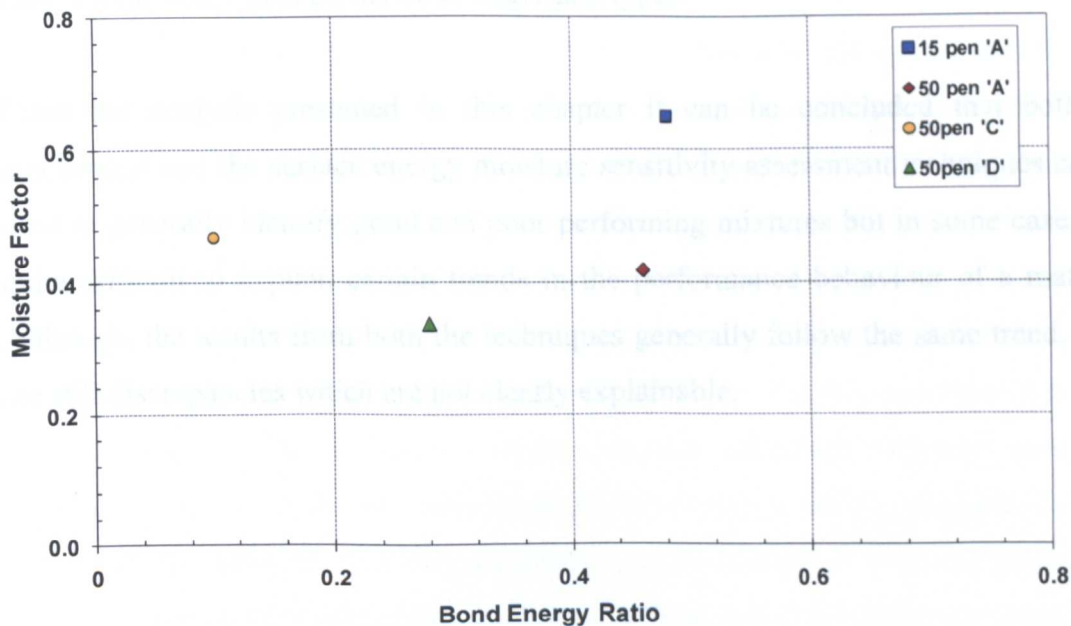


Figure 8.10: SATS Moisture Factors versus SE Bond Ratios

In the figure, the data has been plotted for the asphalt mixtures obtained by using aggregates A, C and D with 50pen binder. Data for aggregate A mixture with 15pen binder is also included. Data for aggregate 'B' has not been included as the bond energy ratios for this material are quite high as compared to the other three aggregate types as shown in Table 8.11. Moisture factors for only the standard SATS test conditions have been plotted.

It can be seen from the figure that both the moisture factor and the bond energy ratio for the 15pen binder are higher as compared to the 50pen. Though, the difference between the bond energy ratios is quite marginal. Similarly, the moisture factor and the bond energy ratio for aggregate A are higher than those for aggregate D. This corroborates well with the general perception that aggregate A performs best in service while aggregate D is related to poor performance (see Table 6.1, Chapter 6). However, in case of aggregate C the results are unexpected. Aggregate C is considered as a better performer as compared to aggregate D from the retained stiffness values from the SATS test (see Figure 6.4) but the bond energy ratio suggests that it is more susceptible to moisture damage and has the worst moisture damage performance among the three aggregates. On the other hand, the moisture factor values for aggregate C suggests that it is even better than the basic aggregate (A). Another major discrepancy was the bond energy ratio for aggregate B which makes it far better than all the other aggregate types.

From the analysis presented in this chapter it can be concluded that both the mechanical and the surface energy moisture sensitivity assessment techniques can be used to generally identify good and poor performing mixtures but in some cases it is quite difficult to explain certain trends in the performance behaviour of a material. Although, the results from both the techniques generally follow the same trend, there are still discrepancies which are not clearly explainable.

CHAPTER 9

CONCLUSIONS AND RECOMMENDATIONS

9.1 Overview

Large amounts of capital are spent throughout the world for the construction, maintenance and rehabilitation of roads. One of the major causes of pavement distresses is moisture. Moisture not only causes damage such as stripping and pot holes but it also increases the severity of already existing distresses. Moisture susceptibility, or in other words the moisture damage performance of an asphalt mixture, is therefore very important for the integrity of a road structure. Damage caused by moisture carries a huge economic impact as it not only results in increased maintenance costs but also decreases the service life of a road structure. The moisture sensitivity of an asphalt mixture is therefore an important parameter to be analysed.

Different techniques have been developed in the past to check the moisture sensitivity of asphalt mixtures. Almost all these techniques use some kind of mechanical test to assess the strength of mixtures once they have been subjected to moisture damage. Even if these techniques accurately predict the performance of a mixture in the field, which is not always the case, they do not provide the reasons for poor or good performance of a mixture. Therefore, it is important to measure the individual material properties in order to understand the mechanisms that are responsible for good or poor adhesion between a road material (bitumen and aggregate). The properties that are responsible for adhesion between the two materials can be referred to as physico-chemical properties. The surface energy properties of the individual materials are responsible for physical adhesion between the two materials and have been used in this research. The surface energy properties of bitumen and aggregates are combined thermodynamically to determine the adhesion between these materials and the effect of the presence of water on this adhesion. Moisture sensitivity parameters, which have been referred to as bond energy ratios, obtained from the surface energy properties of the materials are also compared with the parameters obtained through the SATS protocol (a mechanical moisture sensitivity assessment technique) in order to check the correlation between the two approaches.

9.2 Conclusions

Static contact angle and dynamic contact angle techniques have been used to measure the contact angle values of different probe liquids on bitumen samples. Goniometer and Wilhelmy plate (DCA) devices were used for this purpose. Microcalorimeter and vapour sorption (DVS) systems have been used for measuring the heat of adhesion and adsorption of probe vapours respectively for aggregates analysis. The surface energy properties of these materials were obtained by using the acid-base (Good-Van Oss- Chaudhury) theory. The SATS protocol has been used for mechanical moisture sensitivity analysis of the materials.

The following conclusions are drawn from the study.

- The static contact angle (Goniometer) technique is a fast and accurate technique for measuring the contact angles of different probe liquids with solids. Small amounts of probe liquid are used in this technique which could also be considered as being cost effective. However, when bitumen is used as a solid then contact angle measurements with some probes are quite tricky. Bitumen is non polar in nature and gives consistent results when tested with polar probes but when it is tested with diiodomethane (methylene iodide), which is also non polar, it becomes quite difficult to get reliable and consistent contact angle values. The reasons are that methylene iodide dissolves bitumen because of its non polar nature and readily spreads on the surface of bitumen as it has a high density and molecular weight as compared to other liquids.
- The Wilhelmy plate, which is a dynamic contact angle technique, measures the contact angle of probe liquid on a comparatively larger surface of sample. The binder sample is immersed into the liquid rather than the previous method (Goniometer) which makes it easier to get accurate results with diiodomethane. Also, as it is a more automated technique, consistent results are obtained for each probe liquid. It is however quite important to produce smooth and uniform thickness bitumen slides in order to get consistent results which is dependent on the experience of the operator. It is quite difficult to produce uniform thickness slides with recovered binders as they are quite stiff

because of ageing and only a small quantity can be obtained from a core of asphalt mixture.

- The microcalorimeter technique was used to determine the surface energy properties of the aggregates. It was difficult to get consistent results with the system. The reason for this may be that the system was run at room temperature without connecting it to a water bath. So, variations in temperature could probably be the reason for the inconsistencies.
- The dynamic vapour sorption system was used for the majority of the aggregates testing. It is a gravimetric analysis technique. The aggregate sample is exposed to the vapours of the test liquid under controlled test conditions (temperature, vapour flow rate) and the increase in mass of sample because of the adsorption of probes on the sample surface is measured. The equipment has limitations to the amount and size of sample. Only 2-3 grams of aggregate sample can be used. It is also quite a time consuming technique, however good results can be produced. The heterogeneous nature of the aggregate material itself sometimes results in variations in data which is difficult to avoid as only a small amount of material can be tested at a time. As it is a gravimetric analysis technique it can only account for the physical adsorption of the probe vapours on the aggregate surfaces.
- The surface energy properties of the bitumen and the aggregates are combined into bond energy ratios. Generally, these parameters give good insight into the compatibility of the two materials (bitumen and aggregate) and their moisture damage performance, and can be used as a good material screening tool. There were, however, some discrepancies where these parameters didn't give the expected results.
- The SATS protocol was used to determine the moisture sensitivity factors for combinations of materials. Bond energy ratios for the same combinations were then determined by using the surface energy techniques. Again, bond energy ratios generally correlated well with the SATS moisture factors but there were exceptions as well.

9.3 Recommendations for Future Work

On the basis of the work carried out for this research and the conclusions made in the previous section, the following are recommended:

- Wherever possible, the dynamic contact angle (Wilhelmy plate) technique should be used for the measurement of contact angles of different probes with the bitumen. The results from this technique can be used to determine accurate surface energy properties of the binders. Extreme care should be taken to produce smooth and uniform thickness bitumen slides for accurate surface energy results.
- Further analysis of aggregate materials should be carried out using the microcalorimeter as this equipment has a shorter testing time as compared to the dynamic vapour sorption (DVS) system. The microcalorimeter should be connected with a water bath for better temperature control and consistent results.
- As mentioned earlier, the DVS system cannot account for any chemical reaction between the probe liquid and the aggregate. A loss in mass was observed while testing some materials with some probe liquids at higher partial pressures. This could be because of two reasons. One is that there may be a chemical interaction between the material and the probe liquid. A separate set of probe liquids should be used for such materials as any possibility of a chemical reaction would significantly affect the final surface energy properties of the material. The other reason could be that the molecules of the probe liquid were not able to stick to the aggregate surface beyond a certain pressure. In this case a lower vapour flow rate can be tried or a vacuum chamber may be required to avoid this.
- Further investigation should be carried out by adding active fillers and adhesion promoters (amine based solutions and silanes) in the binders in order to study their effects on the surface energy properties of the materials and the bond energy ratios.

- Chemical analysis for both the bitumen and the aggregate materials is required to be carried out in order to be able to explain the discrepancies from both the mechanical and the surface energy moisture sensitivity assessment techniques.
- Data from field performance tests is required to be incorporated to compare and correlate with the moisture sensitivity ratios obtained from the surface energy properties for the same materials.
- *Aggregates Modification:* Different material (bitumen and aggregate) treatment techniques have been developed in the past to improve the compatibility of the two materials. Anti-stripping agents and polymers are added to bitumen in order to make it hydrophobic and improve its chemical bond with the aggregates. Techniques which are used to waterproof the aggregates and improve their adhesion characteristics include lime treatment and polymeric aggregate treatment. These treatments turn hydrophilic aggregate into a hydrophobic one but this may also reduce the bond strength between bitumen and aggregate.

Aggregate like limestone, which has weak basic character, bonds well with the carboxylic acids in the bitumen. On the other hand, the siliceous aggregates like granite (Tarrer and Wagh, SHRP-91-507, 1991), which has a weak acidic surface, does not adhere well with the bitumen because of a lack of any chemical interaction (MS-24, 2007).

Irradiation is a process in which the material under test is bombarded with radiations such as gamma rays or x-rays. These radiations knock the electrons out of place thus changing the properties of the material. Depending on the type of material and intensity of radiation these changes could be permanent or short termed.

It has been observed that gem stones and diamonds that have been irradiated exhibit lower contact angles (Nassau and Schonhorn, 1977), which is an indication of the hydrophilic nature of the material. After irradiation material/aggregate may behave similar to it being cleaved with the atoms at

the new surfaces being deprived from some of their neighbours, and hence some of their coordination bonds are broken. These atoms seek to form new bonds to replace the old ones (Tarrer and Wagh, SHRP-91-507, 1991). At this stage if bitumen is introduced, the aggregate would form a very strong bond with it. This technique could be useful for both basic and siliceous aggregates.

- *Measurement of Direct Adhesion (intrinsic adhesion versus adhesive fracture energy)*: Intrinsic adhesion between bitumen and aggregate is the adhesive bond energy which is obtained by using the thermodynamic (surface energy) properties of the two materials. The adhesive fracture energy is the bond strength between two materials which is obtained by using some mechanical test. The materials are bonded together and the force required to separate these materials is then referred to as the fracture energy between the two materials. The magnitude of the values obtained by using mechanical tests can however be much larger than the ones obtained by using surface energy theory.

An adhesion test method is required to be developed to determine the adhesive fracture energy for a bitumen-aggregate system. A test method that could provide results relating to the intrinsic adhesion values and repeatable for different bitumen-aggregate systems could then be used to determine the exact nature of the fracture plane and the location of the failure between the bitumen and the aggregates under both dry and wet conditions.

Numerous testing techniques are being used by the adhesive manufacturing industries to determine the bond strength of adhesives with different materials. Some of the popular ones are the double cantilever beam (ASTM D3433) and the peel test (ASTM D1876, D3330) techniques. Similar techniques can be used to measure the adhesive fracture energy between bitumen and aggregate. The values obtained from such tests could then be directly related to the adhesion characteristics (intrinsic adhesive values) of the two materials, and materials could be selected on the basis of the obtained results prior to mix design. This can help in the development of a more reliable and fast material screening protocol to obtain moisture resistant materials.

REFERENCES

AASHTO: T 180-84 (2002). "Coating and Stripping of Bitumen-Aggregate Mixtures: standard method of test", American Association of State Highway and Transportation Officials standards for tests, pp. T182-1 to T182-5.

AASHTO: T 283-03 (2003). "Resistance of Compacted Asphalt Mixtures to Moisture Induced Damage: standard method of test", American Association of State Highway and Transportation Officials standards for tests, pp. T283-1 to T283-8.

AASHTO: T 324-04 (2004). "Hamburg Wheel-Track Testing of Compacted Hot-Mix Asphalt (HMA): standard method of test", American Association of State Highway and Transportation Officials standards for tests, pp. T324-1 to T324-7.

AASHTO: T 315-05 (2005). "Determining the Rheological Properties of Asphalt Binder using a Dynamic Shear Rheometer (DSR)", American Association of State Highway and Transportation Officials standards for tests, pp. T315-1 to T315-31.

Adamson, A.W., and Gast, A.P., (1997). "Physical Chemistry of Surfaces", 6th ed. New York: John Wiley and Sons, Inc.

Adam, N.K., (1941). "The physics and Chemistry of Surfaces", 3rd ed. London: Oxford University Press, 1941.

Airey, G.D., Kinloch, A.J., Blackman, B.R.K., and Taylor, A.C., (2007). "Predicting and Enhancing the Moisture-Damage Performance of Asphalt Mixtures: a case for support for an application to EPSRC", Nottingham Transportation Engineering Centre, University of Nottingham, UK.

Airey, G.D., Masad, E., Bhasin, A., Caro, S., and Little, D., (2007). "Asphalt Mixture Moisture Damage Assessment Combined with Surface Energy Characterization". Proc. Conference on Advanced Characterization of Pavement and Soil Engineering Materials, Athens, Greece.

Airey, G.D., Choi, Y.K., Collop, A.C., Moore A.J.V., and Elliot, R.C., (2005). "Combined Laboratory Ageing/Moisture Sensitivity Assessment of High Modulus Base Asphalt Mixtures", *Journal of the Association of Asphalt Paving Technologists*, 74, pp. 307-345.

Airey, G.D., and Choi, Y.K., (2002). "State of the Art Report on Moisture Sensitivity Test Methods for Bituminous Pavement Materials", *International Journal of Road Materials and Pavement Design*, 3(4), pp. 355-372.

Airey, G. D. and Hunter, A. E. (2003). "Dynamic Mechanical Testing of Bitumen: Sample Preparation Methods", *Proceedings of the Institution of Civil Engineers (ICE)*, Transport 156, May 2003, pp. 85-92, Issue TR2.

Airey, G.D., Choi, Y., Collop, A.C. and Elliott, R.C., (2003). "Development of an accelerated durability assessment procedure for high modulus base (HMB) materials", 6th International RILEM Symposium on Performance Testing and Evaluation of Bituminous Materials, PTEBM'03, Zurich, Switzerland, pp. 160-166.

Airey, G.D., Choi, Y., Collop, A.C., Moore, A.J.V. and Elliott, R.C., (2005). "Combined laboratory ageing / moisture sensitivity assessment of high modulus base asphalt mixtures", *Journal of the Association of Asphalt Paving Technologists*, pp. 307-346.

Annual Local Authority Road Maintenance (Alarm) Survey, (2006). Asphalt Industry Alliance, www.asphaltindustryalliance.com/alarm.asp.

Anon, (2000). "Resistance of compacted bituminous mixtures to moisture induced damage", AASHTO T283-99, American Association of State Highways and Transportation Officials, USA.

Anon, (2004). "Method for the Assessment of Durability of Compacted Asphalt Mixtures using the Saturation Ageing Tensile Stiffness (SATS) Tests", *Manual of Contract Document for Highways Works: Clause 953*, Highways Agency, UK.

Answers .com (2007). "Contact Angle",
<http://www.answers.com/contact+angle?cat=technology>

ASTM: D 3625-96 (2001). "Effect of Water on Bituminous-Coated Aggregate Using Boiling Water: standard practice", American Society for Testing and Materials, pp 345-346.

ASTM: D 1075-96 (2000). "Effect of Water on Compressive strength of Compacted Bituminous Mixtures: standard test method", American Society for Testing and Materials, pp 112-113.

ASTM: D 4867/D 4867M (2004). "Effect of Moisture on Asphalt Concrete Paving Mixtures: standard test method", American Society for Testing and Materials, pp 509-513.

ASTM: D 5100-95a (2004). "Adhesion of Mineral Aggregate to Hot Bitumen: standard test method", American Society for Testing and Materials, pp 263-264.

ASTM: D 5405-98 (2004). "Conducting Time to Failure (Creep-Rupture) tests of Joints Fabricated from Non-bituminous Organic Roof Membrane Material: standard test method", American Society for Testing and Materials, pp 277-281.

Australian Asphalt Pavement Association, (2005). "Asphalt Moisture Sensitivity: Advisory Note 19", AAPA- Australian Asphalt Pavement Association, Victoria, Australia.

Bagampadde, U., Isacson, U. and Kiggundu, B. M., (2006). "Impact of Bitumen and Aggregate Composition on Stripping in Bituminous Mixtures", Journal of Materials and Structures, RILEM, vol. 39, pp. 303-315.

Barton, A., (1997). "States of Matter, States of Min", London: Institute of Physics Publishing.

Bhasin, A. (2006). "Development of Methods to Quantify Bitumen-Aggregate Adhesion and Loss of Adhesion due to Water", PhD thesis, Texas A&M University, USA.

Bhasin, A., and Little, D., (2006). "Characterising Surface Properties of Aggregates using Hot Mix Asphalt", National Technical Information service, Springfield, Virginia, USA, International Centre for Aggregate Research (ICAR/505-2).

Bhasin, A., and Little, D.N., (2007). "Using Surface Energy Measurements to Select Materials for HMA Pavements", NCHRP Research Results Digest 316, NCHRP Project 9-37, Transportation Research Board, Washington DC, USA.

Bhasin, A. and Little, D. N., (2007). "Characterization of Aggregate Surface Energy using the Universal Sorption Device", Journal of Materials in Civil Engineering, Vol. 19, No. 8, ASCE, pp-634-641.

Bhasin, A., Howson, J., Masad, E., Dallas, N. L. and Lytton, R. L., (2007). "Effect of Modification Processes on Bond Energy of Asphalt Binders", 86th Annual Meeting of the Transportation Research Board [CD-ROM], Washington, D.C.

Bhasin, A., Masad, E., Little, D., and Lytton, R., (2006). "Limits on Adhesive Bond Energy for Improved Resistance of Hot-Mix Asphalt to Moisture Damage", Transportation research record: Journal of the Transportation Research Board, No. 1970, Washington D.C., pp. 3-13.

Birgisson, B., Roque R., Tia, M. and Masad, E., (2005). "Development and Evaluation of Test methods to Evaluate Water Damage and Effectiveness of Anti-stripping Agents", Project Number 4910-4504-722-12 from Florida Department of Transportation: Florida.

British Standards Institution (2003a). "Bituminous mixtures – Test methods for hot mix asphalt – Part 33: Specimen prepared by roller compactor", BS EN 12697-33.

British Standards Institution (2003b). “Bituminous mixtures – Test methods for hot mix asphalt – Part 6: Determination of bulk density of bituminous specimens”, BS EN 12697-6.

British Standards Institution (2003c). “Bituminous mixtures – Test methods for hot mix asphalt – Part 8: Determination of void characteristics of bituminous specimens”, BS EN 12697-8.

British Standards Institution (2004b). “Bituminous mixtures – Test methods for hot mix asphalt – Part 26: Stiffness”, BS EN 12697-26.

British Standards Institution (2004c). “Bituminous mixtures – Test methods for hot mix asphalt – Part 35: Laboratory mixing”, BS EN 12697-35.

British Standards Institution (2005). “Coated macadam (asphalt concrete) for roads and other paved areas – Part 1: Specification for constituent materials and for mixtures”, BS 4987-1.

British Standards Institution (2009). “Bituminous mixtures – Test methods for hot mix asphalt – Part 5: Determination of the maximum density”, BS EN 12697-5.

BS EN 828: (1998). “Adhesives Wettability-Determination by Measurement of Contact Angle and Critical Surface Tension of Solid Surface”, British Standards. UK.

BS 2000-143: (2004). “Determination of Asphaltenes (Heptane Insolubles) in Crude Petroleum and petroleum Products”, British Standards. UK.

BS EN 12592: (2007). “Bitumen and Bituminous Binders - Determination of Solubility”, British Standards. UK.

BS DD 213: (1993). “Determination of the Indirect Tensile Stiffness Modulus of Bituminous Mixtures”, British Standards, UK.

BS EN 12607-1: (2007). “Bitumen and Bituminous Binders - Determination of the Resistance to Hardening under the Influence of Heat and Air - Part 1: RTFOT Method”, British Standards, UK.

BS EN 12697-4: (2005). “Bituminous Mixtures – Test Methods for Hot Mix Asphalt - Part 4: Bitumen Recovery – Fractionating Column”, British Standards, UK.

BS EN 14769: (2005). “Methods of Test for Petroleum and its Products. Bitumen and Bituminous Binders – Accelerated Long Term Ageing Conditioning by a Pressure Ageing Vessel (PAV)”, British Standards, UK.

BS EN 14770: (2005). “Methods of Test for Petroleum and its Products. Bitumen and Bituminous Binders - Determination of Complex Shear Modulus and Phase Angle – Dynamic Shear Rheometer (DSR)”, British Standards, UK.

Cahn Instrument, (1999). “Cahn DCA 315 Operator’s Manual”, Scientific and Medical Products Ltd. Cheshire, UK.

Calorimeter, (2007). Encyclopaedia Britannica. 19 Mar. 2007,
<http://www.search.eb.com/eb/article-9018727>

Cheng, D., (2002). “Surface Free Energy of Asphalt Aggregate System and Performance Analysis of Asphalt Concrete based on Surface Free Energy”, PhD thesis, Texas A&M University, USA.

Cheng, D., Little, D.N., Lytton, R.L. and Holste, J.C., (2002). “Surface Energy Measurement of Asphalt and Its Application to Predicting Fatigue and Healing in Asphalt Mixtures”, Transportation Research Record: Journal of the Transportation Research Board, No. 1810, TRB, National Research Council, Washington, D.C., pp. 44-53.

Cheng, D., Little, D.N., Lytton, R.L., and Holste, J.C., (2002). “Moisture Damage Evaluation of Asphalt Mixtures by Considering both Moisture Diffusion and

Repeated-Load Conditions”, *Transportation Research Record: Journal of the Transportation Research Board*. TRR 1832, pp. 42-49.

Choi, Y.K., Collop, A.C., Airey, G.D., Elliott, R.C., Williams, J. and Heslop, M.W., (2002). “Assessment of the durability of high modulus base (HMB) materials”, 6th International Conference on the Bearing Capacity of Roads, Railways and Airfields, Lisbon, Portugal.

Choi, Y.C., (2005). “Development of the saturation Ageing Tensile Stiffness (SATS) Test for High Modulus Base Materials”, PhD thesis, School of Civil Engineering, University of Nottingham, UK.

Collop, A.C., Choi, Y.K., Airey, G.D. and Elliott, R.C., (2004a). “Development of the saturation ageing tensile stiffness (SATS) test”, *Proceedings of the ICE Transport*, 157, pp. 163-171.

Collop, A.C., Choi, Y.K. and Airey, G.D., (2004b). “Development of a combined ageing / moisture sensitivity laboratory test”, *Euroasphalt and Eurobitume Congress*, Vienna, Austria.

Collop, A. C., Choi, Y. and Airey, G. D., (2007). “Effects of Pressure and Ageing in SATS Test. *Journal of Transportation Engineering*”, ASCE/November 2007, pp 618-624.

Collop, A. C., Choi, Y., Airey, G. D. and Elliott, R. C., (2003). “Development of the Saturation Ageing Tensile Stiffness (SATS) Test”, *Proceedings of the Institution of Civil Engineers (ICE), Transport 157*, August 2004, pp. 163-171, Issue TR3.

Coree, B. J., and Kim, S., (2005). “Evaluation of Hot Mix asphalt Moisture Sensitivity using the Nottingham Asphalt Test Equipment”, *Centre for Transportation Research and Education (CTRE Project 02-117)*, Iowa State University, USA.

Edwards, Y., (2006). “Influence of Waxes on Bitumen and Asphalt Concrete Mixture Performance”, PhD thesis, Royal Institute of Technology, Stockholm, Sweden.

Edwards, Y. and Isacsson, U., (2008). "Experience of Adding Wax to Bitumen and Asphalt Mixture Products", Transport Research Arena (TRA) Europe 2008, Ljubljana.

Edwards, Y., Tasdemir, Y. and Isacsson, U., (2005). "Rheological Effects of Commercial Waxes and Polyphosphoric Acid in Bitumen 160/220-Low Temperature Performance", FUEL 85 (2006), pp. 989-997.

Emery, J. and Seddik, H., (1997). "Moisture-Damage of Asphalt Pavements and Anti stripping Additives: Causes, Identification, Testing and Mitigation", Transportation Association of Canada.

Erbil, H. Y., (2006). "Surface Chemistry of Solid and Liquid Interfaces", Blackwell Publishing Ltd.

Fini, E.H., Al-Qadi, I.L., Dessouky, S. H., and Masson, J.F., (2006). "Adhesion of Bituminous Crack sealants to Aggregates", 85th Annual Meeting of the Transportation Research Board [CD-ROM], Washington, D.C.

Fini, E. H., Al-Qadi I. L. and Masson, J. F., (2007). "A New Blister Test to Measure Bond Strength of Asphaltic Materials. Asphalt Paving Technologists", 76, pp. 275-302.

First Ten Angstroms, (1998). "Contact Angle Accuracy: application notes", Portsmouth, Virginia, USA.

<http://www.firsttenangstroms.com/pdfdocs/CAAccuracy.pdf>

Hansen, F.K., (2006). "Program for Contact Angle Measurements by Image Analysis: DROPimage Standard User's Guide 2.0", rame-hart instrument co., Netcong, USA.

Hansen, F.K., (2006). "The measurement of Surface Energy of polymers by means of contact Angle of Liquids on Solid Surface: a short overview of frequently used methods". University of Oslo.

Hefer, A.W., (2004). "Adhesion in Bitumen-Aggregate Systems and Quantification of the Effects of Water on the Adhesive Bond", PhD thesis. Texas A&M University, USA.

Hefer, A.W., Bhasin, A., and Little, D.N., (2005). "Bitumen Surface Energy Characterization using a Contact Angle Approach", *Journal of Materials in Civil Engineering*, Vol. 18, No. 6, ASCE, pp. 759-767.

Immersion Tray Test, (2007). "The Idiots Guide to Highway Maintenance", 23 March, 2007, <http://www.highwaysmaintenance.com/SDdata.html>.

Nicholls, J. C., Airey, G. D., Collop, A. C., Elliott, R. C. and Grenfell, J., (2009). "Assessment of asphalt durability tests; Part 1: Widening the Applicability of the SATS Test", Draft Project Report, TRL, RPN570 2/462_080.

Kandhal P.S., (1994). "Field and Laboratory Evaluation of Stripping in Asphalt Pavements: State of the art", TRR 1454, TRB, Washington, D.C., pp. 36-47.

Kanitpong, K., and Bahia, H., (2005). "Relating Adhesion and Cohesion of Asphalts to Effect of Moisture on Asphalt Mixtures Laboratory Performance", 84th Annual Meeting of the Transportation Research Board [CD-ROM], Washington, D.C.

Kim, Y. R., (2009). "Modelling of Asphalt Concrete", 1st ed. ASCE press USA: McGraw-Hill Construction.

Kinloch, A.J., (1997). "Adhesives in Engineering. Institution of Mechanical Engineers", 1997, 211, pp. 307-335.

Kinloch, A.J., (2002). "The Durability of Adhesive Joints", In: Dillard, D.A., and Pocius, A.V. ed. *Adhesion Science and Engineering-1: The Mechanics of Adhesion*. London: Elsevier, 2002, pp. 661-698.

Kringos, N., and Scarpas, A., (2005). "Ravelling of Asphalt Mixes due to Water Damage: computational identification of controlling parameters", *Transportation*

Research Record: Journal of the Transportation Research Board, No. 1929, Transportation Research Board of the National Academics, Washington, D.C, pp. 79-87.

KSV Instruments, (2007). "Surface Free Energy-Background, Calculation and Examples: by using contact angle measurements", Application Note Number 108. KSV Instruments, Ltd.

Lu, Q., and Harvey, J.T. (2007). "Inclusion of Moisture Effect in Fatigue Test for Asphalt Pavements", 86th Annual Meeting of the Transportation Research Board [CD-ROM], Washington, D.C.

Lytton, R.L., (2003). "Adhesive Fracture in Asphalt Concrete Mixtures", Lecture Notes. Texas A&M University, USA.

Manual Series No. 24 (MS-24), (2007). "Moisture Sensitivity: Best Practices to Minimize Moisture Sensitivity in Asphalt Mixtures", Asphalt Institute, USA.

Mezger, T. G., (2002). "The Rheology Handbook: for Users of Rotational and Oscillation Rheometers", Curt R. Vincentz Verlag, Hannover, Germany.

Miller, J.S. and Bellinger, W.Y., (2003). "Distress Identification Manual for the Long-Term Pavement Performance Program", Publication FHWA-RD-03-031. FHWA, Office of Infrastructure Research and Development, McLean, Virginia.

Morrison, R. T. and Boyd, R. N. (1983). "Organic Chemistry", 4th ed. New York. Allyn and Bacon, Inc.

Mouillet, V., Lamontagne, J., Durrieu, F., Planche, J. P. and Lapalu, L. (2007). "Infrared Microscopy Investigation of Oxidation and Phase Evolution in Bitumen Modified with Polymers", FUEL 87 (2008), pp. 1270-1280.

Nassau, K., and Schonhorn, H., (1977). "The Contact Angle of Water on Gems, Gems and Geology", XV, No. 12, pp. 354-360.

Neumann, A. W., David, R. and Zuo, Y., (2011). "Applied Surface Thermodynamics", 2nd ed. CRC Press Taylor and Francis Group.

Planinsek, O., Pisek, R., Trojak, A. and Srcic, S., (2000). "The Utilization of Surface Free Energy Parameters for the Selection of a Suitable Binder in Fluidized Bed Granulation", *International Journal of Pharmaceutics* 207, pp. 77-88.

rame-hart, (2007). "Automated Dispensing System: User Guide", rame-hart instrument co., Netcong, USA.

Read, J. and Whiteoak, D., (2003). "The Shell Bitumen Handbook", 5th ed., Thomas Telford Ltd., London, UK.

Rieke, P.C., (1997). "Application of Van Oss-Chaudhury-Good theory of Wettability to interpretation of Interfacial Free Energies of Heterogeneous Nucleation", *Journal of Crystal Growth*, 182, pp. 475-484.

Santucci. L., (2002). "Moisture Sensitivity of Asphalt Pavements: technology transfer program", Institute of Transportation Studies, UC Berkeley Institute of Transportation Studies, USA.

Shaw, D. J., (1991). "Introduction to Colloid and Surface Chemistry", 4th ed., Butterworth-Heinemann, Oxford, UK.

SHRP-A-369, (2006). "Blister Test: Selection of an Adhesion Test Method", *Strategic Highway Research Program*, pp. 412-416.

Sing, K. S. W., (1969). "Utilisation of Adsorption Data in the BET Region", *Proceedings; International Symposium on Surface area Determination*, Bristol, UK.

Solaimanian, M., J., Harvey, M., Tahmoressi, and V. Tandon., (2003). "Test Methods to Predict Moisture Sensitivity of Hot Mix Asphalt Pavements", *Proceedings National Seminar on Moisture Sensitivity of Asphalt Pavements*, San Diego, California.

SuperCRC Microcalorimeter, (2006). "Isothermal Mixing and Reaction Calorimeter, Model SuperCRC 20-305-2.4: User Manual", Omnical Technologies, Inc. Houston, Texas, USA.

Superpave Series No. 1 (SP-1), (2003). "Performance Graded Asphalt Binder Specification and Testing", Asphalt Institute, USA.

Surface Measurement Systems, (2007). "DVS-Advantage: Pre-Installation Requirements", DVS Advantage Protocol, DVS-PRO-TAS-001, Surface Measurement Systems, Ltd. Alperton, UK.

Surface Measurement Systems, (2007). "DVS-Advantage: Operation Manual", Revision 1.3, Surface Measurement Systems, Ltd. Alperton, UK.

Surface Measurement Systems, (2007). "DVS-Advantage: Automated Multi-Vapour Gravimetric Sorption Analyzer for Advanced Research Applications", brochure, Surface Measurement Systems, Ltd. London, UK.

Tarrer, A.R., and Wagh, V., (1991). "The Effect of Physical and Chemical Characteristics of Aggregate on Bonding", Strategic Highway Research Program, National Research Council Washington, D.C. (SHRP-91-507), USA.

Terrel R.L. and Al-Swailmi S., (1994). "Water Sensitivity of Asphalt-Aggregate Mixes: Test Selection", SHRP-A-403, Strategic Highway Research Program, National Research Council, Washington, D.C.

Van Lent, D. Q., Molenaar, A. A. A., and Van de Ven, M. F. C., (2009). "The Effect of Specimen Preparation Techniques on the Surface Characteristics of Aggregates", 88th Annual Meeting of the Transportation Research Board [CD-ROM], Washington, D.C.

Van Oss, C.J., Chaudhury, M.K., and Good, R.J., (1987). "Monopolar Surfaces. Advances in Colloid and Interface Science", vol. 28, pp. 35-64.

Van Oss, C.J., Chaudhury, M.K., and Good, R.J., (1988). "Interfacial Lifshitz-van der Waals and Polar Interactions in Macroscopic Systems", Department of Chemical Engineering, State University of New York at Buffalo, New York 14260, Chem. Rev. 1988, 88, pp. 927-941.

Vialit Plate Test, (2007). "The Idiots Guide to Highway Maintenance", 23 Mar. 2007, <http://www.highwaysmaintenance.com/vialit.htm>

Volpe, C. D. and Siboni, S., (1997). "Some Reflections on Acid-Base Solid Surface Free Energy Theories", Journal of Colloid and Interface Science 195, pp. 121-136. Article No. CS975124.

Wikipedia, the free encyclopaedia, (2007). "Goniometer", <http://en.wikipedia.org/wiki/Goniometer>

Wikipedia, the free encyclopaedia, (2007). "Calorimeter", <http://en.wikipedia.org/wiki/Calorimeter>

Williams, D. R. and Levoguer, C. L., (2008). "Measuring BET Surface Areas using Organic Probe Molecules", Application Note Number 18. Surface Measurement Systems, UK.

APPENDIX A

Measurement of Contact Angle Using Goniometer

Introduction

Goniometer is an instrument that is generally used for measuring the contact angle between a liquid and a solid. The term goniometry is a combination of two Greek words, *gonia*, meaning angle and *metron*, meaning measure (<http://en.wikipedia.org/wiki/goniometer>, 2007).

The contact angle goniometer was invented by Dr. William Zisman of the United States Naval Research Laboratory in Washington, DC and the first of this type of instrument was built by Ramehart during the 1960s. Goniometers are used not only for contact angle and surface energy applications, but also for surface tension measurement using pendant drop, sessile drop and other techniques (<http://en.wikipedia.org/wiki/goniometer>, 2007). The sessile drop method is normally used for contact angle measurement. This method is used to estimate wetting properties of a localized region on a solid surface. Angle between the baseline of the drop and the tangent at the drop boundary is measured. This is ideal for curved samples or where one side of the sample has different properties than the other.

The contact angle is specific for any given system and is determined by the interactions across the three interfaces. Consider a small drop of liquid resting on a flat horizontal solid surface. The **contact angle** is the angle at which this liquid and vapour interface meets with the solid surface (<http://www.answers.com/contact>, 2007).

On many hydrophilic surfaces water gives a contact angle of 10° to 30° and it readily spreads on extremely hydrophilic surfaces with an effective contact angle of 0° . On hydrophobic surfaces water exhibits contact angle of 70° to 90° which may even go up to 150° or even nearly 180° for highly hydrophobic surfaces. In this case water droplets simply rest on the surface, without actually wetting it (<http://www.answers.com/contact>, 2007).

Equipment

The main equipment includes;

- Goniometer assembly, shown in Figure A1
- Micro-syringe with needle
- Light source (illuminator) with cordset
- Calibration tool
- Calibration Reference Tools
- Automated dispensing system
- Computer with monitor

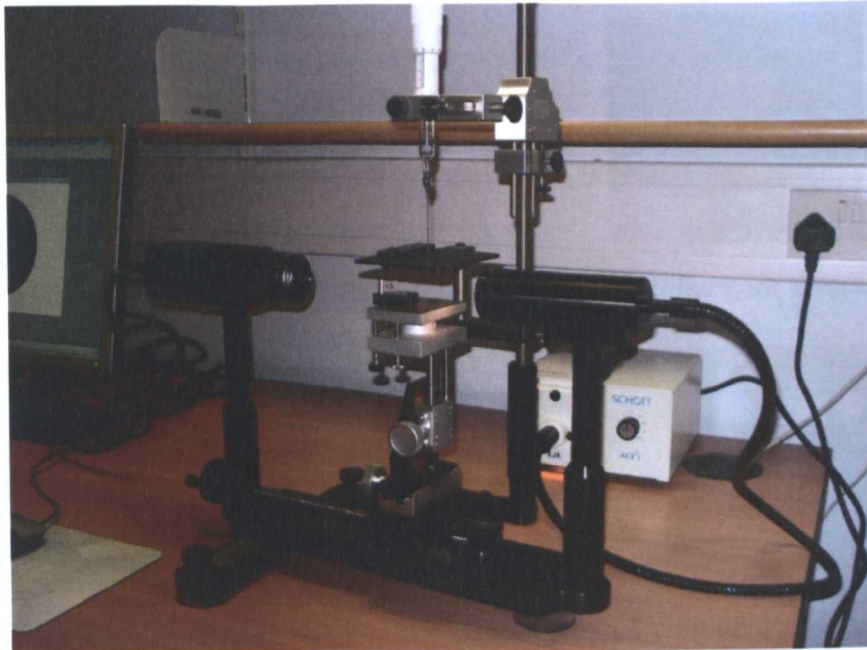


Figure A1: Goniometer

Materials Required

- Surface to be evaluated i.e. substrate (Bitumen)
- Reagents with 99 percent purity (HPLC Grade):
 - Glycerol
 - Formamide
 - Diiodomethane
 - Ethylene glycol
 - Deionised water

Conditioning and Test Temperatures

Adhesives and substrates are conditioned at a room temperature of $23^{\circ}\text{C} \pm 2^{\circ}\text{C}$ and $50\% \pm 5\%$ relative humidity for 24 hours.

Sample Preparation

A glass slide with substrate/Bitumen on the top is prepared for testing with Goniometer. The following two methods can be used for the preparation of glass slides:

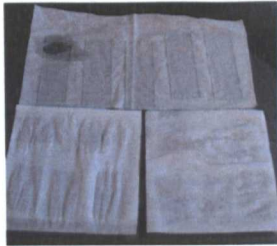
- I. *Hot Pour Method:* The bitumen is heated in an oven, at its mixing temperature, till it becomes pourable. Temperature of about 150°C is sufficient for base bitumen while a temperature of 170°C to 180°C is used for PMB's. The glass slides which are to be used for the test are washed with deionised water and acetone and then allowed to dry at room temperature. The heated bitumen is stirred and poured on the glass slide. Just before pouring the bitumen, the glass slides are passed through the flame of a gas torch in order to get rid of any residue/lint. A complete step-by-step slide preparation procedure is shown in Figure A2.



a). Use wash bottles to rinse the slides



b). Wash the slides with acetone & water



c). Place the slides on lint-free wipes



d). Dry by placing on a slide holder



e). Heat the bitumen at mixing temperature



f). Pass slides through the flame



g). Stir the heated bitumen before pouring



h). Pour bitumen on the slides



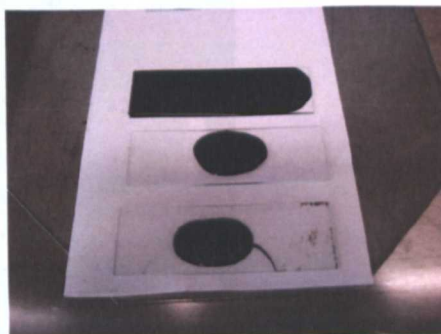
i). Store in a desiccator for about 24 hours

Figure A2: Sample Preparation (Hot Pour Method)

II. *Hot Plate Method*: Small amount of bitumen is poured on the glass slide. The glass slide is then placed on a preset hot plate at the mixing temperature of the bitumen. The bitumen liquefies and spreads on the surface of the slide, as shown in Figure A3, which is then placed in a desiccator for pre-conditioning at room temperature.



a). Bitumen slides on a pre-heated hot plate



b). Final prepared slides

Figure A3: Sample Preparation (Hot Plate Method)

This technique is used when the material is available in limited quantity. The slides obtained by using this technique are not completely levelled and also the availability of a smaller area for contact angle measurement makes it difficult to obtain good results.

Measurement of Contact Angle

In order to obtain a contact angle measurement by Goniometer, the following procedure may be used:

- Check that the equipment is completely levelled by looking at the level bubble, attached to the base of the equipment, as shown in the Figure A4 below. In the figure below the thumb is pointing towards a levelling screw which is provided on both sides of equipment base and is used to level the equipment.

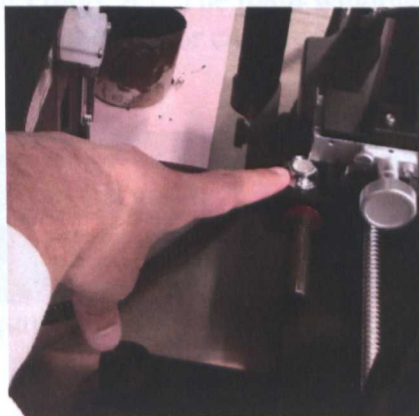


Figure A4: Levelling the Equipment

- Level the stage of the Goniometer by using a two axis bubble spirit level as shown in Figure A5. The screws provided at the bottom of the stage, both along the longer and shorter axis, are used to raise or lower the stage along these axes.



Figure A5: Levelling the Stage

- Turn-on the automated dispenser and the illuminator (light source), as shown in Figure A6, before turning-on the computer. The pointer on the knob of the illuminator should be directing straight-up as shown below.

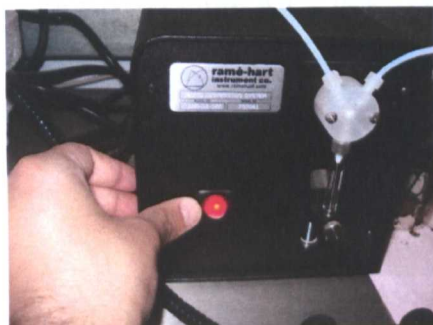


Figure A6: Turning-on the Equipment

- Turn-on the software by double clicking the **DropImage** software icon on the desktop, as shown in Figure A7. The main window containing the main menu, speed buttons panel and the live or captured image viewport appears as shown in Figure A8.



Figure A7: DropImage; Software Icon

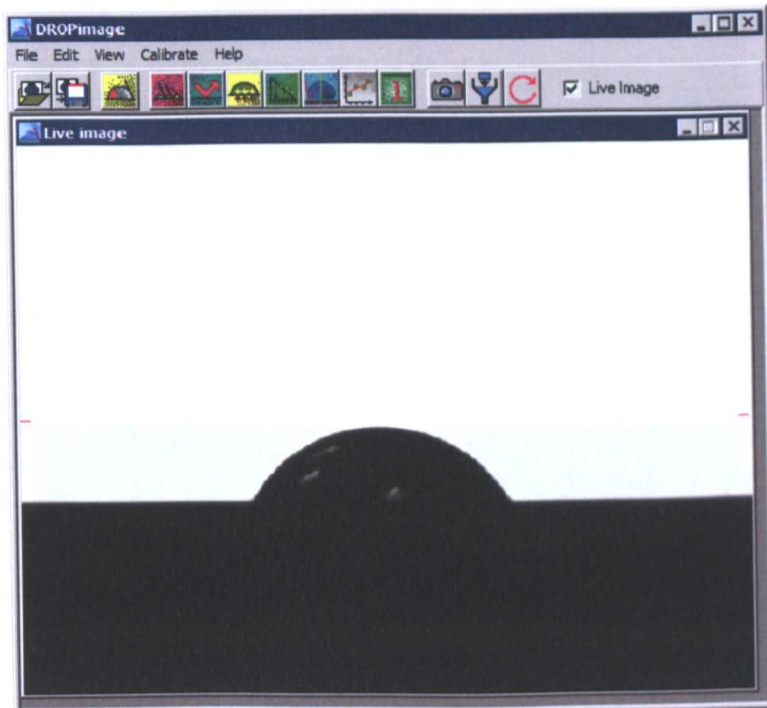


Figure A8: DROPimage Main Window
(Hansen, rame-hart instrument co. user guide, 2006)

- Software will prompt for the initialization of the automated dispenser as shown in Figure A9. Click 'Yes'.

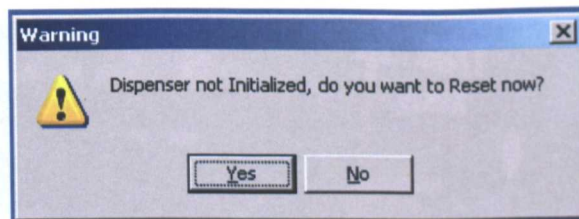


Figure A9: Dispenser Initialization

- Remove the cover from the camera lens as shown in Figure A10. The lens should always remain covered when the equipment is not in use.



Figure A10: Fire-Wire Camera

- Check the Live Image box in the toolbar in order to activate the camera and obtain live image of the pipette tip and stage as shown in Figure A11.

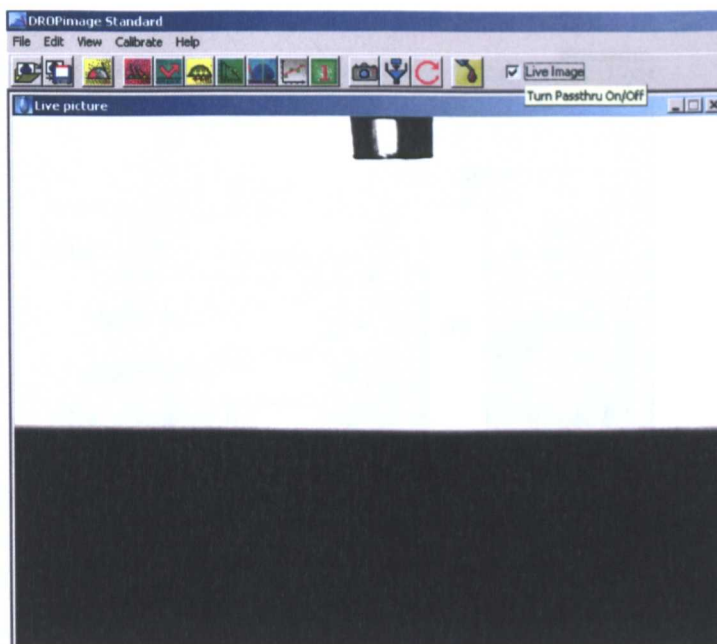


Figure A11: Camera Activation

- Use the focus knob, shown in Figure A12 below, to focus the dispenser tip. Note that only the tip is focused, not the stage. Tip and the front edge of the stage are not at the same position and cannot be focused simultaneously. Also, we are interested in focusing the point where the drop will rest on the stage and/or the drop itself to get a good contact angle value.

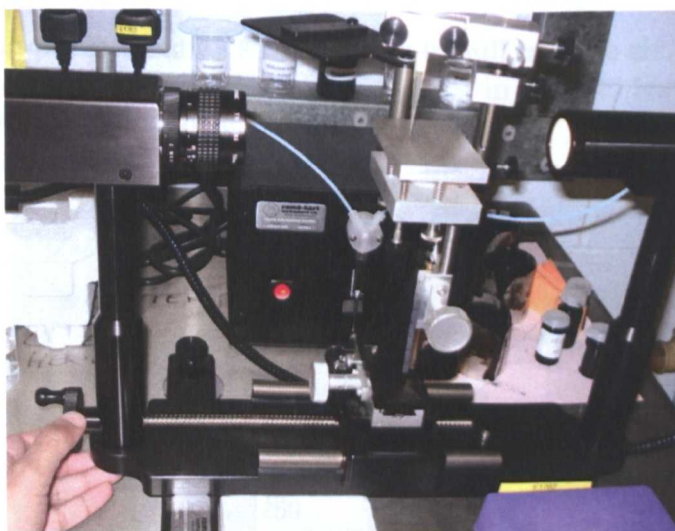


Figure A12: Focusing the Camera

- Click on the dispenser icon , in the main toolbar as shown in Figure A13, a drop volume control window opens as shown in Figure A14. Click yes if it is prompted to initialize the device.



Figure A13: Drop Volume Control Icon

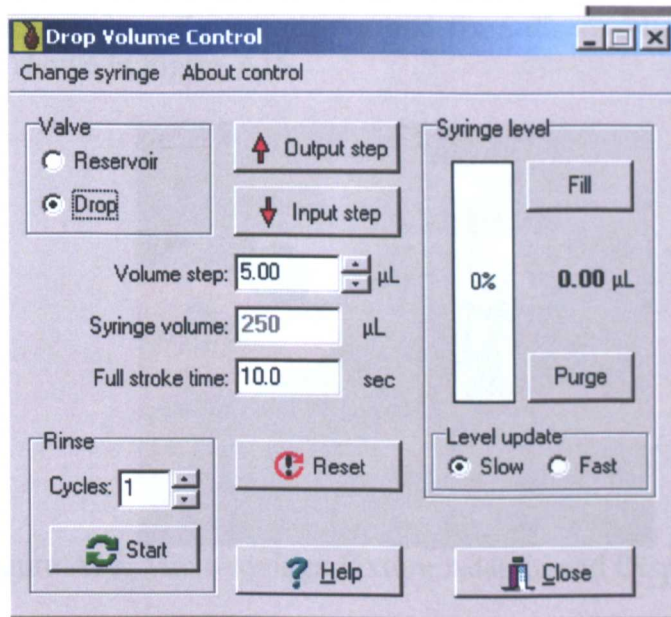


Figure A14: Syringe Control Window

- In the drop volume control dialogue box click reset to initialize the process.
- Enter number of rinse cycles in the rinse section and click start to prime the lines and syringe. Three to four rinse cycles are recommended. Click purge to eject any water that is currently in the tip.
- Click the in-put step button several times to pull in some air. Fill about 40% of the syringe volume, as shown in Figure A15, in order to leave a small air gap between the water and the test fluid.

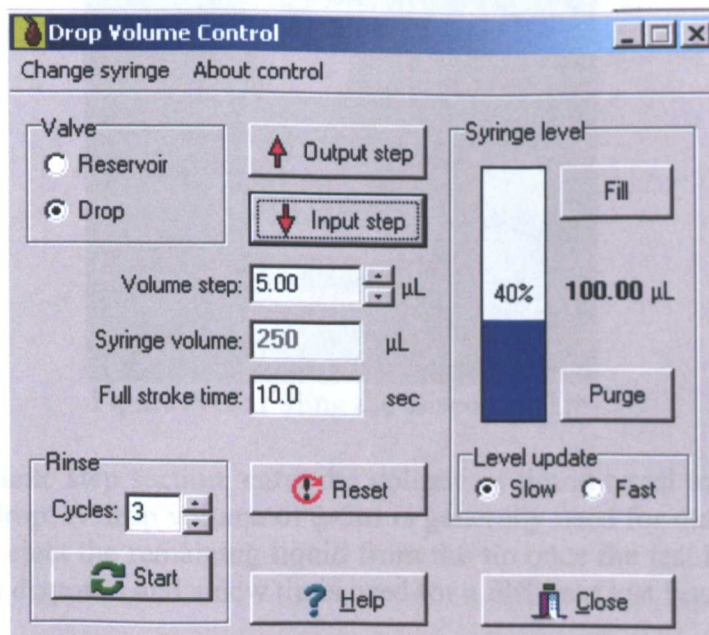


Figure A15: Drop Volume Control

- Place the end of left tube submerged in a beaker of distilled water. Fit the right tube to micro-syringe fixture adaptor and fix a disposable tip on the end of adaptor as shown in Figure A16.



Figure A16: Micro-syringe Fixture Adaptor and Disposable Tip

- Place a beaker filled with the required probe liquid on the stage of the equipment as shown in Figure A17. Immerse the pipette tip in the liquid and fill it by clicking the input step in the drop volume window. The syringe level in the drop volume control window should show 100% volume.



Figure A17: Filling the Dispenser Tip

- In the volume step section, enter the volume of liquid equal to the volume of required drop. A drop volume of 2-5 μ l is generally used for the test. Purge tab is used to eject the remaining liquid from the tip once the test is finished. The used tip is disposed and a new tip is used for a different test liquid.
- Remove the beaker and place the glass slide coated with the solid to be tested on the stage of the Goniometer with the edge of the slide flush with the front of the stage plate (British Standard, BS EN 828, 1998), as shown in Figure A18.

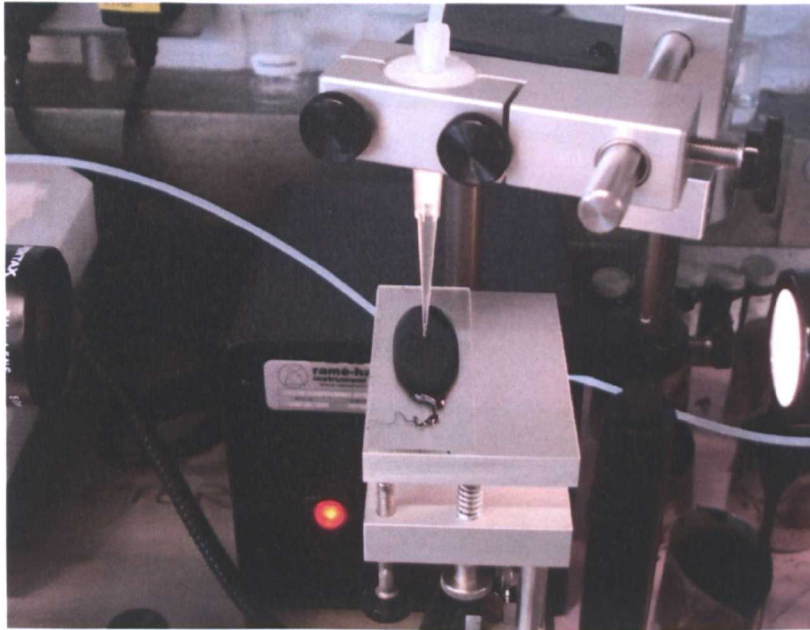


Figure A18: Placing the Slide

- Raise the stage of the Goniometer by using the knob at the front of the equipment as shown in Figure A19. The stage is raised so that it covers almost half of the live image window, as shown in Figure A20, but it should not go beyond the half mark (red marks, half-way on both sides of the live picture window) as then it would give an error in the reading.



Figure A19: Stage Position Adjustment

Figure A22: Contact Angle Window
(Hanson, ramé-hart instrument co. user guide, 2006)

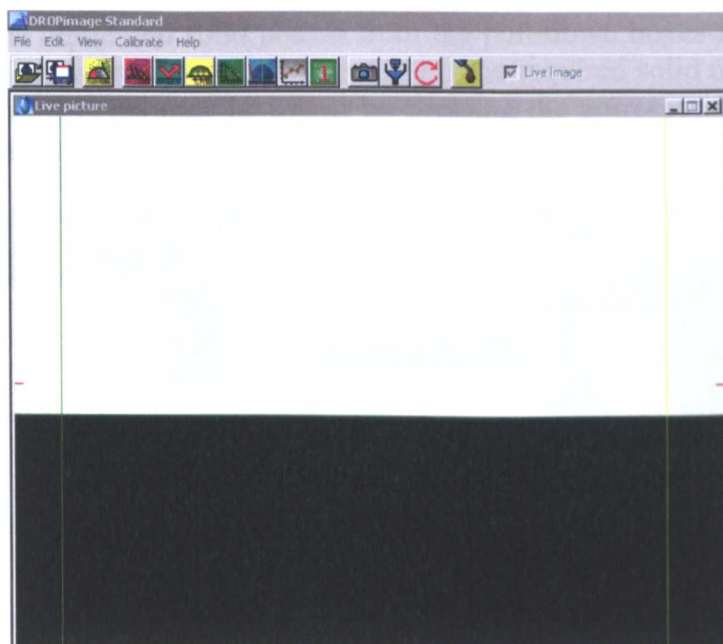


Figure A20: Live Picture Window

- Open the Contact Angle window by pressing the contact angle tool icon  shown in Figure A21, in the main toolbar. It opens the contact angle window as shown in Figure A22.



Figure A21: Contact angle Tool Icon

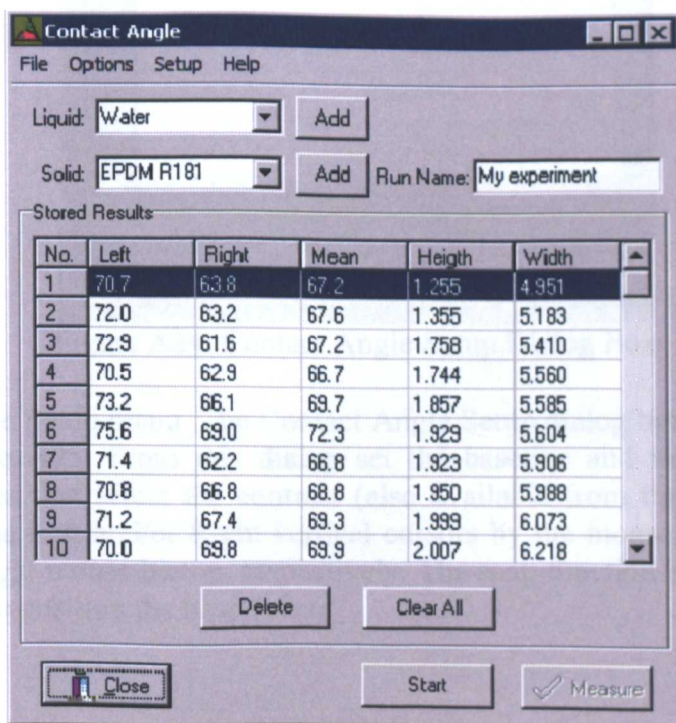


Figure A22: Contact Angle Window
(Hansen, rame-hart instrument co. user guide, 2006)

- Select the liquid and solid phases from the pull-down boxes in the upper part of the window as shown in Figure A23. If the required solid or liquid is not in the list, new items may be added by pressing the corresponding Add button. They may also be added and edited by the Phase Editor.

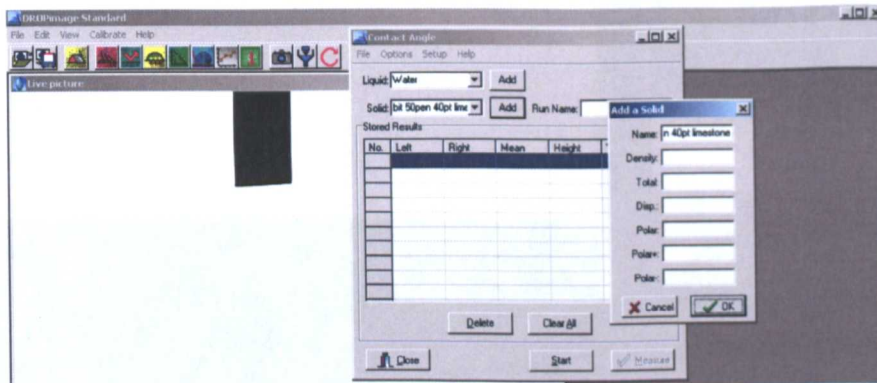


Figure A23: Liquid/Solid Phase Editor

- Enter a Run Name, as shown in Figure A24.

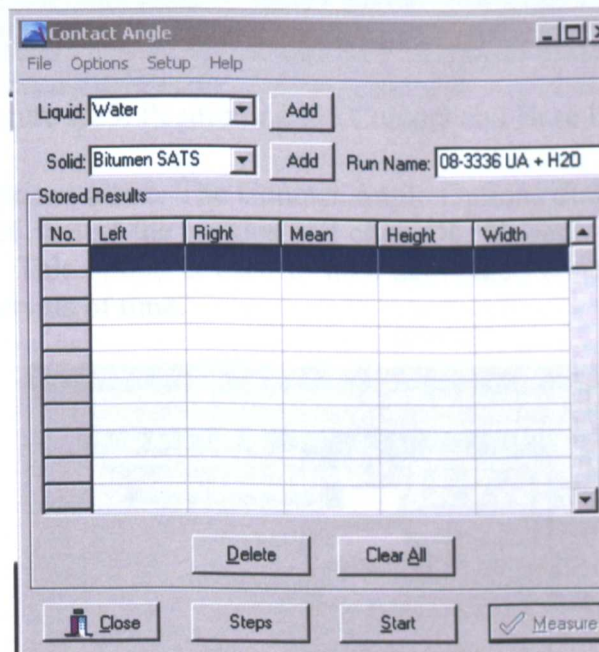


Figure A24: Contact Angle Setup Dialog Box

- Select the Setup menu. The Contact Angle Setup dialog box appears as shown in Figure A25. From this dialog set the baseline and the black and white intensities that affect the contrast (also available from the View Menu) and adjust the Left and/or Right vertical cursors by the mouse, holding down the left or right mouse button, respectively. The snap function in the “setup” menu is used to position the base-line.

Figure A26: Contact Angle Options Window

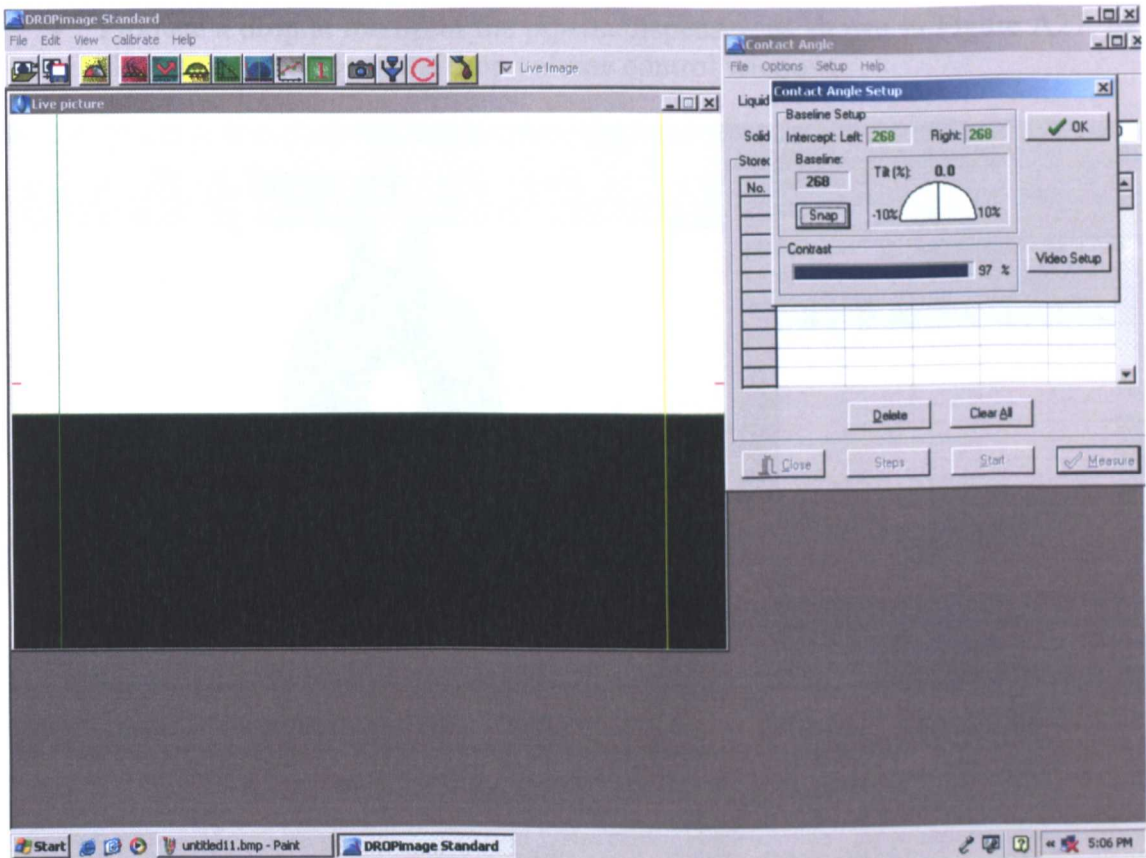


Figure A25: Positioning the Cursors and Base line

- Select the Options menu. The Contact Angle Options dialog appears as shown in Figure A26. Select the options and click Ok. Options will be kept between experiments. This option is used to take automated contact angle readings at specified intervals of time.

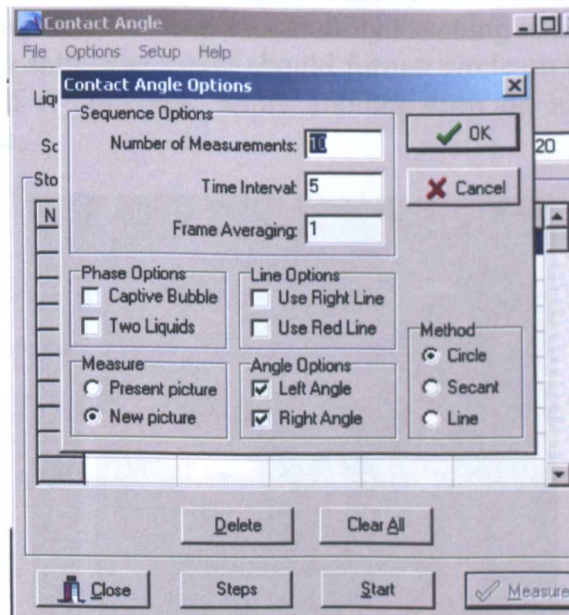


Figure A26: Contact Angle Options Window

- Produce a drop at the tip of the pipette/dispenser, as shown in Figure A27, by clicking output step in the drop volume control window.

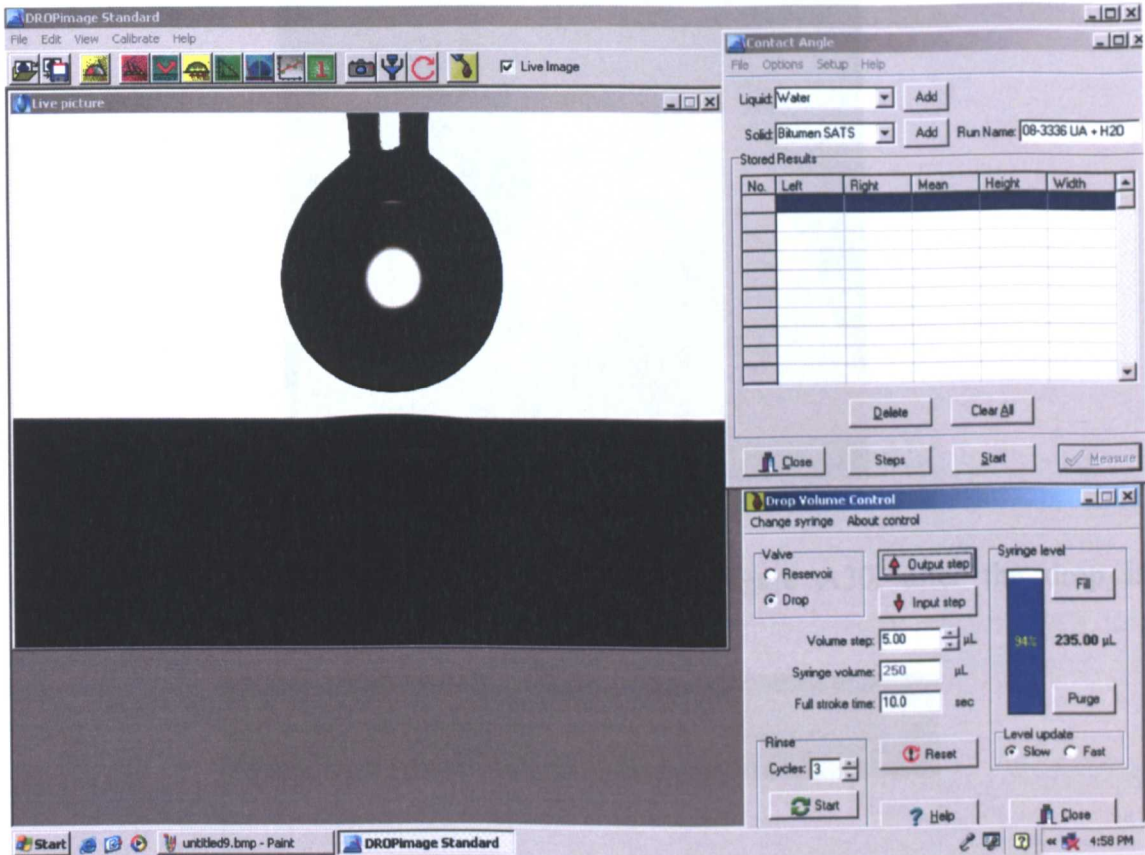


Figure A27: Dispensing the Probe Liquid

- Lower the dispenser tip by using the thumb-screw attached to the micro-syringe fixture as shown in Figure A28. It is recommended to lower the syringe and dispense the drop by carefully touching it with the substrate, such that it does not split. The liquid should form a circle on the panel, as shown in Figure A29, if it does not; apply another drop on a clean portion of the panel/substrate.



Figure A28: Depositing the Drop on the Bitumen

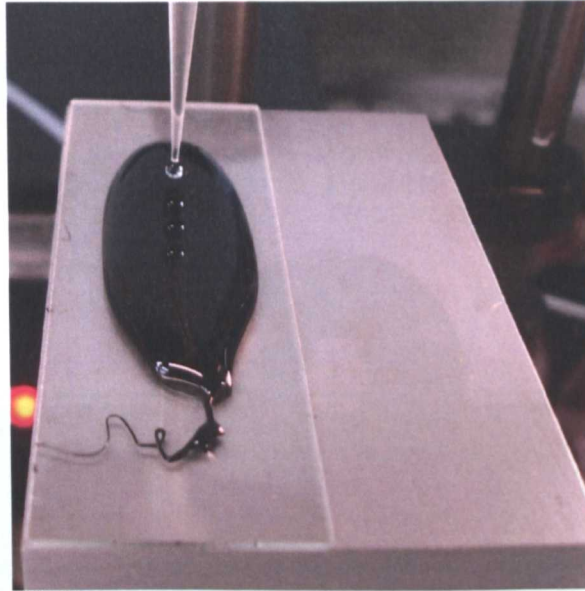


Figure A29: Liquid Drops on Substrate

- The live picture will appear as follows, Figure A30, after the drop is dispensed.

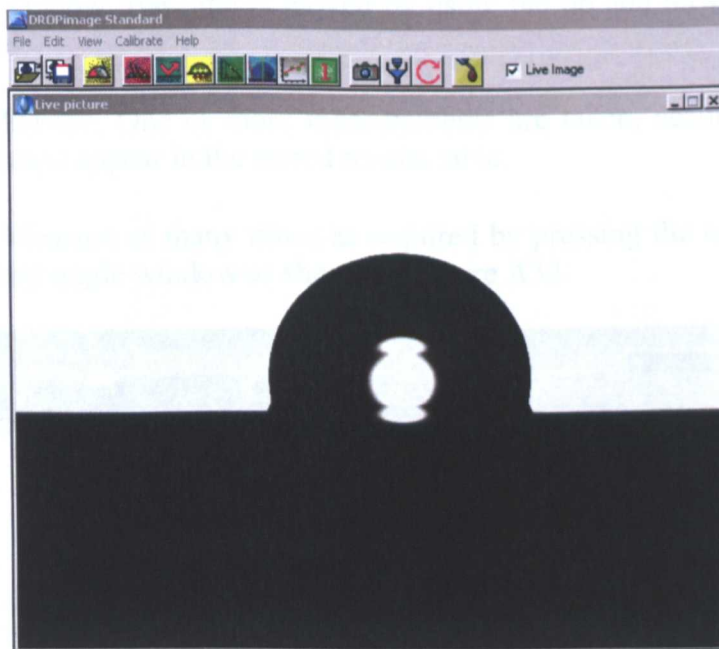


Figure A30: Dispensed Drop

- Refocus the microscope on the drop.
- It is better to look down the sample at an angle of 3° (camera angle) to get a good reflection of the drop, in order to define a clear position of baseline (FTA instrument, application notes, 2007). For an exact horizontal view, the baseline is barely adequate. In case of our equipment camera is already fixed and the sample stage is adjusted/levelled to get a good clear drop reflection.
- Click the Start button on the contact angle window. The Crosshairs Cursor lines appear as shown in Figure A31.

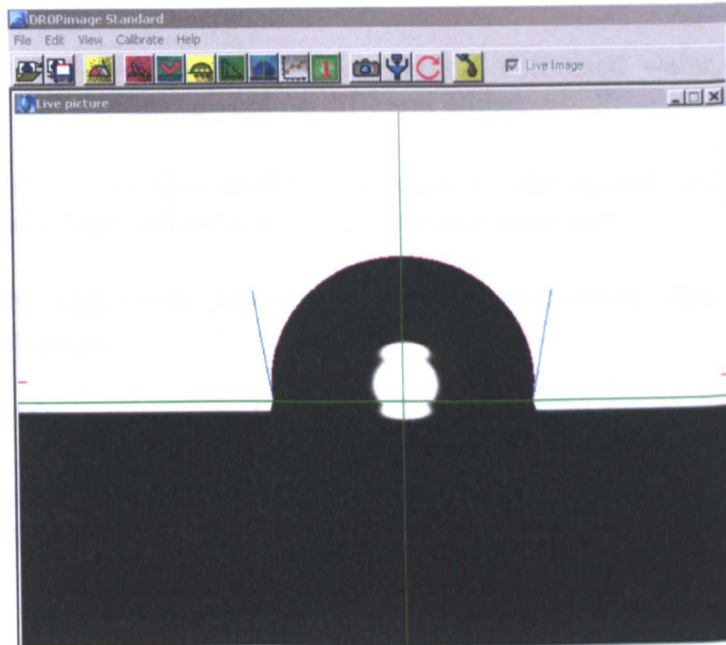


Figure A31: Visible Crosshair Cursor Lines

- Place the baseline exactly where the drop and its image meets in the live picture window. Baseline is moved by using the up and down buttons on the keyboard.
- Press Measure. One or more measurements are taken, according to options. The result(s) appear in the stored results table.
- Repeat Measure as many times as required by pressing the measure button in the contact angle window as shown in Figure A32.

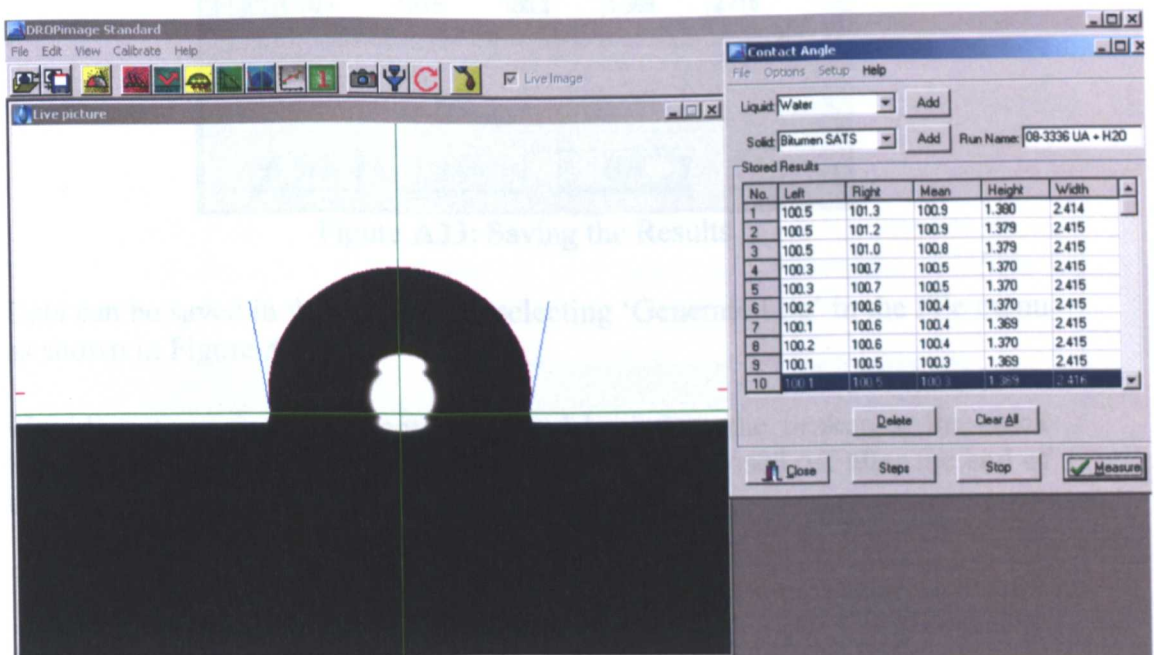


Figure A32: Contact Angle Measurement Window

- Ensure that the angle forms a tangent at the point where the drop contacts the surface.

- Measure the contact angles of formamide, deionised water, diiodomethane, glycerol and ethylene glycol on different slides.
- Record minimum four readings for each of the liquids. Disregard readings which have been influenced by dust, contamination etc.
- When finished, press Stop (same as the Start button). The crosshair cursor lines disappear.
- Start and Stop may be used as many times as required.
- Save the Contact Angle file by selecting Save As on the File menu, as shown in figure A33 below.

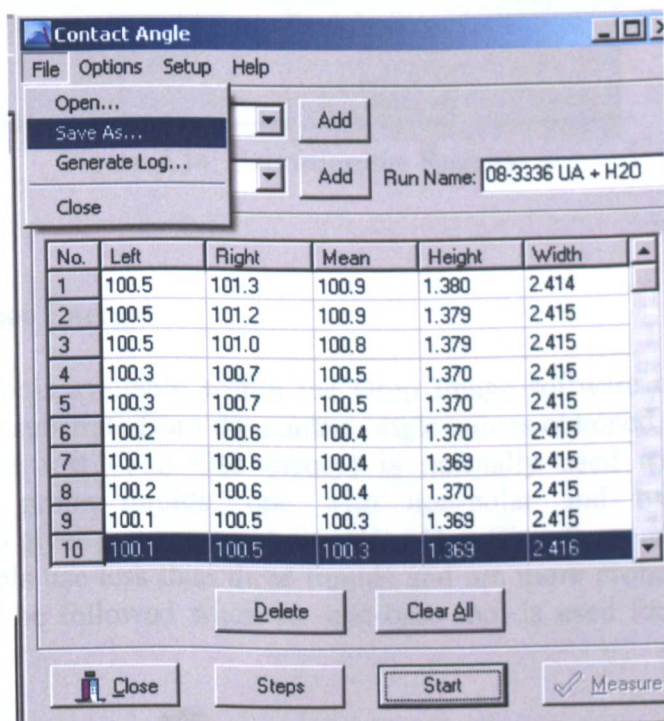


Figure A33: Saving the Results

- Data can be saved in the text file, by selecting 'Generate Log' in the File menu as shown in Figure A34.
- Liquids not required shall not be poured back into the beaker or the stock bottle. They are to be rejected and to be properly disposed off after the end of the measurements.



Figure A34: Exporting the Results

Calculation of Surface Energy

There are different tools available within the Drop Image software to calculate the surface energy of the substrate from the contact angle values obtained from the probe liquid. The acid-base test (Van Oss theory) is normally used as it takes into consideration three probe liquids, one with non-polar and two with polar characteristics, which gives good repeatability (Van Oss, Chaudhury and Good, 1988) while some other tools use less than three liquids and are more prone to errors. The following steps may be followed when an acid-base tool is used for calculation of surface free energy.

- Click the acid-base icon , shown in Figure A35, in order to open the acid-base surface energy tool, as shown in Figure A36 (Hansen, rame-hart instrument co. user guide, 2006)



Figure A35: Drop-Image Toolbar-Surface Energy Tool

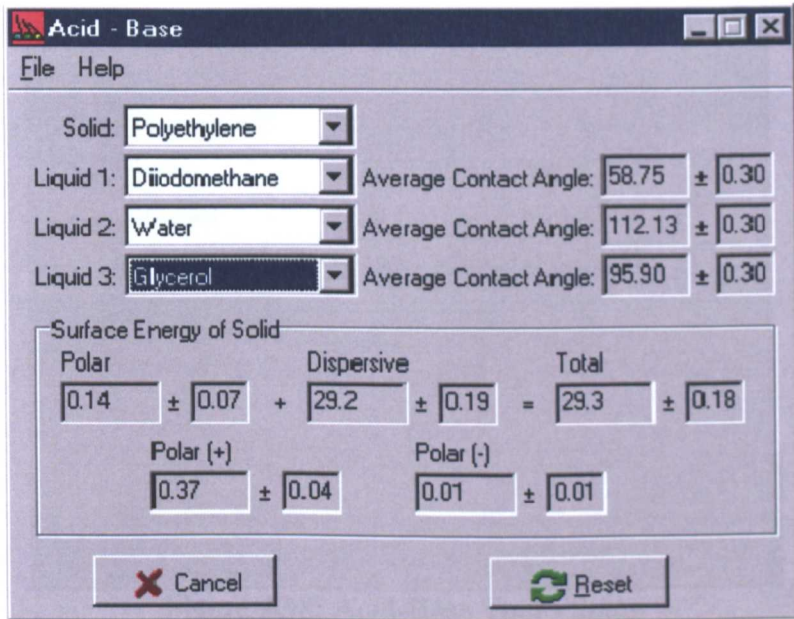


Figure A36: Surface Energy Measurement Tool

- Select file in the contact angle window and open the required files generated by the contact angle tool as shown in Figure A37 below. When a contact angle file is opened it shows all the active data in the contact angle window.

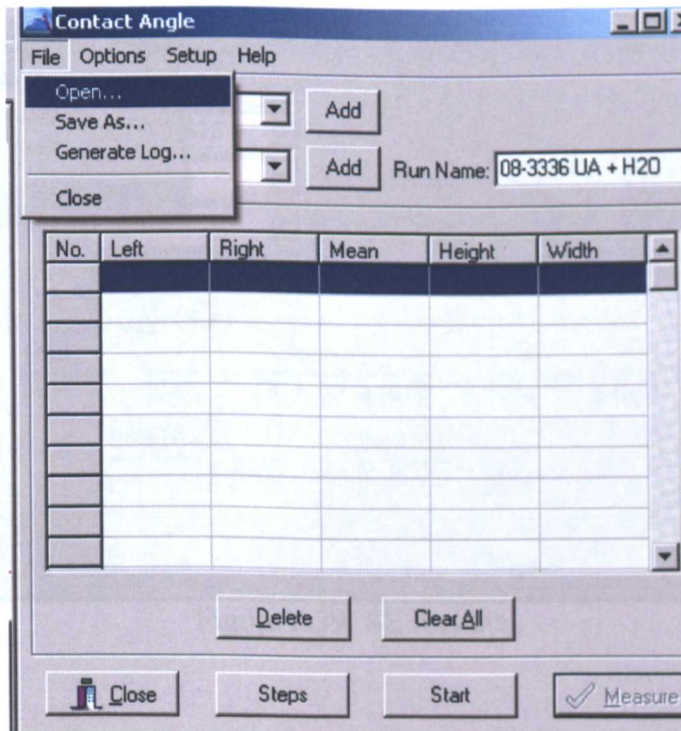


Figure A37: Opening the Contact angle Data

- Select the required solids and liquids from the drop-down list in Acid-Base tool as shown in Figure A38.

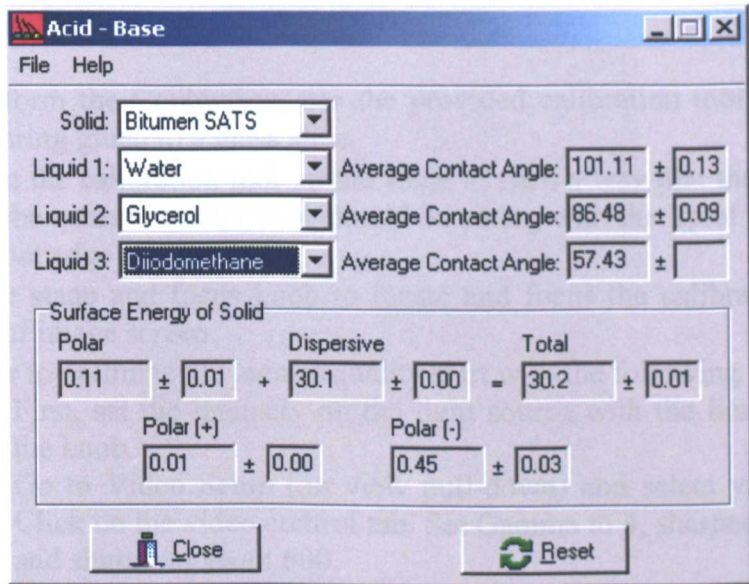


Figure A38: Acid-Base Tool - Setup

- The surface energy values are calculated and displayed in the same acid-base window which can then be saved by clicking 'Generate Log' in the file menu as shown in Figure A39. The results are saved in a text file and can be opened by using Microsoft Excel.

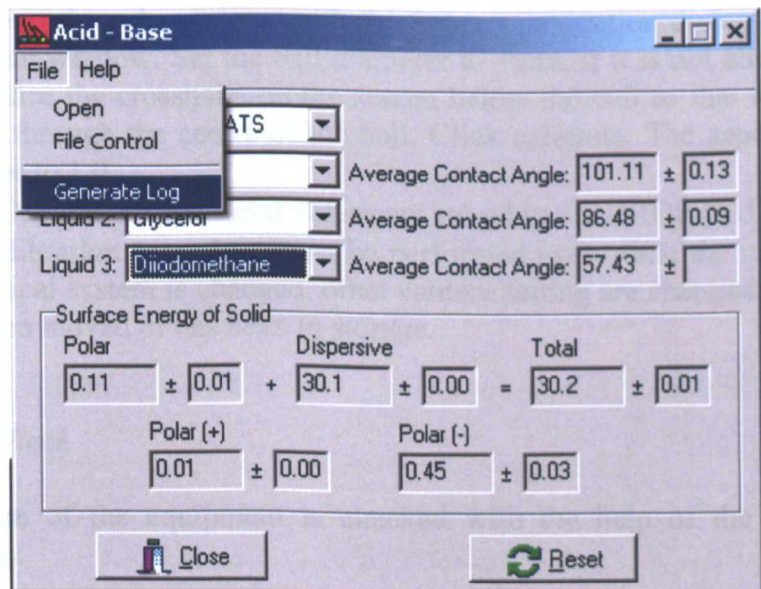


Figure A39: SE Results

The drop calibration reference tool includes images of drops on a transparent film substrate as shown in Figure A40. Images are named as A, B, C and D with fixed angles of 30°, 45°, 60° and 75° respectively. The tool is placed on the stage with the lip of the tool aligned with the front edge of the stage. The front side of the tool should be facing the camera. The contact angles of the drops are measured and compared with the values stated in the calibration certificate provided with the tool to check the accuracy of the measurement.

Equipment Calibration

- To perform the Calibration, use the provided calibration tool, which is steel ball bearing glued to a glass slide.
- Position the calibration tool on the stage in such a way that the ball should be facing the camera and the tool should be sitting with the lip of the tool aligned with front edge of the stage.
- Use the stage and focus knob to locate and focus the calibration ball in the centre of image screen.
- In order to optimize the picture quality start with the following settings:
 - First, set the intensity on the light source with the line straight up on the knob.
 - Go to Video Setup (on view pull-down) and select video properties. Click on the video control tab. Set Gamma to 4, sharpness to about 550 and shutter to about 600.
 - Turn off auto for both contrast and backlight comp. Adjust brightness (typically between 200 and 600) and contrast (typically between 100 and 300) until an optimal picture appears with the background completely white and the ball completely black. It is best to keep video properties static as frequent changes can affect the results of the data collected.
- Pull down the *Calibration* Menu; choose *New calibration* and then *Sphere*.
- Picture of the sphere along with the Sphere Calibration dialog box appears in the Main window. Set the ball diameter to 4mm, if it is not already, and click OK. Place the crosshairs on the screen below the ball so that the vertical line passes through the centre of the ball. Click calibrate. The aspect ratio should be close to 1.0.
- Click OK and the measured values are stored in the DROP.CAL file.
- The calibration procedure must be performed every time the magnification of the optical system is changed, other camera setting are changed and equipment has been moved or has been in storage.

Calibration Check

The calibration of the equipment is checked with the help of the following two reference tools:

- 1) Fixed Drop Calibration Reference Tool
- 2) Reference Solid PTFE

The fix drop calibration reference tool includes images of drops on a transparent film as shown in Figure A40. Images are named as A, B, C and D with fixed angles of 30°, 60°, 90° and 120° respectively. The tool is placed on the stage with the lip of the tool aligned with the front edge of the stage. The front side of the tool should be facing the camera. The contact angles of the drops are measured and compared with the values stated in the calibration certificate provided with the tool, to check the accuracy of the equipment.

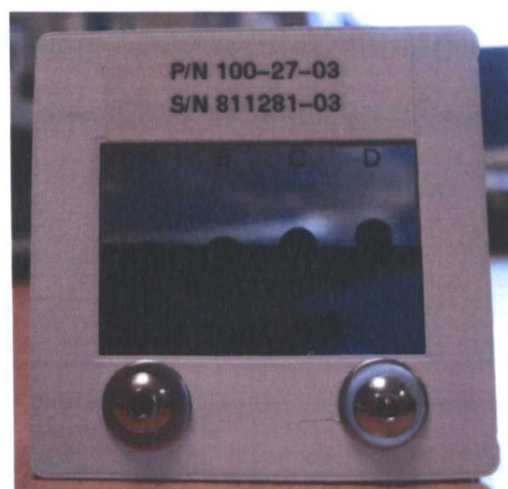


Figure A40: Fixed Drop Calibration reference Tool

The reference solid PTFE, shown in Figure A41, is placed on the levelled stage of the Goniometer and the angle of contact of deionised water on its surface is measured. Drops of the volume of $4\mu\text{l}$ are used for the purpose. The results are compared with the standard values provided with the calibration certificate.

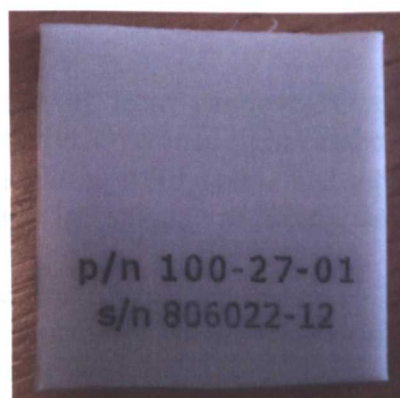


Figure A41: Reference Solid (PTFE)

The results from one of the calibration checks are provided in Table 20 for reference.

Table A1: Calibration Check; Results

Goniometer Contact Angle Results with PTFE as Reference Solid								
Measured Values								
Liquid	Solid	Run	No.	Left	Right	Mean	Height (mm)	Width (mm)
Water	Polyethylene	Water	1	105.5	106.6	106	1.375	2.191
Water	Polyethylene	Water	2	105.5	106.5	106	1.37	2.191
Water	Polyethylene	Water	3	105.4	106.5	105.9	1.37	2.191
Water	Polyethylene	Water	4	105.2	106.7	106	1.369	2.19
Water	Polyethylene	Water	5	105.4	106.5	106	1.369	2.191
Water	Polyethylene	Water	6	105.2	106.5	105.8	1.369	2.191
Water	Polyethylene	Water	7	105.3	106.4	105.8	1.369	2.192
Water	Polyethylene	Water	8	105.1	106.7	105.9	1.368	2.191
Water	Polyethylene	Water	9	105.1	106.8	106	1.368	2.19
Water	Polyethylene	Water	10	105.3	106.7	106	1.368	2.19

Expected Contact Angle Range (from Calibration Certificate) 101.4°-105.9°

Goniometer Contact Angle Results from Calibration Reference Tool						
Measured Values	Ref. No.	Left	Right	Mean	Height (mm)	Width (mm)
	A	29.6	31.1	30.3	0.259	2.009
	B	60.5	61.1	60.8	1.004	3.491
	C	88.8	90.6	89.7	1.997	4.048
	D	120.3	117.3	118.8	3.006	3.512
Actual Values (from Calibration Certificate)	Ref. No.	Left	Right	Mean	Height (mm)	Width (mm)
	A	30.2	31.6	30.9	0.267	2.066
	B	60.5	61.3	60.9	1.024	3.591
	C	88.6	90.6	89.6	2.06	4.156
	D	121.2	117.4	119.3	3.104	3.579
Tolerance ± 1%						

Precautions

- Keep the instrument away from windows. Outside light and excessive side lighting affects the results. Overhead light can be avoided by using the shade.
- The work surface should be solid, stable and vibration free. Goniometer table or bench should not be shared with any instrument which vibrates or oscillates.
- Instrument must be covered when not in use.
- When not in use, the lens cover should be attached to keep the lens free of dust and particles which may scratch the surface.
- Remove the micro-syringe barrel and needle and clean all components after each use daily and between liquids.
- Fire-wire cable should be connected before booting up the system, so that the software can detect the camera automatically when it is turned on.
- Do not disturb or remove the fire-wire cable while the system is in operation.
- Do not move the equipment while it is in *stand by* or *on* position.
- Exit the software and turn off the illuminator before shutting down the system.

APPENDIX B

Measurement of Contact Angle Using Wilhelmy Plate Device

Introduction

When a liquid comes in contact with a solid, it either spreads across the surface or repelled by that solid surface. The contact angle, θ , as illustrated below, is a thermodynamic quantity that characterizes the interaction between a solid and a liquid surface at the point of interaction.

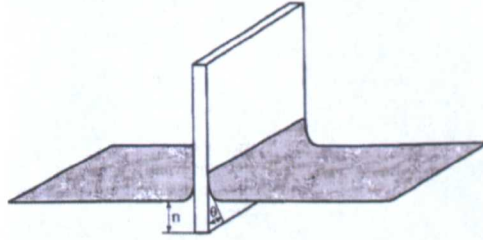


Figure B1: Contact Angle at Solid/Liquid/Vapour Contact Point
(Cahn WinDCA, user manual, 1999)

Wilhelmy plate device/Dynamic Contact Angle Analyser-DCA performs indirect contact angle measurement which involves immersing a glass or platinum plate of known dimensions into a liquid and then deriving the contact angle from the measured force (Adamson and Gast, 1997). It is used to measure the surface properties of solid and liquid samples. DCA consists of a highly sensitive balance, a moving stage mechanism and a control station. It uses WinDCA, a Windows based software program, to control the DCA system, collect data and perform data analysis (Cahn WinDCA, user manual, 1999).

Scope

- Measured contact angle values are used to calculate three surface energy components of the bitumen
- The method is not suitable for bitumen that contains particulate additives

Significance and use

The surface energy components of bitumen combined with that of aggregates can be used to determine the work of adhesion of the two materials, and the susceptibility of asphalt to water damage (Hefer, Bhasin and Little, 2005).

Equipment

The main equipment includes;

- Wilhelmy Plate Device, shown in Figure B2
- Computer System
- Slotted slip holder
- Microscope glass slip

- Crocodile clips
- Glass beakers
- Desiccator



Figure B2: DCA-System

Materials Required

- Approximately 50 grams of bitumen per sample
- Reagents with 99 percent purity (HPLC Grade):
 - Glycerol
 - Formamide
 - Diiodomethane
 - Ethylene glycol
 - Distilled water

Glass beakers labelled with the names of the Reagents/probe liquids are washed, dried and filled with the respective probes prior to test as shown in Figure B3. One beaker should be used for one liquid only.



Figure B3: Beakers Filled with Probes

Conditioning and Testing Temperatures

Additives and substrates are conditioned for 24 hours, at room temperature of $23^{\circ}\text{C} \pm 2^{\circ}\text{C}$ and at relative humidity of $50\% \pm 5\%$.

Sample Preparation

Microscope glass slides (24 mm x 40 mm, No. 1.5) are used for preparation of bitumen films. Each slide can only be used once. At least four measurements for a sample are made with each probe liquid.

The following procedure is used to prepare the sample slides.

- A tin filled with bitumen or mastic sample is placed in oven at the appropriate mixing temperature. After about 15 minutes, the tin is removed from the oven and placed on a hot plate to maintain temperature. The sample is thoroughly stirred as shown in Figure B4.



Figure B4: Sample/substrate Tin

- Glass slides are cleaned with acetone and then rinsed with distilled water as detailed in appendix A. Both sides of the slides are passed through a blue flame, as shown in Figure B5, in order to remove any moisture or organic matter from the slide.



Figure B5: Cleaning of Glass Slide

- The clean glass slide is dipped into and out of the molten sample (approximately up-to 15mm depth) as shown in Figure B6. The slide is then

immediately inverted to allow the sample/bitumen to drain down evenly coat the slide.



Figure B6: Sample Preparation

- The prepared slides are then carefully placed onto a slide holder and kept in a desiccator for 24 hours as shown in Figure B7 below.



Figure B7: Samples placed in a Desiccator

Measurement of Contact Angle

In order to make a contact angle measurement, the following procedure is followed:

- Turn on the equipment and the computer system.
- Fill a 100ml beaker with the required probe liquid up to a depth of 50ml and place it on the stage of the equipment. For expensive probes like diiodomethane and formamide a 50ml beaker is used and is filled up-to about 25ml.
- Open the WinDCA software by double clicking the software icon, shown in Figure B8 below.

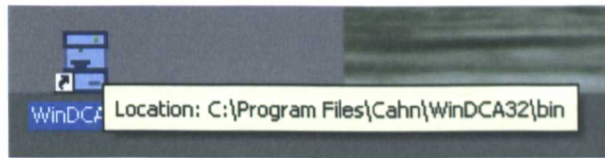


Figure B8: WinDCA Icon

- Load a contact angle method from the method drop-down menu in the main menu toolbar as shown in Figure B9 and B10 respectively. A new method can be created by selecting the required option.

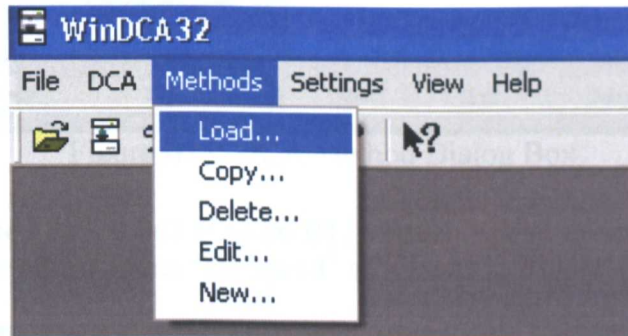


Figure B9: Method Drop-Down Menu

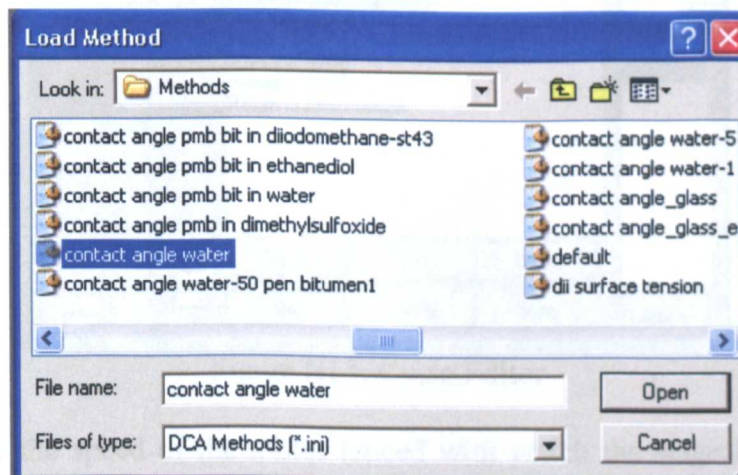


Figure B10: Load Method window

- Once the required method is loaded, select the edit option in the method drop-down menu shown in Figure B11. The DCA method dialog box appears as shown in Figure B12.

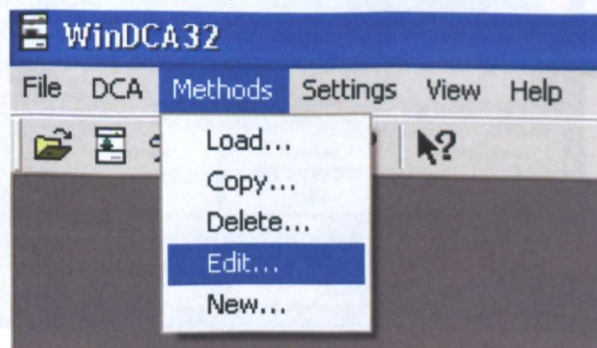


Figure B11: Method Editor

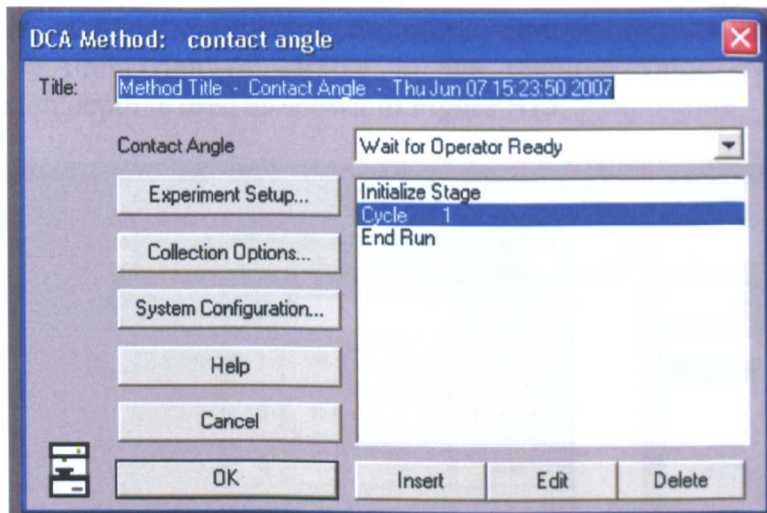


Figure B12: DCA Method Dialog Box

- In the method dialog box (Figure B12) select 'cycle' option and click edit tab. In the cycle editor select 'set speed' as shown in Figure B13 below and click edit.

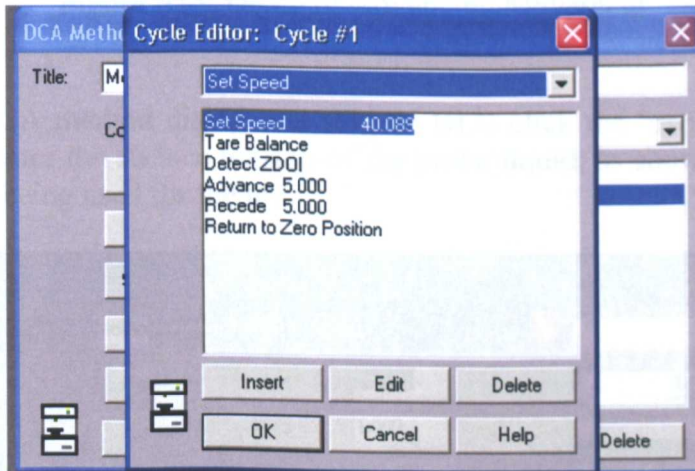


Figure B13: Cycle Editor

- Change the speed of the motor (speed with which the stage is moved or the sample slide is immersed in the probe liquid) to the required as shown in Figure B14 and click done. A speed of 40microns/sec is used in our case.



Figure B14: Stage Speed Editor

- In the cycle editor the advance and recede options are selected to change the depth of immersion of sample to the required value. Normally 5mm immersion depth is used as shown in Figure B15.

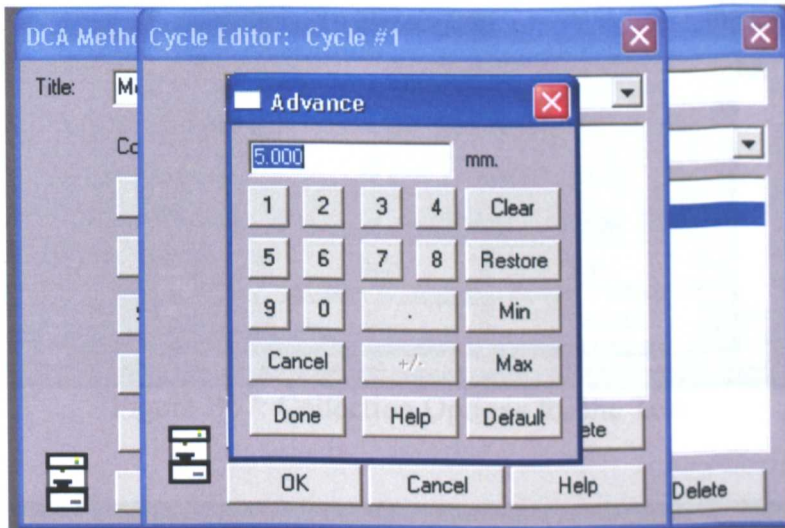


Figure B15: Depth of Advancing Movement

- In the DCA method dialog box (Figure B12) click the ‘experimental set-up’ tab and enter the surface tension of the probe liquid, as shown in Figure B16, which is being used for the test.

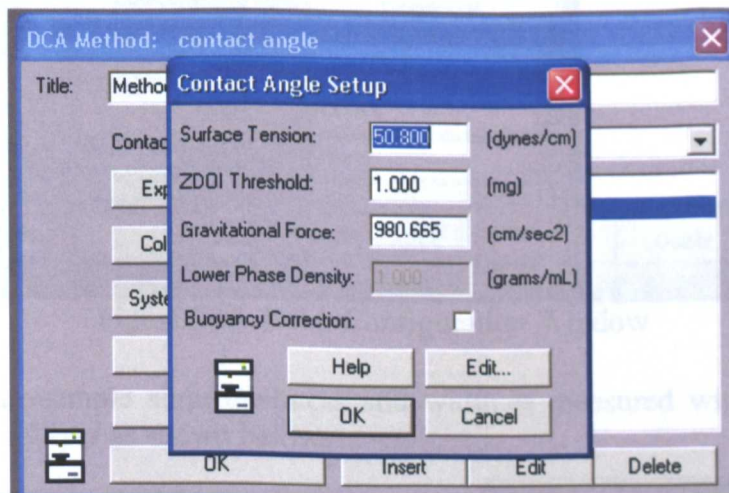


Figure B16: Contact Angle Set-up

- Click ‘collection options’ tab in the DCA method dialog box (Figure B12) and enter the operator and sample identities in the respective fields as shown in Figure B17. Similarly the ‘system configuration’ tab is used to enter the plate/sample slide dimensions as shown in Figure B18 below.

Figure B19: Measuring the Slide Dimensions

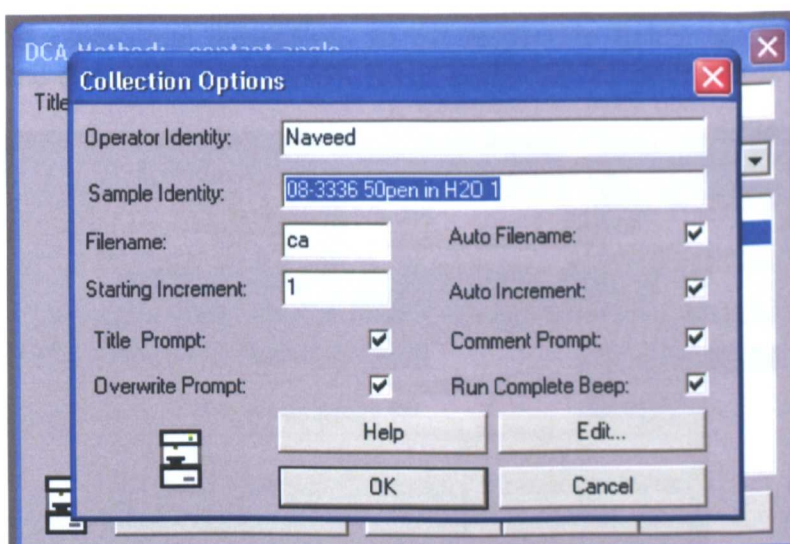


Figure B17: Collection Options for the Test



Figure B18: DCA Configuration Window

- The plate/sample slide thickness and width is measured with the help of a vernier calliper as shown below.



Figure B19: Measuring the Slide Dimensions

Figure B.2. Securing the Glass Slide on the Sample Support

- Enter the measured dimensions in the respective fields, as shown in Figure B20, and click Ok.

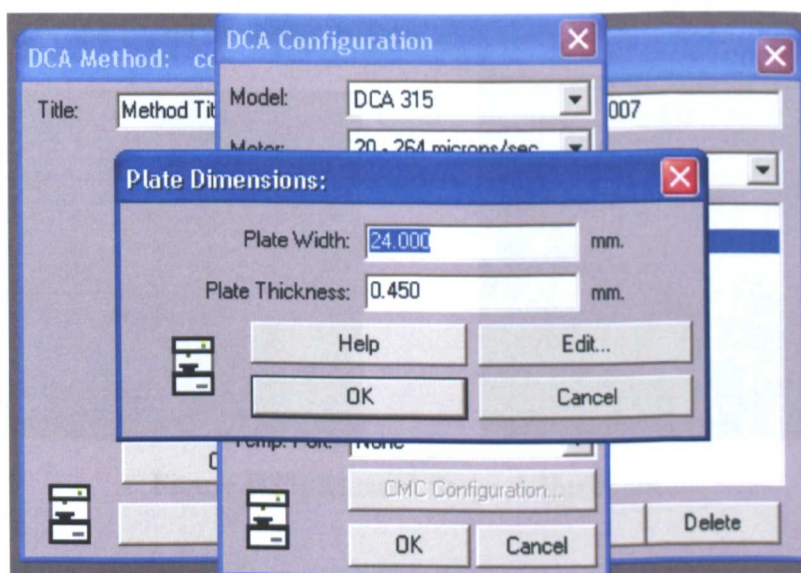


Figure B20: Entering the Slide Dimensions

- The software will prompt for saving the changes as shown below. Click Ok.

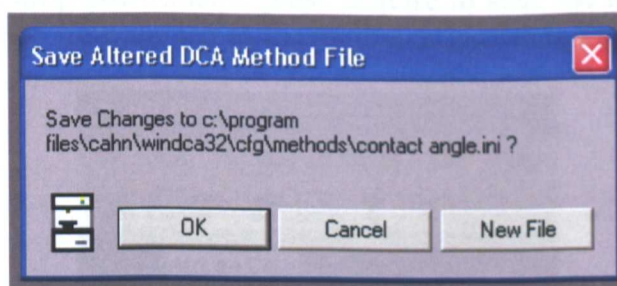


Figure B21: Saving the Method File

- The measured sample slide is attached with the provided copper clip and is hanged on the sample stirrup with the help of a forceps as shown in Figure B22.

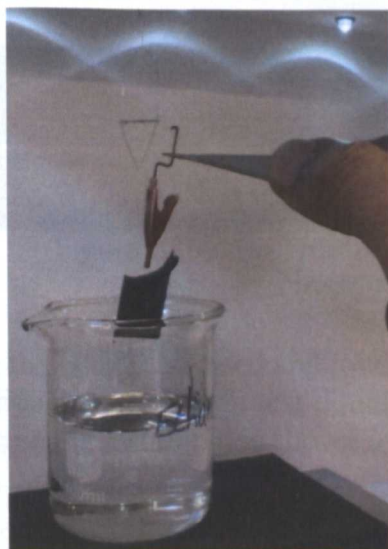


Figure B22: Securing the Glass Slide on the Sample Stirrup

- The bottom edge of the hanged glass slip/slide should be parallel to the surface of the liquid in the beaker. Now manually adjust the height of the stage so that the bottom of the slide is within a distance of approximately 5mm from the surface of the liquid as shown below.

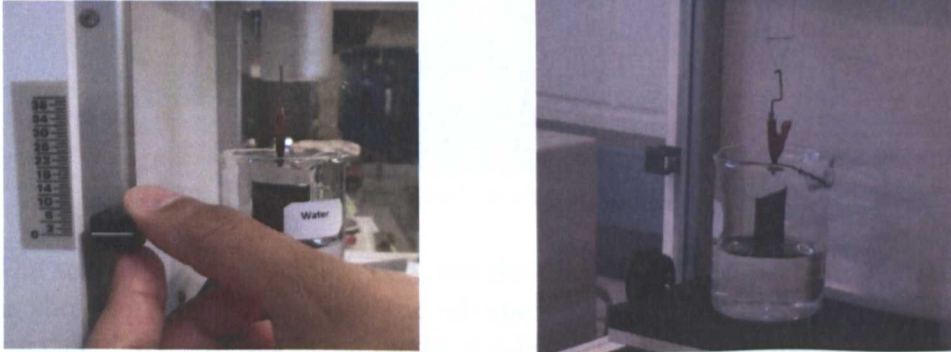


Figure B23: Manual Stage Adjustment

- Close the front cover of the equipment and wait till the slide stops swinging and become stable.
- In the DCA drop-down menu, press acquire to start the test. Or simply press the second icon from the left in the toolbar as shown in Figure B24.



Figure B24: Initialising the Test

- The software will prompt for the file title as shown in Figure B25. Change the title if required and click 'done'.

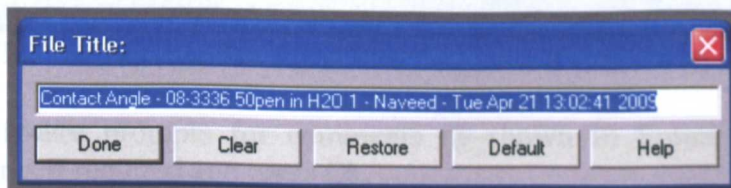


Figure B25: File Title

- The stage containing the beaker is raised and lowered at pre-entered speed and depth. The sample slide is immersed in test liquid during the stage movement. A sample slide immersed in test liquid is shown in Figure B26.

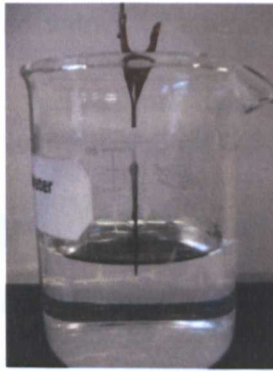


Figure B26: Sample Slide Immersed in Test Liquid

- The software draws a graph between the mass of slide and depth of immersion as shown in Figure B27, and the advancing and receding contact angle values are calculated and displayed on the top-left corner of the graph.

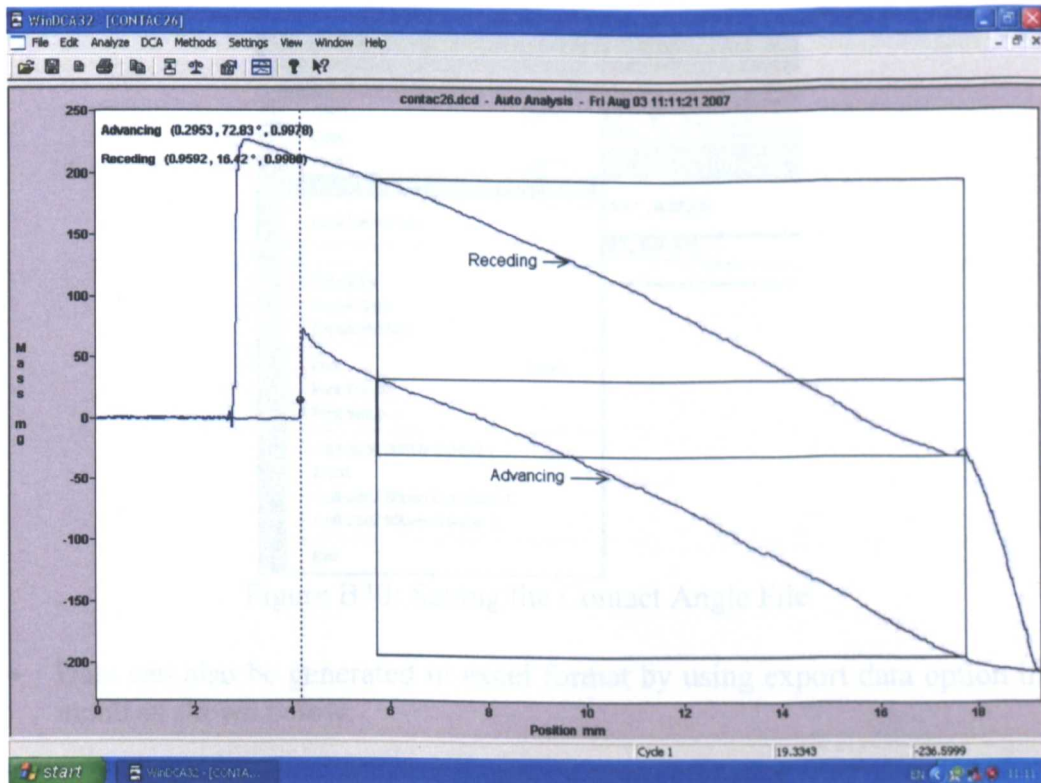


Figure B27: Advancing-Receding Plot for Contact Angle Measurements

- The software prompts for comments as shown in Figure B28. Enter the comments if required and press Ok.

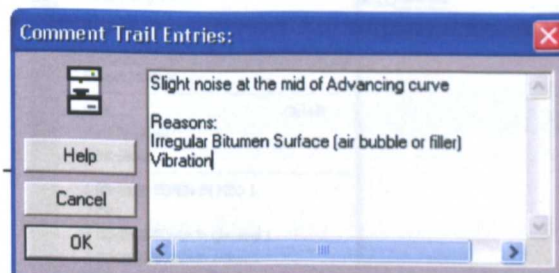


Figure B28: Comment Field for the Test

- In order to obtain accurate values of contact angles a smooth portion of the graph can be selected by using the manual option in the analyse drop-down menu, as shown in Figure B29, and selecting the required portion of the advancing and receding plot by using the right button of the mouse.

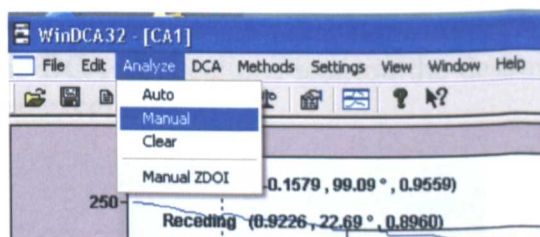


Figure B29: Manual Analysis Option

- The obtained results are saved by using the 'save as' option from the file drop-down menu, as shown below, and can be printed directly through software.

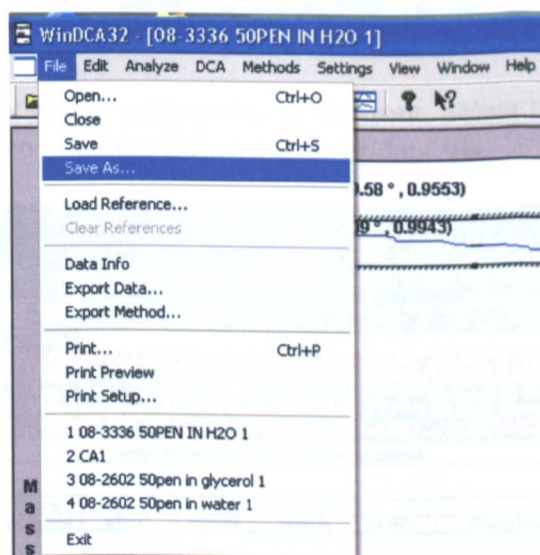


Figure B30: Saving the Contact Angle File

- Data can also be generated in excel format by using export data option in file menu as shown below.

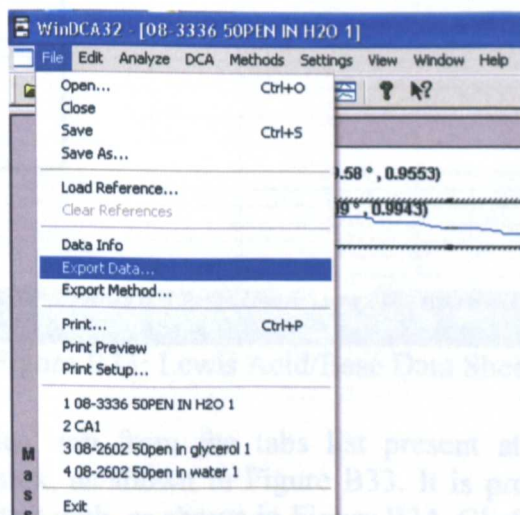


Figure B31: Exporting the Data

Calculation of Surface Energy

Surface energy components are calculated by using the macros installed in an excel spread sheet provided with the software. The following steps may be followed for the purpose:

- Double click the DCA applications icon on the desktop, as shown below, to open the required excel sheet.

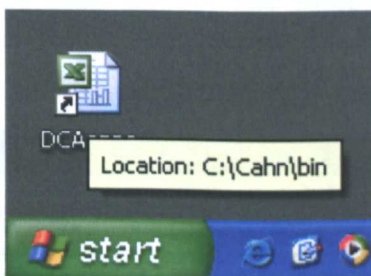


Figure B32: DCA applications Icon

- The sheet opens with a main menu at the front. Select Lewis Acid/Base option from the menu to open the following sheet/data file.

Lewis Acid/Base: Data Files Selected							
Analysis Done:							
#	Advancing cosine(theta)	Receding cosine(theta)	gamma ^l	gamma ^{lv}	gamma ^{p-}	gamma ^{p+}	Constants ID
1							

Solutions	
	$\gamma_s^{p-} =$
Adv	$\gamma_s^{p+} =$
	$\gamma_s^{lv} =$
	$\gamma_s =$
	$\gamma_s^{p-} =$
Reo	$\gamma_s^{p+} =$
	$\gamma_s^{lv} =$
	$\gamma_s =$

Figure B33: Lewis Acid/Base Data Sheet

- Click 'open files' tab from the tabs list present at the top of the sheet, highlighted in pink, as shown in Figure B33. It is prompted to select a non-polar liquid to start with, as shown in Figure B34. Click Ok.

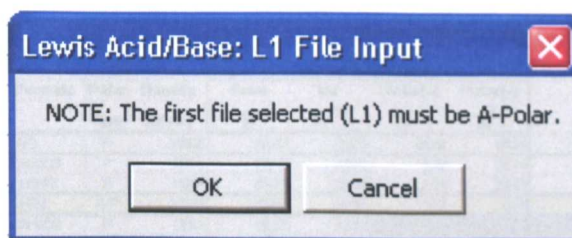


Figure B34: Lewis Acid/Base File Input Window

- Select the contact angle data file for the sample which is required to be analysed. Select the file which was created for a non-polar liquid and click open as shown below.

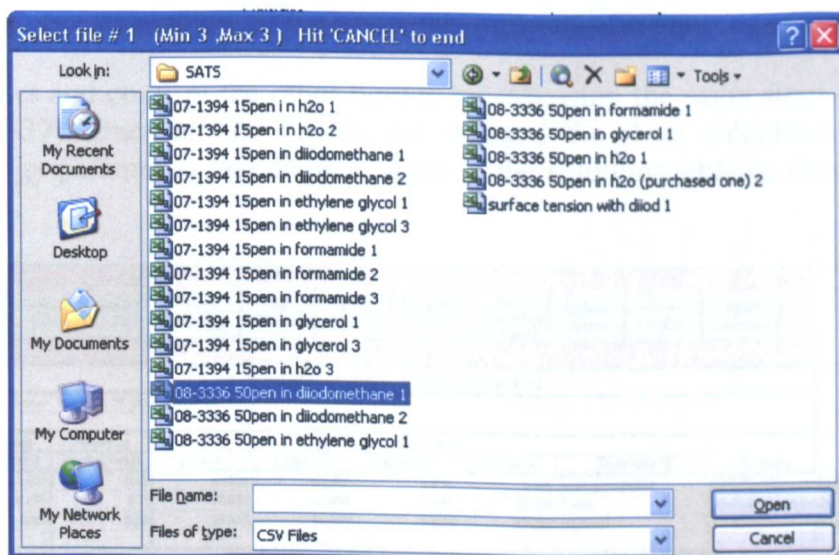


Figure B35: File selection for SE analysis

- When prompted, find the number for the liquid which has been selected in the previous step from the table displayed on the screen (Figure B37) and enter the selected number in the constants field shown below.

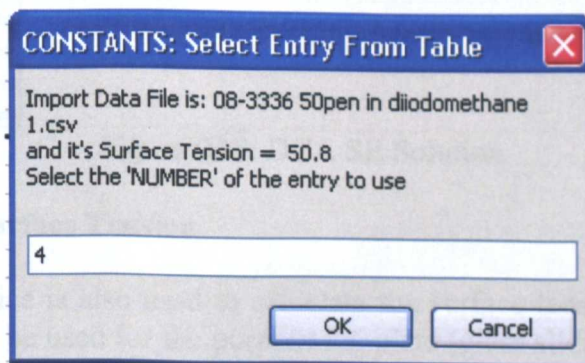


Figure B36: Probe Constants Entry

- The software highlights the selected liquid and prompts to confirm the selection. Confirm the selection by clicking Ok as shown in Figure B37.

Liquid Specifications					Values			
#	Liquid ID	Formula	Polar Type	Density (g/mL)	LEWIS ACID/BASE			
					Total γ_L	LW γ_L^{LW}	Polar(+) $\gamma_L^{(+)}$	Polar(-) $\gamma_L^{(-)}$
1	Water	H2O	P	1.0000	72.80	21.80	25.50	25.50
2	Glycerol	C3H8O3	P	1.2613	63.40	34.00	3.92	57.40
3	Formamide	CH3NO	P	1.1334	58.20	39.00	2.28	38.60
4	Methyleneiodide	CH2I2	A-P	3.3212	50.80	50.80	0.00	0.00
5	Ethylene glycol	C2H6O2	P	1.1088	48.30	28.00		
6	Iodomethane	CH2I2	A-P	3.3212	46.50	46.50		
7	Bromonaphthalene	C10H7Br	A-P	1.8050	44.60	43.50		
8	Dimethyl sulfoxide	(CH3)2SO	P	1.1000	43.50	36.00		
9	Chloroform	CHCl3	P	1.4850	27.15	27.15		
10	Dithioglycol	C3H8OS2	P	1.2340				
11	Tricresylphosphate	C21H21PO4	A-P	1.1620				
12	Dimethylformamide	C3H7ON	A-P	1.1737				
13	Dicyclohexyl	C12H22	A-P	0.8833				
14	2-ethoxyethanol	H3OCH2CH	P	0.9663				
15	Hexadecane	C17H31	A-P	0.7733				

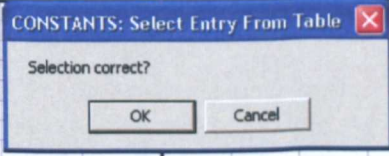


Figure B37: Probe Selection Confirmation

- Select and confirm the other liquids by following the same steps (Figure B33 to B37). Once all the liquids are selected the sheet calculates the surface energy parameters and displays them in the solutions table as shown in Figure B38.

Clear Tables Open Files New L1 File Print Tables Re Calculate View Headers View File Table View Solutions Table Delete Entry Save Table Main Menu										
Lewis Acid/Base: Data Files Selected										
Analysis Done: Tue April 21, 2009 @ 1:31PM										
#	Advancing		Receding		Constants			Constants ID	File Name	
	cosine(theta)	cosine(theta)	gamma ^l	gamma ^{lw}	gamma ⁺	gamma ⁻				
1	0.557	0.84	50.800	50.800	0.000	0.000	Methyleneiodide	08-3336 50pen in diiodomethane 1.osv		
2	-0.075	0.71	72.800	21.800	25.500	25.500	Water	08-3336 50pen in h2o 1.osv		
3	0.102	0.94	63.400	34.000	3.320	57.400	Glycerol	08-3336 50pen in glycerol 1.osv		

Solutions	
Adv	$\gamma_s^{D-} =$ 2.63
	$\gamma_s^{P+} =$ 0.01
	$\gamma_s^{lw} =$ 30.78
	$\gamma_s =$ 31.04
Rec	$\gamma_s^{D-} =$ 18.58
	$\gamma_s^{P+} =$ 3.68
	$\gamma_s^{lw} =$ 43.10
	$\gamma_s =$ 59.64

Figure B38: DCA SE Solution

Measurement of Surface Tension

Wilhelmy plate device is also used to calculate the surface tension of the test liquid. Two techniques can be used for the purpose i.e. plate (glass slide) method or DuNuoy ring method. The glass slide method is normally used. A clean glass slide is hanged on the sample stirrup and the liquid which is being tested for the surface tension value is placed on the equipment stage beneath the glass slide.

A step by step method for calculation of Surface tension using glass slide approach is explained below with the help of figures.

• All total parameters can be changed by using the Edit option in the WinAdv drop-down menu. A DCA method edit window is shown in Figure B-41 below.

- Double click the WinDCA software icon on desktop, the WinDCA main window is opened as shown in Figure B39.

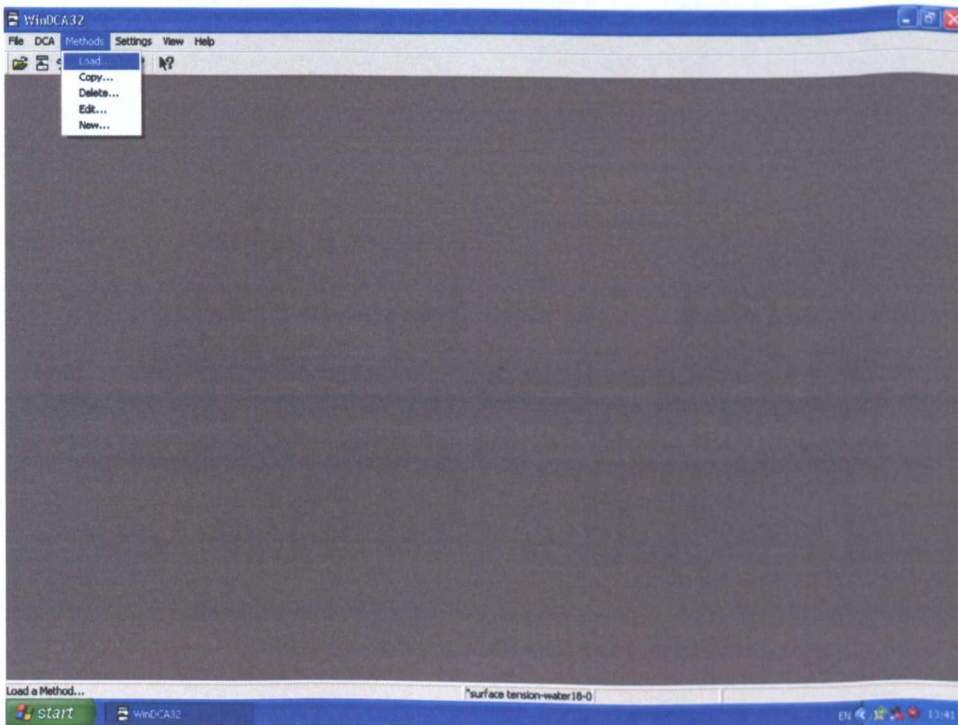


Figure B39: WinDCA Main Window

- Load the surface tension method for the liquid by clicking *method* and then *load* in the Method drop-down menu as shown in Figure B40.

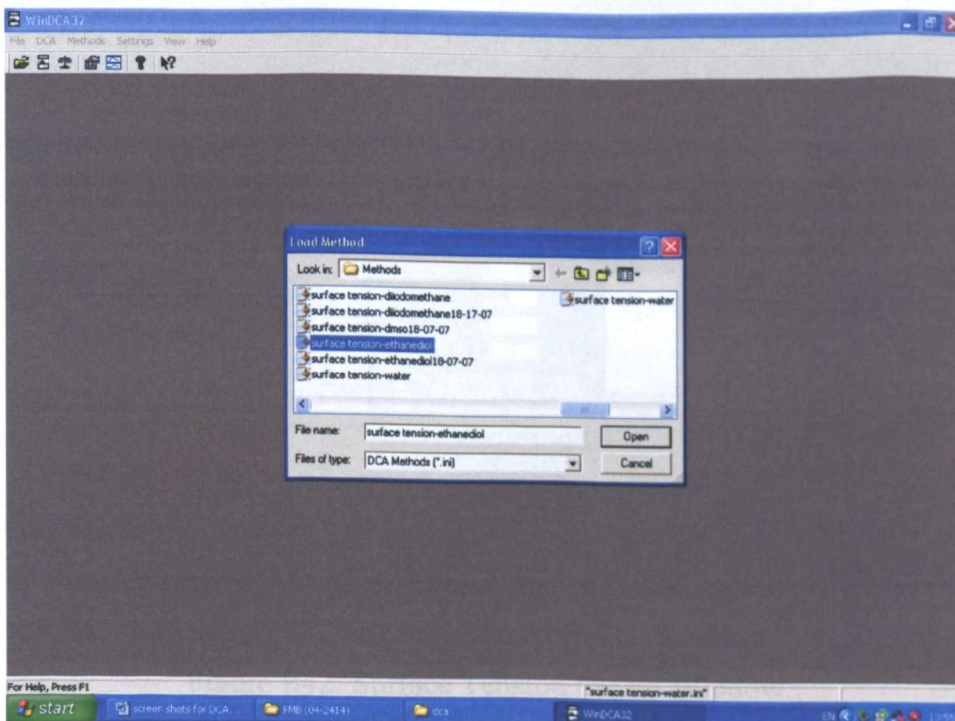


Figure B40: WinDCA Load Method Window

- Method parameters can be changed by using the *Edit* option in the *Method* drop-down menu. A DCA method edit window is shown in Figure B41 below.

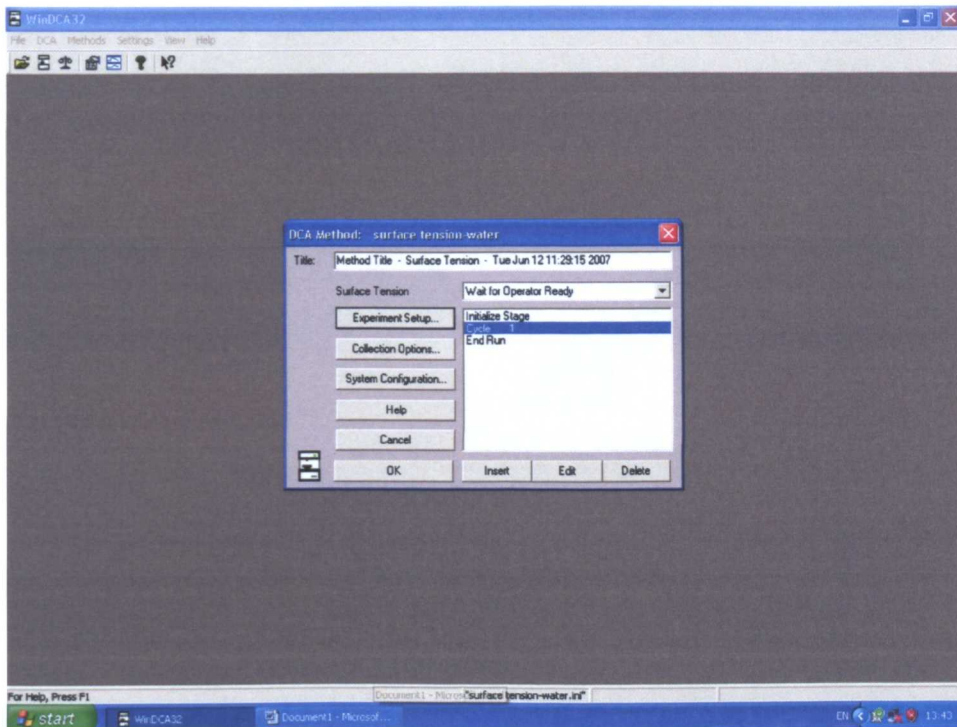


Figure B41: DCA Method; Edit Window

- Different surface tension test parameters like maximum time and ZDOI threshold etc., shown in Figure B42, can be changed by clicking *Experimental Set-up* in the Edit Window.

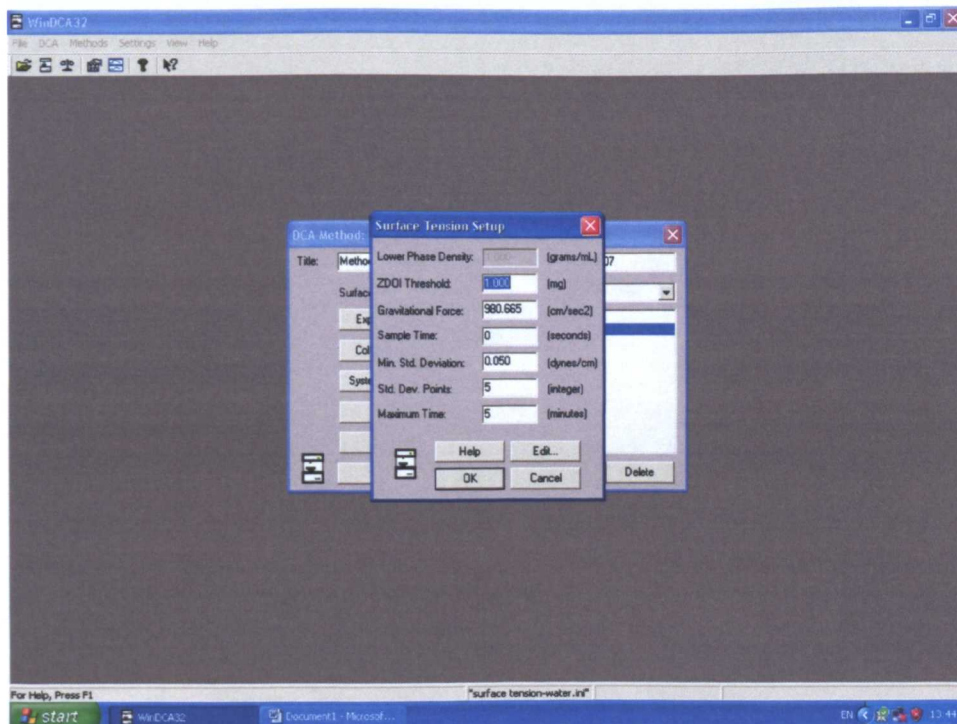


Figure B42: Surface Tension Set-up Window

- *Collection Option* tab in the Edit Window is used to change the operator and sample identity as shown in Figure B43 below.

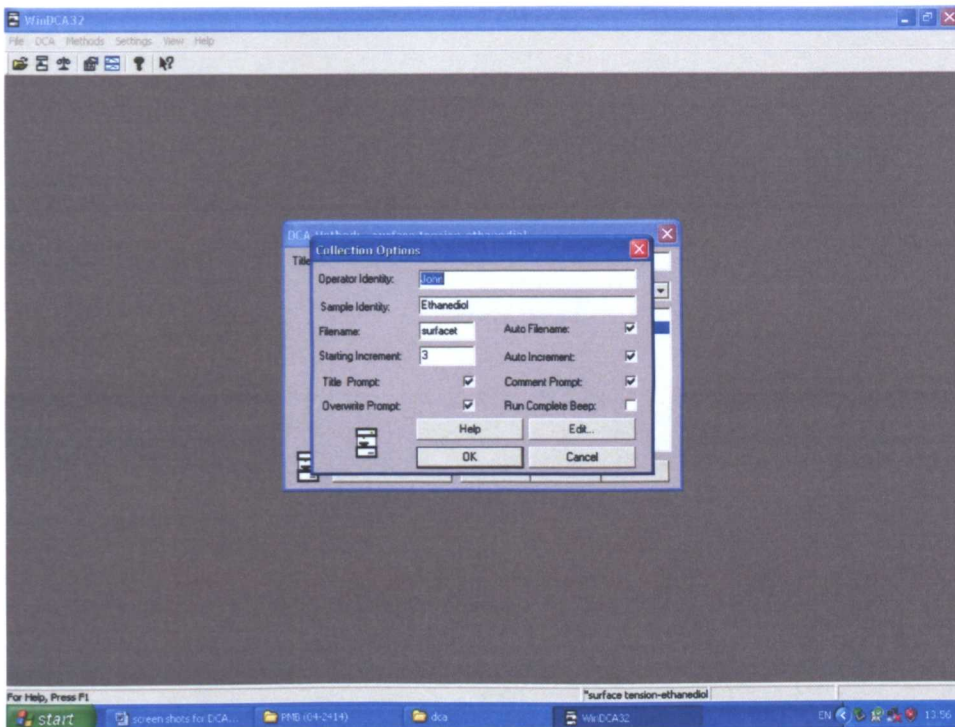


Figure B43: Collection Option Window

- Parameters like speed of motor and plate dimensions are changed through system configuration window as shown in Figure B44 below.

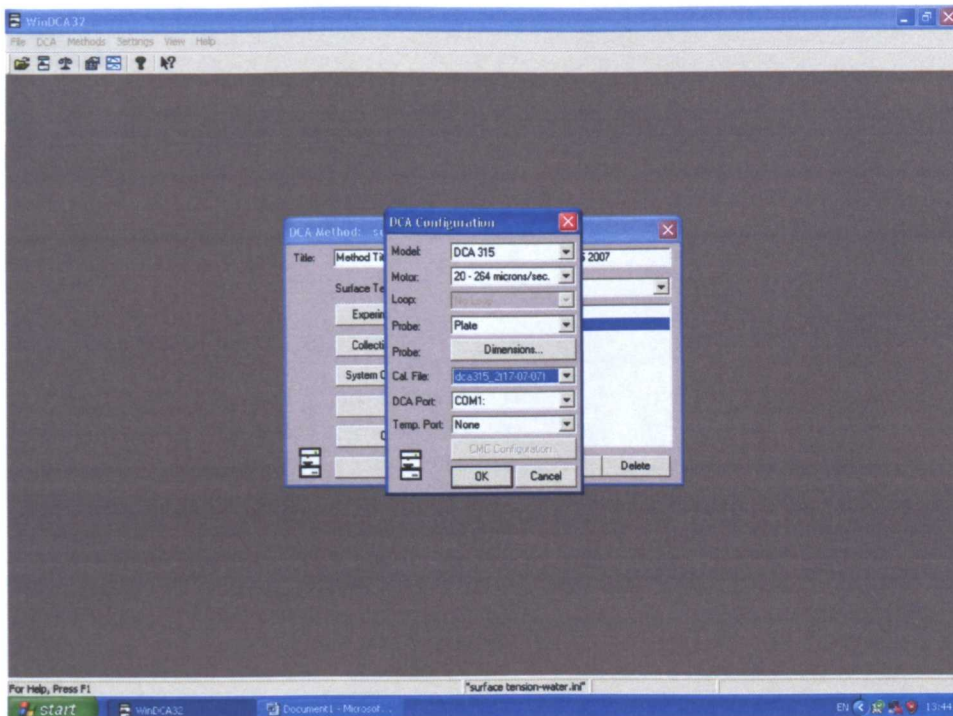


Figure B44: DCA Configuration Window

- All the changes made in the surface tension method can be saved by clicking *OK*, or by saving the changed method as a separate file as shown in Figure B45.

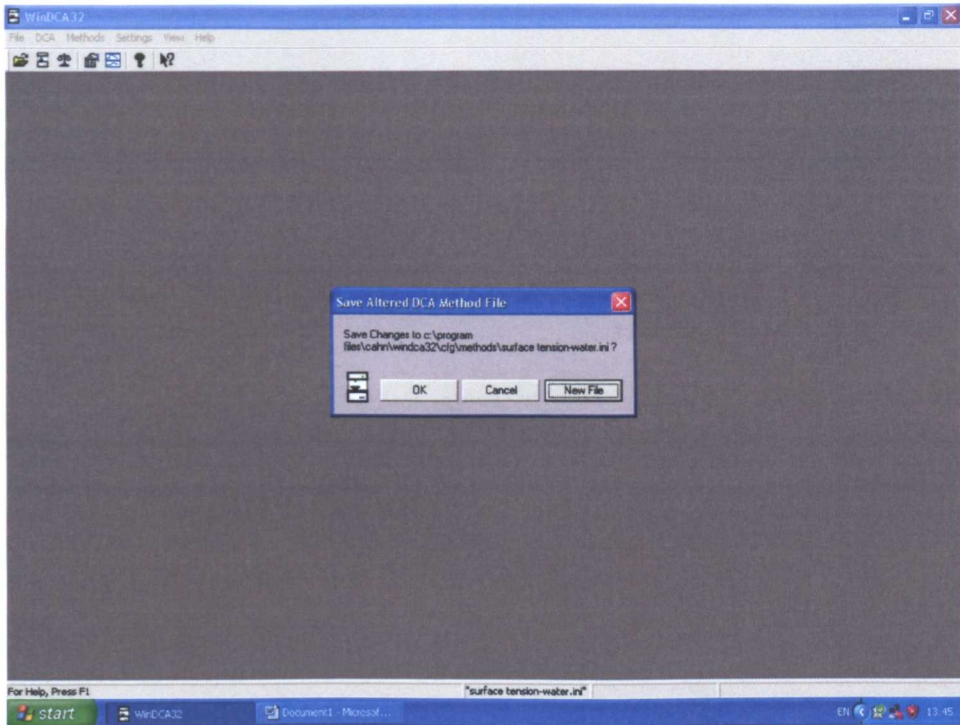


Figure B45: Saving a DCA Method File

- Once the required changes have been made, click *Acquire* in the DCA drop-down menu to start the test as shown in Figure B46 below.

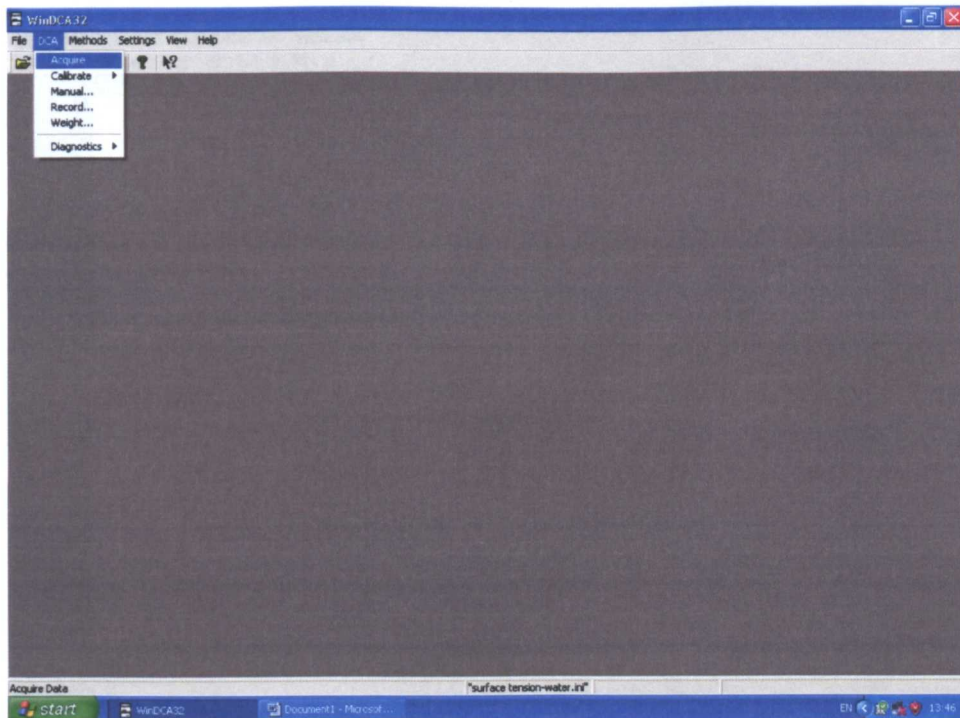


Figure B46: DCA Data Acquire Window

- When the software prompts for a File Title, enter the file details and click *Done* to start the test. File title window is shown in Figure B47 below.

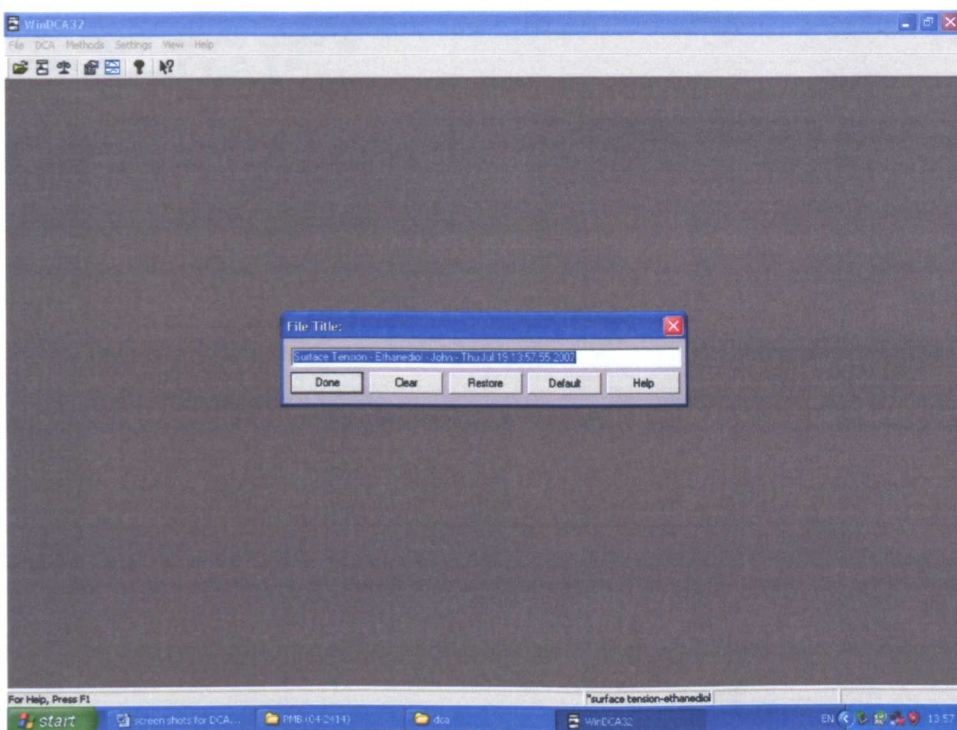


Figure B47: DCA File Title Window

- The software draws a graph between the mass of slide and depth of immersion as shown in Figure B48, and the surface tension values are calculated

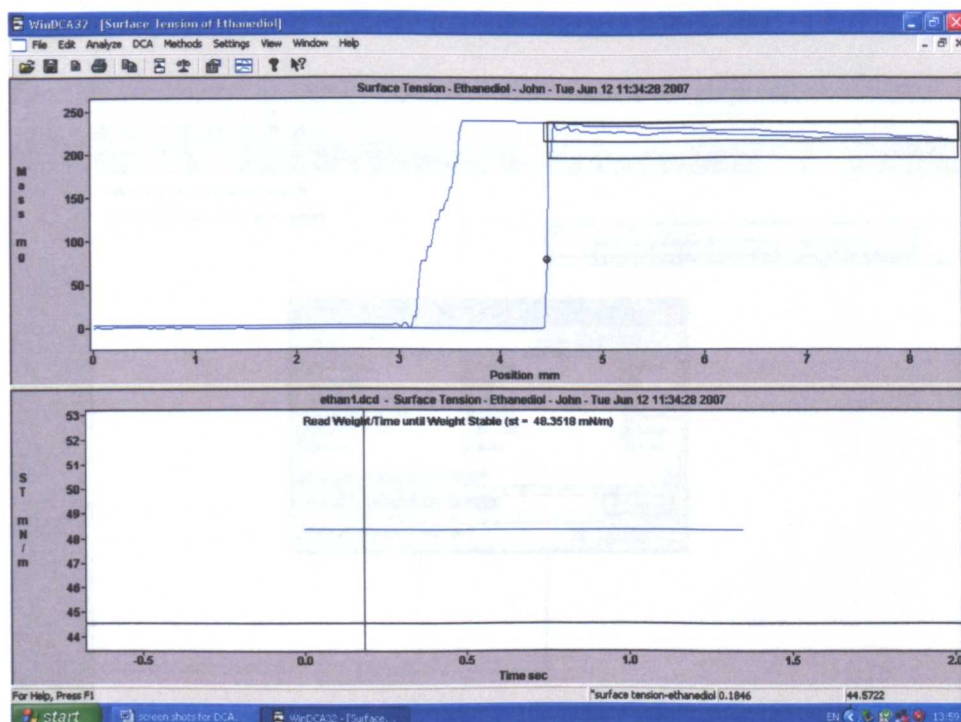


Figure B48: Advancing-Receding Plot for Surface Tension Measurements

- In order to obtain a precise value of surface tension a smooth portion of the graph can be selected by using the manual option in the analyse drop-down menu as shown in Figure B49.

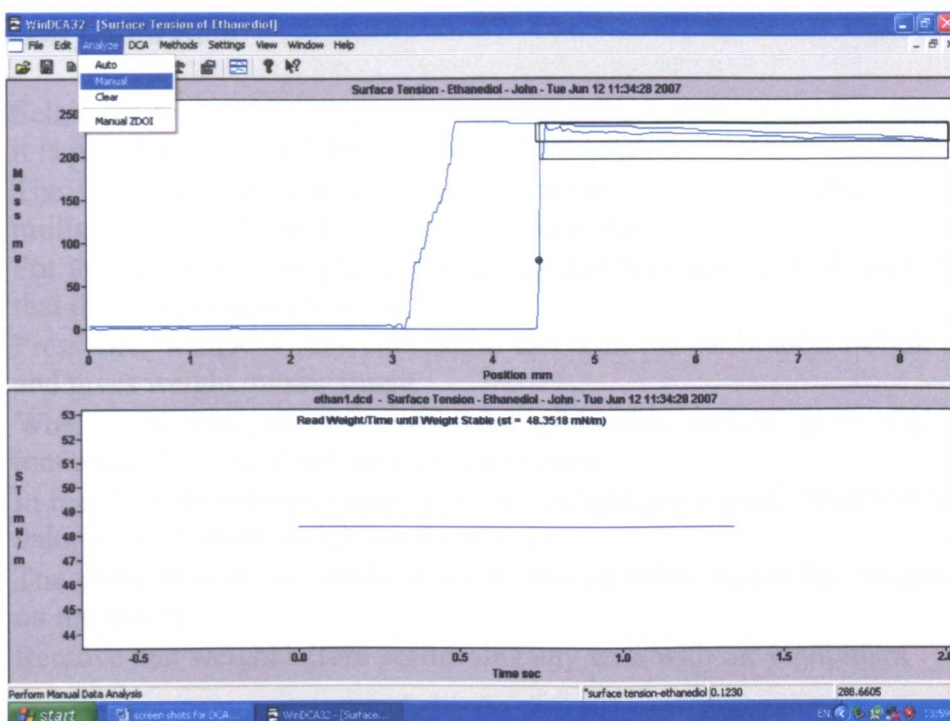


Figure B49: Manual Analysis Window

- Surface tension value for the advancing slide movement is calculated and displayed in the main window as shown in Figure B50. The obtained results are then saved by clicking *save as* option in the file drop-down menu. The data is generally saved in a separate surface tension sub-folder.

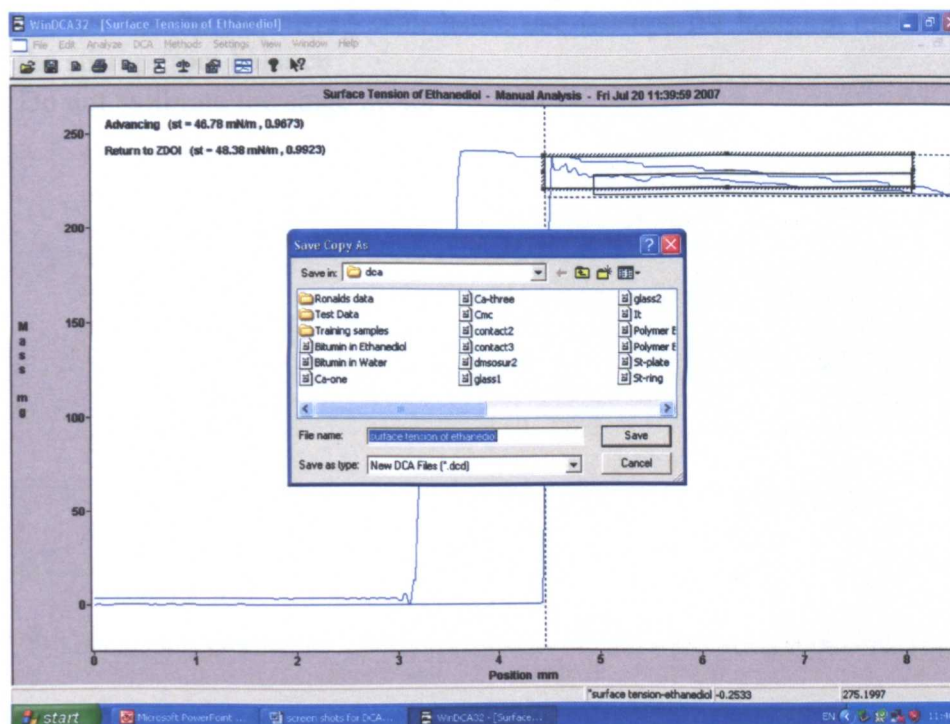


Figure B50: DCA, Save File Window

Equipment Calibration

- Select *calibrate* and then *balance* from the DCA menu. Install a stirrup when it is prompted and click OK to continue calibration
- The DCA balance calibration dialog appears, enter the calibration weight in milligrams, you intend to use and then click *start*
- Put the calibration weight on the stirrup and wait for a couple of minutes so that the stirrup stops swinging
- Press OK. WinDCA runs calibration test with the calibration weight in place and gives weight measurement
- When it is prompted to remove the calibration weight, press OK without removing the weight and save the calibration
- In the DCA drop down menu, go to *record* and press *start*. WinDCA gives the value of the present weight on the stirrup
- The calibration is successful if the measured value equals the weight present on the stirrup
- Remove that weight before performing any tests with the equipment

Precautions

- The work surface should be solid, stable and vibration free
- Instrument must be covered when not in use
- Width of glass slip (plate) should not be more than $2/3^{\text{rd}}$ of the diameter of the beaker
- Always rinse and dry the beakers before pouring in the test liquid
- Do not handle the stirrup with hand, use forceps for hanging and dislodging the stirrup from balance
- Do not calibrate the stage motor

APPENDIX C

Measurement of Vapour Sorption of Aggregates using DVS Advantage System

Introduction

The DVS Advantage is designed to accurately measure a sample's change in mass as it sorbs precisely controlled concentrations of water or organic vapours in an inert carrier gas. The sample is hung from a microbalance in a sample pan (an empty pan is usually hung on the other side of the balance as a 'reference'). Air carrying the test vapours is then passed over the sample at a well-defined flow-rate and temperature. The sample mass readings from the microbalance then reveal the vapor adsorption/desorption behavior of the sample (DVS-Advantage, operation manual, 2007). Surface energy components of the aggregates are then determined using adsorption isotherm, on the basis of sorption of vapor probes by aggregates.

A schematic diagram of a DVS Advantage system is shown below:

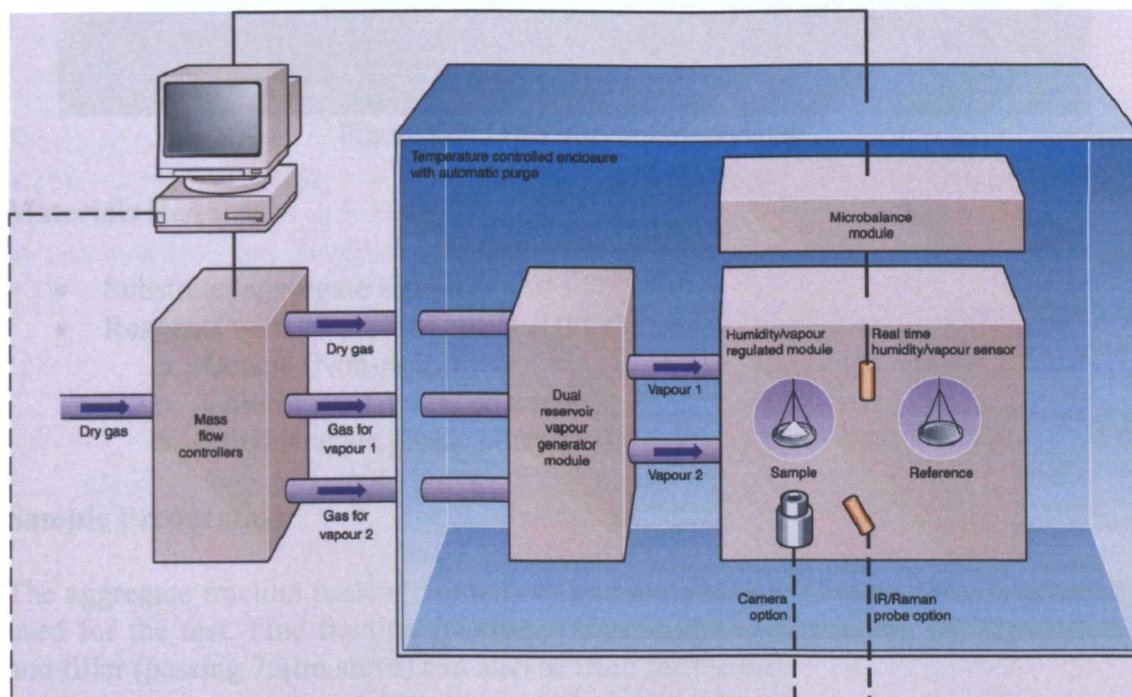


Figure C1: DVS-Advantage Schematic
(Surface Measurement Systems, DVS-Advantage, 2007)

Equipment

The DVS Advantage system is shown in Figure C2. Other main parts include;

- Mass flow controller
- Temperature probes
- Optical vapour sensor
- Environmental chamber with DVS Manifold
- Computer System

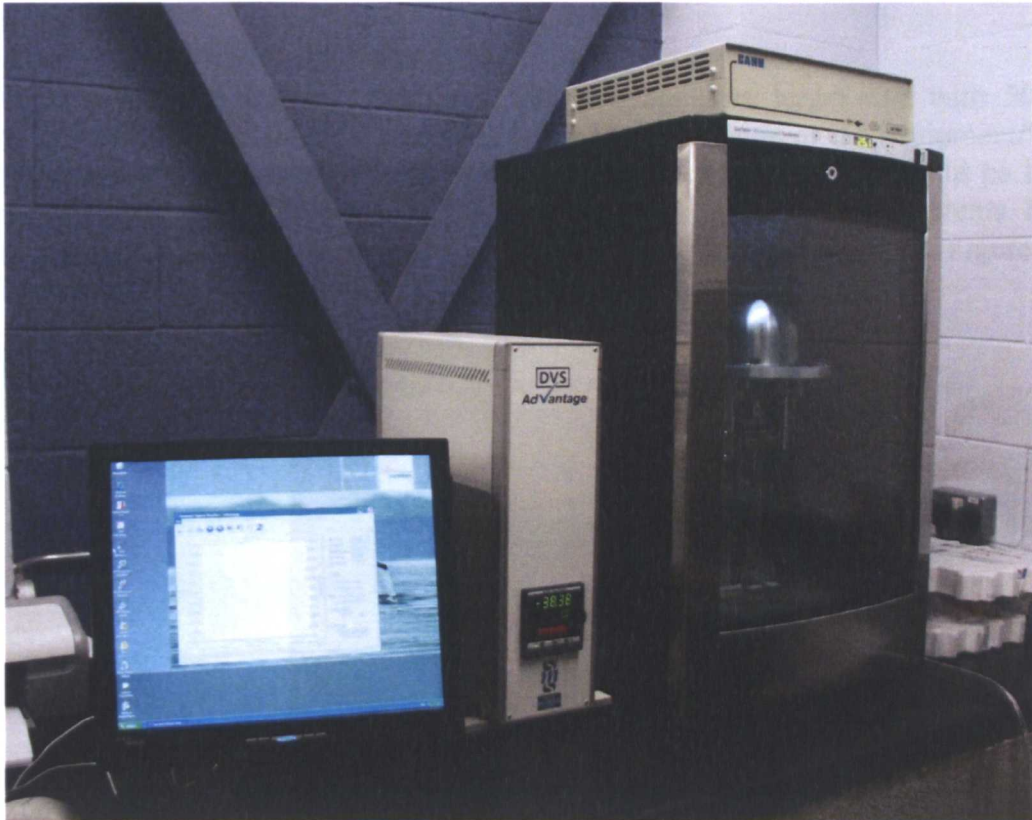


Figure C2: DVS Advantage System

Materials Required

- Substrate; aggregate sample
- Reagents with 99 percent purity (HPLC Grade):
 - Octane (Non-Polar)
 - Chloroform (Acidic character)
 - Ethyl Acetate (Basic character)

Sample Preparation

The aggregate fraction passing 5mm sieve and retaining on 2.36mm sieve is generally used for the test. Fine fraction (passing 150 μ m sieve and retaining on 75 μ m sieve) and filler (passing 75 μ m sieve) can also be used for the test.

Aggregate samples are thoroughly washed and then dried in an oven before testing with DVS. Samples are stored in glass vials as shown in Figure C3 below (left to right; Limestone, Granite and Basalt).



Figure C3: Aggregate Samples

Test procedure

The DVS system is provided with two glass bottles. The larger one with 500ml capacity is indicated as bottle A and is screwed on the left side of the equipment/DVs chamber. It is recommended that this be used for water. The bottle should be half-filled with either deionised water and should be labelled to indicate its contents. Pour the probe liquid into the smaller (250ml) Pyrex bottle/bottle B, as shown in Figure C4, until it is approximately half-full.



Figure C4: DVS; Probe Liquid Bottles

The bottles should be cleaned and they should be free of any solvents from the previous experiments. It is always good to label the bottle with the name of the solvent contained within and use one bottle for one solvent only. The bottles are then placed in the Bottle A and Bottle B position in the Advantage manifold- they should be screwed into the chosen position until hand-tight. The DVS advantage manifold with bottles on both sides is shown in Figure C5 below.

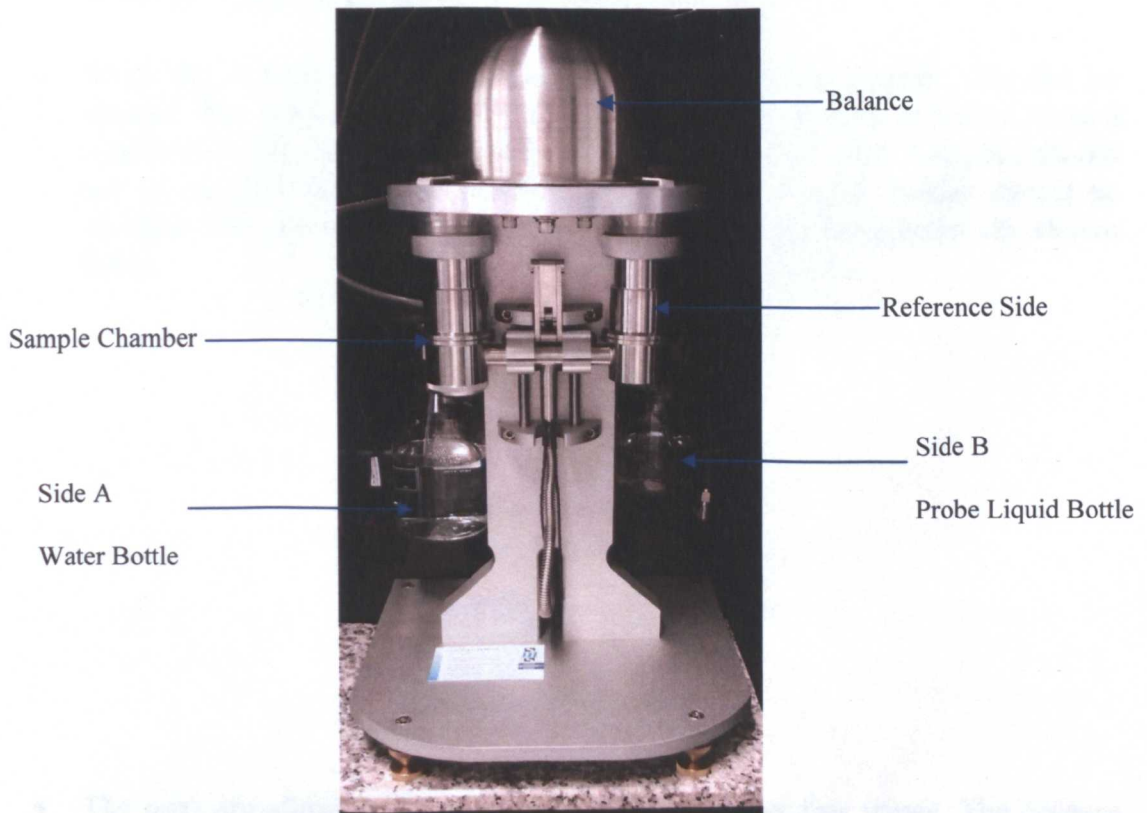


Figure C5: DVS Manifold

Always use a separate bottle for each probe liquid. Flush out any old probe vapour from the system by running the dry nitrogen through the system with an empty bottle at manifold B, before starting a new test.

The sample and reference side pans are hanged with the balance with the help of hanging wires. The DVS manifold is levelled with the help of thumb screws provided at the bottom of the manifold, as shown in Figure C6, to make sure that the hang wires do not touch the walls of the sample or reference chamber.



Figure C6: DVS Manifold; Levelling Screws

The following steps are followed in order to set-up the equipment for a test.

- Turn on the computer system.
- Check the pressure regulator on the gas cylinder for a pressure of 15Psi/1.5bar and adjust it if required. The regulator should always be set for a pressure of 1.5bar.
- Check the temperature of the environmental chamber containing the DVS manifold. It should always be set at 25°C.
- Wash the sample and the reference pans with deionised water followed by ethanol. The pans are washed by holding them with the help of forceps over a beaker and spraying the liquid with the help of a wash bottle. The pans should not be handled directly by hands at any stage. The wash bottles should be labelled with the required liquid. The bottles that are being used are shown below.



Figure C7: DVS; Wash Bottles

- The pans are allowed to dry by placing them on lint free wipes. The counter weights, if used, should also be washed every time before starting a new test.

Steel ball bearings are used as counter weights. It is recommended to use separate forceps for handling pans/weights and aggregates as shown in Figure C8 below.



Figure C8: Aggregate Sample, Reference Pan with Counter weights and Forceps

- The solvent bottle is filled with the required probe liquid and screwed into the manifold B as shown below.

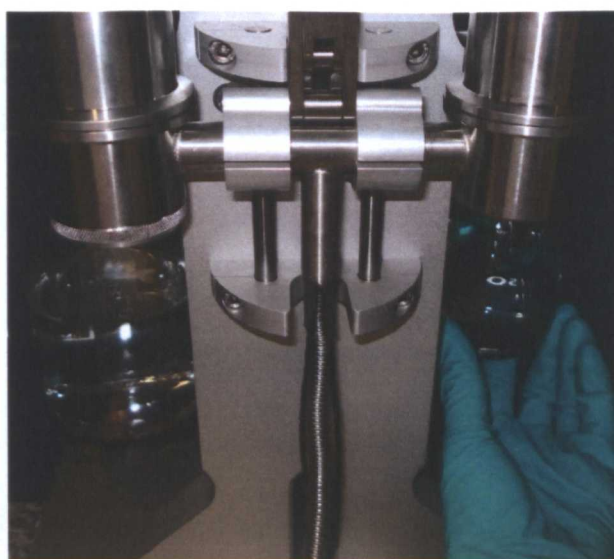


Figure C9: Attaching the Probe Liquid Bottle

- The other manifold which is not in use should not be left empty. It is recommended to be attached with an empty bottle.

In order to run an automated experiment, following main steps are followed:

- Double click the DVS Advantage control software icon on the desktop, as shown in Figure C10, to open the software.

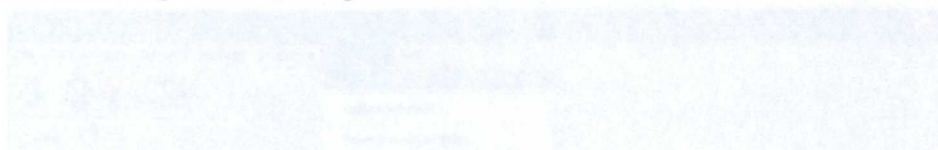


Figure C10: DVS Advantage control software icon on the desktop



Figure C10: DVS Control Software Icon

- First of all go to the diagnostic panel, shown in Figure C11, by clicking the diagnostic tab at the bottom of the main software window. The clean mirror value (CMV) should read about 120. If it is more than that, then the dew point analyser (DPA) sensor is required to be cleaned.

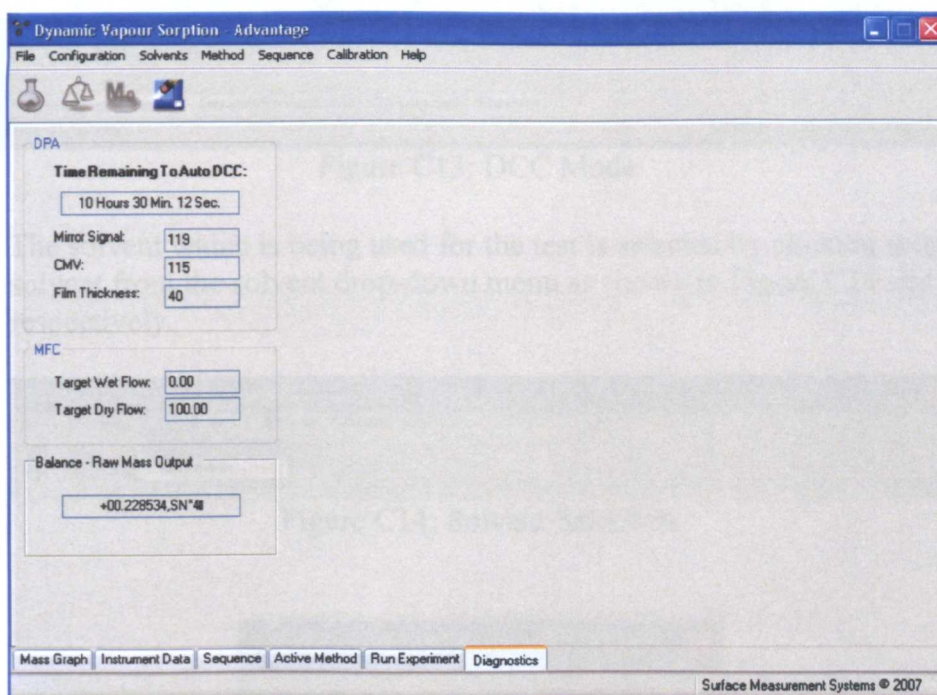


Figure C11: DVS Control Software; Diagnostic Panel

- The DPA sensor can be cleaned by selecting decontaminate optical sensor option from the calibration drop-down menu as shown in Figure C12 below.

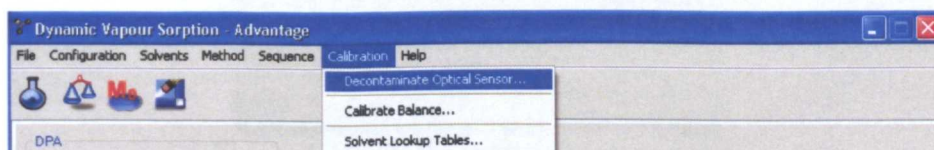


Figure C12: Decontamination of Optical Sensor

- The system automatically cleans the sensor and the CMV value goes down to about 120. During this dynamic decontamination control (DCC) process the system goes into a hold mode for about five minutes. It can be seen by looking into the instrument data panel, as the indicators for DCC mode and hold mode lights up as shown in Figure C13. At the end of a DCC cycle the measuring indicator lights-up and the system goes back into the ready or save data mode.

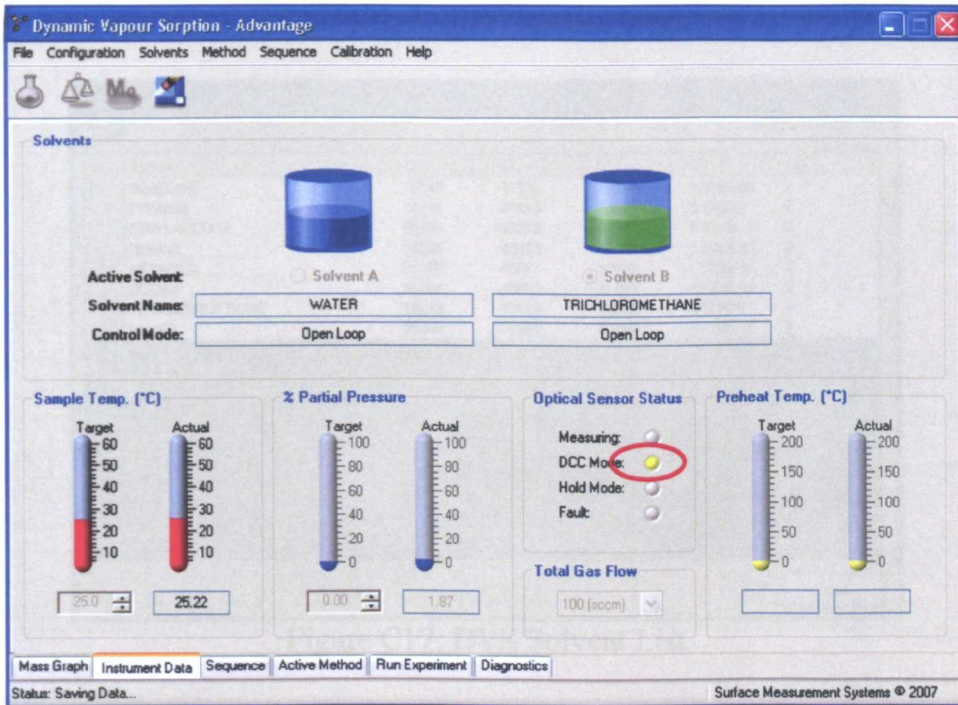


Figure C13: DCC Mode

- The solvent which is being used for the test is selected by clicking select solvent from the solvent drop-down menu as shown in Figure C14 and C15 respectively.

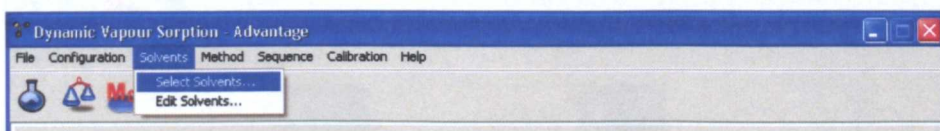


Figure C14: Solvent Selection

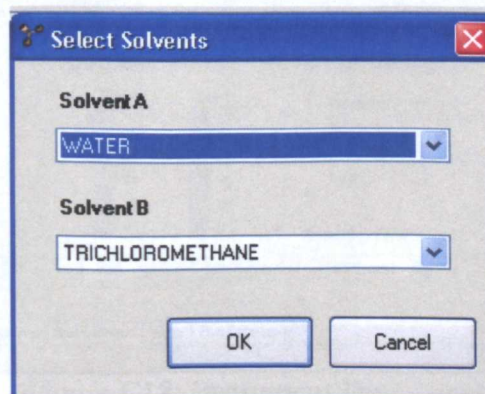


Figure C15: DVS; Select Solvents Menu

- If the required solvent is not in the list, a new solvent can be added through edit solvent menu, as shown in Figure C16, and filling-in the required constants for that solvent in the solvent list window shown in Figure C17.

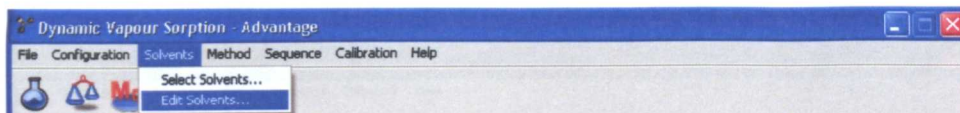


Figure C16: Edit Solvent Menu

Solvent	C1	C2	C3	C4	C5
DODECANE	137.47	-11976	-16.698	8.0906E-06	2
ETHANOL	74.475	-7164.3	-7.327	3.134E-06	2
ETHYL ACETATE	66.824	-6227.6	-6.41	1.7914E-17	6
HEXANE	104.65	-6995.5	-12.702	1.2381E-05	2
METHANOL	81.768	-6876	-8.7078	7.1926E-06	2
OCTANE	96.084	-7900.2	-11.003	7.1802E-06	2
TRICHLOROMETHANE	146.43	-7792.3	-20.614	0.024578	1
WATER	73.649	-7258.2	-7.3037	4.1653E-06	2

Figure C17: DVS Solvent List

- Once the solvents have been added the manifold containing the solvent which is going to be used for the test is selected from the instrument data panel shown below.

The Instrument Data Panel displays the following information:

- Solvents:** Two solvent reservoirs are shown. Solvent A is selected (radio button checked) and contains 'WATER'. Solvent B is unselected and also contains 'WATER'. Both are in 'Closed Loop' control mode.
- Sample Temp. (°C):** Target is 25.0, Actual is 25.00.
- % Partial Pressure:** Target is 0.00, Actual is 0.00.
- Optical Sensor Status:** Measuring (green dot), DCC Mode (grey dot), Hold Mode (grey dot), Fault (grey dot).
- Preheat Temp. (°C):** Target and Actual fields are empty.
- Total Gas Flow:** Set to 200 (sccm).

At the bottom, there are tabs for 'Mass Graph', 'Instrument Data', 'Sequence', 'Active Method', 'Video', and 'Run Experiment'. The status is 'Ready...' and the copyright is 'Surface Measurement Systems © 2007'.

Figure C18: Instrument Data Panel

- Input the experiment details onto the Run Experiment panel, as shown in Figure C19. These include Sample Name, Sample Description, and the Output directory. This provides useful information for later analysis of the DVS data.

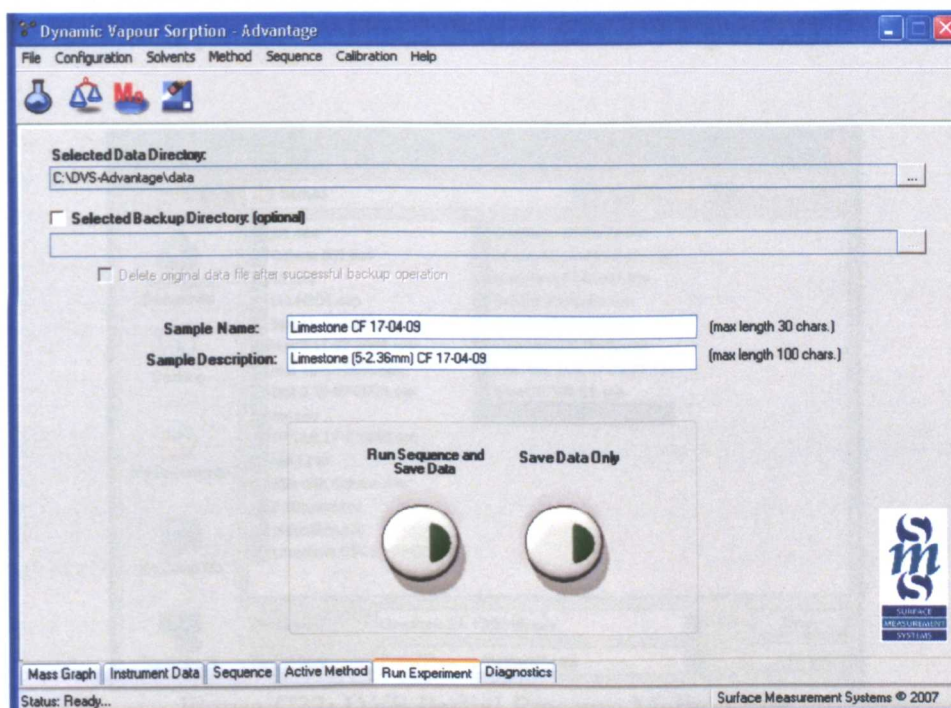


Figure C19: The DVS Control Software, Run Experiment Panel

- Create any DVS Methods to be used via the New Method menu item that is located on the Method menu as shown in Figure C20. Click the New Method option to call up the New Method Setup window as shown in Figure C21.

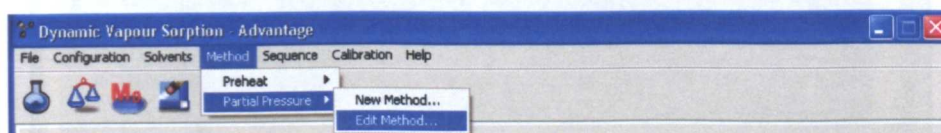


Figure C20: Method Menu Selection

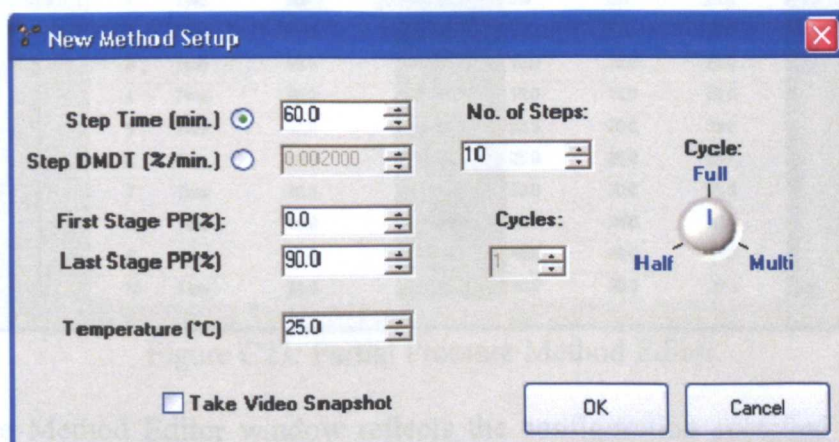


Figure C21: The New Method Setup Window

- The New Method Setup window provides an efficient way of selecting the initial configuration of the new Partial Pressure Method. An already created method can also be selected from the method file shown in Figure C22 by choosing the edit method option from the method drop-down menu. Once the Partial Pressure configuration has been specified, click the OK button to call up the Partial pressure Method Editor as shown in Figure C23.

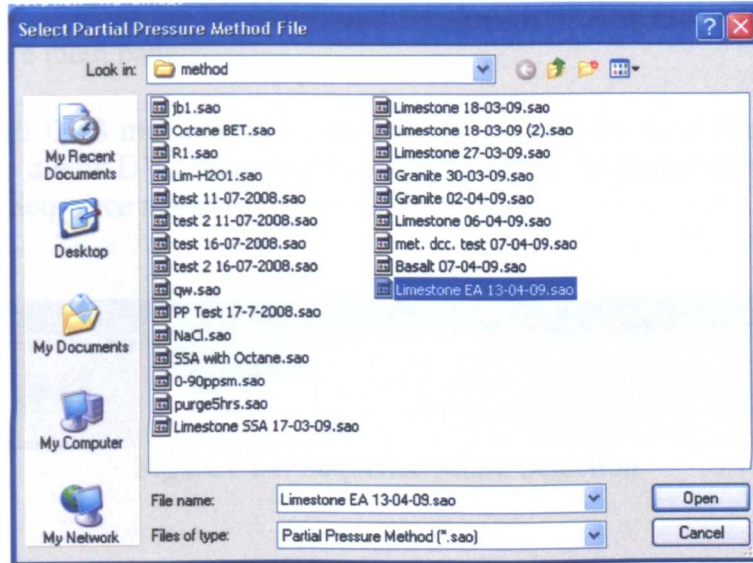


Figure C22: DVS Partial Pressure Method File

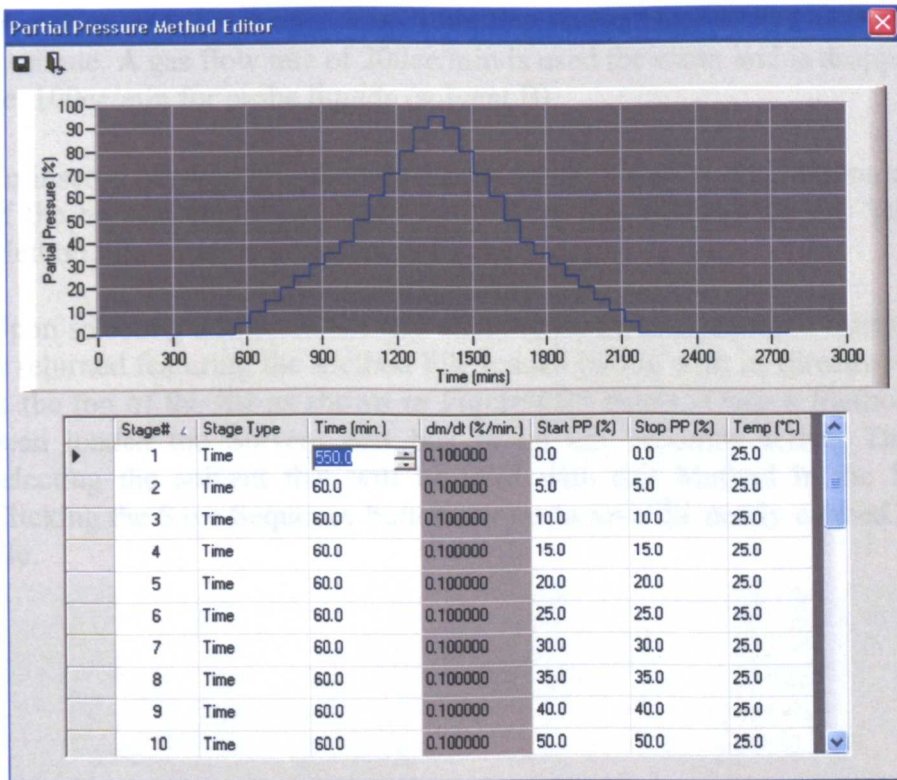


Figure C23: Partial Pressure Method Editor

The Method Editor window reflects the configuration specified in the New Method Setup panel. It features a graph and grid which show the details of the

experiment. The Partial Pressure Method may be edited using the grid. In the stage type select time and dry the material as much as required.

After performing any of the operations described above, the graph at the top of the Method Editor window immediately reflects the alterations to the Method. Clicking the Save Method button allows to save the newly created Method file. By default, the software immediately goes to the directory specified in the Preferences option. Upon specifying the Method name, clicking Save will save the file and close the Method Editor window, returning to the DVS Advantage Software main panel.

- Once all DVS methods to be used in the experiment have been created, add them to a new DVS Sequence by using the New Sequence menu item located on the Sequence menu as shown in Figure C24.

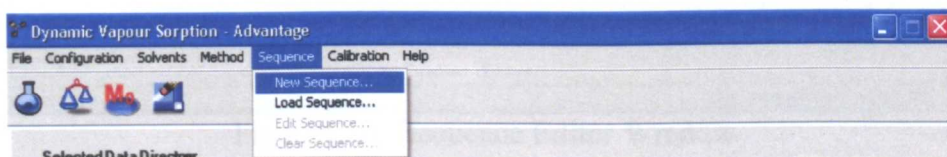


Figure C24: Sequence Menu Selection

The Sequence Editor allows loading the Methods that are to be run and also configure that which solvent is to be used for each particular Method. The control mode is set at open loop, sampling rate at 1second and save data rate at 1 minute. A gas flow rate of 200cc/min is used for water and is dropped to half i.e. 100cc/min for probe liquids (solvent B).

- To insert a Method into the new Sequence the Load Method button at the end of the highest empty box must be clicked, this will call up the Select DVS Method File window as shown in Figure C22.

Upon selecting a Method file and clicking Open, the Sequence Editor window is returned featuring the Method File loaded (along with its directory location) at the top of the list as shown in Figure C25 below. Once a Method file has been loaded the Solvent edit box to its left becomes active. This allows selecting the solvent that will be used with this Method in the Sequence. Clicking the Save Sequence button allows to save the newly created Sequence file.



Figure C22: Selecting the Sample's Solvent

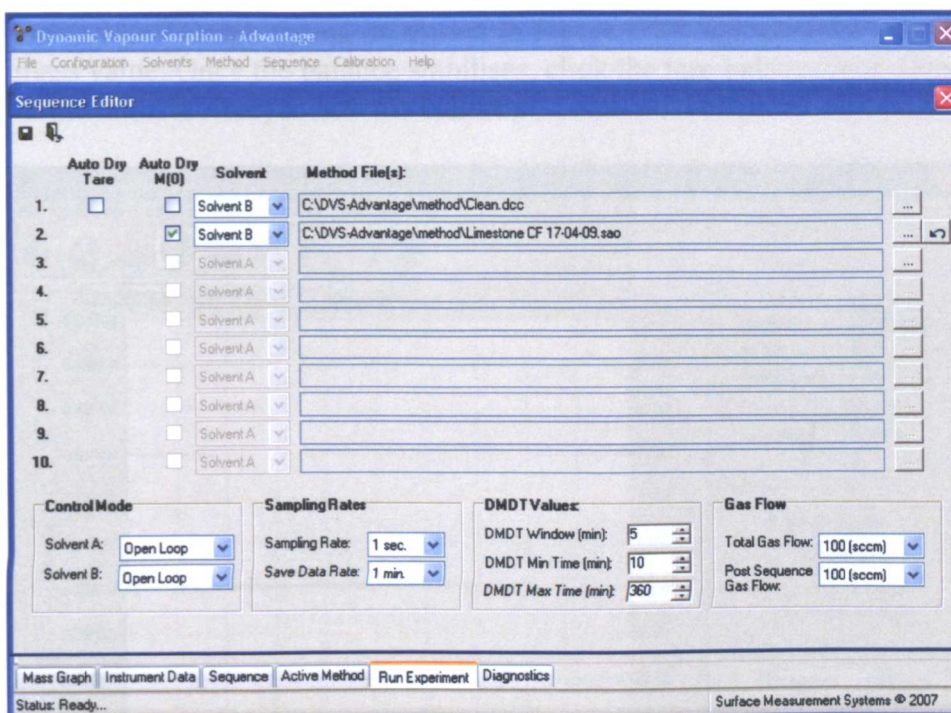


Figure C25: Sequence Editor Window

- Go to the sequence drop down menu in the menu bar and click Load sequence in order to load already saved sequence. Once a DVS sequence is loaded the experiment may be commenced.
- Carefully hang the cleaned sample and reference pans in the respective chambers with the help of a forceps as shown below.



Figure C26: Handling the Pans

- Allow the pans to settle and then close the chamber as shown in Figure C27.



Figure C27: Securing the Sample Chamber

- Go to Mass Graph menu, as shown in Figure C28, and observe the displayed mass value. Once the balance stabilises, click the tare balance icon (second left in the main toolbar) to tare the balance.

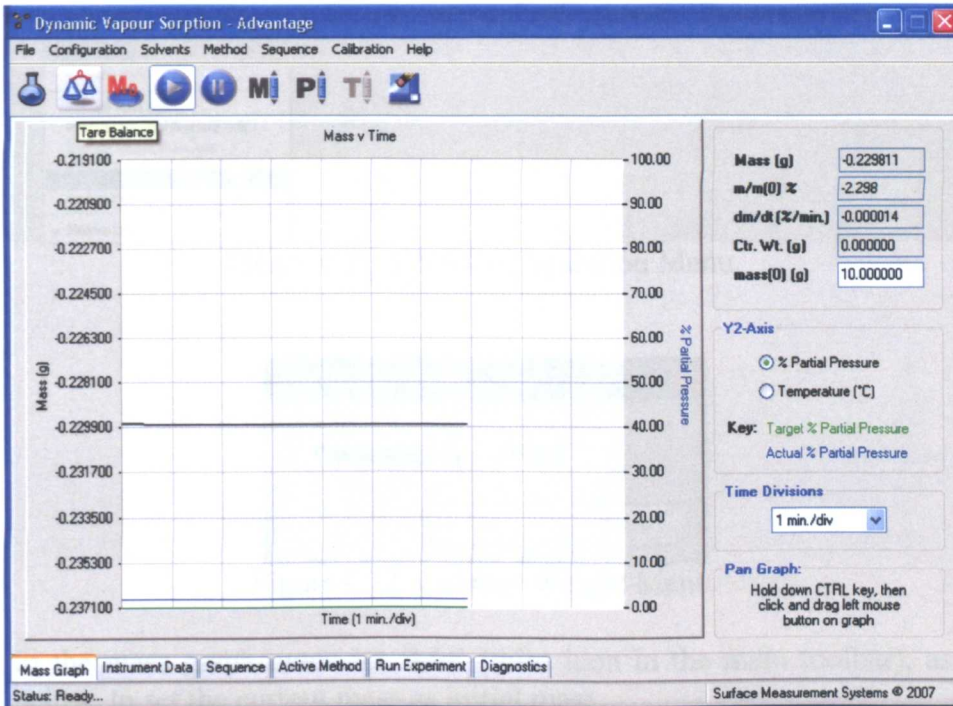


Figure C28: The DVS Control Software Mass Graph Panel

- Software asks for confirmation as shown in Figure C29. Click 'yes'.

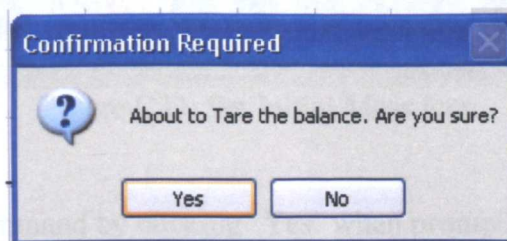


Figure C29: Balance Tare

- Now, take out the pans and add the required amount of aggregate sample (normally 2 to 3 grams of sample is used) and counter weight/steel ball bearings in the respective pans. Carefully hang them back on the stirrups/hang wires, as shown below, and close the camber.



Figure C30: Placing the Sample in the Manifold

- In the configuration menu select counter weight, as shown in Figure C31, and add the weight of the steel ball bearings in the required field as shown in Figure C32.

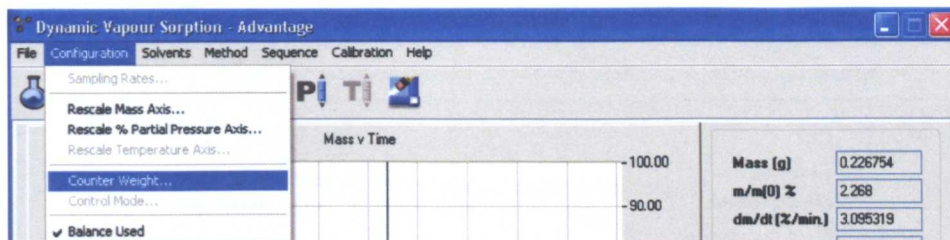


Figure C31: DVS Configuration Menu

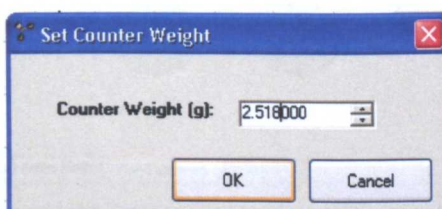


Figure C32: Counter Weight Menu

- In the mass graph menu hit 'Mo' (third icon in the main toolbar), as shown below, to set the current mass as initial mass.

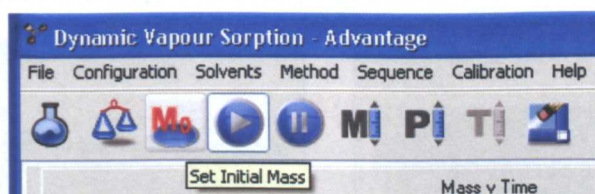


Figure C33: Set Initial Mass Icon

- Confirm the command by clicking 'Yes' when prompted as shown below.

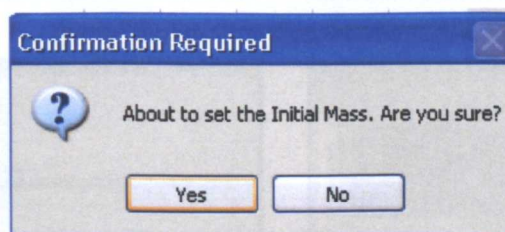


Figure C34: Setting the Initial Mass

- Select the Run Experiment panel and then click the Run Sequence and Save data button shown in Figure C35.

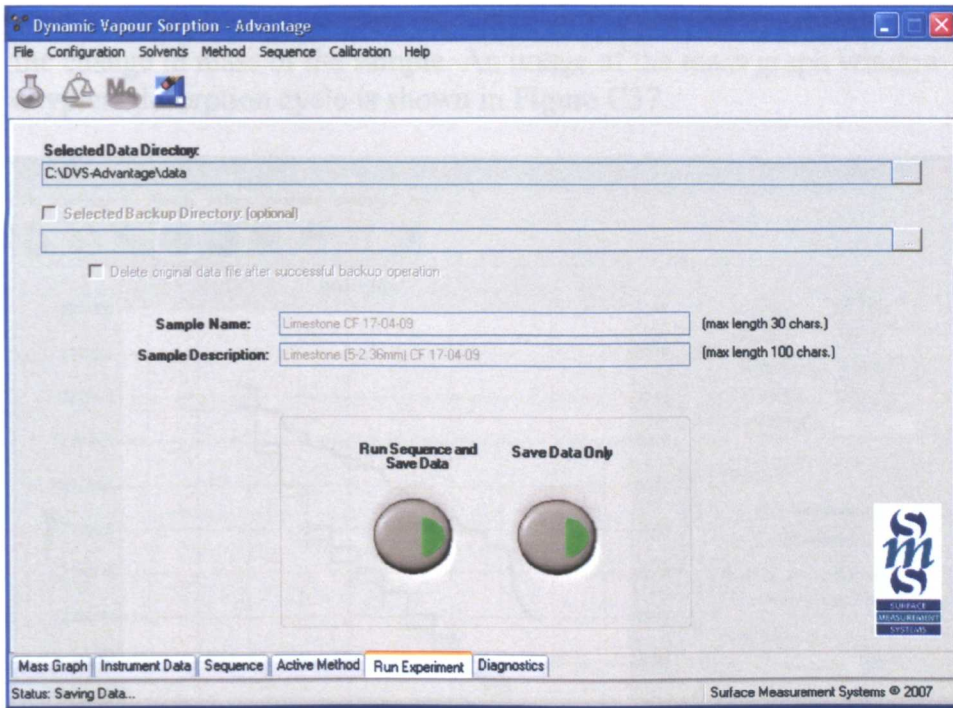
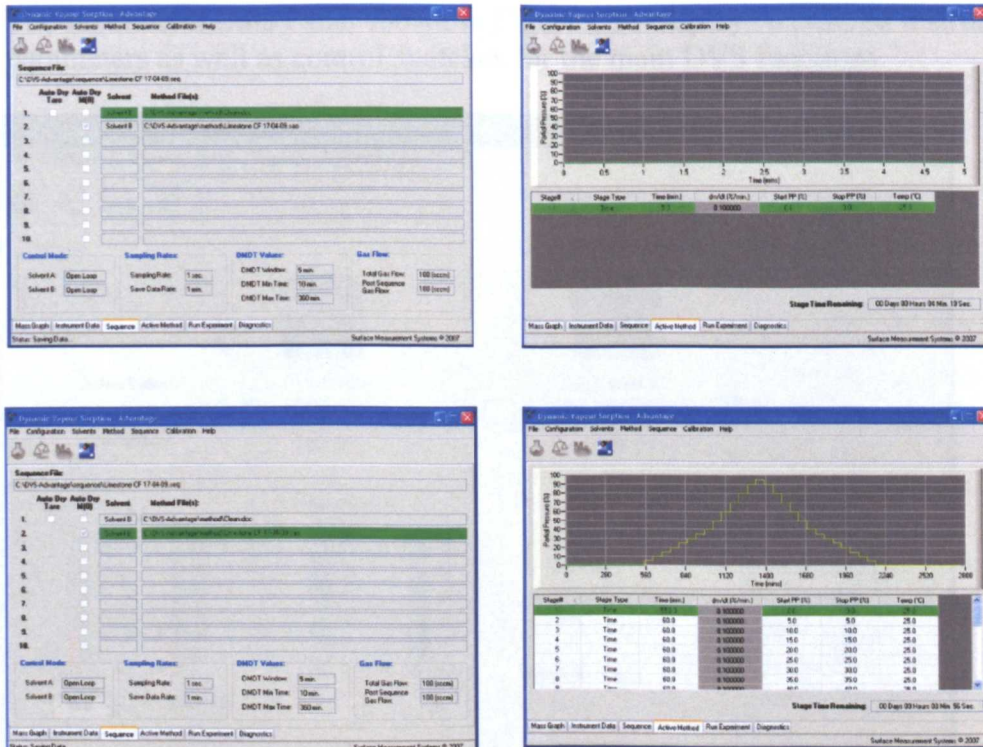


Figure C35: Run Sequence and Save Data Button

- The DVS Advantage will instantly start sequentially running the Methods contained in the active DVS Sequence, as shown in Figure C36, and saving the DVS data to the output directory specified.



- The mass graph window plots the actual and target partial pressure along with the change in mass of the sample. An image of the mass graph window during a typical desorption cycle is shown in Figure C37.

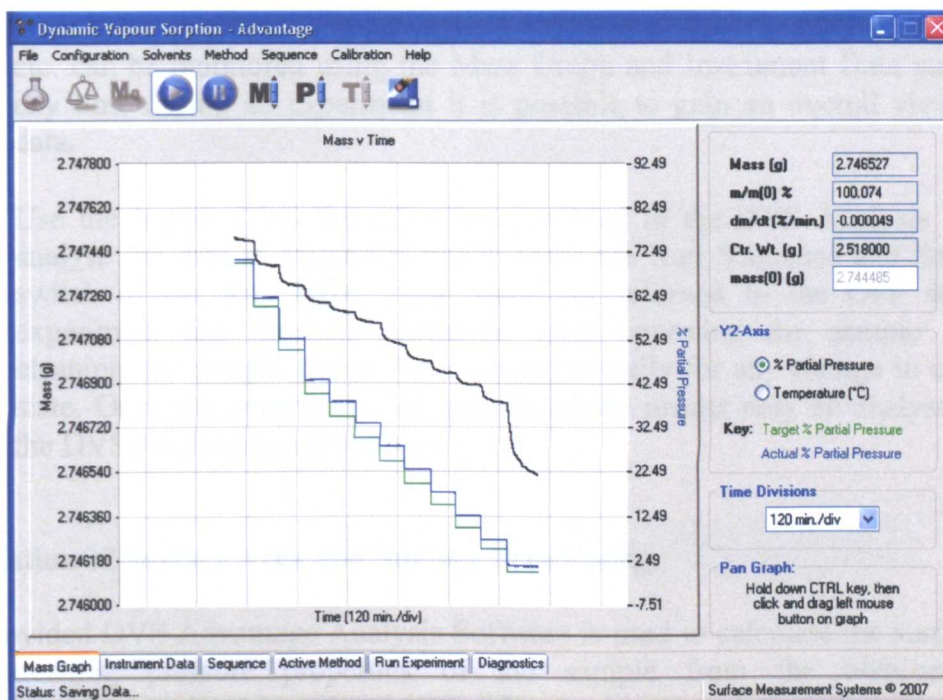


Figure C37: Mass Graph window; Desorption Cycle

- The Instrument Data Panel shown in Figure C38 displays measured instrument parameters as well as control switches for the main DVS functions.

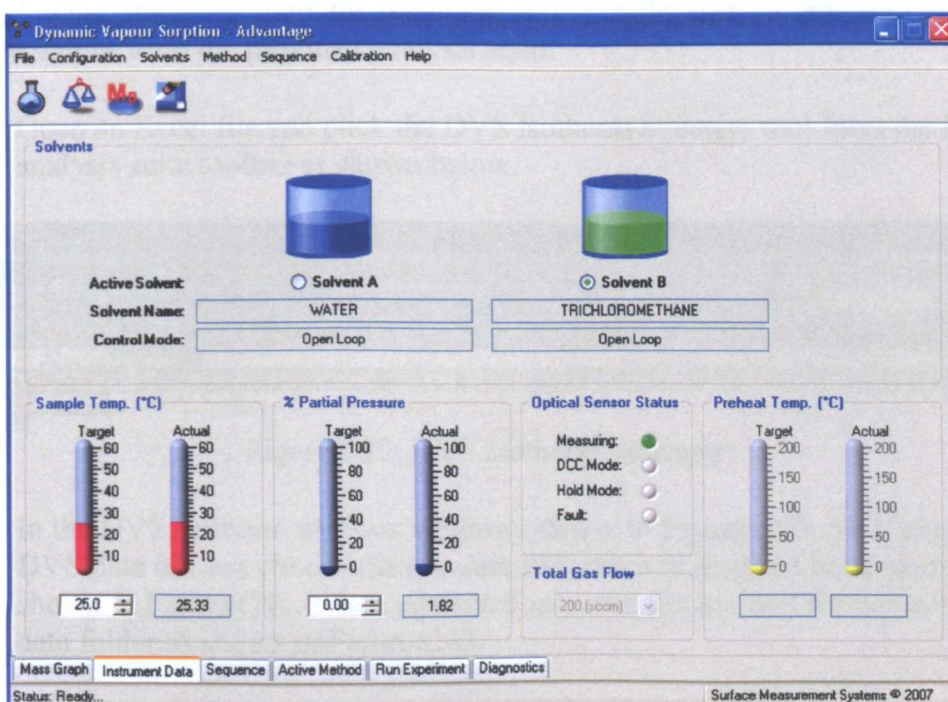


Figure C38: The DVS Control Software, Instrument Data Panel

When a Sequence is running, the Instrument Data panel serves only as a display of the system's parameters, none of the parameters it indicates may be

altered. However, if there is no Sequence running, then the Instrument Data panel may be used to input set-points for almost all of the system parameters displayed.

Once the experiment is in progress, the change in mass, humidity, Stage time, etc. can be monitored using the Mass Graph and Instrument Data panels. At any time during an experiment it is possible to gain an overall view of the data.

- Use the Import DVS Data function provided in the DVS Analysis Suite to analyse the data in Microsoft Excel. Once the Run Sequence and Save Data switch of the Run Experiment panel has returned to the OFF state, the experiment has finished. However, after removing the sample pan for cleaning, the sample should be inspected visually for any change in colour or state. Once the experiment has completed the results may be analysed using the DVS Analysis Suite software.

Calculation of Surface Area and Surface Free Energy

The provided DVS Advantage Analysis Software is used to calculate the surface area and spreading pressure properties of the sample from the obtained mass change/sorption results, when tested with different vapour probes. The surface energy parameters are then calculated from the obtained surface area and spreading pressure values. The complete calculation procedure is provided in the earlier part of this report.

The following steps are used for obtaining the specific surface area and spreading pressure values from the provided analysis suite.

- Open an Excel file and click the DVS isotherm manager tool from the DVS analysis suite toolbar as shown below.

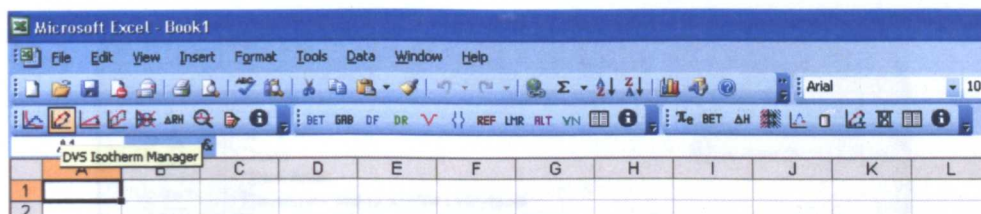


Figure C39: DVS Isotherm Manager

- In the DVS isotherm analysis window, shown in Figure C40, click import DVS data tab and choose the test data file which is required to be analysed as shown in Figure C41. When prompted save the file in excel format in the DVS data folder as shown in Figure C42.

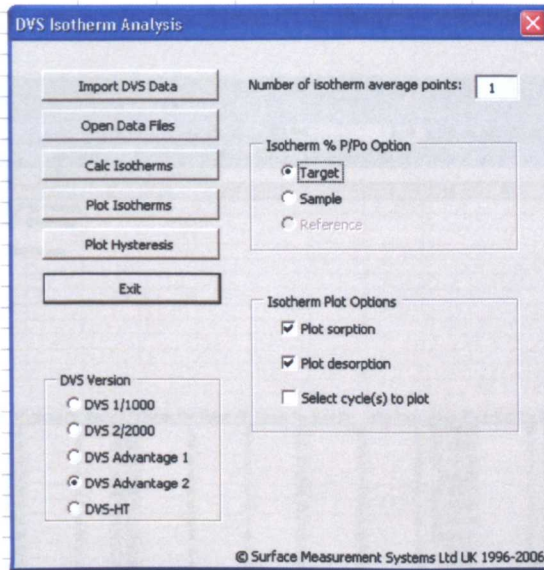


Figure C40: DVS Isotherm Analysis Window

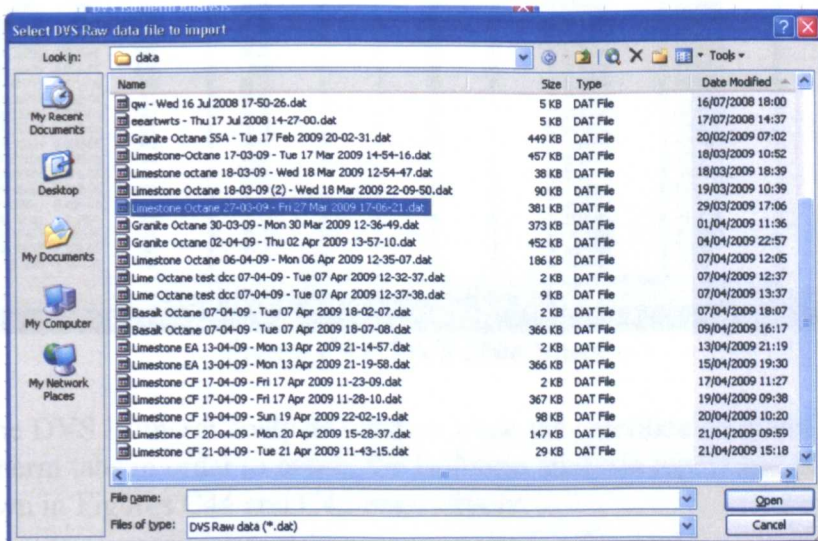


Figure C41: DVS Raw Data

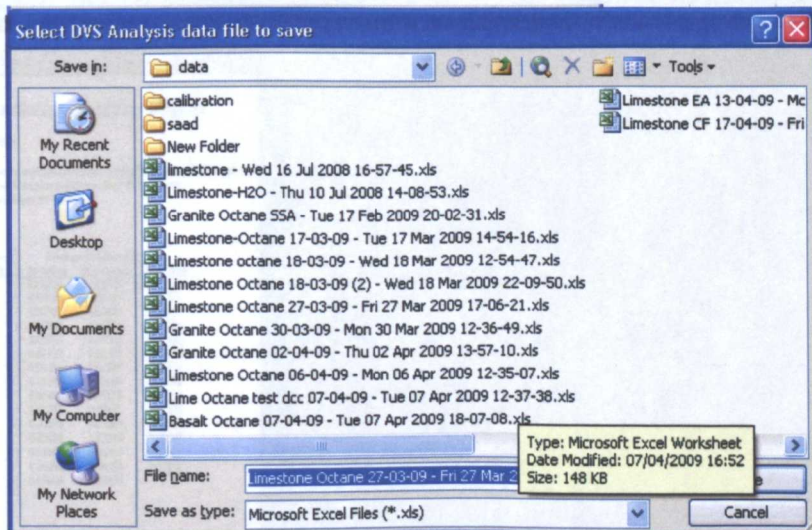


Figure C42: DVS Analysed Data Folder

- The selected file opens in the form of a sheet as shown below.

DVS WINDOWS DATA FILE - VERSION 4.02 (DVS 2/Advantage)

1 DVS WIN DVS DATA FILE - VERSION 4.02 (DVS 2/Advantage) 2861 16
 2 Sequence C:\DVS-Advantage\sequence\Limestone 27-03-09.seq 16 617
 3 Sequence Fri Mar 27 16:00:09 2009
 4 Method File C:\DVS-Advantage\method\Limestone 27-03-09.seq
 5 Method File Fri Mar 27 15:55:58 2009
 6 Sample No Limestone Octane 27-03-09
 7 Sample W 2.730276
 8 Sample D Limestone (2.36-5mm) Octane 27-03-09
 9 Raw Data Fri Mar 27 17:06:21 2009
 10 Author User
 11 Data Sawin 60
 12 Control Mc Open
 13 Solvent B: OCTANE
 14 Solvent A

Time (min)	Mass	dm	dm/dt	Actual PP	Actual PP	Sample Tg	Target P	Target PP	Target Tg	Sine RH	Sine Freq	Actual P	Actual Dry dm (%)	d	User Defn	User Defn	Reserved	Target PP	Ac
0.01	2.73027	99.99978	7.158268	0.6	0	26.05	5	0	25	0	0	23.78933	0	0.007765	0	0	0	0	0
1.01	2.730267	99.99967	-0.00029	0.6	0	25.93	5	0	25	0	0	23.76821	0	0.007656	0	0	0	0	0
2.01	2.730267	99.99967	-0.00024	0.62	0	25.8	5	0	25	0	0	23.76128	0	0.007656	0	0	0	0	0
3.01	2.730258	99.99934	-0.00021	0.59	0	25.69	5	0	25	0	0	23.8229	0	0.007326	0	0	0	0	0
4.01	2.730249	99.99901	-0.0002	0.59	0	25.59	5	0	25	0	0	23.83043	0	0.006986	0	0	0	0	0
5.01	2.730246	99.9989	-0.00021	0.59	0	25.5	5	0	25	0	0	23.83449	0	0.006886	0	0	0	0	0
6.01	2.73024	99.99868	-0.00023	0.58	0	25.43	5	0	25	0	0	23.76733	0	0.006686	0	0	0	0	0
7.01	2.730237	99.99857	-0.00021	0.59	0	25.38	5	0	25	0	0	23.86421	0	0.006657	0	0	0	0	0
8.01	2.730231	99.99835	-0.00017	0.59	0	25.33	5	0	25	0	0	23.861	0	0.006337	0	0	0	0	0
9.01	2.730228	99.99824	-0.00015	0.58	0	25.29	5	0	25	0	0	23.8684	0	0.006227	0	0	0	0	0
10.01	2.730221	99.99799	-0.00014	0.59	0	25.27	5	0	25	0	0	23.87764	0	0.005971	0	0	0	0	0
11.01	2.73022	99.99796	-0.00015	0.61	0	25.25	5	0	25	0	0	23.89558	0	0.005934	0	0	0	0	0
12.01	2.730219	99.99791	-0.00014	0.6	0	25.24	5	0	25	0	0	23.84892	0	0.005897	0	0	0	0	0
13.01	2.73021	99.99758	-0.00013	0.59	0	25.26	5	0	25	0	0	23.86214	0	0.005658	0	0	0	0	0
14.01	2.73021	99.99758	-0.00014	0.59	0	25.26	5	0	25	0	0	23.9352	0	0.005658	0	0	0	0	0
15.01	2.73021	99.99758	-0.00011	0.6	0	25.25	5	0	25	0	0	23.91991	0	0.005658	0	0	0	0	0
16.01	2.730204	99.99736	-0.00011	0.59	0	25.24	5	0	25	0	0	23.90465	0	0.005348	0	0	0	0	0
17.01	2.730203	99.99733	-0.0001	0.6	0	25.23	5	0	25	0	0	23.90985	0	0.005311	0	0	0	0	0
18.01	2.730201	99.99725	-7.55E-05	0.61	0	25.22	5	0	25	0	0	23.89457	0	0.005238	0	0	0	0	0
19.01	2.7302	99.99722	-8.61E-05	0.59	0	25.2	5	0	25	0	0	23.84892	0	0.005201	0	0	0	0	0
20.01	2.730197	99.99711	-7.47E-05	0.6	0	25.17	5	0	25	0	0	23.84975	0	0.005091	0	0	0	0	0
21.01	2.730196	99.99707	-6.48E-05	0.6	0	25.16	5	0	25	0	0	23.90011	0	0.005055	0	0	0	0	0
22.01	2.730195	99.99703	-6.39E-05	0.61	0	25.15	5	0	25	0	0	23.81433	0	0.005018	0	0	0	0	0
23.01	2.730195	99.99703	-4.80E-05	0.6	0	25.16	5	0	25	0	0	23.83632	0	0.005018	0	0	0	0	0
24.01	2.730191	99.99689	-5.86E-05	0.6	0	25.17	5	0	25	0	0	23.80321	0	0.004872	0	0	0	0	0
25.01	2.730187	99.99674	-7.27E-05	0.6	0	25.17	5	0	25	0	0	23.89441	0	0.004725	0	0	0	0	0
26.01	2.730187	99.99674	-8.67E-05	0.61	0	25.18	5	0	25	0	0	23.88971	0	0.004725	0	0	0	0	0
27.01	2.730183	99.99659	-8.74E-05	0.61	0	25.18	5	0	25	0	0	23.9263	0	0.004579	0	0	0	0	0
28.01	2.730178	99.99641	-9.43E-05	0.62	0	25.19	5	0	25	0	0	23.84874	0	0.004386	0	0	0	0	0
29.01	2.730178	99.99641	-0.0001	0.6	0	25.18	5	0	25	0	0	23.90784	0	0.004386	0	0	0	0	0
30.01	2.730178	99.99641	-9.30E-05	0.6	0	25.16	5	0	25	0	0	23.8684	0	0.004386	0	0	0	0	0
31.01	2.730177	99.99637	-7.36E-05	0.61	0	25.17	5	0	25	0	0	23.85195	0	0.004359	0	0	0	0	0
32.01	2.730175	99.9963	-3.76E-05	0.59	0	25.17	5	0	25	0	0	23.88146	0	0.004266	0	0	0	0	0

Figure C43: DVS Data Sheet

- In the DVS isotherm analysis window click the calculate isotherm and plot isotherm tabs in order to obtain the isotherm analysis report and plotted data as shown in Figures C44 and C45 respectively.

DVS Isotherm Analysis Report

Date: 27 Mar 2009
 Time: 5:06 PM
 File: C:\Documents and Settings\User\Desktop\Images\Ravil Analysis images\Limestone Octane test.xls
 Meth: C:\DVS-Advantage\method\Limestone 27-03-09.seq
 Sample: Limestone Octane 27-03-09
 Temp: 25.1 °C
 M(0): 2.730276

Sample % PPs	Change in Mass (%) - dry	
	Sorption	Description Hysteresis
0.6	0.00000	0.00128
3.5	0.00524	0.00663 0.00139
9.5	0.00711	0.00824 0.00114
14.5	0.00883	0.01004 0.00121
19.5	0.01004	0.01245 0.00242
25.0	0.01132	0.01425 0.00293
30.5	0.01253	0.01557 0.00304
35.5	0.01366	0.01689 0.00322
40.5	0.01483	0.01839 0.00355
46.5	0.01773	0.02172 0.00399
57.5	0.02095	0.02622 0.00527
70.2	0.02696	0.03333 0.00637
80.0	0.03601	0.04414 0.00813
89.3	0.05425	0.06256 0.00831
94.4	0.07656	0.07656

DVS - The Sorption Solution © Surface Measurement Systems Ltd UK 9998-2008

Figure C44: Isotherm analysis Report

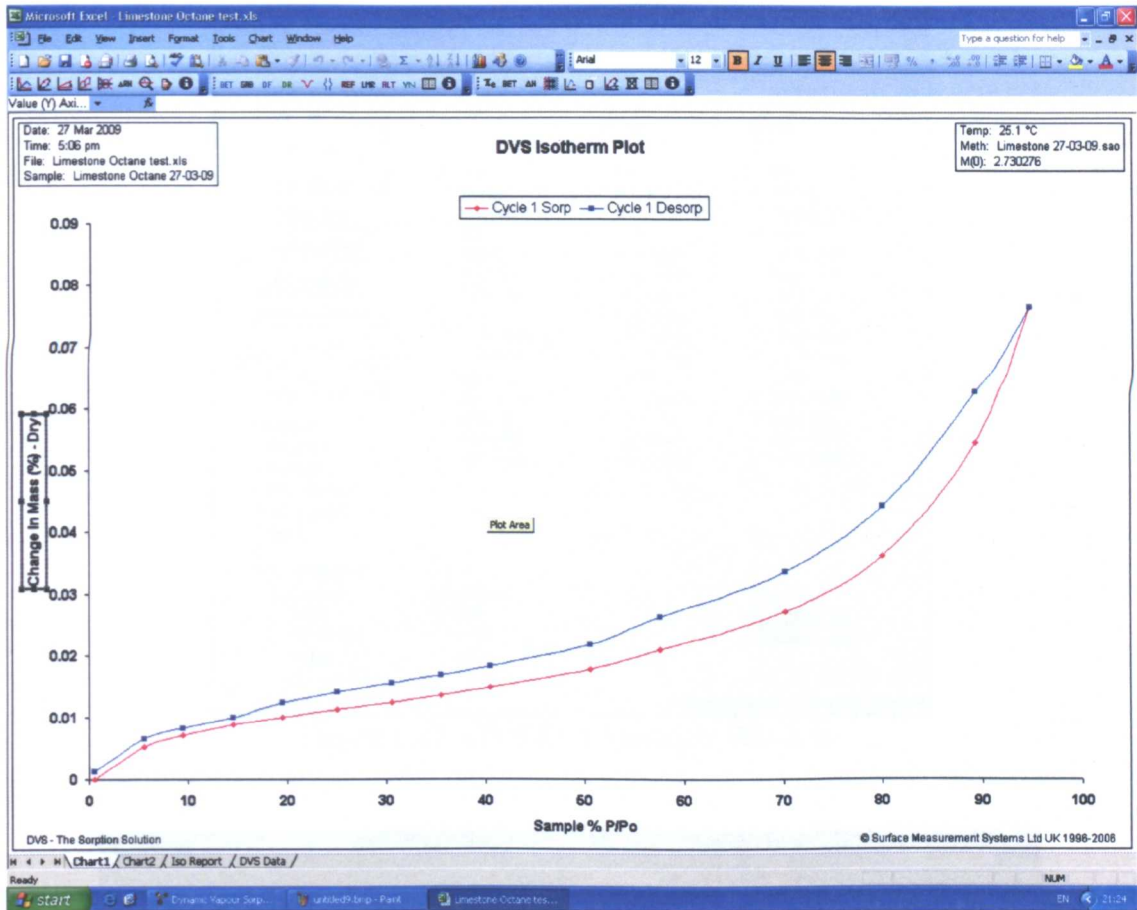


Figure C45: Typical Isotherm Plot

- Now click the DVS plot manager tab from the analysis suite toolbar, as shown in Figure C46, to open the DVS plot manager window.

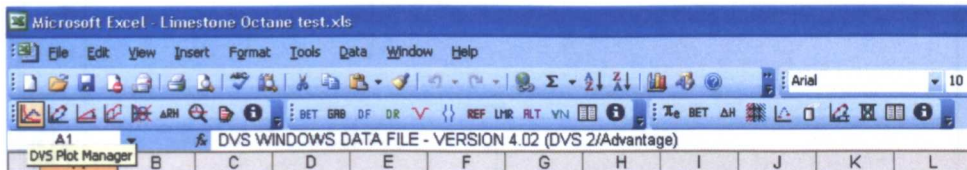


Figure C46: DVS Plot Manager

- The DVS plot manager, shown in Figure C47, is used to plot all the available data. All the tabs on the left side of the window can be used to obtain plots for different combinations of data.

A custom plot can also be obtained by selecting the required data from the window and selecting custom plot tab.

The DVS partial pressure and the mass plots are shown in Figure C48 and C49 respectively.

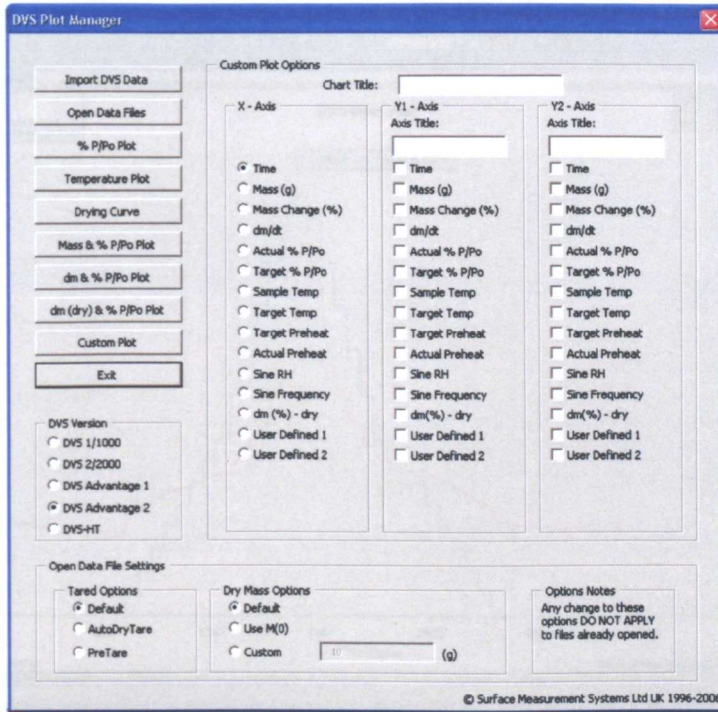


Figure C47: DVS Plot Manager Window

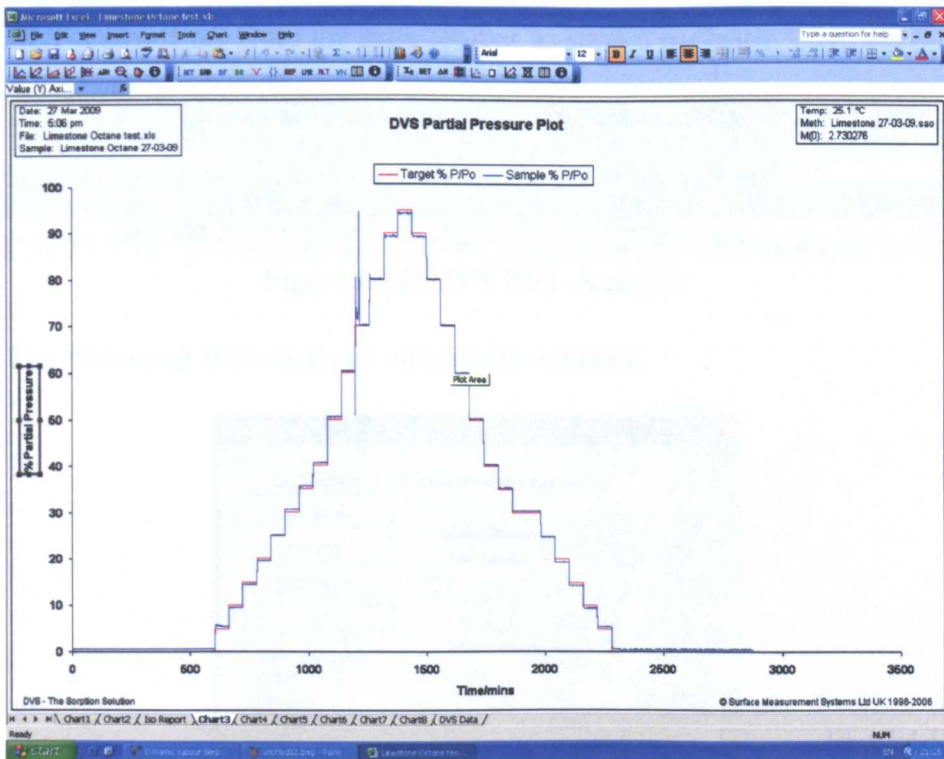


Figure C48: DVS Partial Pressure Plot

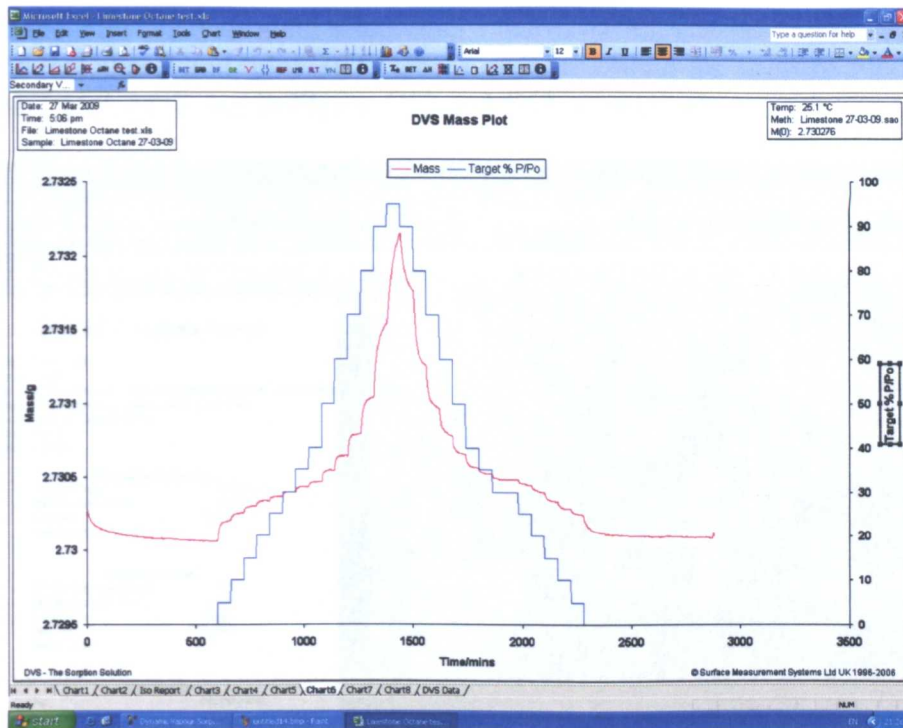


Figure C49: DVS Mass Plot

- The specific surface area of the tested material is calculated by selecting the BET analysis tab from the suite toolbar as shown in Figure C50 below.

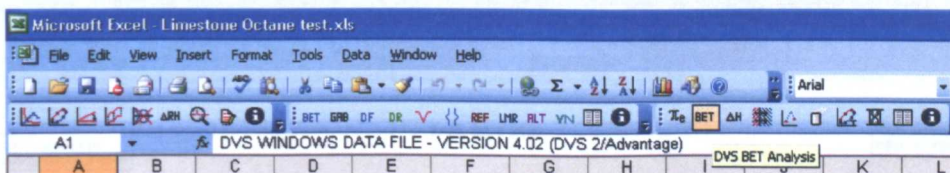


Figure C50: DVS BET Analysis

- The following BET analysis window is obtained.

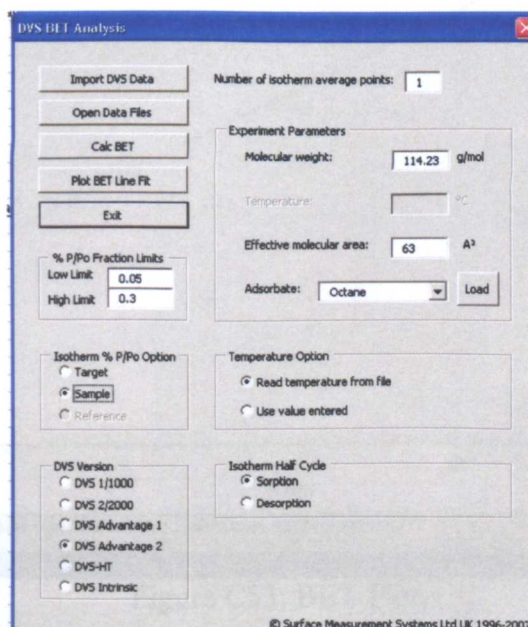


Figure C51: BET Analysis Suite

- In the BET analysis suite select the isotherm partial pressure option and click the ‘calculate’ and ‘plot BET’ tabs in order to obtain the analysis report and BET plot, as shown in Figure C52 and C53 respectively.

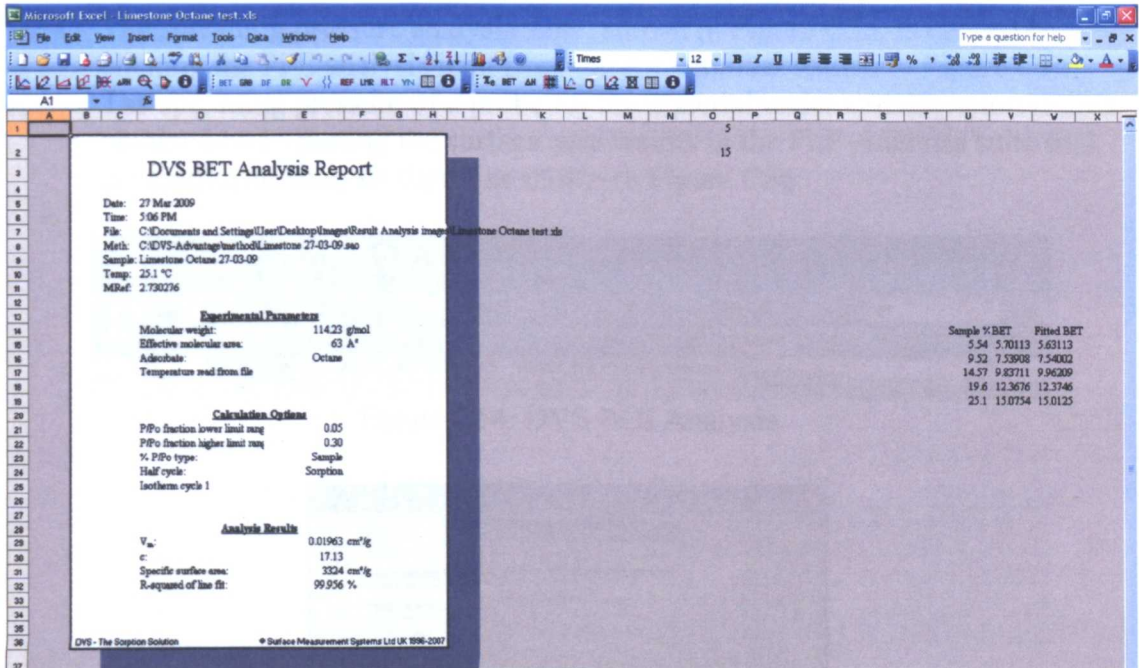


Figure C52: BET Analysis Report

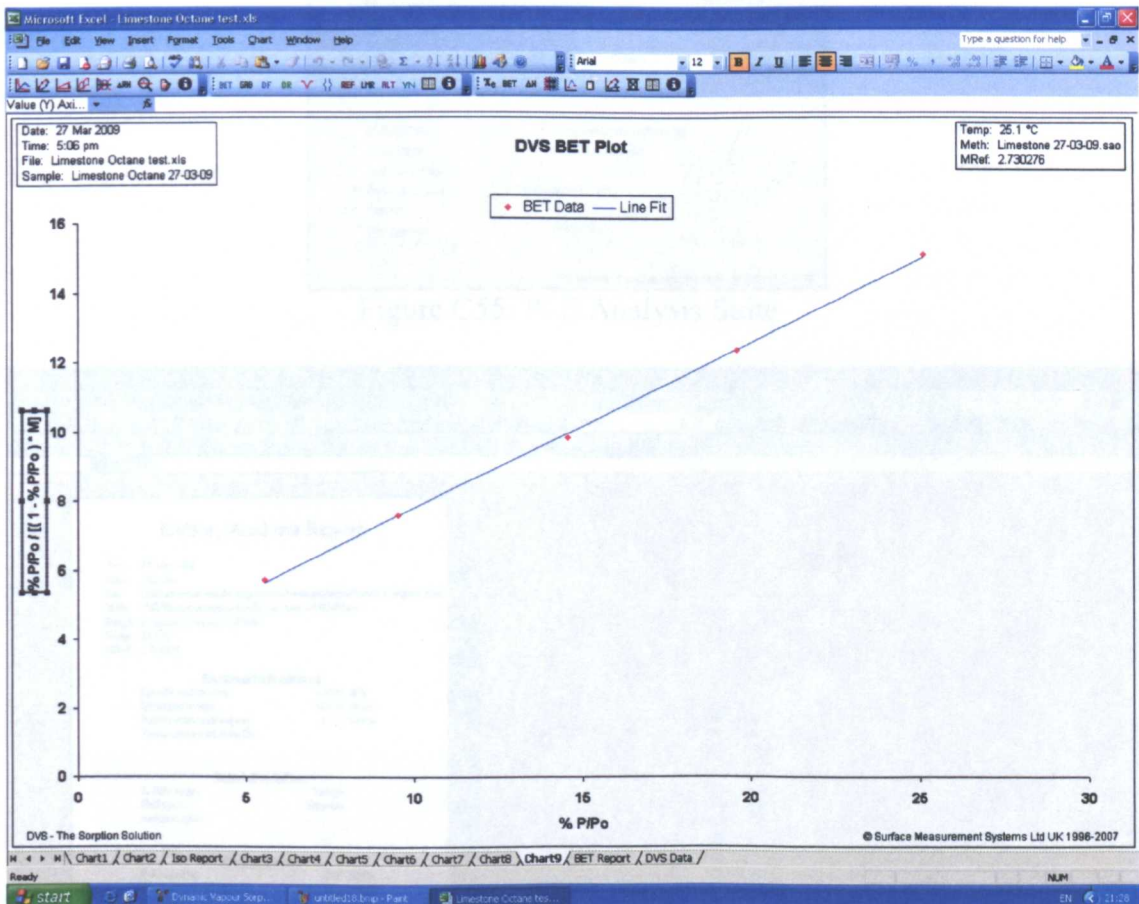


Figure C53: BET Plot

Figure C54: Spreading Pressure Analysis Report

- The analysis report provides with the specific surface area and BET constants for the material. Only the data from a non-polar probe is used to calculate the specific surface area of that material.
- The spreading pressure analysis suite, shown in Figure C55, is opened by clicking the Pi E analysis icon from the suite toolbar shown in Figure C54. The spreading pressure of a probe for the material under consideration is then obtained by in-putting the surface area results in the Pi E Analysis suite and generating an analysis report as shown in Figure C56.

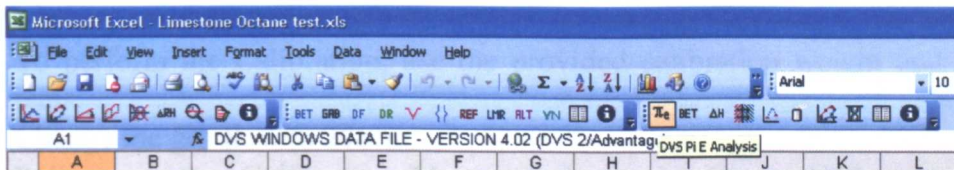


Figure C54: DVS Pi E Analysis

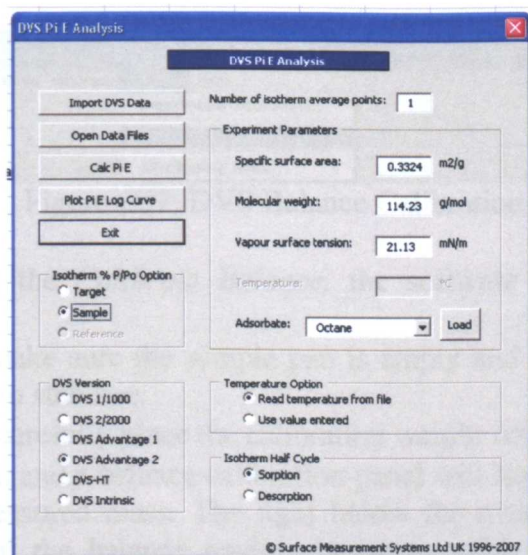


Figure C55: Pi E Analysis Suite

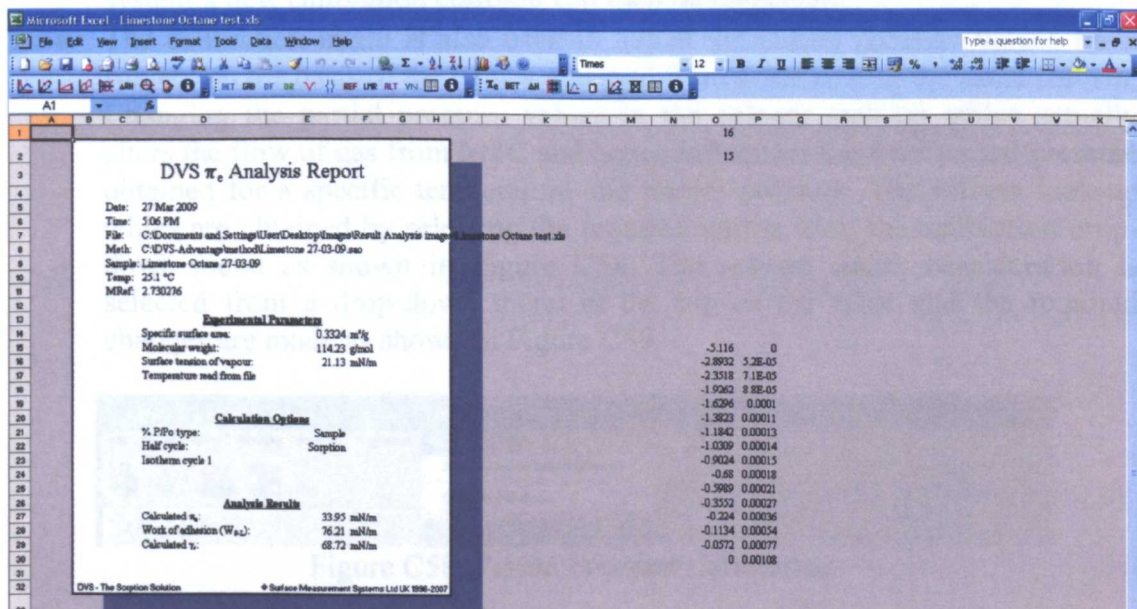


Figure C56: Spreading Pressure Analysis Report

Equipment Calibration

The microbalance needs to be calibrated against a certified calibration weight for optimum system performance. It is recommended that the microbalance be calibrated whenever:

- The microbalance is turned off
 - The DVS system is moved to a new location or repositioned
 - The experimental temperature of the incubator is changed, and;
 - At least every month during routine usage.
- To perform the Calibration, use the provided calibration weight and sample pans.
 - Change the gas flow to 20ccm.
 - Pull down the *Calibration* Menu as shown in Figure C57, and choose *calibrate balance*.

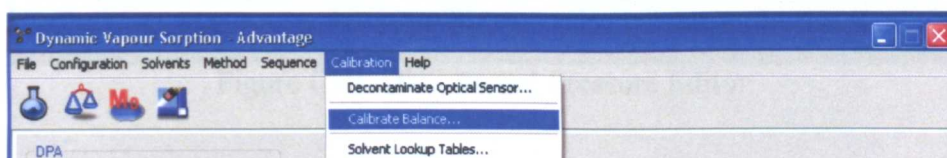


Figure C57: DVS Balance Calibration

- Upon clicking the *Calibrate Balance*, the software prompts to empty the sample pan.
- At this point make sure the sample pan is empty and clean. Tare the balance and wait for it to stabilise.
- Click OK and carefully place the calibration weight when prompted
- Click OK again and a balance calibration panel will appear. The panel displays the current measured mass. The light below the mass will be red, and will remain so until the balance reading becomes stable (this typically takes 5 minutes). When the mass reading is stable the light will turn green and the system's new calibration constant can then be registered.
- The calibration menu is also used to adjust the partial pressure values for a solvent on the basis of the values obtained from a test run for the same solvent. Changing the partial pressure values in the solvent look-up tables actually alters the flow of gas from MFC and hence influences the final partial pressure obtained for a specific temperature and partial pressure. The solvent look-up tables are obtained by selecting the required option from the calibration drop-down menu as shown in Figure C58. The solvent under consideration is selected from a drop-down menu at the top of the table and the required changes are made as shown in Figure C59.

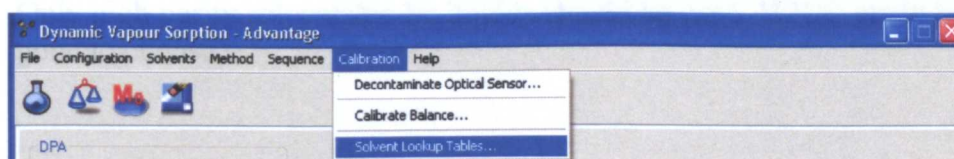


Figure C58: Partial Pressure Calibration

Dynamic Vapour Sorption - Advantage

File Configuration Solvents Method Sequence Calibration Help

Solvent Lookup Table Editor

Partial Pressure Table for: OCTANE

Temp	Flow	0.00	10.00	20.00	30.00	40.00	50.00	60.00	70.00	80.00	90.00	98.00
20	100	0.00	8.00	18.00	29.00	39.00	49.00	59.00	69.50	80.00	90.00	99.00
20	150	0.00	8.00	18.00	29.00	39.00	49.00	59.00	69.50	80.00	90.00	99.00
20	200	0.00	8.00	18.00	29.00	39.00	49.00	59.00	69.50	80.00	90.00	99.00
30	100	0.00	8.00	18.00	29.00	39.00	49.00	59.00	69.50	80.00	90.00	99.00
30	150	0.00	8.00	18.00	29.00	39.00	49.00	59.00	69.50	80.00	90.00	99.00
30	200	0.00	8.00	18.00	29.00	39.00	49.00	59.00	69.50	80.00	90.00	99.00
40	100	0.00	8.00	18.00	29.00	39.00	49.00	59.00	69.50	80.00	90.00	99.00
40	150	0.00	8.00	18.00	29.00	39.00	49.00	59.00	69.50	80.00	90.00	99.00
40	200	0.00	8.00	18.00	29.00	39.00	49.00	59.00	69.50	80.00	90.00	99.00
50	100	0.00	8.00	18.00	29.00	39.00	49.00	59.00	69.50	80.00	90.00	99.00
50	150	0.00	8.00	18.00	29.00	39.00	49.00	59.00	69.50	80.00	90.00	99.00
50	200	0.00	8.00	18.00	29.00	39.00	49.00	59.00	69.50	80.00	90.00	99.00
60	100	0.00	8.00	18.00	29.00	39.00	49.00	59.00	69.50	80.00	90.00	99.00
60	150	0.00	8.00	18.00	29.00	39.00	49.00	59.00	69.50	80.00	90.00	99.00
60	200	0.00	8.00	18.00	29.00	39.00	49.00	59.00	69.50	80.00	90.00	99.00

Mass Graph Instrument Data Sequence Active Method Run Experiment Diagnostics

Status: Ready... Surface Measurement Systems © 2007

Figure C59: DVS Partial Pressure Editor

Precautions

- The DVS requires a flat stable surface. It should not be susceptible to vibrations from other equipment in the lab or from excessive movement from personnel walking in the laboratory. This is important because of the sensitivity of the Micro Balance.
- A clearance of at least 1.0m above the work area is required (Surface Measurement Systems, DVS-Advantage protocol, 2007).
- The lab should be maintained at a stable ambient temperature preferably between 21 to 26 degrees Celsius (Surface Measurement Systems, DVS-Advantage protocol, 2007).
- The relative humidity in the lab should be less than 60% (Surface Measurement Systems, DVS-Advantage protocol, 2007).
- Dry nitrogen or air with less than 0.1% H₂O, with a pressure regulated to a minimum of 15 psi (1.5 Bar) should be used. Normal instrument grade air or nitrogen as used for Gas Chromatography is suitable.
- The Organic Vapour vent of the DVS should be connected to a vent facility suitable for the safe removal of toxic or flammable vapours. Always check that the vent facility exhaust fan is switched-on and running.
- The organic vapour detector in the environmental chamber should be engaged and running.
- Only high purity solvents/probe liquids should be used, HPLC grade is a level good to choose.

APPENDIX D

Measurement of Heat of Adhesion Using Micro-Calorimeter

Introduction

A calorimeter is used for measuring the heat of chemical reactions or physical changes and heat capacity. The word calorimeter is derived from the Latin word *calor*, meaning *heat*. The most common types of calorimeters are Differential Scanning Calorimeters, Isothermal Micro-calorimeters, Titration Calorimeters and Accelerated Rate Calorimeters (Encyclopaedia Wikipedia, 2007).

The design of a typical calorimeter is as shown in Figure D1 (Encyclopaedia Britannica, 2007).

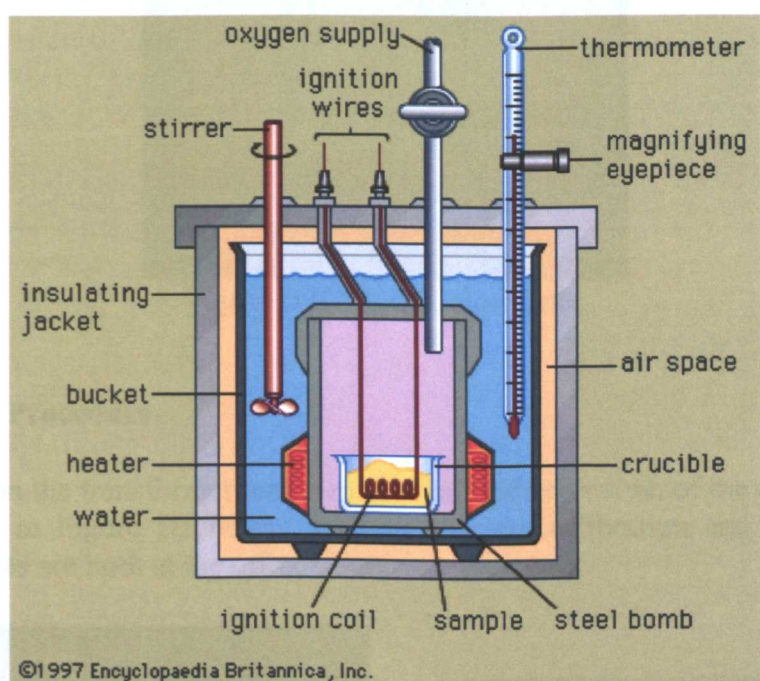


Figure D1: Cross-section of a typical calorimeter (Encyclopaedia Britannica, 2007)

The micro-calorimeter is a generic differential isothermal system which has the advantage of shorter testing time, lower capital cost, less operator training, and direct energy measurements (Omnical Technologies, Inc. user manual, 2007).

Equipment

The equipment includes;

- Micro-Calorimeter, shown in Figure D2
- Vial Picking Needles
- Computer System
- Vials with Caps and Septum
- Syringes with Needles
- RPM Gauge (Tachometer)

- Borescope
- Pipettes

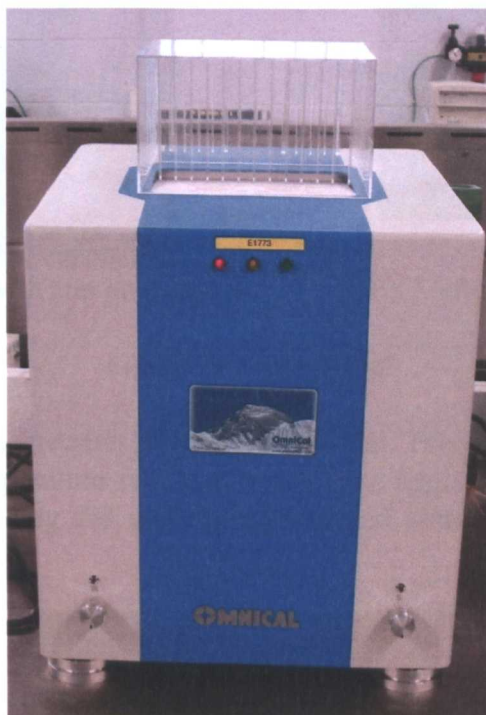


Figure D2: Micro-Calorimeter

General Test Procedure

- Turn-on the transformer and then the main power switch of the calorimeter, as shown in Figure D3 below. Be sure that the calibration and stirring motor switches are both at the off position.



Figure D3: Turning-On the Equipment

- A typical 16ml glass vial with black teflon cap and a septum is shown in Figure D4 (a) below. Take a glass vial, unscrew the cap and check the size of the vial by inserting it into a vial size-check tool as shown in Figure D4 (b) below. Sometimes a slightly oversize vial may jam in the thermal well of the calorimeter during the test. The tool is of the size of the thermal well of the calorimeter and is used to select the vials of the correct size.



a). Vial with cap and septum



b). Vial size-check tool

Figure D4: Glass Vial

- Add substrate (aggregates) to the empty vial. Precondition the aggregates at the required temperature for three hours. The aggregates are conditioned on a hot plate, by placing the vials in a preheated aluminium holder as shown in Figure D5.

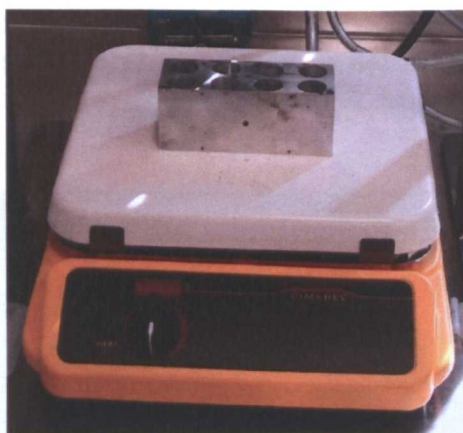


Figure D5: Vial Holder with Hot Plate

- Vials are weighed when empty and then after the addition of substrate, as shown in Figure D6, in order to get the exact weight of the substrate. Cap the vial and insert a 6-inch needle as a vial picking tool.

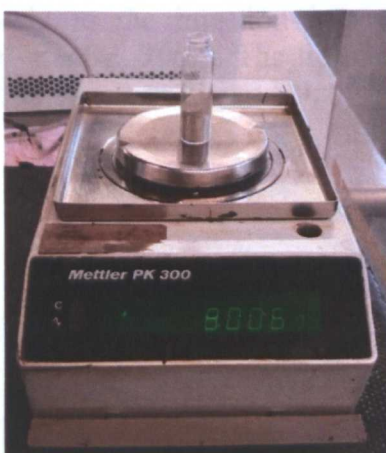


Figure D6: Weighing the Sample

Figure D9: Silicone Syringe

- Attach a refrigerated circulator/water bath to the calorimeter and set the temperature (a circulator is used if the ambient/room temperature is more than the required test temperature)
- Take plastic syringes, pull out the plungers and cover the tips of the plungers with a PTFE thread seal tape as shown in Figure D7. This is done to avoid any dissolution of the plunger tip by chemicals like chloroform.



Figure D7: Covering the Syringe Plungers with PTFE Tape

- Put the required chemical in a glass beaker and fill the syringes with the required amount of chemical in a fume cupboard as shown in Figure D8. Pull some air into the syringes so the plunger is not in contact with the liquid. The air gap at the top of the syringes helps block heat from travelling down from the plunger.



Figure D8: Filling the Syringe

- Pull a little air into the needle tip to make sure the contents of the syringe do not drip out prematurely to the injection into the sample vial (Omnicel Technologies, Inc. user manual, 2007). The tip of the syringe is also covered with a silicone stopper, as shown in Figure D9, to avoid any premature drip for the needle.

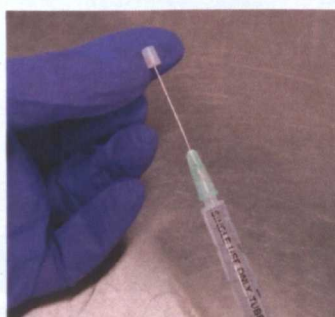


Figure D9: Silicone Stopper

- Place a sample vial into the sample-side thermal well and an empty vial to the reference-side thermal well as shown in Figure D10 below.



Figure D10: Placing the Vials in Thermal Well

- Place chemical-filled syringes into the sample injection ports and also into the reference injection ports as shown in Figure D11. Be sure that any of the syringe needles do not pierce the silicone septum of the vials.

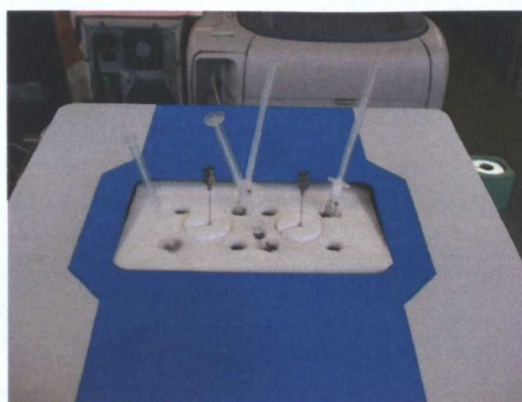


Figure D11: Placing the Needles in Injection Ports

- Cover the thermal wells with Teflon caps and place the plastic cover on the top of the calorimeter to block the airflow as shown in Figure D12.



Figure D12: Calorimeter-Top Cover

- On the PC desktop, double click **WinCRC** shortcut icon, as shown in figure D13, to start the control program.

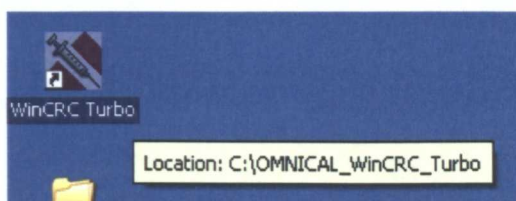


Figure D13: WinCRC Icon

- In the setup panel enter test details, upper temperature (set temperature 2°C more than what is required) and ramp rate. Leave all the other fields of setting as they are. A filled set-up panel is shown in Figure D14 below.

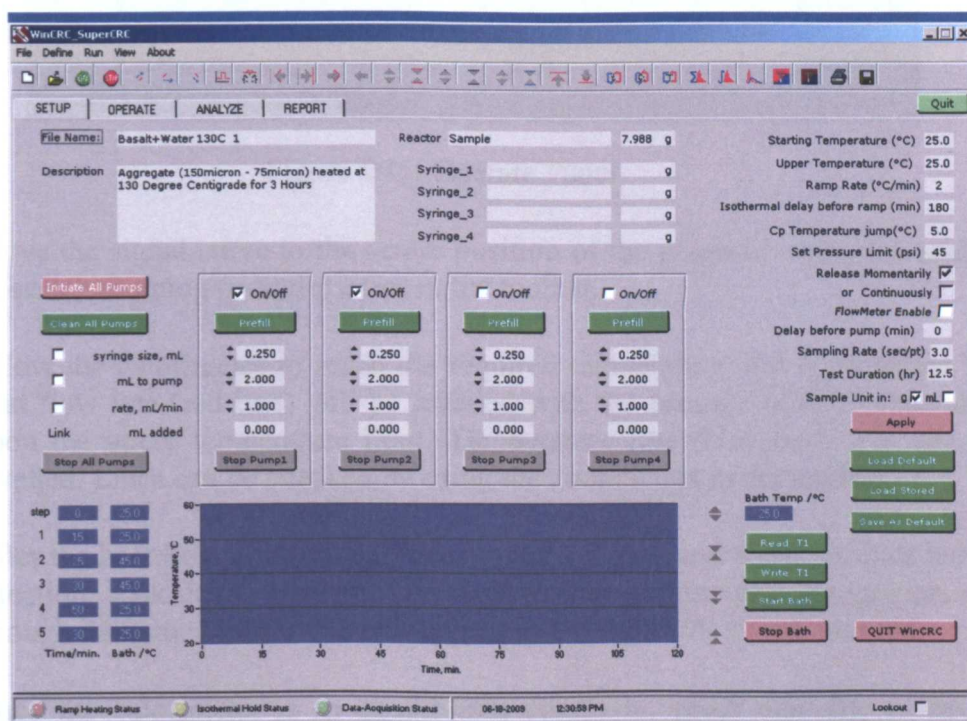


Figure D14: WinCRC Software Set-up Panel

- Always remember to toggle **Apply** before going to the OPERATE or ANALYZE panel. The colours of all the fields should turn into grey. To change the inputs toggle Apply/Change again. After the change(s) made, click **Apply** to initiate the settings. To empty all of the fields, simply click the 1st icon in the toolbar.
- Go to the **operate** panel, shown in Figure D15 to monitor the instrument operation. Click **GO** and **Ramp** icon in the toolbar to start data collection

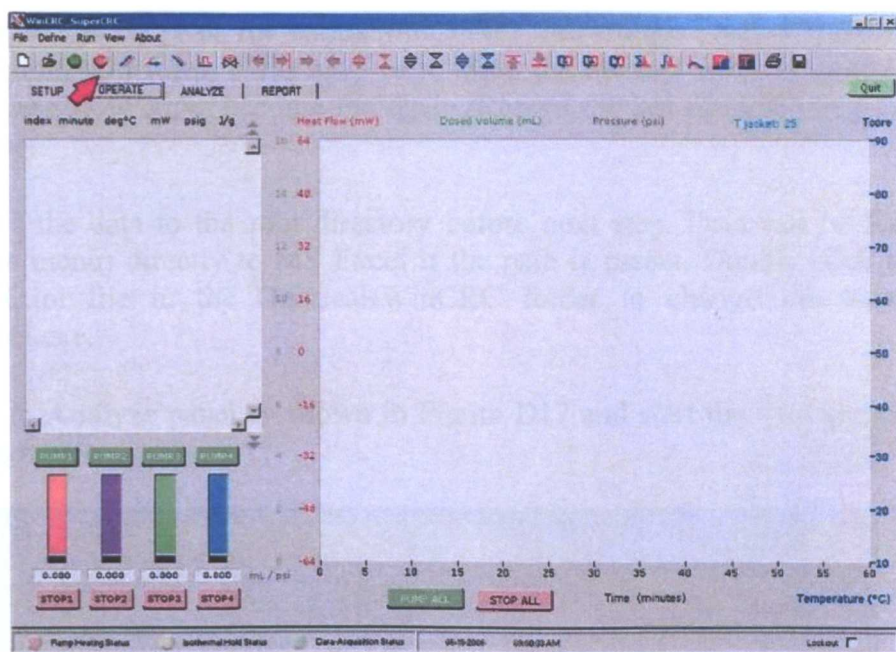


Figure D15: Operate Panel

- Move the signal curve to the centre position of the graph by using the scaling (x-scale) zooming (y-scale) icons in the toolbar.
- Allow the calorimeter to reach the required temperature and equilibrate. The heat flow line (red line) will be levelled with the passage of time depending upon the upper temperature limit. Temperature line (blue line) will also be levelled. Lines can be checked by using the zoom icons in the toolbar.
- After the heat flow baseline stabilizes to the $\pm 20\mu\text{W}$ and a few seconds before injection, click the 3rd icon from the right to start runtime peak integration, and a rough integrated heat value will appear in the right side of the data list.
- Once the calorimeter is in equilibrium condition, press **new file** to restart readings and indices. Allow the indices (difference between two indices is 3 seconds) to reach to a minimum of 25.
- Inject all syringe contents into both reference and sample vials by pressing the syringe plungers as shown in Figure D16 and cover the top with the plastic calorimeter cover.

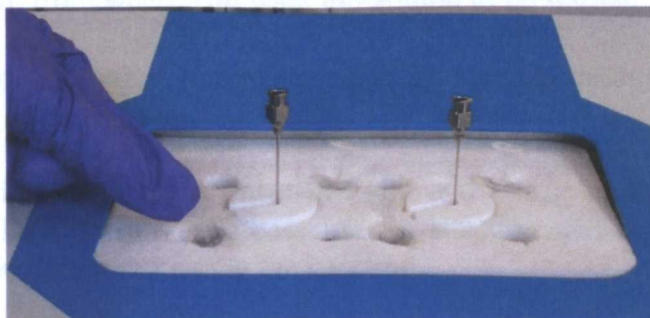


Figure D16: Injecting the Probe Liquid

- A new graph, peak for exothermic (+ve) and trough (-ve) for endothermic reaction, will form. Click **stop** icon when the thermal event is complete and the heat flow curve become flat again. Record the last runtime integrated heat value.
- **Save** the data to the root directory before next step. Data can be **Exported** (File menu) directly to MS Excel if the path is preset. Double click the WinCRC.ini file in the Omnical-WinCRC folder to change the location of Excel.exe.
- Go to **Analyze** panel as shown in Figure D17 and start the data analysis sub-program.

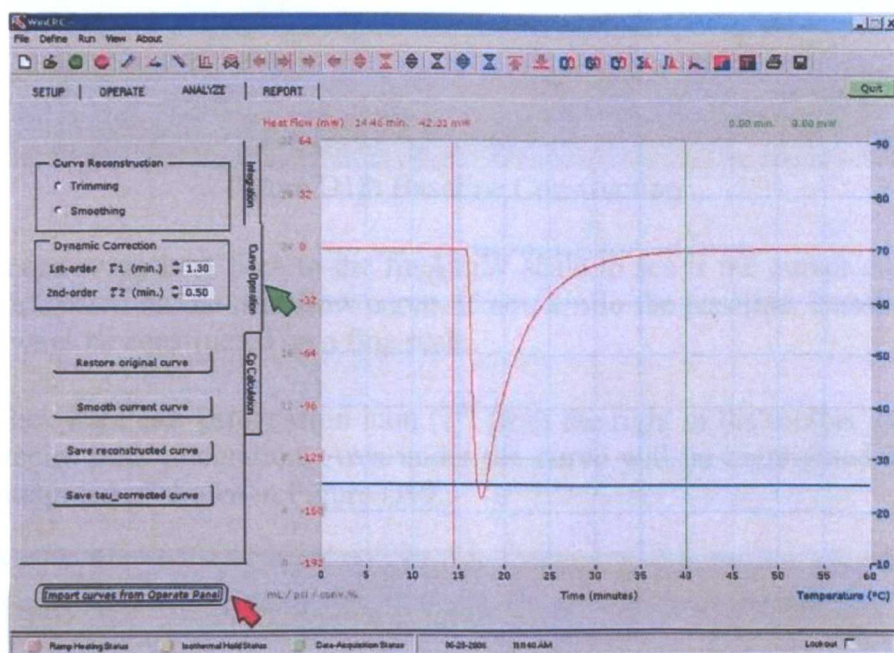


Figure D17: Analyze Panel

- Click **Import Curve** button to populate the data curve from **operate** panel.
- Use the scaling and zooming icons in the toolbar in order to move the thermogram toward the centre of the graph. Do not use Baseline-up or down icon.
- Drag the red vertical line to the left side of the peak. Be sure the cross mark is on the curve from where you want integration to be started.
- Drag the green vertical line to the right. Be sure the cross mark is located on the curve.
- In integration menu select **Point-to-Point** and Linear or non-linear, as shown in Figure D18, to draw the base line. A baseline will be formed on graph. Click **Undo** before redrawing the baseline.

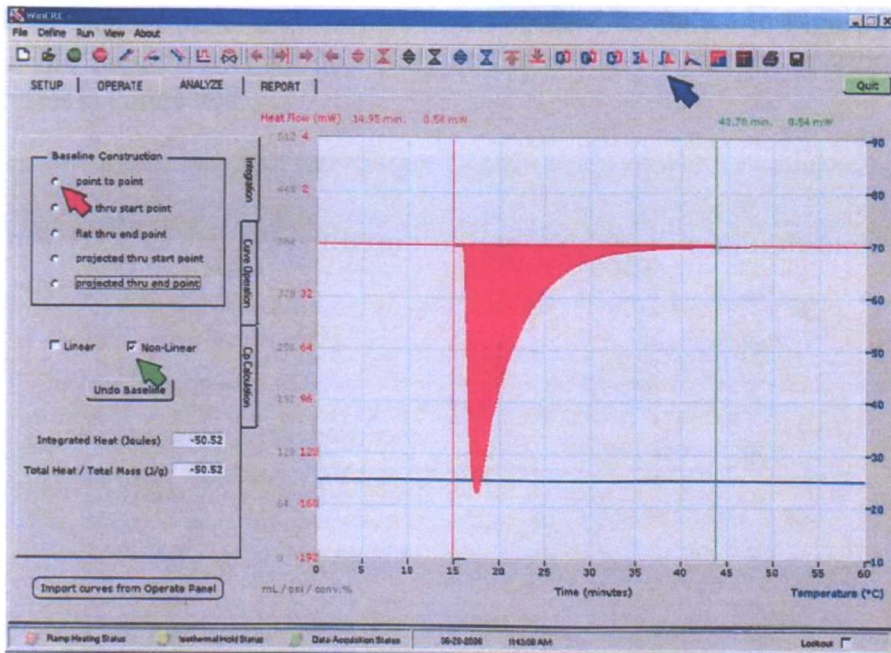


Figure D18: Baseline Construction

- Zoom in the heat flow to the final mW scale to see if the cursor cross marks are located on the heat flow curve. If not, **Undo** the baseline. Baseline should always be constructed on a fine scale.
- Click the **Peak Integration** icon (2nd from the right in the toolbar section) for precise peak integration. Area under the curve will be highlighted in red and integrated as shown in Figure D19.

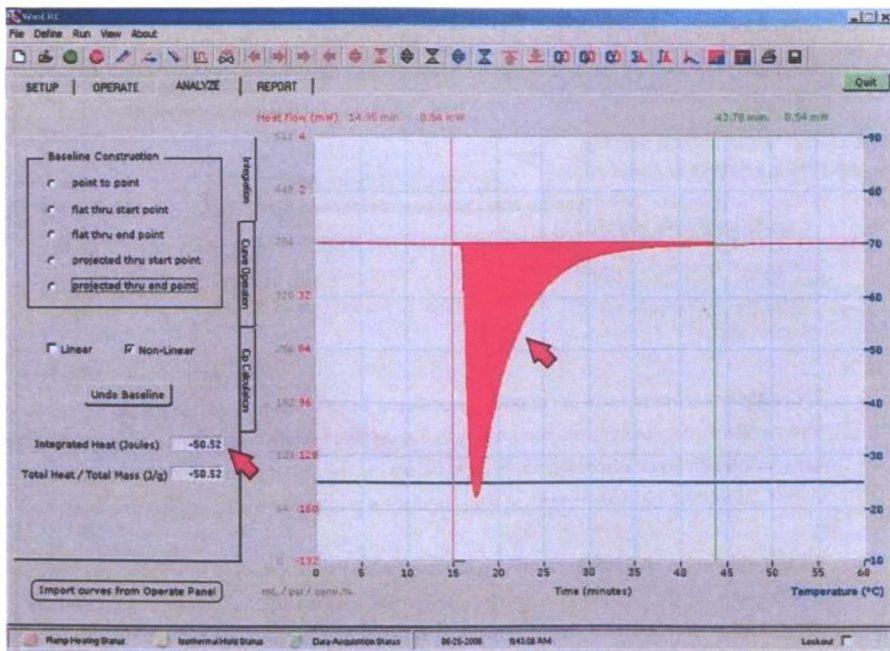


Figure D19: Peak Integration

- Go to **Report** panel and start a **Print Preview**, as shown in Figure D20, from the file menu. Enter all necessary comments and **Print** the thermogram if a printer is connected

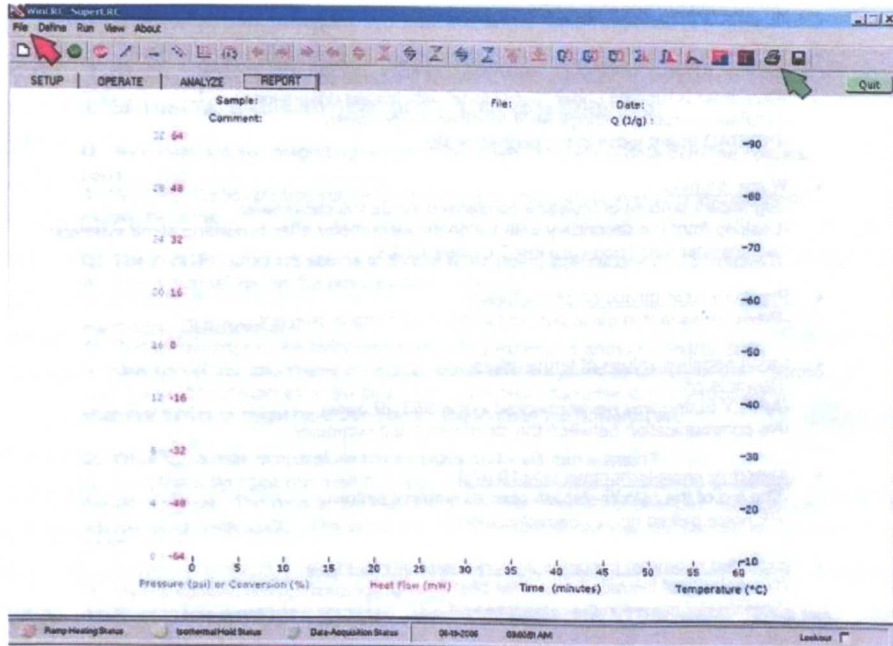


Figure D20: Print Preview

- A typical integrated heat curve showing the pre-equilibrium and post-test states is shown in Figure D21 below.

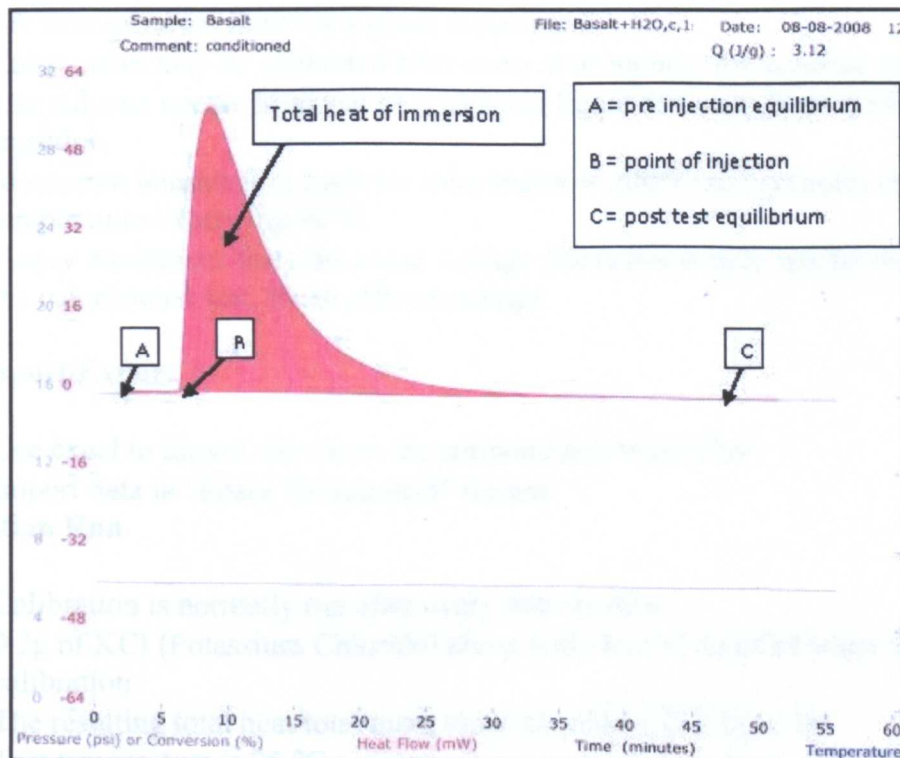


Figure D21: Post-Test Integrated Heat Curve

Precautions

- Never apply force against the internal structure of the Calorimeter
- Never use mineral oil or silicone oil, or any halogenated heat transfer fluid for the external circulating bath.
- Never run a sub-ambient calorimetric experiment without placing the calorimeter inside a dry or purge box or a glove bag
- External circulating bath must be used for near-ambient or sub-ambient isothermal temperature control
- Never circulate hot fluid to the cold calorimeter. For fast cool down, purge with ambient air first and then circulate tap water or other cold fluids when bath temperature is below 90 °C
- Never inject sample outside the sample vial. Make sure that the sample syringe needle pierces the septum before injection
- Never use oversize glass vial that may plug in the calorimeter thermal well.
- The control PC should not be connected to the network
- The calorimeter should be installed in an area free from dust, fumes, humidity and mechanical vibration
- The calorimeter should not be in the direct path of heating and cooling vent
- Purge the calorimeter with air before performing a high temperature experiment with the internal heater
- Samples and syringe barrels must be thermally equilibrated to the calorimeter heat sink temperature before injection
- The maximum relief pressure should be set to 50psi for glass vessels
- Place an empty vessel in the reference well to balance the vessel thermal masses for both sample and reference wells
- To reduce the equilibration time ramp the calorimeter with the sample
- Dynamic curve correction should be applied for very fast reactions
- Set a temperature limit for a given experiment
- Calorimeter may be calibrated after every four months for accurate results
- Use silicone needle head stoppers to avoid liquid drain out from syringe before injection
- Maximum temperature limit for calorimeter is 200°C and syringes cannot take temperature exceeding 90°C.
- Heavy equipment that can cause voltage fluctuations may not be used during the calorimetric test, it can affect readings.

Data Import/Export

- Use excel to import data from the software generated files
- Import data in "Space Delimited" format

Calibration Run

- Calibration is normally run after every four months
- 0.2g of KCl (Potassium Chloride) along with 4ml of distilled water is used for calibration
- The resulting total heat/total mass value should be 230 J/g \pm 3%
- Test temperature is 25 °C

Calculation of Surface Energy

Specific surface area values of the materials are required for calculating the final surface energy parameters. A step-by-step procedure outlining the calculation of surface energy from the integrated heat values is provided in the earlier part of this document.

Apparatus Set-up for Bitumen-Aggregate Test

- Fill the vial with approximately 5ml of bitumen with no bitumen sticking outside the vial.
- A pipette is used for injection of aggregates in the vial (Bhasin and Little, 2006).
- Make a hole in the septum of the size of the diameter of pipette
- Cover the mouth of the vial with a soft paper and then close it using vial cap with punched septum in place.
- Place the pipette filled with aggregates on the septum in an inverted position so that the paper underneath can be punched to initiate the reaction, as shown in Figure D22.
- Quantity of bitumen is selected in such a way that they can be easily get drowned or coated by the bitumen.
- Turn on the calorimeter and the control PC system.
- Cover the top of the calorimeter with the provided plastic cap and allow the system to equilibrate to the required upper temperature.
- After equilibration, remove the cap and push the pipette through the paper so that all the aggregates fall in the vial.
- Use provided software to measure heat of adhesion.

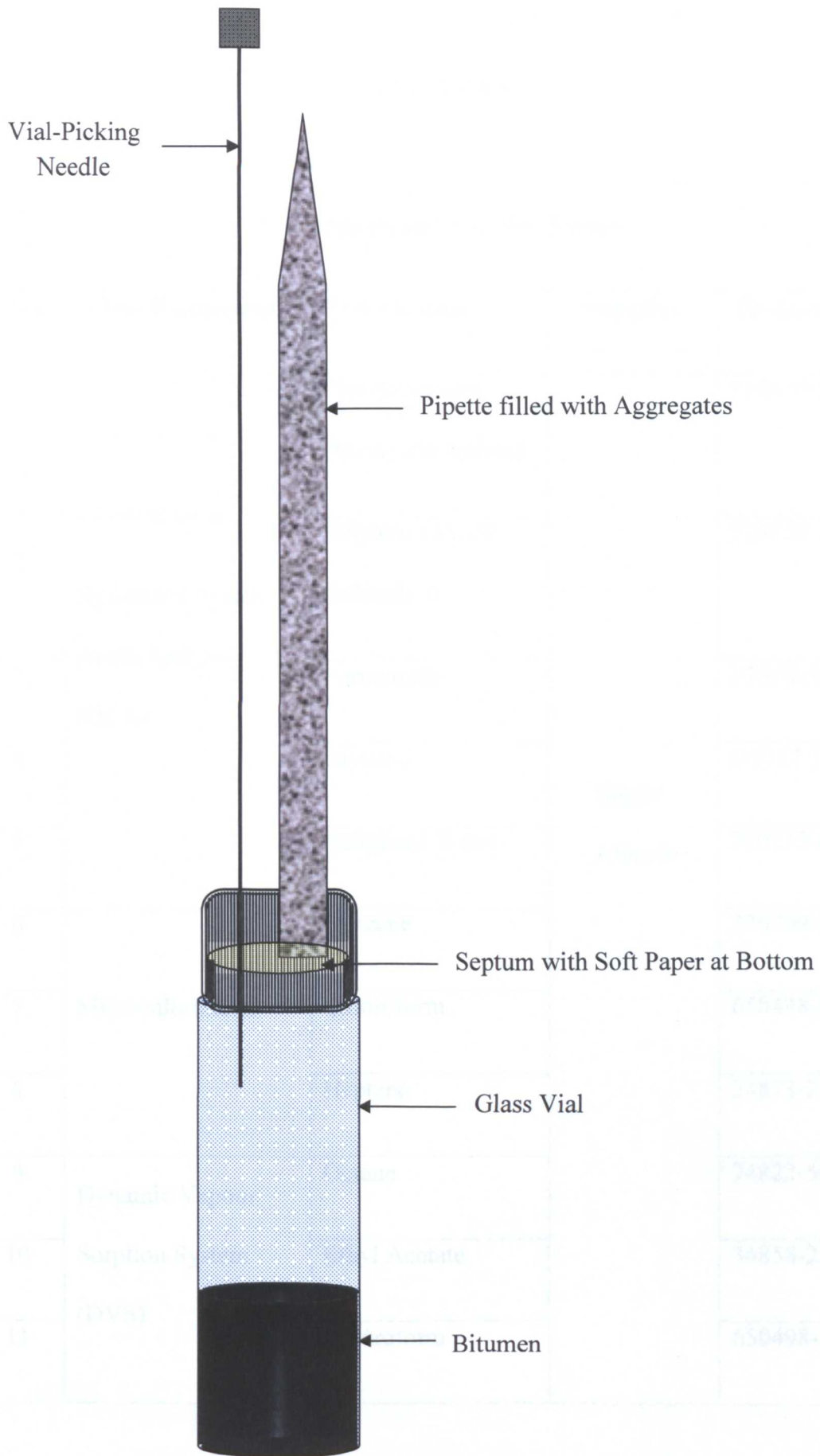


Figure D22: BITUMEN-AGGREGATE ADHESION TEST SETUP

APPENDIX E

Test Liquids and Supplier Codes				
S. No.	Test Equipment	Probe Liquid	Supplier	Product Code
1	Goniometer & Dynamic Contact Angle Analyser (DCA)	Diiodomethane (Methylene Iodide)	Sigma- Aldrich	158429-500ml
2		Ethylene Glycol (Ethandiol)		324558-1L
3		Formamide		F7503-500ml
4		Glycerol		G7757-1L
5		Deionised Water		270733-4L
6	Microcalorimeter	Benzene		270709-1L
7		Chloroform		650498-1L
8		Heptane		34873-2.5L
9	Dynamic Vapour Sorption System (DVS)	Octane		74822-500ml
10		Ethyl Acetate		34858-2.5L
11		Chloroform		650498-1L

APPENDIX F

COSHH Assessment Record

Process Identification:			Assessment
Characterising Surface Properties of Aggregates used in Hot Mix Asphalt			01
Work Area: NTEC, Asphalt Testing Laboratory 2			Room: B16
Persons at Risk:		Storage Location:	
Technical Staff and Researchers		Room B16 (Asphalt Testing Lab. 2, NAT Room)	
Substance Used:	Hazards	Quantity	Record No.
Octane (> 99%, High Performance Liquid Chromatography-HPLC Grade)	Harmful	90ml of liquid bottle is attached with the equipment for multiple tests	
	Fire (Highly Flammable)		
	Dangerous for the Environment		
Equipment Involved:			
Vapour sorption system	Vapour leak* ¹		
Dry nitrogen cylinder	Leakage* ²		
<p>*¹ Sorption system is supplied with a leak detector/sensor which shuts down the system and stops the supply of chemical in case of leakage through the system. The detector can be checked by putting a small amount of chemical on a piece of cotton and introducing it in front of the detector.</p> <p>*² The nitrogen cylinder should be checked for leakage at place where gas regulator is fitted, every time the cylinder is changed.</p>			
Process Steps	Hazard	Controls	Exposure
<p>1). Approximately 3g of aggregate sample is placed in a sample pan which is then hanged with the equipment balance.</p> <p>2). 90ml of probe liquid is poured in the provided glass bottle which is then screwed into the equipment manifold till it is hand-tight</p> <p>3). Dry Nitrogen gas is flowed through the liquid bottle and the aggregate sample at a rate of 100ccm.</p> <p>4). When the gas carrying the probe liquid vapours flows through the aggregate sample, some of the vapours get adsorbed at the aggregate surface.</p> <p>5). Change in mass of aggregate because of adsorption of vapour probes is measured</p> <p>6). Vapour concentration can be changed between 0-98% p/p₀</p>	Irritant	<p>Nitrile Gloves,</p> <p>Safety Goggles,</p> <p>Fume Cupboard</p>	1-2 minutes

<p>7). The gas flow, through the liquid and the sample, is carried out in a sealed environment until it enters into a separate exhaust system connected with the equipment and is exhausted out of the laboratory</p> <p>8). The equipment has a leak sensor which automatically stops the gas flow and shuts-down the system in case of any leakage.</p>			
Controls Used:			
Fume Cupboard			
Personal Protection Equipment Requirements:			
Nitrile Gloves, Safety Glasses/chemical splash goggles, Laboratory Coat			
Maintenance, Examination and Testing of Controls			
Personnel are only exposed at the time when the equipment glass bottle is filled with the probe liquid.			
A test normally takes more than a day.			
Storage requirements			
Store in a cool, dry place away from direct light. Store in flammables area/cupboard.			
Transport			
Chemical transport to and from FC and storage cabinet should be done in double containment. Available metal tins can be used for the purpose.			
Record keeping			
An equipment log book should be maintained. The name of the researcher, project and project duration (start-finish dates) should be mentioned in the record.			
Workplace Air Monitoring	Limits	Measured (in case of spill)*³	
WEL (workplace exposure limit)	1751mg/m ³	170.42mg/m ³	
Lower explosion limits	0.8%	2.4x10 ⁻⁵ %	
Flash Point	13°C		
Auto Ignition Temperature	220°C		
Oxygen concentration (In case of release of entire content of compressed nitrogen from the cylinder)	19%-23.5%	20.31% * ⁴	
<p>*³ There is no direct exposure to the chemical as dispensing is done in fume cupboard and the test process is undertaken in sealed conditions. The exposure values have been measured by considering the maximum possible volume of spill that can take place through equipment chemical bottle during a test.</p> <p>Order the chemical in small quantities (≤ 500ml) so that any possible spillage through supply container can be reduced to minimum. Always follow the spill emergency procedure in case of a spillage.</p>			

*⁴ Under normal conditions the concentration of oxygen in the atmosphere is given as 21%. A separate sheet providing the detail quantitative assessment for **nitrogen**, in case of release of entire content of compressed gas, is attached at the end of this record as reference.

Health Surveillance

Information, Instruction and Training

Staff/Researchers involved must be trained for operation and emergency procedures

Action Required	Responsibility	Date

Procedures in case of an Emergency

Emergency Procedure	Availability
Spill: In case of a spill, open all the windows, ask other personnel to leave the room. Remove all sources of ignition. Absorb spill with inert material (e.g. vermiculite, sand or earth), then place in suitable container. Do not use combustible material such as sawdust. Person handling the spill should use a respirator (Half mask respirator for protection against organic vapours: complying with EN: 140 or EN: 405). Better options are 3M series 4000, 6000 or 7500. Store the respirators in an appropriate/designated storage box.	
	Training
Fire: Use dry chemical, carbon dioxide or appropriate foam.	

Disposal Procedure for Waste Products

Method of Disposal
Tested aggregates and the remaining probe liquid in the equipment bottle are stored in a separate container for disposal. Dispose off as hazardous waste.
Person Responsible for Disposal
Request for disposal of the waste material should be forwarded to the laboratory manager.

Assessment of Exposure

My Assessment of the Risk to Exposure to this Process is:-

Risk: Low

$$\begin{aligned}
 \text{Risk} &= \text{Hazard Severity}^{*5} \times \text{Likelihood of Occurrence}^{*6} \\
 &= \quad 6 \quad \quad \quad \times \quad \quad \quad 1 \\
 &= \quad 6
 \end{aligned}$$

*⁵ *⁶ 'Hazard Severity' and 'Likelihood of Occurrence' are defined on a scale of 0 to 10.

'Hazard Severity' is defined on the basis that 'how hazardous is the substance/chemical', which would be used for the test.

As the test will be carried out under controlled conditions i.e. proper ventilation, trained staff and availability of proper protection equipment, the 'Likelihood of Occurrence' is given a value of '1'.

Always handle in a fume cupboard.

Get immediate medical aid in case of eye contact, ingestion or excessive inhalation.

In case of skin contact, wash thoroughly with water.

Store in a cool, dry place away from sources of ignition. Store in flammables area/cupboard.

Signature of the Assessor <div style="text-align: center;">Naveed Ahmad</div>	Date: 16/09/2008
Signature of the Project Supervisor	Date

Date of Next Assessment

The supervisor MUST pass on the findings of this assessment to the personnel involved in the work and a copy of the assessment MUST be placed in the Departmental Safety Appendix.

It is the responsibility of the supervisor to ensure that the work is carried out in compliance with this assessment. In the event of the control limits being exceeded or work practices changing, then a new assessment must be made.

Quantitative Assessment for Release of Entire Contents of Compressed Gas from Cylinders

1 Calculate volume of gas released in worst case scenario

Example 1 50 litre Nitrogen cylinder charged to 200bar used in room with free air volume of 75 m³

Example 2 50 litre of hydrogen charged to 200bar in room with volume of 75m³

1 Nitrogen
200
0.05
1.013
9.87

Initial pressure of gas in cylinder [bar] P1
 Cylinder vol. in m³ [litres/1000] V1
 Atmospheric pressure [bar] P2
 Volume of gas at atmospheric m³ V2

2 Hydrogen	Our Case
200	230
0.05	0.05
1.013	1.013
9.87	11.35

2. Calculate concentration of gas in room and compare with WEL where one has been assigned or flammability/explosion limits [for flammable gases]

1 Nitrogen
9.87
75
13.16

Volume of gas at atmospheric pressure
 Volume of room in m³
 Concentration of gas in room %

2 Hydrogen	Our Case
9.87	11.35
75	373.9
13.16	3.035571

#DIV/0
!

Hydrogen is an extremely flammable gas with a wide flammability band in air of 4 to 75%. The result in the above example is over 10 times the BCGA recommended maximum gas concentration of 25% of the lower flammability limit - this equates to 1%. There is therefore sufficient gas to cause a dangerous atmosphere and a detailed risk assessment is required to make the situation acceptable - e.g. monitoring zoning of area, removal of sources of ignition and electrical equipment from area, use of flash back arrestors.

Nitrogen does not have a WEL assigned, but some gases do. These are shown in ppm - to convert to % divide by 10000. Were this sulphur hexafluoride WEL 1000ppm /0.1% [8hr TWA] and 1250ppm /0.12% STEL a concentration of 13.16% would be considered dangerous.

3. Calculate Oxygen concentration after release of gas.

Volume of room m^3 V_r

Vol. gas at atmospheric V_g

$V_r - V_g$

$V_o = 0.21 (V_r - V_g)$

% Oxygen after release = $100 \times V_o / V_r$

	1 Nitrogen	Our Case
Volume of room m^3 V_r	75.00	373.90
Vol. gas at atmospheric V_g	9.87	11.35
$V_r - V_g$	65.13	362.55
$V_o = 0.21 (V_r - V_g)$	13.68	76.14
% Oxygen after release	18.19	20.31

Normal Conc. of Oxygen is 21% - concentrations below 18% present serious risk of asphyxiation. BCGA recommend a minimum oxygen concentration of 19% and maximum concentration of 23.5%, and evacuation of area at 18%. In this example (1) monitoring is recommended as level is only just above 18%

Note: In our case the concentration of Oxygen in the atmosphere, after the release of Nitrogen gas, is well within the limits

CURRICULUM VITAE

Name: Naveed Ahmad

Address: Nottingham Transportation Engineering Centre (NTEC)
Pavement Research Building
Department of Civil Engineering
University of Nottingham
University Park, Nottingham NG7 2RD, UK

Email: evxna1@nottingham.ac.uk

Education:

December 2006 Onward

PhD Student
Nottingham Transportation Engineering Centre (NTEC),
Department of Civil Engineering,
University of Nottingham, UK

2004-2006

M.Sc, Civil Engineering
University of Engineering & Technology Taxila, Pakistan

1999-2003

B.Sc Honours, Civil Engineering
University of Engineering and Technology Taxila, Pakistan

Work Experience:

May 2009 Onward

Research Associate
Nottingham Transportation Engineering Centre (NTEC),
Department of Civil Engineering,
University of Nottingham, UK

January 2004 to December 2006

Teaching/Research Associate
Department of Civil Engineering,
University of Engineering and Technology Taxila, Pakistan

March-May 2005

Intern, Parliamentary Internship Program
The Senate of Pakistan

August 2003 to January 2004

Trainee Engineer
National Highway Authority (NHA) Pakistan